THE ROLE OF HYDROGEN SULFIDE IN CENTRAL CARDIOVASCULAR REGULATION AND CEREBRAL ARTERY TONE

A thesis submitted in fulfilment of the requirements for the degree of Doctor of Philosophy

Eloise Yvonne Streeter
Bachelor of Pharmacy

College of Science, Engineering and Health
School of Medical Sciences
RMIT University

October 2012

INDEX

Declaration

I certify that, except where due acknowledgement has been made, the work is that of the author alone; the work has not been submitted previously, in whole or in part, to qualify for any other academic award; the content of the thesis is the result of work which has been carried out since the official commencement date of the approved research program; any editorial work, paid or unpaid, carried out by a third party is acknowledged; and ethics procedures and guidelines have been followed.

Eloise Streeter

Date:

Acknowledgements

My primary acknowledgements are to my supervisors. Thank-you to my primary supervisor, Emilio Badoer, for allowing me the opportunity to complete a PhD, and work in his laboratory. Throughout my PhD, Emilio has been patient and supportive and provided me with continual helpful advice and guidance, enabling my development into a competent researcher. A special thank-you to my second supervisor, Joanne Hart, who provided me with invaluable instruction, helping with experimental design and direction in my later studies. Joanne has consistently made herself available for impromptu discussions on the direction of my work and for this, I am extremely grateful.

Thank-you for the support of members of my research group, especially Joo-Lee Cham and Melissa Dworak for their technical assistance in my early studies; Indrajeet Rana, for allowing me to utilise the facilities at his new position at the Baker Institute; Samin Kosari for performing several renal nerve recordings for some preliminary experiments and Martin Stebbing for his repeated help with use of the confocal microscope, as well as helpful suggestions regarding my work and presentations.

I would also like to thank Donny Camera, for his extensive advice and assistance in performing RT-PCR experiments; Mohammad Al-magableh for his lending his expertise in performing western blotting and Leo Chen for his assistance and suggestions regarding myography and lucigenin assays. Simon Potocnik enhanced the quality of my immunofluorescence work immensely through his guidance and suggestions, thank-you.

Thanks also the many people who have lent a sympathetic ear and helpful suggestions throughout my PhD, especially Jennifer Lawrence and Trisha Jenkins. Finally thanks so much to my husband, Daniel, for putting up with me and supporting me throughout my PhD.

Abstract

Hydrogen sulfide (H_2S), a gas long known for its smell and toxicity, is now increasingly recognised as a gasotransmitter, in addition to nitric oxide (NO) and carbon monoxide (CO). It is produced endogenously by several enzymes and has various biological effects, including neuromodulation, cardiovascular and antioxidant effects. In the peripheral cardiovascular system, H_2S causes vasodilation and systemic administration of a H_2S donor, sodium hydrogen sulfide (NaHS), reduces blood pressure in a dose dependent manner. H_2S is also produced in the central nervous system, suggesting that it may have a role in the central regulation of the cardiovascular system, similar to NO. There are few studies investigating the role of H_2S in the brain in cardiovascular regulation or in cerebral artery tone. The thesis has investigated: i) the effect of H_2S in the brain on blood pressure (BP), heart rate (HR), and lumbar sympathetic nerve activity (LSNA); ii) the mechanism of H_2S-induced vasodilation of middle cerebral arteries (MCA); iii) the influence of diabetes on the H_2S-induced MCA response.

Cardiovascular diseases, such as hypertension and heart failure, are associated with increased sympathetic nerve activity (SNA), the pathophysiology of which is incompletely understood. The rostral ventrolateral medulla (RVLM) and the hypothalamic paraventricular nucleus (PVN) are brain nuclei with key cardiovascular regulatory functions and demonstrated involvement in the increased SNA of cardiovascular pathologies. The possible role of H_2S as a central cardiovascular regulator via the RVLM and PVN was therefore investigated. The presence of the H_2S producing enzyme, cystathionine β synthase (CBS) in the RVLM and PVN was demonstrated by western blotting and immunohistochemistry. Nerve recording studies were performed on anaesthetised male Wistar Kyoto (WKY) and spontaneously hypertensive rats (SHR). Bilateral microinjections of NaHS (0.2 – 2000 pmol/side), or inhibitors of CBS (hydroxylamine, HA, 0.2 – 2.0 nmol/side; or amino-oxyacetate, AOA, 0.1 –

1.0 nmol/side) into the RVLM did not significantly affect BP, HR or LSNA, compared to vehicle in WKY rats. Microinjections into the PVN of NaHS, HA and AOA had no consistent significant effects on BP, HR or LSNA compared to vehicle in WKY rats. NaHS microinjected into the PVN or RVLM of SHR rats did not significantly affect BP, HR or LSNA compared to vehicle. Together, these results suggest that H_2S may not have a major cardiovascular regulatory role in the RVLM and PVN.

H_2S is produced in peripheral blood vessels via the enzyme cystathionine-γ-lyase (CSE). It is thought to be an important endogenous vaso-active mediator, since CSE gene deletion has resulted in increased blood pressure. Although there are numerous studies investigating the mechanism of H_2S-induced vasodilation in peripheral vessels, in cerebral blood vessels, the mechanism has not been extensively studied. Vasorelaxation studies were performed on middle cerebral arteries (MCA) from male Sprague-Dawley rats using wire myography. Immunofluorescence staining showed the H_2S producing enzyme cystathionine-γ-lyase (CSE) was present in the smooth muscle layer of middle cerebral arteries. Consistent with this, the CSE substrate L-cysteine (10 μM-100 mM) induced vasorelaxation in middle cerebral arteries that was independent of endothelium, suggesting conversion of L-cysteine to H_2S via CSE occurred in the vascular smooth muscle. NaHS (0.1-3.0mM) produced concentration-dependent relaxation of MCA, which was unaffected by endothelium removal. Inhibiting K^+ conductance with KCl (50mM) significantly attenuated NaHS-induced relaxation, increasing the EC_{50} by 4 fold. 4,4-diisothiocyanatostilbene-2,2-disulfonic acid (DIDS, 300μM) caused a significant 10-fold rightward shift of the NaHS concentration-response curve. Nifedipine (3μM), a blocker of L-type calcium channels, significantly reduced the maximum relaxation elicited by NaHS by 30%. These findings suggest that H_2S mediated relaxation of middle

cerebral arteries is DIDS sensitive and partly mediated by inhibition of L-type calcium channels with an additional contribution by potassium channels.

Cardiovascular pathologies, including hypertension and diabetes, alter the structure and function of cerebral vessels, increasing the risk of stroke and dementia. The mechanisms inducing this dysfunction are incompletely understood, but are thought to involve reactive oxygen species (ROS) inducing endothelial dysfunction. H_2S has antioxidant effects and has been shown to protect against endothelial dysfunction. The effect of diabetes on the MCA response to H_2S was therefore investigated. Cerebral vessels were harvested from streptozotocin (50mg/kg) induced diabetic rats 10 weeks after streptozotocin treatment, and their age-matched controls. Diabetes induced an attenuation of bradykinin-induced vasorelaxation, suggesting endothelial dysfunction. The response to NaHS was unchanged by diabetes, however, L-cysteine-induced relaxation was enhanced in diabetic vessels. The mechanism of H_2S-induced vasodilation was investigated using DIDS (300μM), nifedipine (3μM) and KCl (50mM) – similar to in non-diabetic rats, DIDS induced a significant rightward shift of the dose-response curve, while nifedipine and KCl both significantly inhibited the maximum relaxation induced by NaHS. The lucigenin assay, an *in vitro* assay for superoxide (O_2^-) generation, demonstrated increased O_2^- generation from both aorta and cerebral vessels of diabetic animals. NaHS decreased O_2^- generation from diabetic, but not control MCA. The results suggest that the mechanism and vascular response to H_2S is unchanged in diabetic MCA, although production of H_2S may be increased. H_2S appears to act as an antioxidant in diabetic MCA *in vitro*.

Publications and Communications

Journal publications

Streeter E, Al-magableh M, Hart JL, Badoer E (2011) Hydrogen sulfide in the RVLM and PVN has no effect on cardiovascular regulation. *Front. Physio.* **2**:55.

Streeter E, Hart J, Badoer E (2012) An investigation of the mechanisms of hydrogen sulfide-induced vasorelaxation in rat middle cerebral arteries*, Naunym Schmeidebergs Arch Pharmacol*. **385** (10):991-1002

Abstracts presented at meetings

Streeter E, Hart J, Badoer E (2009) Effect of hydrogen sulfide in the brain on cardiovascular regulation, *Proceedings of the Australasian Society of Clinical and Experimental Pharmacologists and Toxicologists*, 2, 28

Streeter E, Hart J, Badoer E (2010) Hydrogen sulfide relaxes middle cerebral arteries in rats. *Proceedings of the Australasian Society of Clinical and Experimental Pharmacologists and Toxicologists*, 14

Streeter E, Hart J, Badoer E (2011) Mechanisms contributing to the hydrogen sulfide induced vasorelaxation of middle cerebral arteries in the rat, *Proceedings of the Australasian Society of Clinical and Experimental Pharmacologists and Toxicologists*, 176

Abbreviations

3-MST	3-mercaptopyruvate sulfurtransferase
4-AP	4-aminopyridine
a-CSF	artificial cerebrospinal fluid
ADRF	adipocyte-derived relaxing factor'
AOA	amino-oxyacetate
AT_1	angiotensin II type 1
ATP	adenosine triphosphate
BK	bradykinin
BK_{Ca}	large-conductance calcium-activated potassium channels
$[Ca^{2+}]_i$	intracellular calcium concentration
cAMP	cyclic adenosine monophosphate
CAT	cysteine aminotransferase
CBS	cystathionine-β-synthase
cGMP	cyclic guanosine monophosphate
CHF	congestive heart failure
CO	carbon monoxide
COX	cyclooxygenase
CSE	cystathionine-γ-lyase
DIDS	4,4'-diisothio-cyanostilbene-2,2'-disulfonicacid
DOPA	3,4 dihydroxyphenylalanine
DPI	diphenylene iodonium
EDHF	endothelium derived hyperpolarising factor
EDRF	endothelium derived relaxing factor
eNOS	endothelial nitric oxide synthase
GABA	γ-aminobutyric acid
H_2O_2	hydrogen peroxide
H_2S	hydrogen sulfide
HA	hydroxylamine
HHcy	hyperhomocysteinaemia
HR	heart rate
IK_{Ca}	intermediate-conductance calcium-activated potassium channels
IML	intermediolateral column
iNOS	inducible nitric oxide synthase
IP	cell surface prostacyclin receptor
K_{ATP}	adenosine triphosphate-sensitive potassium channels
K_{Ca}	calcium-activated potassium channels
K_{IR}	inwardly rectifying potassium channels
K_V	voltage-gated potassium channels
L-NAME	$L\text{-}N^G$-Nitroarginine methyl ester
LSNA	lumbar sympathetic nerve activity
MCA	middle cerebral artery
MAP	mean arterial pressure
Na_2S	sodium sulfide
NADH	nicotinamide adenine dinucleotide

NADPH	nicotinamide adenine dinucleotide phosphate
NaHS	sodium hydrogen sulfide
NNDP	N,N-dimethylphenyldiamine sulphate
nNOS	neuronal nitric oxide synthase
NOS	nitric oxide synthase
NO	nitric oxide
NOD	non-obese diabetic mice
Nox	nicotinamide adenine dinucleotide phosphate oxidase
NTS	nucleus tractus solitarius
$O_2^{\cdot-}$	superoxide
$OH^{\cdot}$	hydroxyl
$ONOO^-$	peroxynitrite
PH	posterior hypothalamus
pH_i	intracellular pH
PLP	pyridoxal 5'-phosphate
PGI_2	prostacyclin
PPG	propargylglycine
PVN	paraventricular nucleus of the hypothalamus
ROS	reactive oxygen species
RSNA	renal sympathetic nerve activity
RT-PCR	real-time quantitative polymerase chain reaction
RVLM	rostral ventrolateral medulla
sGC	soluble guanylate cyclase
SHR	spontaneously hypertensive rats
SK_{Ca}	small-conductance calcium-activated potassium channels
SNA	sympathetic nerve activity
SOD	superoxide dismutase
STZ	streptozotocin
SUR	sulphonylurea receptor
VGCC	voltage gated calcium channels
VSM	vascular smooth muscle
WKY	Wistar Kyoto

Chapter 1: Introduction

Hydrogen sulfide (H_2S) has a well-ingrained reputation as a toxic, malodorous gas. However, it is now increasingly recognised as a gasotransmitter, in addition to nitric oxide (NO) and carbon monoxide (CO) as it is produced endogenously by several enzymes (Kimura, 2011; Shibuya *et al.*, 2009b; Yang *et al.*, 2008) and induces various biological effects. H_2S displays anti-oxidant properties (Kimura *et al.*, 2010) and several cardiovascular actions of H_2S have been described, including vasorelaxation (Zhao *et al.*, 2001), protection against ischaemia reperfusion injury (Calvert *et al.*, 2009) and inhibition of high glucose-induced endothelial dysfunction (Suzuki *et al.*, 2011). This introductory chapter begins with an overview of the biochemistry of H_2S, including how it is produced and pharmacological tools that are used to study H_2S-induced effects. The biological effects of H_2S are briefly overviewed in section 1.1.3 (p.21), with pertinent effects being revisited in detail under sections 1.2-1.4 (p.22-62). Sections 1.2-1.4 (p.22-62) explain each of the physiological systems and pathological changes investigated in this research project with reference to the rationale for investigating each of these phenomena, and evidence of H_2S-induced effects.

1.1 Hydrogen sulfide as an endogenous mediator

1.1.1 Biochemistry

Enzymatic production

H_2S is synthesised in bacteria by the reduction of sulphate or elemental sulfur (Escobar *et al.*, 2007). Since mammals lack the ability to reduce elemental sulfur, H_2S is produced endogenously via the catabolism of sulfur containing amino acids, predominantly by the transsulfuration enzymes – cystathionine-β-synthase (CBS, EC 4.2.1.22) (Kimura, 2011); and cystathionine-γ-lyase (CSE, EC 4.4.1.1) (Yang *et al.*, 2008). For example, H_2S is released during the conversion of cysteine to serine by CBS and cysteine to pyruvate by CSE (figure 1.1). A recent study indicates that a third enzyme, 3-mercaptopyruvate sulfurtransferase (3-MST, EC 2.8.1.2) can also generate H_2S. 3-MST acts in concert with cysteine aminotransferase (CAT, EC 2.6.1.75) to catabolise cysteine, generating pyruvate and H_2S (figure 1.1) (Shibuya *et al.*, 2009a). CBS is a major contributor to H_2S production in the brain, as CBS expression levels are relatively high, and inhibition of CBS using hydroxylamine and amino-oxyacetate suppresses the production of brain H_2S (Abe *et al.*, 1996). CSE levels predominate in most peripheral tissues, and mice with genetic deletion of CSE have reduced endogenous H_2S levels in aorta, heart, serum, and fail to generate H_2S in liver (Mustafa *et al.*, 2009b; Yang *et al.*, 2008). 3-MST appears to contribute to H_2S production in both the periphery and central nervous system (Shibuya *et al.*, 2009a) (Shibuya *et al.*, 2009b).

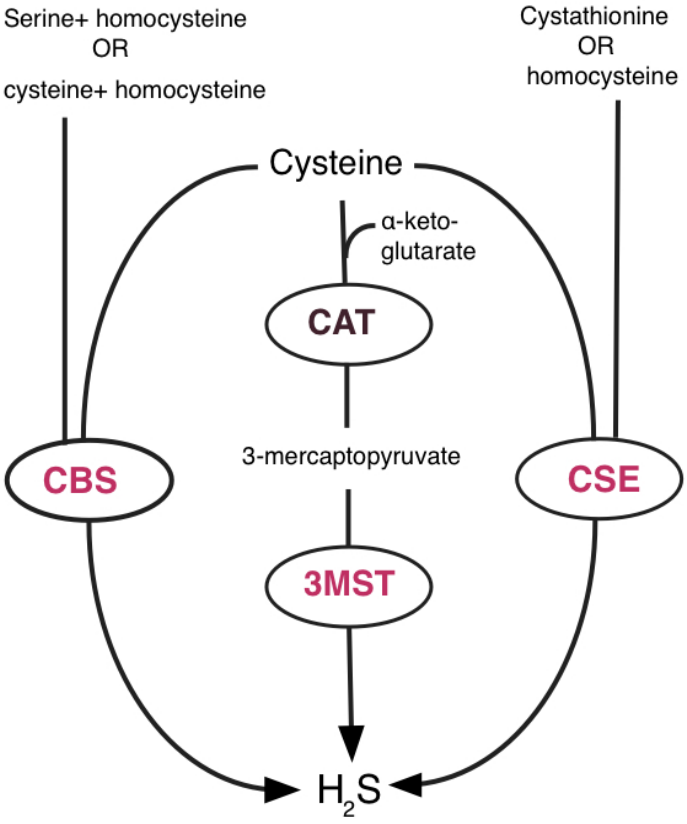

Figure 1.1 Schematic illustrating pathways contributing to endogenous H_2S production

H_2S can be produced via the enzymes CBS, CSE or 3-MST. All three enzymes can utilise cysteine as a substrate for H_2S production, with the 3-MST pathway requiring an intermediate step where cysteine is converted to 3-mercaptopyruvate via CAT. CBS can also use serine plus homocysteine or cysteine plus homocysteine as substrates, and CSE can use cystathionine or homocysteine as substrates. The byproducts of cysteine metabolism other than H_2S are dependent on the pathway and the substrate, and for reasons of clarity, have been omitted from this diagram pertaining to H_2S production. For example, the 3-MST pathway also releases pyruvate as a byproduct. CBS, cystathionine-β-synthase; CSE, cystathionine-γ-lyase; 3-MST, 3-mercaptopyruvate sulfurtransferase, CAT, cysteine amino transferase. Adapted from Shibuya *et al.* (Shibuya *et al.*, 2009b).

Concentration of H_2S in Tissues

Free H_2S is maintained at low levels in basal conditions through absorption and storage as bound sulfur, which cannot function as a gaseous messenger (Ishigami *et al.*, 2009). Previous studies show very high concentrations of H_2S (brain: 50-160 μM, (Goodwin *et al.*, 1989; Savage *et al.*, 1990); plasma: 40-300 μM (Kimura, 2002)) compared to recent studies (brain: 15 nM (Furne *et al.*, 2008); plasma:<15 nM (Whitfield *et al.*, 2008). The disparity is likely due to the harsh chemical treatment (either strong acid or strong base) required for the assays used in previous studies, which may have released sulfur from its stored forms. Recent developments have allowed for more direct measurements of free H_2S using either gas chromatography (Furne *et al.*, 2008) or a polagraphic H_2S sensor (Whitfield *et al.*, 2008). The actual concentration of H_2S in mammalian tissues remains to be conclusively determined, but is likely to be much lower than original estimates.

1.1.2 Pharmacological tools

There are various pharmacological tools useful for investigating the potential functions of H_2S. These include donors, precursors to H_2S production, inhibitors of H_2S producing enzymes and genetic knock-down of H_2S producing enzymes.

H_2S donors

H_2S donors release or generate H_2S upon addition to solution, and are therefore useful for determining whether exogenously administered H_2S can produce biological effects. Most studies investigating the biological effects of H_2S have used one of two commonly available sulfide salts: sodium sulphide (Na_2S) or sodium hydrogen sulphide (NaHS). Both donors rapidly generate H_2S upon addition to solution by first dissociating - Na_2S dissociates to Na^+ and S^{2-}, and NaHS to Na^+ and HS^- - followed by formation of equilibrium according to:

$$S^{2-} + H^+ \longleftrightarrow HS^- + H^+ \longleftrightarrow H_2S$$

Since the pKa of HS^- is greater than 12, only a trace amount of S^{2-} exists at physiological pH (Olson, 2012). The pKa of H_2S is 6.77 at 37 ^oC, resulting in approximately 18.5% being present as H_2S, with 81.5% existing as the HS^- anion (Dombkowski *et al.*, 2004). It is not known which form of H_2S (H_2S, HS^- or S^{2-}) is physiologically active, or whether all three forms are active to varying extents, however, the active component is commonly termed 'hydrogen sulfide', and it will therefore be referred to throughout the present thesis as H_2S.

The formation of H_2S from Na_2S involves accepting two protons from the solution, whereas H_2S formation from NaHS requires only one proton. Thus, while solutions of both compounds are alkaline, Na_2S forms considerably more alkaline solutions for the same amount of H_2S produced. This is likely the reason for a general preference among the literature for use of NaHS, as opposed to Na_2S. Since NaHS was the most commonly used H_2S donor at the time of research, and does not cause significant alkalinisation of physiologically buffered solutions within the concentrations applied in the present studies (Al-Magableh *et al.*, 2011), NaHS was used as a H_2S donor for all studies in the present thesis.

Recently, a number of slow-releasing H_2S compounds have been developed, including GYY4137 (Li *et al.*, 2008). Due to the lack of knowledge regarding the efficacy and selectivity of such compounds in the time frame of the present studies, NaHS was the preferred donor here. However, these slow-releasing compounds are proving useful pharmacological tools, particularly in studies observing chronic effects of H_2S.

L-cysteine as a precursor to H_2S production

L-cysteine is commonly used to determine the effects of endogenously produced H_2S (d'Emmanuele di Villa Bianca *et al.*, 2009; Elsey *et al.*, 2010). It acts as a substrate for both CBS and CSE, resulting in the endogenous production of H_2S (figure 1.1). However, L-cysteine also scavenges nitroxyl anion and has been used in studies investigating nitroxyl anion-induced vascular effects (Andrews *et al.*, 2009).

Inhibitors of CBS and CSE

The tonic production of H_2S can be inhibited using inhibitors of either of the H_2S producing enzymes, CBS or CSE. CBS and CSE are both dependent on pyridoxal 5'-phosphate (PLP), and like nitric oxide synthase, are regulated by calcium in the presence of calmodulin (Eto *et al.*, 2002; Finkelstein *et al.*, 1975) (Yang *et al.*, 2008). Several pharmacological tools are available for the manipulation of these enzymes. The work described in the present thesis employed amino-oxyacetate (AOA) and hydroxylamine (HA) to inhibit CBS; and D,L-propargylglycine (PPG) to inhibit CSE.

AOA inhibits CBS by covalently binding to its cofactor, PLP (McMaster *et al.*, 1991). AOA is relatively non-specific, since it inhibits all enzymes which require PLP as a cofactor. Other PLP dependent enzymes include 3,4 dihydroxyphenylalanine (DOPA) decarboxylase and γ-aminobutyric acid (GABA)-transaminase (Amadasi *et al.*, 2007). AOA inhibition of GABA-transaminase results in increased brain GABA levels, which is thought to be partly responsible for the anticonvulsant properties of AOA (McMaster *et al.*, 1991). HA is similarly non-specific, as it causes reversible dissociation of PLP from CBS and other PLP-dependent enzymes (Braunstein *et al.*, 1971). HA also acts as a nitric oxide donor (Taira *et al.*, 1997). PPG covalently binds to the PLP binding site of the CSE enzyme, thus may also influence other PLP-dependent enzymes (Johnston *et al.*, 1979). A relatively poor cell-permeability of PPG (Marcotte *et al.*, 1976) necessitates the use of fairly high concentrations (1-20mM) in biological experiments.

Genetic knock-down models: $CSE^{-/-}$ and $CBS^{-/-}$

$CSE^{-/-}$ mice have been developed and used by several studies to investigate the cardiovascular role of H_2S (Mustafa *et al.*, 2011; Yang *et al.*, 2008). Aside from reduced plasma H_2S levels, these mice develop significant hyperhomocysteineamia, which is known to adversely affect cardiovascular function, decreasing NO availability (Weiss *et al.*, 2002), and reducing endothelium derived hyperpolarising factor mediated responses (Cheng *et al.*, 2011). In contrast to $CSE^{-/-}$ mice, $CBS^{-/-}$ are not used in the study of H_2S-induced effects. This is due to the severity of pathological consequences of the $CBS^{-/-}$ model, including hyperhomocysteinaemia, liver injury and death typically within 2-3 weeks of birth (Maclean *et al.*, 2010).

In summary, the currently available pharmacological tools used to investigate the biological effects of H_2S suffer various limitations, such as non-specificity of enzyme inhibitors. Newer methods, such as highly selective enzyme inhibitors, are yet to be developed. At present, the tools described are the best at our disposal, and are therefore in common use to examine the biological effects of H_2S.

1.1.3 Biological effects of H_2S

In 1996, Abe and Kimura were the first to attribute a physiological response to H_2S. They showed that application of NaHS to hippocampal rat brain slices resulted in facilitation of long-term potentiation (Abe *et al.*, 1996). Since then, a range of physiological effects of H_2S have been observed, including: neuromodulation (Abe *et al.*, 1996; Austgen *et al.*, 2011; Dawe *et al.*, 2008; Nagai *et al.*, 2004), vasorelaxation (Zhao *et al.*, 2001), attenuation of endothelial dysfunction and atherosclerosis (Suzuki *et al.*, 2011; Wang *et al.*, 2009; Zhao *et al.*, 2011), antioxidant (Chai *et al.*, 2012; Kimura *et al.*, 2006; Kimura *et al.*, 2010; Muzaffar *et al.*, 2008) and anti- and pro-inflammatory actions (di Villa Bianca *et al.*, 2010; Wallace *et al.*, 2007) (for review see (Whiteman *et al.*, 2011)). Several of these effects are reminiscent of NO, and both gaseous mediators are produced by calcium-calmodulin dependent enzymes (Eto *et al.*, 2002; Yang *et al.*, 2008). Such parallels have led to intensive research into the roles of H_2S in physiology and pathophysiology, particularly in the cardiovascular system.

To date there has been very little research on the role of H_2S in the central regulation of the cardiovascular system or cerebrovascular tone. The present research project has therefore investigated i) the role of H_2S in central regulation of the cardiovascular system; ii) the role of H_2S regulation of middle cerebral artery (MCA) tone and iii) diabetes induced changes to the MCA H_2S-induced response. The following sections shall review each of these physiological and pathophysiological processes in turn, emphasising the rationale for investigating each, and any known relevant effects of H_2S.

1.2 Cardiovascular regulation by the brain

The central nervous system plays a key role in regulating cardiovascular function, particularly via several nuclei within the brainstem and hypothalamus known as 'premotor nuclei' (Guyenet, 2006) (Dampney, 1994). The premotor nuclei contain presympathetic neurons that project directly to the sympathetic preganglionic motor neurons in the intermediolateral column (IML) of the spinal cord. These motor regions send inputs to sympathetic post-ganglionic nerves. These peripheral sympathetic nerves innervate the heart, blood vessels, kidneys and the adrenal medulla to regulate cardiovascular function (Guyenet, 2006) (figure 1.2). Of the premotor nuclei, the present studies have focused on the rostral ventrolateral medulla (RVLM), as it has a profound influence on cardiovascular regulation (Dampney, 1994), and the paraventricular nucleus of the hypothalamus (PVN), as it is an important integrative site for cardiovascular function (Badoer, 2001; Badoer, 2010; Deering *et al.*, 2000).

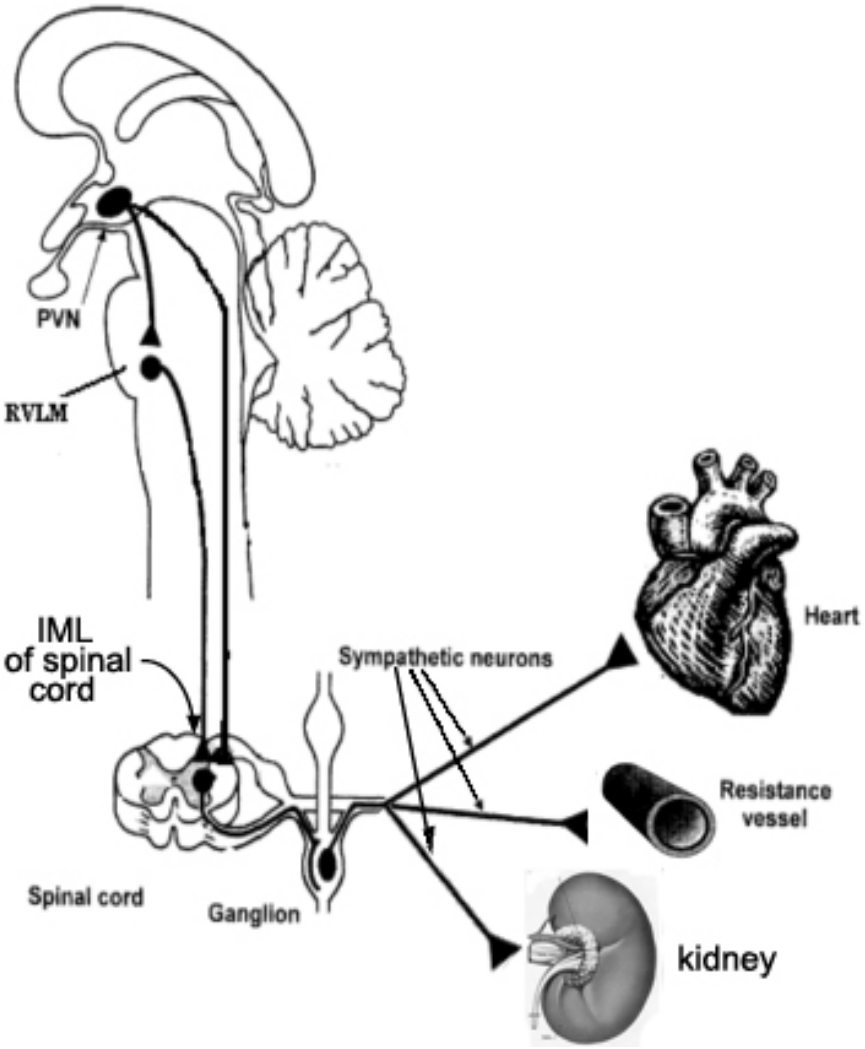

Figure 1.2. Diagram illustrating sympathetic innervation via the RVLM and PVN Presympathetic neurons within the PVN and RVLM send projections to the IML of the spinal cord. The motor neurons in the IML project to sympathetic post-ganglionic neurons to ultimately influence sympathetic effector organs including heart, kidney and resistance vessels. IML, intermediolateral column; RVLM, rostral ventrolateral medulla; PVN, paraventricular nucleus. Modified from (Pyner, 2009).

Peripheral sympathetic nerve activity enhancement is observed in patients with hypertension, congestive heart failure, diabetes, obesity and chronic kidney diseases. The most common form of human hypertension is neurogenic hypertension – hypertension associated with sympathetic overdrive (Esler, 2010). It is now well established that increased sympathetic nerve activity (SNA) contributes to the development of hypertension (Tsioufis *et al.*, 2011), as well as a plethora of pathophysiological consequences independent of raised blood pressure, such as myocardial hypertrophy and vascular remodelling. Sympathetic overactivity is associated with augmented neuronal activity in premotor nuclei including the RVLM (Kumagai *et al.*, 2012) and PVN (Li *et al.*, 2003; Takeda *et al.*, 1991). The aetiology of this augmented neuronal activity in premotor nuclei is incompletely understood. However, accumulating evidence suggests the involvement of pathological changes within premotor nuclei, such as the RVLM (Kishi *et al.*, 2004; Nishihara *et al.*, 2012; Oliveira-Sales *et al.*, 2010) and PVN (Allen, 2002; Li *et al.*, 2003; Takeda *et al.*, 1991). The importance of the RVLM and PVN in cardiovascular regulation, and their potential involvement in the pathogenesis of cardiovascular diseases are outlined below.

1.2.1 The rostral ventrolateral medulla

Role of the rostral ventrolateral medulla in cardiovascular regulation

The pre-sympathetic neurons in the RVLM appear to play a pivotal role in the tonic and reflex control of sympathetic vasomotor activity, such that bilateral inhibition of neurons in the RVLM results in a dramatic decrease in both arterial pressure and sympathetic vasomotor activity (Dampney, 1994; Guyenet, 2006). The RVLM has a key role in regulating SNA. It integrates central and peripheral signals, for appropriate adjustment of sympathetic nerve output. The arterial baroreflex is an example of a peripheral signal integrated by the RVLM, such that sudden elevation of blood pressure activates arterial baroreceptors which stimulate a neuronal pathway to suppress RVLM activity (Pilowsky *et al.*, 2002). SNA is thus reduced, restoring blood pressure. The RVLM also mediates sympathoexcitatory reflexes, such as the chemoreflex (Koshiya *et al.*, 1996) and the somatic pressor reflex (Kiely *et al.*, 1994). Central inputs from other autonomic-related nuclei, such as the PVN (Badoer, 2001), dorsolateral periaqueductal grey (Lovick, 1993) and midline raphe nuclei (Bago *et al.*, 2001), also influence the tonic activity of the RVLM.

Involvement of the rostral ventrolateral medulla in cardiovascular disease

Mounting evidence indicates that within the RVLM, elevation of the renin-angiotensin system, as well as oxidative stress, contribute to several cardiovascular pathologies including spontaneous hypertension, heart failure and renovascular hypertension (Campos *et al.*, 2011). The RVLM of spontaneously hypertensive rats (SHR) have an exaggerated response to stimulation with L-glutamate (Tsuchihashi *et al.*, 1998), implicating the RVLM in the pathogenesis of hypertension. This anomaly is partly normalised by oral treatment with an angiotensin II type 1 (AT_1) receptor antagonist (Lin *et al.*, 2005). Nicotinamide adenine dinucleotide phosphate (NADPH) oxidase, a major source of central reactive oxygen species (ROS), is upregulated by activation of AT_1 receptors (Peterson *et al.*, 2006). The resultant oxidative stress in the RVLM contributes to spontaneous hypertension, since microinjection of a superoxide dismutase (SOD) mimetic into the RVLM, or over-expression of the SOD producing gene in the RVLM suppressed sympathetic neurogenic vasomotor tone in SHR, but not Wistar Kyoto (WKY) rats (Nishihara *et al.*, 2012; Tai *et al.*, 2005).

Oxidative stress in the RVLM has also been shown to contribute to heart failure and renovascular hypertension. ROS scavengers microinjected into the RVLM attenuated the cardiac sympathetic afferent reflex in rats (Zhong *et al.*, 2009), a reflex which contributes to the enhanced sympathetic activity observed in congestive heart failure (CHF) (Zucker *et al.*, 2004). In 2 kidney-1 clip rats, a model of renovascular hypertension, over-expression of SOD in the RVLM using an adenoviral vector normalised RVLM superoxide levels and completely reversed hypertension (Oliveira-Sales *et al.*, 2009). The RVLM is evidently a key region for the development of pathological sequelae in cardiovascular disease, and therefore a potential target for the development of novel therapeutics.

1.2.2 The Paraventricular nucleus of the hypothalamus

Role of the paraventricular nucleus in cardiovascular regulation

Interest in the PVN was sparked by the observation that it has spinally projecting neurons, allowing it to influence SNA and thus the cardiovascular system (Swanson *et al.*, 1983) (Badoer, 2001) (figure 1.2, p.23). PVN neurons also project to several sites known to influence SNA such as the RVLM, the raphe nuclei and parabrachial nucleus (Coote *et al.*, 1998; Shafton *et al.*, 1998).

The PVN plays an important role in the regulation of the cardiovascular system, since activation of the PVN, either electrically or using excitatory neurotransmitters, produces changes in blood pressure and sympathetic nerve activity, which vary from increases to decreases (Kannan *et al.*, 1989; Kannan *et al.*, 1987). The effect of PVN stimulation is probably dependent on the precise location within the PVN which is stimulated (Deering *et al.*, 2000). The PVN plays a critical role in the regulation of physiological cardiovascular reflex functions. For example, neuronal projections from the parvocellular PVN mediate baroreflex regulation of lumbar sympathetic nerve activity (LSNA) (Patel *et al.*, 1988) and contribute to reflex reduction in sympathetic nerve activity (Ng *et al.*, 2004) and renal vasorelaxation (Chen *et al.*, 2011; Lovick *et al.*, 1993) in response to an acute volume load. Secretion of oxytocin and vasopressin from PVN magnocellular neurons is also involved in blood volume control (Petersson, 2002; Poulain *et al.*, 1982). These important cardiovascular regulatory functions have led to research into the involvement of the PVN in cardiovascular pathophysiology.

Involvement of the paraventricular nucleus in cardiovascular disease

Abnormal functioning of the PVN appears to be involved the sympathetic overactivity which occurs in certain cardiovascular diseases, including CHF, arterial hypertension and myocardial ischaemia (Malliani *et al.*, 2002) (Li *et al.*, 2003). Notably, electrolytic lesions in the PVN prevented the development of hypertension (Takeda *et al.*, 1991), and LSNA and blood pressure were dramatically reduced by inhibition of the PVN in SHR rats (Allen, 2002). One of the major complications of heart failure, excess sympathoexcitation, is associated with increased sympathetic drive from the PVN (Li *et al.*, 2003; Patel *et al.*, 2012; Xu *et al.*, 2012). Changes within the PVN such as up-regulation of pro-inflammatory cytokines (Kang *et al.*, 2009) and neuronal nitric oxide synthase (nNOS) down-regulation (Zheng *et al.*, 2011) associated with diminished GABA sensitivity of PVN neurons (Patel, 2000), contribute to increased sympathetic drive. ROS generation in the PVN also appears to play an important role in CHF-induced enhanced sympathetic drive, since PVN superoxide scavengers almost abolished CHF sympathetic overdrive (Han *et al.*, 2007). In aldosterone/salt-induced hypertension, gene silencing of NADPH oxidase isoforms 2 and 4 using siRNA injections into the PVN significantly attenuated hypertension, implicating involvement of NADPH oxidase generated ROS (Xue *et al.*, 2012).

1.2.3 Possible involvement of H_2S in cardiovascular regulation by the brain

H_2S has been shown to perform several neuromodulatory roles, including facilitation of long term potentiation (Abe *et al.*, 1996), induction of calcium waves in astrocytes (Nagai *et al.*, 2004) and regulation of release of corticotrophin releasing hormone from the hypothalamus (Dello Russo *et al.*, 2000). Peripherally, H_2S has several cardiovascular effects, including vasorelaxation (Zhao *et al.*, 2001) and protection against cardiac ischaemia reperfusion injury (Calvert *et al.*, 2009). It has been proposed that H_2S may regulate resting blood pressure, since CSE knockout mice had elevated blood pressure in one study (Yang *et al.*, 2008), although a more recent study showed no effect of CSE knockout on blood pressure (Ishii *et*

al., 2010). Given its neuromodulatory effects and peripheral cardiovascular effects, the question arises as to whether or not H_2S may function as a central cardiovascular regulator.

Indeed, there is limited evidence that H_2S may be important in cardiovascular regulation via the brain. For example, a 60 minute infusion of NaHS (0.4 μmol) into the lateral cerebral ventricle resulted in an increase in blood pressure (Ufnal *et al.*, 2008). Conversely, a rapid cerebroventricular infusion of higher amounts of NaHS (3-303 μmol over 30 seconds) resulted in significant decreases in blood pressure and heart rate (Liu *et al.*, 2011a). Another study focused specifically on the posterior hypothalamus (PH) (Dawe *et al.*, 2008). Microinjection of NaHS into the PH slightly reduced blood pressure (by approximately 5mmHg), and the CBS inhibitors, AOA and HA, both slightly increased blood pressure (Dawe *et al.*, 2008). The nucleus tractus solitarius (NTS) is an integratory site for visceral afferents such as baroreceptor and chemoreceptor fibres (Austgen *et al.*, 2011). Administration of NaHS to brain stem slices augmented pre-synaptic transmission in the NTS, whereas AOA depressed synaptic activity (Austgen *et al.*, 2011). In a recent study, microinjection of NaHS into the RVLM induced reductions in LSNA, blood pressure and heart rate, while AOA induced elevations of these parameters (Guo *et al.*, 2011). However, at the time of this study, the role of H_2S in cardiovascular regulation via the RVLM or PVN, regions with profound influences on cardiovascular regulation (see above 1.2.1, p.24 and 1.2.2, p.26), had not been investigated.

1.3 Middle cerebral artery tone

The brain has a minimal storage of energy sources, and thus relies on a steady delivery of adequate oxygen and glucose via blood flow through cerebral vessels. Interruption of blood flow to the brain can result in irreversible neuronal damage within minutes (Pagnussat *et al.*, 2007). The regulation of cerebrovascular tone is crucial for maintaining appropriate blood flow to the brain.

1.3.1 Function of the middle cerebral artery

The middle cerebral artery (MCA) is the largest cerebral artery and arises from a trifurcation of the internal carotid artery (figure 1.3). It supplies most of the temporal lobe, anterolateral frontal lobe (and the majority of the primary motor cortex), parietal lobe (and the majority of the somatosensory cortex), nearly all of the basal ganglia, and the posterior and anterior internal capsules. In contrast to the peripheral vasculature, large cerebral arteries, such as the MCA, are important contributors to cerebral vascular resistance (Faraci *et al.*, 1990). Thus, the tone of the MCA is an important determinant of overall cerebral blood flow. Aberrant MCA tone can be involved in the pathophysiology of certain conditions, such as Alzheimer's disease and stroke.

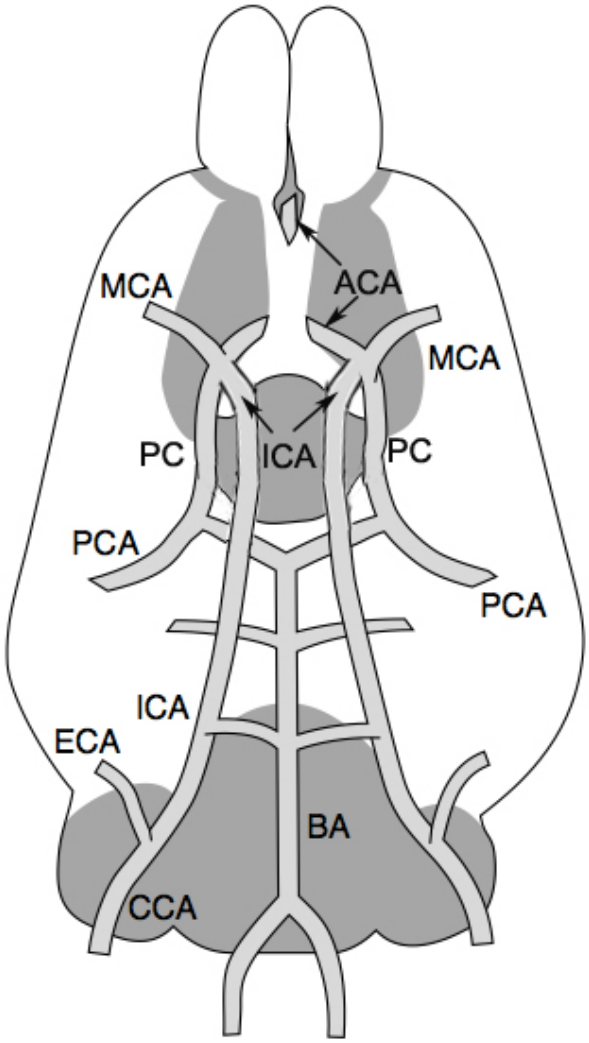

Figure 1.3 Diagram illustrating position of middle cerebral artery

Ventral view of a rat brain showing the position of the middle cerebral artery, among other major cerebral arteries. The trifurcation of the internal carotid artery into middle cerebral artery, posterior communicating artery and anterior cerebral artery is also demonstrated. The circle of Willis is also pictured – a circle of arteries formed by the junction of the posterior communicating arteries, posterior cerebral arteries and anterior cerebral arteries. MCA, middle cerebral artery; ACA, anterior cerebral artery; ICA, internal carotid artery; PC, posterior communicating artery; PCA, posterior cerebral artery; ECA, external carotid artery; BA, basilar artery; CCA, common carotid artery. Adapted from (O'Neill *et al.*, 2001).

1.3.2 Implications of middle cerebral artery tone in pathophysiology of disease

Alzheimer's Disease

Although the traditional hypothesis for the pathophysiology of Alzheimer's disease involves the accumulation of β-amyloid resulting in neuronal dysfunction (Kelley *et al.*, 2007), accumulating evidence suggests that cerebral vasculopathy plays an additional role (Iadecola, 2004). Notably, Alzheimer's disease patients have an increased incidence of ischaemic brain lesions and atherosclerosis of cerebral vessels (Roher *et al.*, 2003; Skoog *et al.*, 2006). Several lines of evidence from animal models suggest that β-amyloid may be involved in the genesis of this vasculopathy, for example, β-amyloid attenuates endothelium dependent responses (Iadecola *et al.*, 1999) and impairs cerebrovascular autoregulation (Niwa *et al.*, 2002). It is well established that hypertension disrupts cerebrovascular tone regulation and causes atherosclerosis (Iadecola *et al.*, 2008). A growing body of evidence suggests that these hypertension-induced changes increase susceptibility to Alzheimer's disease (Iadecola *et al.*, 2008).

Haemorrhagic stroke

After a subarachnoid haemorrhage, cerebral vasospasm occurs in vessels including the MCA (Kasprowicz *et al.*, 2012). This vasoconstriction contributes to delayed ischaemic neurological deficits and increases the risk of ischaemic stroke (Qi *et al.*, 2011). During the acute phase (1-5 days) after a haemorrhagic stroke, there is also an impairment of cerebral autoregulation, or the ability of cerebral vessels to respond to changes in transmural pressure (Diedler *et al.*, 2009). Since cerebral autoregulation normally protects the brain from fluctuations in perfusion, this impairment results in an increased risk of subsequent cerebrovascular events, such as haemorrhage or ischaemia. Also during the acute phase after subarachnoid haemorrhage, upregulation of receptors for vasoconstrictor substances, such as endothelin and serotonin, has been observed (Edvinsson *et al.*, 2011), yielding dramatic changes in the contractility of vessels, and compounding increased risk of subsequent cerebrovascular events.

Ischaemic stroke

After ischaemic stroke, progressive damage to cerebral vessels occurs (Fagan *et al.*, 2004). In the acute phase (hours post stroke) myogenic reactivity of the MCA is decreased (Cipolla *et al.*, 1997), and endothelium dependent responses are abolished due to enhanced ROS production (Kontos, 2001). In the chronic phase (days to months post stroke) atherosclerosis occurs as a result of enhanced production of apoptotic and angiogenic factors in endothelial cells (Fagan *et al.*, 2004). Both acute and chronic effects may decrease brain tissue perfusion, causing further damage to the compromised, but salvageable, penumbra and increasing the risk of secondary stroke.

A great number of neuroprotective agents have been trialled for protection against post-stroke neuronal cell death, without success (O'Collins *et al.*, 2006). Due to the anomalous cerebrovascular tone regulation post ischaemic and haemorrhagic stroke (Cipolla *et al.*, 1997) ((Kontos, 2001), there is increasing focus on the development of therapeutics which target vascular mechanisms (Moskowitz *et al.*, 2010).

Thrombotic stroke

Inappropriate MCA tone may increase the risk of thrombotic stroke by reducing blood flow. Although thrombotic strokes often occur in smaller, penetrating arteries (Cho *et al.*, 2007), they may also occur in MCA (Yoo *et al.*, 1998). Reduced blood flow enhances the risk of clot formation in diseased cerebral vessels. For example, sleep apnoea has been demonstrated to reduce blood flow in the MCA and may be responsible for the increased risk of stroke observed in these patients (Franklin, 2002; Netzer *et al.*, 1998).

The maintenance of physiological tone of the MCA is crucial to maintain appropriate cerebral blood flow, and failure can result in severe pathological sequelae. Understanding the intricate mechanisms in place to regulate tone may allow for the development of therapeutic tools.

1.3.3 Control of middle cerebral artery tone

There are marked differences between peripheral and cerebral artery tone regulation, notably since cerebral arteries must maintain adequate blood flow to the brain over a wide range of systemic pressure and internal demands. In order to achieve a relatively constant blood flow, cerebral vessels respond to changes in perfusion pressure with a profound change in resistance (Faraci *et al.*, 1998). Myogenic tone, whereby vessels constrict upon increased perfusion pressure, plays a particularly important role in cerebral blood flow autoregulation.

This section reviews the influence of several relevant factors and their influence on cerebrovascular tone: ion channels, bicarbonate exchange, endothelial derived factors and ROS.

Ion channels

Ion channels play a crucial role in the regulation of vascular smooth muscle (VSM) tone by regulating intracellular calcium concentration via effects on membrane potential. VSM cells express a variety of calcium, potassium, chloride and stretch-activated cation channels (Jackson, 2000). The major channels which were investigated for their involvement in the H_2S-induced response in the present thesis were potassium and calcium channels, because previous studies suggested that these are the most likely targets. Therefore, the role of potassium and calcium ion channels in VSM is outlined below, with reference to their influence on cerebrovascular tone.

Potassium Channels: Opening of potassium channels hyperpolarises the cell membrane through efflux of potassium ions, thus causing closure of voltage gated calcium channels (VGCC) and leading to vasorelaxation (Brayden, 2002) (figure 1.4, p.44). The activity of potassium channels on smooth muscle membranes is a major determinant of vascular tone, since the change in activity of only a few K^+ channels can alter membrane potential significantly, and affect vascular tone (Nelson *et al*., 1995b).

Adenosine triphosphate-sensitive potassium channels (K_{ATP}) play an important role in regulating resting membrane potential of VSM, such that blockade of K_{ATP} causes depolarisation of VSM and subsequent increased tone (Nakashima *et al*., 1995; Nelson *et al*., 1990). K_{ATP} contain two distinct types of protein subunits, the inwardly rectifying potassium channel subunits (of which there are two isoforms $K_{IR}6.1$ or $K_{IR}6.2$) and the sulphonylurea receptor (SUR, of which multiple isoforms exist: SUR1, SUR2A, SUR2B) (Brayden, 2002). In cerebral vessels, K_{ATP} channel subunits $K_{IR}6.1$ and SUR2B are prominently expressed on smooth muscle cells (Adebiyi *et al*., 2011; Ploug *et al*., 2006) and opening of K_{ATP} induces pharmacological relaxation associated with hyperpolarisation (Faraci *et al*., 1998).

K_{ATP} are coupled to cellular metabolic activity, such that a decrease in the ratio of intracellular adenosine triphosphate (ATP) to adenosine diphosphate concentration results in channel opening, and thus vasorelaxation. This is suggestive of a mechanism to allow blood vessels to respond directly to inadequate oxygenation. Indeed, blockade of K_{ATP} has been shown to inhibit hypoxic vasorelaxation in both peripheral and cerebral vessels (Liu *et al.*, 1998; Reid *et al.*, 1993), although the role of K_{ATP} in hypoxic vasorelaxation remains controversial (Adebiyi *et al.*, 2011). Studies in VSM suggest that nucleoside concentration may not be the most important determinant of K_{ATP} opening or closure, and the ATP

concentration may serve only to set a low background open probability, while other factors, such as sulfhydration or phosphorylation, may be more likely to cause K_{ATP} opening (Quayle *et al.*, 1997; Zhang *et al.*, 2010). Notably, it has been demonstrated that H_2S sulfhydrates K_{ATP} *in vitro*, which reduces ATP binding to the $K_{IR}6.1$ subunit, thus enhancing K_{ATP} open probability (Mustafa *et al.*, 2011).

Inwardly rectifying potassium channels (K_{IR}) are channels which allow K^+ to pass more readily into a cell than out (Quayle *et al.*, 1993). These channels are present in a diverse range of arteries and arterioles, including the rat middle cerebral artery (Johnson *et al.*, 1998), and play a role in vasorelaxation induced by increased extracellular K^+ (Quayle *et al.*, 1993). Since neuronal activity stimulates K^+ release, these channels play an important role in coupling neuronal function to cerebral blood flow in rats (Filosa *et al.*, 2006). The observation that barium chloride (BaCl), a K_{IR} channel blocker, induces a dose dependent constriction of rat MCA (Johnson *et al.*, 1998) indicates that these channels are also important in regulation of resting cerebrovascular tone.

Three types of calcium-activated potassium channels (K_{Ca}) are present in cerebral vessels in various species: large, intermediate and small conductance (BK_{Ca}, IK_{Ca} and SK_{Ca}, respectively). BK_{Ca} form an integral part of the response to 'calcium sparks'- local, intracellular calcium transients caused by the release of Ca^{2+} from a cluster of ryanodine-sensitive calcium channels on the sarcoplasmic reticulum (Jaggar *et al.*, 2000). Calcium sparks are initiated by the entry of calcium through voltage gated calcium channels, and the resultant Ca^{2+} release from the sarcoplasmic reticulum activates BK_{Ca} causing hyperpolarisation and thus vasorelaxation (Nelson *et al.*, 1995a). Blockade of BK_{Ca} results in vasoconstriction of large cerebral arteries, demonstrating their critical role in the regulation of

normal cerebrovascular tone (Nelson *et al.*, 1995a). There is no evidence that BK_{Ca} are expressed in endothelial cells in intact vessels, except in some pathological states (Hughes *et al.*, 2010). IK_{Ca} and SK_{Ca} are present in rat cerebrovascular endothelial cells, and are involved in the activity of EDHF (Zygmunt *et al.*, 1996).

Voltage-gated potassium channels (K_V) open in response to depolarisation, and they are thus suggested to provide an important negative feed-back to arterial constriction (Nelson *et al.*, 1995b). K_V channels are a highly diverse family of potassium channels, composed of 4 pore-forming subunits, which arise from at least 11 different gene families (K_V1- K_V11), each composed of several different members (Coetzee *et al.*, 1999; Ottschytsch *et al.*, 2002). Inhibitors of K_V cause cerebral artery constriction, indicating that K_V are involved in maintenance of cerebral artery tone (Knot *et al.*, 1995; Zhong *et al.*, 2010).

Voltage gated calcium channels: VGCC open in response to depolarisation, or close in response to hyperpolarisation of the cell membrane, thus regulating entry of extracellular calcium, and vascular tone. There are 10 molecular sub-types of VGCC, which are assigned into three groups (Ca_V1, 2 and 3). Ca_V1 (1.1-1.4) are all L-type channels, $Ca_V2.1$ are P/Q, $Ca_V2.2$ are N and $Ca_V2.3$ are R and all Ca_V3 (3.1-3.3) are T-type channels (Kuo *et al.*, 2011). Of these channel subtypes, L-type calcium channels play a dominant role in the maintenance of VSM tone (Moosmang *et al.*, 2003), and overactivity of L-type calcium channels is associated with hypertension (Pesic *et al.*, 2004) and cerebrovascular disease (Koide *et al.*, 2011). Pharmacological as well as histological evidence also point to a role for T-type calcium channels in the maintenance of cerebrovascular (Kuo *et al.*, 2011; Lam *et al.*, 1998; Navarro-Gonzalez *et al.*, 2009) and peripheral vascular tone (Cribbs, 2001), although this remains controversial (Kuo *et al.*, 2011). P/Q, N and R type channels are largely confined to neurons (Catterall *et al.*, 2005) and it is not known if these channels play a role in the maintenance of cerebrovascular tone.

VSM tone is regulated by a large array of dilating and constricting substances, but the vast majority of these elicit their vasoactivity through a change in smooth muscle intracellular calcium concentration ($[Ca^{2+}]_i$) (Nelson *et al.*, 1990). VGCC are important in regulating $[Ca^{2+}]_i$ via changes in membrane potential (figure 1.4, p.44). However, voltage-independent regulation of $[Ca^{2+}]_i$ also occurs, via release of calcium from internal stores (Kuo *et al.*, 2011). The contribution of each mechanism to vascular tone in peripheral vessels varies according to vessel type, with conduit arteries depending more on calcium release from internal stores, and resistance vessels depending more on VGCC (van Breemen *et al.*, 1989). In the middle cerebral artery, both mechanisms play an important role, although their relative contribution depends on species and age (Long *et al.*, 2000; Skarby *et al.*, 1985).

Bicarbonate exchange

The major transport mechanisms that regulate intracellular pH (pH_i) in smooth muscle cells are: Cl^-/HCO_3^- exchange (which functions to acidify the cell), Na^+/H^+ exchange and Na^+ dependent Cl^-/HCO_3^- (which both function to alkalinise the cell) (Madden *et al.*, 2001). Maintenance of physiological pH_i is crucial to the function of VSM, since enzymes are pH sensitive, and modification of pH_i may disrupt the activity of a vast array of enzymes and ion channels (Schulz *et al.*, 2011). For example, reduced pH_i in endothelial cells disrupts endothelial nitric oxide synthase (eNOS) activity, thereby reducing NO bioavailability (Boedtkjer *et al.*, 2011). In smooth muscle cells, decreased pH_i reduces opening probability of BK_{Ca} (Schubert *et al.*, 2001) and L-type calcium channels (Klockner *et al.*, 1994) (figure 1.4, p.44), as well as reducing the sensitivity of the contractile machinery to calcium (Gardner *et al.*, 1988; Peng *et al.*, 1998). The overall effect of altered pH_i on vascular tone depends on the vessel type, as well as the degree of tone present (Wray *et al.*, 2004), although generally, decreased pH_i causes vasorelaxation, while increased pH_i causes vasoconstriction (Aalkjaer *et al.*, 1997).

Bicarbonate exchange is important in recovery from acid or base challenge, as demonstrated by experiments using 4,4'-diisothio-cyanostilbene-2,2'-disulfonicacid (DIDS), a general inhibitor of bicarbonate exchangers (Parks *et al.*, 2009), although DIDS is recognised to have other actions (see section 1.3.4 Proposed mechanisms of H_2S-induced vasorelaxation, bicarbonate exchange, p.48). DIDS inhibits recovery from an acute acid (Carr *et al.*, 1995) as well as base (Aickin, 1988) load in smooth muscle cells. The influence of acid handling within cells of the cerebral vasculature is particularly important, since cerebral artery tone is acutely sensitive to plasma or extracellar pH via pCO_2 (Brian *et al.*, 1996). Evidence suggests that Na^+ dependent Cl^-/HCO_3^- exchange is involved in the recovery of cerebral microvascular endothelium from an acid load (Hsu *et al.*, 1996). There is also evidence that bicarbonate

exchange may be important in myogenic tone development, since DIDS and a bicarbonate free medium both inhibited myogenic tone in rabbit posterior cerebral artery (Henrion *et al.*, 1994).

The endothelium

The endothelium produces and releases potent relaxing and constricting factors that regulate the tone of underlying VSM. Three of the most influential endothelial derived vasoactive factors are NO, prostacyclin (PGI_2) and endothelium derived hyperpolarising factor (EDHF). The influence of NO, PGI_2 and EDHF on cerebrovascular tone are discussed below.

Nitric Oxide: The vasoactivity of endothelium derived relaxing factor (EDRF) has been attributed to NO (Palmer *et al.*, 1987). NO is produced via a family of isoenzymes known as nitric oxide synthases (NOS). Named according to the cell type in which they were initially discovered, NOS isoenzymes include endothelial NOS (eNOS), neuronal NOS (nNOS) and inducible NOS (iNOS, initially discovered in macrophages). Like H_2S, NO is a small, gaseous molecule, and therefore, once produced in endothelial cells, NO freely diffuses to the adjacent smooth muscle cells. NO induces relaxation via stimulation of soluble guanylate cyclase (sGC), resulting in an increase in intracellular cyclic guanosine monophosphate (cGMP) concentration (figure 1.4, p.44), and this activates protein kinase G (Schmidt *et al.*, 1994), which activates myosin light-chain phosphatase increasing the dephosphorylation of myosin regulatory light chain (Surks, 2007). In MCA, two isoforms of NOS, eNOS and nNOS are constitutively expressed (Briones *et al.*, 2002) and NO produces potent vasorelaxation of cerebral vessels (Salom *et al.*, 1999; Salom *et al.*, 1998). It has been demonstrated that NO influences cerebrovascular tone under basal conditions, and plays a crucial role in the regulation of cerebral blood flow (Faraci, 1993; Toda *et al.*, 2009).

Prostacyclin: Prostacyclin (PGI_2) belongs to the family of prostanoids, bioactive lipid mediators formed from arachadonic acid via cyclooxygenase (COX). Arachadonic acid is formed mainly from cell membrane phospholipids by the action of phospholipase A_2 (Bogatcheva *et al.*, 2005). COX converts arachadonic acid to prostaglandin H_2, the precursor to prostanoids, which is then converted to PGI_2 via prostacyclin synthase. Arachadonic acid may also be acted on by either lipoxygenases, or cytochrome P450 monooxygenases to produce vasoactive arachodonic acid metabolites (Bogatcheva *et al.*, 2005). PGI_2 is the major product of COX in endothelial cells (Moncada *et al.*, 1976). The actions of PGI_2 are mediated mainly by its action on two receptor types: the cell surface prostacyclin receptor (IP), and the intracellular peroxisome proliferator-activated receptor β/δ (Mitchell *et al.*, 2008). IP receptors are present on smooth muscle cells and their activation by PGI_2 increases 3′-5′-cyclic adenosine monophosphate (cAMP) formation resulting in vasorelaxation via cAMP-dependent protein kinase A activation (figure 1.4, p.44)(Stitham *et al.*, 2007). In MCA, COX and prostacyclin synthase expression (Ospina *et al.*, 2002) as well as IP receptor expression, have been demonstrated and IP receptor activation induces vasorelaxation (Myren *et al.*, 2011). PGI_2 plays an important role in cerebral vessel endothelium-mediated responses in neonates, although this role declines with maturation, such that in adulthood, PGI_2 plays only a minor role, with responses mainly mediated by NO and EDHF (Zuckerman *et al.*, 1996).

Endothelium derived hyperpolarising factor (EDHF): After inhibition of production of NO and PGI_2, a residual endothelium dependent relaxation exists, that is concurrent with VSM cell hyperpolarisation and activation of K^+ channels (Feletou *et al.*, 1988; Komori *et al.*, 1988). This hyperpolarisation was initially attributed to a single entity, termed EDHF. However, more than 20 years of research have demonstrated that the EDHF response is attributable to multiple signaling pathways between endothelial cells and VSM, only some of which involve the release of factors (Edwards *et al.*, 2010). All EDHF pathways are

dependent on an initial increase in endothelial intracellular calcium (Fukao *et al.*, 1995). The ensuing pathways causing VSM depolarisation can be divided into two broad categories. The 'classical' pathway involves subsequent activation of endothelial SK_{Ca} and IK_{Ca}, resulting in endothelial cell hyperpolarisation (Zygmunt *et al.*, 1996) (figure 1.4, p.44). But exactly how endothelial cell hyperpolarisation causes smooth muscle cell hyperpolarisation remains a topic of debate. Mounting evidence implicates involvement of myoendothelial gap junctions in EDHF mediated relaxations in both peripheral and cerebral vessels (Ujiie *et al.*, 2003; Xu *et al.*, 2002) (figure 1.4, p.44). There are also various lines of evidence that K^+ escaping from endothelial cell K_{Ca} can hyperpolarise VSM via activation of Na^+/K^+-ATPases and/or K_{IR} channels (Edwards *et al.*, 2010). The other EDHF pathway does not involve endothelial cell hyperpolarisation. Instead, diffusible factors may be released from the endothelium upon increased intracellular calcium, causing activation of BK_{Ca} and K_{ATP} channels on VSM (Edwards *et al.*, 2010) (figure 1.4 p.44). Candidates for diffusible factors released via this second pathway include NO, nitroxyl anions, PGI_2, epoxyeicosatrienoic acids, hydrogen peroxide, C-naturetic peptide (Luksha *et al.*, 2009) and H_2S (Mustafa *et al.*, 2011; Yang *et al.*, 2008).

The contribution of EDHF to endothelium dependent relaxation varies depending on the vessel type, generally increasing as the vessel size decreases (Tomioka *et al.*, 1999). Evidence suggests that this is also the case in cerebral vessels, whereby EDHF mediated the majority of endothelium induced vasorelaxation in rat MCA branches, but nitric oxide was the dominant mediator of the response in MCAs (You *et al.*, 1999).

Reactive oxygen species

ROS can be divided into free radicals, such as superoxide ($O_2^{\cdot-}$) and hydroxyl ($OH^{\cdot}$); non-radicals, such as hydrogen peroxide (H_2O_2); and reactive nitrogen species, such as NO (technically, $NO^{\cdot}$, since it is a radical gas, with an unpaired electron) and peroxynitrite ($ONOO^-$). In vascular cells, there are multiple sources for the generation of ROS, including mitochondria, cyclooxygenases and NADPH oxidases, indicating a physiological importance for ROS (Faraci, 2006). Indeed, ROS are generated at low levels in cerebral vessels (Miller *et al.*, 2005) and are essential for normal vascular cell physiology, having multiple functions, including regulation of tone. $O_2^{\cdot-}$ and H_2O_2 were examined for their possible involvement in H_2S-induced vasorelaxation of MCA in the present research project, since $O_2^{\cdot-}$ is the parent ROS molecule, and H_2O_2 is regarded a particularly important ROS molecule in regulation of vascular function, due to its stability and ability to diffuse across membranes (Miller *et al.*, 2006).

$O_2^{\cdot-}$ is formed from molecular oxygen via oxidases and is a precursor for H_2O_2 formation (via SOD), as well as reactive nitrogen species (Miller *et al.*, 2006). Due to its poor membrane permeability and short half-life, $O_2^{\cdot-}$ itself is unlikely to play an important role in regulation of VSM tone under physiological conditions (Miller *et al.*, 2006), although pathologically increased production may alter this. In the cerebral vasculature, $O_2^{\cdot-}$ generation from NADPH or nicotinamide adenine dinucleotide (NADH) causes relaxation of rabbit and mouse cerebral arteries at low substrate concentrations (Didion *et al.*, 2002a; Park *et al.*, 2004), which is blocked by tetraethylammonium, indicating involvement of K^+ channels (Didion *et al.*, 2002a). Conversely, at higher substrate concentrations constriction of rabbit cerebral arteries was observed (Didion *et al.*, 2002a). In peripheral vessels, vasoconstriction by $O_2^{\cdot-}$ is thought to be due to the rapid reaction of $O_2^{\cdot-}$ with NO and subsequent loss of vasodilator influence of NO. Evidence in cerebral vessels also indicates that $O_2^{\cdot-}$ induced constriction occurs via decreasing basal vasodilator effects of NO (Demchenko *et al.*, 2002).

Exogenous and endogenous H_2O_2 have been demonstrated to produce vasorelaxation of cerebral vessels (Wei *et al.*, 1996; Yang *et al.*, 1998). H_2O_2-induced relaxation of cerebral vessels has been variably attributed to endothelium-dependent (Yang *et al.*, 1998) and -independent (Fraile *et al.*, 1994) mechanisms; opening of K_{Ca} (Sobey *et al.*, 1997), and opening of K_{ATP} (Wei *et al.*, 1996).

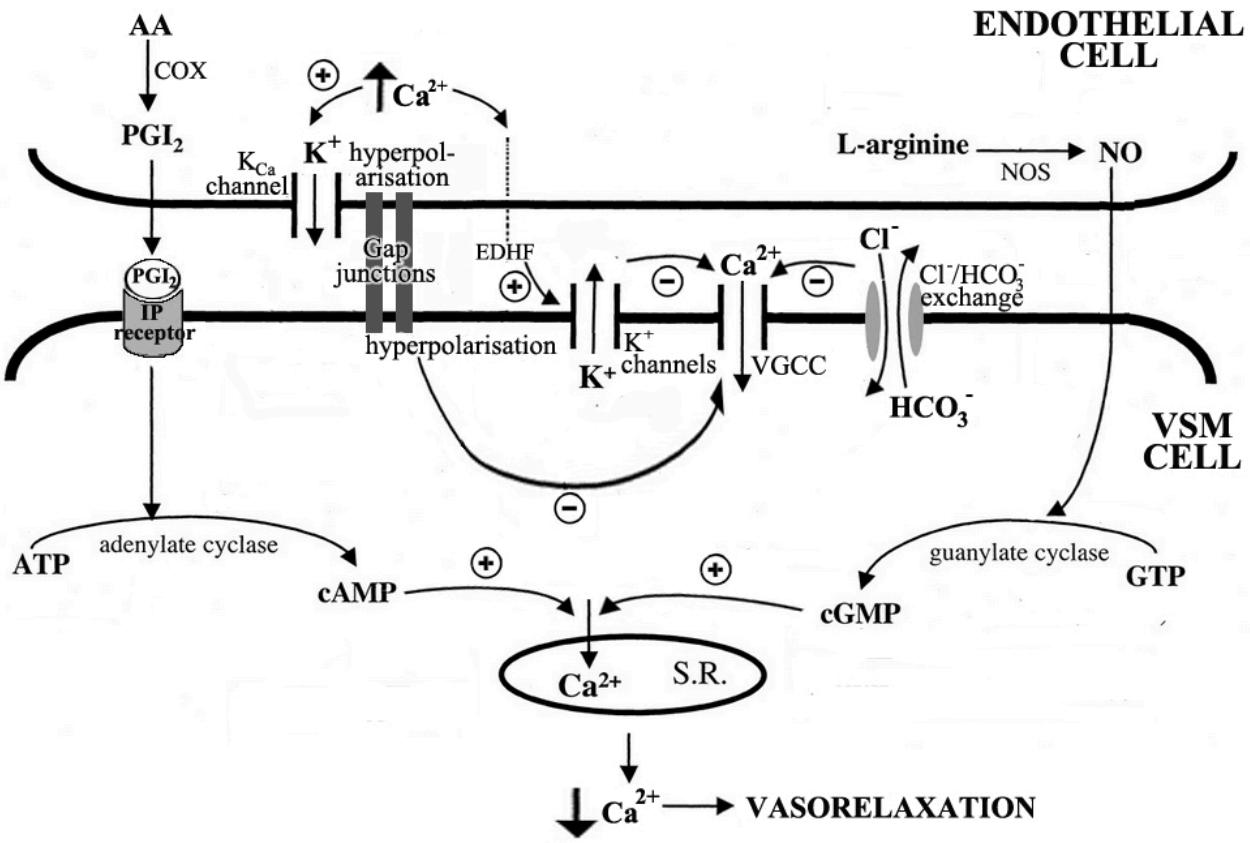

Figure 1.4 Diagram illustrating mechanisms contributing to vasorelaxation of smooth muscle cells

In VSM, hyperpolarisation causes closure of VGCC, decreasing intracellular Ca^{2+} and eliciting vasorelaxation. Various mechanisms lead to hyperpolarisation of VSM, including efflux of K^+ through VSM K^+ channels and EDHF. The EDHF pathway consists of an initial increase in intracellular calcium in endothelial cells which causes VSM hyperpolarisation via various pathways, including transfer of hyperpolarisation via gap junctions, or release of diffusible factors from endothelium which activate BK_{Ca} and K_{ATP} channels on VSM. NO and PGI_2, are produced in endothelial cells before diffusing to adjacent smooth muscle cells to increase cGMP and cAMP levels, respectively, thus causing vasorelaxation. Activation of Cl^-/HCO_3^- exchange on VSM causes intracellular acidification, which reduces the open probability of VGCC, causing vasorelaxation. VSM, vascular smooth muscle; VGCC, voltage-gate calcium channels; EDHF, endothelial derived hyperpolarising factor; NO, nitric oxide; PGI_2, prostacyclin; NOS, nitric oxide synthase; COX, cyclo-oxygenase; cAMP, cyclic adenosine monophosphate; cGMP, cyclic guanosine monophosphate; GTP, guanosine triphosphate; ATP, adenosine triphosphate.

1.3.4 Proposed mechanisms of H_2S-induced vasorelaxation

Paucity of data in cerebral vessels

Apart from the present research, there are only three recent studies that have investigated the mechanism of H_2S-induced vasorelaxation of cerebral vessels. The latest study demonstrated that H_2S increased the frequency of Ca^{2+} sparks in piglet cerebral arteriole smooth muscle cells, causing an increase in the frequency of transient K_{Ca} current, and thus vasorelaxation (Liang *et al.*, 2012). In an *in vivo* study, using piglet pial arterioles (50 μm diameter), the vasorelaxation response to a H_2S solution was found to be entirely mediated by K_{ATP} channels (Leffler *et al.*, 2010). In another study, using piglet cerebral arterioles (200μm diameter) *in vitro*, only 55% of the vasorelaxation could be attributed to K_{ATP} channels (Liang *et al.*, 2011). Additionally, the latter study showed that the Na_2S (a H_2S donor) mediated vasorelaxation of cerebral vessels of SUR2 (a K_{ATP} subunit) knockout mice was only 50% of the wild type mice (Liang *et al.*, 2011). Thus, K_{ATP} channels play a variable role in the H_2S-induced vasorelaxation of cerebral vessels. The mechanism of H_2S-induced vasorelaxation of cerebral vessels is incompletely understood, and contributing mechanisms other than K_{ATP} and K_{Ca} channels have not been investigated. In contrast, numerous studies have investigated H_2S function in peripheral vessels.

Proposed mechanisms of H_2S-induced vasorelaxation in peripheral vessels

Evidence on the contribution of various mechanisms to the H_2S-induced relaxation of peripheral vessels is reviewed below.

Ion channels

Ion channels which have been shown to be involved in the H_2S-induced vasorelaxation of peripheral vessels include: potassium channels, specifically K_{ATP}, K_{Ca}, K_{IR} and K_V; and VGCC.

Potassium channels: K_{ATP} channel opening has been reported as a key mechanism for H_2S-induced vasorelaxation in various studies in peripheral vessels (Cheng *et al*., 2004; Zhao *et al*., 2001). However, the role of K_{ATP} channels in the H_2S-induced vasorelaxation in peripheral vessels remains controversial. In some studies, using rat and mouse aorta, only partial inhibition of the relaxation induced by NaHS was demonstrated by blockade of K_{ATP} channels (Al-Magableh *et al.*, 2011; Cheng *et al.*, 2004; Zhao *et al.*, 2001). By contrast, other studies using rat mesenteric arteries, and rat and mouse aorta, failed to demonstrate any role of K_{ATP} channels in the vasorelaxation mediated by H_2S (Jackson-Weaver *et al.*, 2011; Kiss *et al.*, 2008; Kubo *et al.*, 2007).

One study suggests a role for K_{IR} channels, since 30μM BaCl, a concentration which is relatively selective for K_{IR} channels, inhibited H_2S-induced vasorelaxation of mouse aorta (Al-Magableh *et al.*, 2011). A recent study suggests involvement of BK_{Ca} in the relaxation induced by H_2S in rat small mesenteric arteries (Jackson-Weaver *et al.*, 2011), although these channels were not involved in the H_2S-induced relaxation of the chicken ductus arteriosis (van der Sterren *et al.*, 2011). The role of IK_{Ca} and SK_{Ca} in H_2S-induced vasorelaxation shall be discussed under section 1.3.4 The endothelium, EDHF (p.49).

The contribution of K_V to H_2S-induced vasorelaxation varies depending on the tissue and species studied. A K_V channel blocker induced a small attenuation of the H_2S-induced relaxation in rat coronary arteries (Cheang *et al.*, 2010) and mouse aorta (Al-Magableh *et al.*, 2011), although it had no effect on H_2S-induced relaxation of rat aorta or chicken ductus arteriosis (Kiss *et al.*, 2008; van der Sterren *et al.*, 2011; Zhao *et al.*, 2001).

The specific sub-type, K_V7 may be involved in the vasorelaxation induced by H_2S. This evidence comes from an investigation into the possible involvement of H_2S in producing the anti-contractile effect of fat (Schleifenbaum *et al.*, 2010). It has been shown previously that perivascular fat attenuates noradrenaline induced aortic vasoconstriction (Soltis *et al.*, 1991), an effect that is mediated by a transferable 'adipocyte-derived relaxing factor' (ADRF) (Lohn *et al.*, 2002). A major mechanism of ADRF is via opening of K_V (Verlohren *et al.*, 2004). Schleifenbaum *et al.* show that the inhibition of contraction by ADRF is sensitive to selective inhibition of K_V7 (Schleifenbaum *et al.*, 2010). Interestingly, the anti-contractile effect of fat was also sensitive to inhibition of H_2S production. These observations, taken together with the findings that H_2S-induced relaxation is K_V7 sensitive (Schleifenbaum *et al.*, 2010), and CSE is expressed in perivascular adipose tissue (Fang *et al.*, 2009), suggest that H_2S is an ADRF. Another line of evidence that H_2S is an ADRF comes from a study where the vasoconstrictors, phenylephrine, serotonin and Angiotensin II, all increased the release of H_2S from periadventitial adipose tissue (Fang *et al.*, 2009). Further investigations, perhaps using CSE gene-silencing techniques, will be required to confirm the interesting hypothesis that H_2S is an ADRF.

Voltage gated calcium channels (VGCC): Among VGCC sub-types; L-type calcium channels have the most clearly defined role in the maintenance of VSM tone and have therefore been studied for their involvement in H_2S-induced vasorelaxation. Nifedipine is a dihydropyidine VGCC blocker with high selectivity towards L-type calcium channels (Furukawa *et al.*, 1999). H_2S-induced relaxation of rat aorta is inhibited by a calcium free bath solution (Zhao *et al.*, 2002), and nifedipine inhibited H_2S relaxation of both rat and mouse aorta (Al-Magableh *et al.*, 2011; Zhao *et al.*, 2002). In the study by Al-magableh *et al.*, NaHS 10mM inhibited contraction to the replacement of calcium in the presence of 100mM KCl to depolarise VGCC, indicating that H_2S blocks entry of extracellular calcium through VGCC. It has also been demonstrated by patch clamp that H_2S inhibits L-type calcium channel current, albeit in cardiomyocytes (Sun *et al.*, 2008).

Bicarbonate exchange

Bicarbonate exchange is important in maintenance of smooth muscle pH_i and thus vascular function (see section 1.3.3 Control of MCA tone, bicarbonate exchange, p.38). The bicarbonate exchange inhibitor, DIDS, abolished H_2S-induced vasorelaxation of rat aorta (Kiss *et al.*, 2008; Lee *et al.*, 2007), and attenuated the relaxation in mouse aorta (Al-Magableh *et al.*, 2011). Both studies in the rat aorta attribute the vasorelaxant action of H_2S to decreased smooth muscle pH_i (Kiss *et al.*, 2008; Lee *et al.*, 2007). One study attributes this decreased pH_i to NaHS-induced enhancement of the Cl^-/HCO_3^- exchanger (Lee *et al.*, 2007). In the study by Kiss *et al*, it is hypothesised that decreased pH_i is due to metabolic inhibition (Kiss *et al.*, 2008), since H_2S is a known inhibitor of cytochrome c oxidase (Khan *et al.*, 1990). In support of their hypothesis, they observed that a H_2S solution decreased the ATP content of rat aortic rings and that H_2S-induced vasorelaxation was enhanced in the absence of oxygen (Kiss *et al.*, 2008). DIDS has several non-specific effects, including inhibition of sodium channels (Liu *et al.*, 1998) and activation of ryanodine channels (Hill *et al.*, 2002) confounding results of the aforementioned studies. Further research will be required to interpret the implications of DIDS-sensitivity upon our understanding of the mechanism of H_2S-induced vasorelaxation.

The endothelium

H_2S-induced vasorelaxation has been shown to be partially dependent on the endothelium in some studies in rat aorta and mesenteric artery (Cheng *et al.*, 2004; Zhao *et al.*, 2002; Zhao *et al.*, 2001). However, not all studies are in agreement, some showing no effect of endothelium removal on the H_2S-induced relaxation of rat and mouse aorta (Al-Magableh *et al.*, 2011; Hosoki *et al.*, 1997; Kubo *et al.*, 2007). Any influence of H_2S on endothelial-induced relaxation may be mediated via altered production, release or action of endothelial-derived vasoactive factors. For example, some studies indicate that H_2S may act synergistically with NO to induce vasorelaxation (Liew *et al.*, 2007; Zhao *et al.*, 2002; Zhao *et al.*, 2001).

Evidence on the involvement of the endothelial derived factors, NO, PGI_2 and EDHF in the mechanism of H_2S-induced relaxation is discussed below. There is controversial evidence that H_2S may be responsible for at least part of the EDHF response, which is also reviewed (see endothelial derived hyperpolarising factor, p.50).

Nitric oxide: In rat aorta, H_2S-induced relaxation was attenuated by inhibition of NO synthesis using L-NAME (Zhao *et al.*, 2002; Zhao *et al.*, 2001). The relaxation induced by NaHS was greatly enhanced in the presence of the NO and vice-versa (Hosoki *et al.*, 1997). These observations suggest that H_2S enhances either the action or production of NO. The hypothesis that H_2S enhances the production of NO is supported by the observation that Na_2S applied to bovine aortic endothelial cells resulted in a two-fold increase in NO production (Predmore *et al.*, 2011). However, the effect of H_2S on NO production remains controversial, since several studies in rat and mouse aorta and rat mesenteric artery showed no effect of L-N^G-Nitroarginine methyl ester (L-NAME) on H_2S-induced relaxation (Al-Magableh *et al.*, 2011; d'Emmanuele di Villa Bianca *et al.*, 2011; Kiss *et al.*, 2008; Streeter *et al.*, 2012).

Furthermore, several studies indicate that H_2S actually decreases vascular NO levels, and current opinion leans more towards this hypothesis, than that of vascular synergy between the two gases (Ali *et al.*, 2006; Geng *et al.*, 2007; Kubo *et al.*, 2007; Liu *et al.*, 2010) (see 1.3.5 biphasic effect: H_2S-induced vasoconstriction, p.54).

Prostacyclin: Studies in peripheral vessels generally report that COX blockade using indomethacin does not influence H_2S-induced vasorelaxation (Cheang *et al.*, 2010; Li *et al.*, 2008) (Al-Magableh *et al.*, 2011; d'Emmanuele di Villa Bianca *et al.*, 2011; Kiss *et al.*, 2008; Zhao *et al.*, 2001), suggesting a lack of involvement of PGI_2 in the peripheral vasodilator H_2S response. However, two studies indicate that H_2S-induced vasorelaxation may involve the release of arachidonic acid metabolites in rat mesenteric arteries (d'Emmanuele di Villa Bianca *et al.*, 2011) and trout branchial arteries (Dombkowski *et al.*, 2004). In the rat mesenteric arteries, it was concluded that H_2S did not release PGI_2, since relaxation was sensitive to inhibition of cytochrome P450 or phospholipase A_2 but not COX. In trout branchial arteries, PGI_2 was possibly involved, since indomethacin produced a similar attenuation of the H_2S-induced vascular response to a cocktail of indomethacin, clotrimazole and esculetin (COX, cytochrome-p450, and lipooxygenase inhibitors, respectively).

Endothelial derived hyperpolarising factor: Several observations have led to the assertion that H_2S may be an EDHF (Mustafa *et al.*, 2011; Yang *et al.*, 2008). Firstly, the channels involved in the 'classical' EDHF response, SK_{Ca} and IK_{Ca} (see section 1.3.3 Control of MCA tone, the endothelium, EDHF, p.39), have a demonstrated involvement in H_2S-induced vasorelaxation (Al-Magableh *et al.*, 2011; Cheng *et al.*, 2004; d'Emmanuele di Villa Bianca *et al.*, 2011; Zhao *et al.*, 2001). Other lines of evidence supporting a role of H_2S as an EDHF include: CSE is expressed in the endothelial cell layer of bovine aorta, human umbilical vein and rat mesenteric artery (Yang *et al.*, 2008); cultured bovine aortic endothelial cells produce measurable H_2S (Yang *et al.*, 2008); stimulation of bovine aortic endothelial cells by

acetylcholine produced a marked increase in H_2S level that was blocked by a muscarinic antagonist (Yang *et al.*, 2008) and CSE mutant mice had attenuated relaxation and virtually abolished hyperpolarisation to a muscarinic agonist (Mustafa *et al.*, 2011; Yang *et al.*, 2008). However, whether H_2S is an EDHF remains to be conclusively determined, since not all laboratories show a sensitivity of H_2S-induced vasorelaxation to SK_{Ca} and IK_{Ca} blockade (Li *et al.*, 2008). In rat mesenteric arteries, while H_2S-induced relaxation was sensitive to blockade of SK_{Ca} and IK_{Ca} channels, it was also attenuated by blockade of production of cytochrome p-450 derived prostanoids (d'Emmanuele di Villa Bianca *et al.*, 2011). In light of evidence that EDHF could be a cytochrome p450 derivative of the arachidonic acid cascade (Campbell *et al.*, 2007), the study by D'Emmanuel di Villa Bianca *et al* suggests that H_2S, rather than itself being an EDHF, may induce the release of EDHF. Furthermore, studies using the CSE knockout model may be confounded by the hyperhomocysteinaemia and resultant endothelial dysfunction induced by this model (Edwards *et al.*, 2012).

Reactive oxygen species

One study observed that H_2S-induced vasorelaxation was enhanced by a SOD mimetic in rat aortic rings (Liu *et al.*, 2010). Despite repeated observations that H_2S influences ROS (Chai *et al.*, 2012; Kimura *et al.*, 2006; Kimura *et al.*, 2010; Muzaffar *et al.*, 2008), the role of ROS in H_2S-induced vasorelaxation has not been thoroughly investigated.

Overview of possible mechanisms contributing to H_2S-induced vasorelaxation

In summary, there is evidence that H_2S-induced vasorelaxation in peripheral vessels may be mediated by various mechanisms, including: opening of potassium channels, such as K_{ATP}, K_{Ca}, K_{IR} K_V; blockade of VGCC, enhanced production or activity of endothelial derived factors, such as NO, PGI_2 and EDHF and decreased pH_i (see table 1). There is also controversial evidence that H_2S may itself be an EDHF. However, in cerebral vessels, only K_{ATP} and K_{Ca} channels have been examined for their contribution to the H_2S-induced vasorelaxation.

Table 1.1 Summary of findings of studies investigating the mechanism of H_2S-induced vasorelaxation

Study	**Species**	**Vessel**	**Involvement of channel/pathway**			**Additional findings**
K^+ channels			**K_{ATP}**	**K_V**	**K_{Ca}**	
Schleifenbaum, 2011	Rat	Aorta	-	↓	-	Inhibition of H_2S production inhibited the anti-contractile effect of fat
Kiss, 2008	Rat	Aorta	No Δ	No Δ	-	
Zhao, 2001	Rat	Aorta	↓	No Δ	↓S&I	H_2S increased K_{ATP} currents
Li, 2008	Rat	Aorta	↓	-	No Δ S&I	Used a compound which slowly releases H_2S, GYY4137. GYY4137 also dilated renal vasculature and exhibited antihypertensive activity
Zhao, 2002	Rat	Aorta	-	-	↓S&I	H_2S reduced the vasorelaxation to SNP
Kubo, 2007	Rat	Aorta	↓	-	-	NaHS reduced eNOS activity
Kubo, 2007	Mouse	Aorta	No Δ	-	-	
Al-Magableh, 2011	Mouse	Aorta	↓	↓	↓S&I	K_{IR} were also involved
Jackson-weaver, 2011	Rat	Mes-enteric	No Δ	-	↓B	Ischaemic hypoxia enhanced myogenic tone by decreasing H_2S production
D'Emmanuel, 2011	Rat	Mes-enteric	-	-	↓S&I	NaHS caused migration of cytosolic PLA_2 close to the nucleus, indicating PLA_2 activation
Cheng, 2004	Rat	Mes-enteric	↓	-	↓S&I	
Mustaffa, 2011	Mouse	Mes-enteric	↓	-	↓S&I	Genetic CSE deletion abolished EDHF activity
Cheang, 2010	Rat	Coron-ary	No Δ	↓	No Δ B	NaHS-induced hyperpolarisation also sensitive to 4-AP, but not glibenclamide
Leffler, 2010	Piglet	Pial	↓	-	-	Hypercapnia increased H_2S concentration in CSF, and relaxation to hypercapnia was inhibited by PPG
Liang, 2011	Piglet	Pial	↓	-	-	Na_2S activated K^+ channel currents, that were sensitive to K_{ATP} channel blockade
Liang, 2012	Piglet	Pial	-	-	↓ B	Na_2S increased Ca^{2+} spark frequency
Dombkowski, 2004	Trout	Bran-chial	↓	-	-	NaHS induced a triphasic response: relaxation, constriction, relaxation. Note: only effects on final relaxation are considered here

Table 1.1 Continued

Ca^{2+} channels			**VGCC**			
Al-Magableh, 2011	Mouse	Aorta	↓			NaHS also inhibited contraction to calcium replacement
Zhao, 2002	Rat	Aorta	↓			A calcium-free medium also inhibited H_2S-induced relaxation
Bicarbonate exchange			**Cl^-/HCO_3^- exchange**			
Lee, 2007	Rat	Aorta	↓			NaHS-induced intracellular acidification
Kiss, 2008	Rat	Aorta	↓			H_2S relaxation via metabolic inhibition
Al-Magableh, 2011	Mouse	Aorta	↓			
Endothelium			**Endo remo val**	**NO**	**sGC**	
Zhao, 2001	Rat	Aorta	↓	↓	-	
Zhao, 2002	Rat	Aorta	↓	↓	↑	Inhibition of sGC potentiated H_2S-induced relaxation
Li, 2008	Rat	Aorta	↓	↓	↓	Inhibition of PGI_2 production had no effect
Kubo, 2007	Rat	Aorta	↓	↑	↑	A very small inhibition of maximum relaxation was observed upon endothelium removal.
Kubo, 2007	Mouse	Aorta	No Δ	No Δ	↑	Endothelium removal had no effect on NaHS-induced relaxation, but abolished constriction. Constriction possibly due to reduced NO production, since NaHS reduced eNOS activity and reduced the relaxant effect of ACh, but not SNP
Al-Magableh, 2011	Mouse	Aorta	No Δ	No Δ	No Δ	Inhibition of PGI_2 production had no effect
Cheng, 2004	Rat	Mes-enteric	↓	-	-	Inhibition of EDHF (by blocking K_{Ca}) also inhibited H_2S-induced relaxation
Cheang, 2010	Rat	Coron-ary	No Δ	No Δ	No Δ	Inhibition of PGI_2 production had no effect

↓,↑ and 'No Δ' denote effects of inhibition of the relevant channel or pathway on H_2S-induced relaxation. Symbols indicate that H_2S-induced relaxation was:↓ attenuated (indicating an involvement of that channel or pathway in H_2S-induced relaxation); ↑ potentiated; 'No Δ' no effect; or '–' not investigated. S&I, small and intermediate conductance K_{Ca}; B, large conductance K_{Ca}; CSF, cerebrospinal fluid; SNP, sodium nitroprusside; PLA_2, phospholipase A_2; 4-AP, 4-aminopyridine; PPG, propargylglycine; sGC, soluble guanylate cyclase.

1.3.5 Biphasic effect of H_2S: H_2S-induced vasoconstriction

The most well-reported vascular action of H_2S is as a vasorelaxant (Liu *et al.*, 2011b). However, several studies report a biphasic vascular action of H_2S depending on its concentration: constriction at low NaHS concentrations (10-100 μM) and relaxation at higher NaHS concentrations (100-1600 μM) (Ali *et al.*, 2006; Kubo *et al.*, 2007; Lim *et al.*, 2008). The following is a summary of the proposed mechanisms of vasoconstriction induced by H_2S.

H_2S-induced vasoconstriction may involve the endothelium, since endothelium removal blocked the vasoconstrictor effect of H_2S (Kubo *et al.*, 2007). This indicates that H_2S may reduce the production or action of endothelial derived vasodilators. Reduction of NO levels by H_2S may be responsible for H_2S-induced vasoconstriction, since L-NAME attenuates the vasoconstrictor effect of NaHS in rat aorta (Kubo *et al.*, 2007; Lim *et al.*, 2008), as well as the increase in blood pressure induced by an NaHS infusion (10 μmol kg^{-1} min^{-1}) in rats (Ali *et al.*, 2006). Several studies indicate that H_2S decreases vascular NO levels by various putative mechanisms, including: directly reacting with NO, forming a vaso-inactive nitrosothiol (Ali *et al.*, 2006; Whiteman *et al.*, 2006), extracellular transport of $O_2^{\cdot-}$, which then reacts with NO (Liu *et al.*, 2010)(see below), inhibition of eNOS (Geng *et al.*, 2007; Kubo *et al.*, 2007) or reduced L-Arginine transport (Geng *et al.*, 2007). Blockade of COX has been shown to inhibit the vasoconstrictor action of H_2S in rat thoracic aorta, suggesting that PGI_2 may be involved (Koenitzer *et al.*, 2007).

H_2S-induced vasoconstriction may also involve $O_2^{\cdot-}$, since NaHS-induced vasoconstriction was attenuated by a SOD mimetic in rat aortic rings (Liu *et al.*, 2010). Those authors also observed that the bicarbonate exchange inhibitor, DIDS, inhibited NaHS-induced vasoconstriction and that NaHS decreased NO production in aortic rings, but only in the presence of bicarbonate. They hypothesised that H_2S induces constriction by increasing the

transport of $O_2^{\cdot-}$ out of the cell via the Cl^-/HCO_3^- exchanger, and $O_2^{\cdot-}$ then reacts with NO to decrease NO levels.

However, it has been shown that the constrictor effect of H_2S is only partially inhibited by endothelium removal (Lim *et al.*, 2008), indicating endothelium-independent mechanisms. One such mechanism appears to be by down-regulation of cyclic adenosine monophosphate (cAMP), since NaHS reversed the vasorelaxation caused by forskolin, a selective adenylyl cyclase activator, and reduced cAMP accumulation in VSM cells (Lim *et al.*, 2008). In mesenteric arteries, the constrictor effect of H_2S was found to involve a constrictor effect of arachidonic acid itself, not its endothelial derived metabolites (d'Emmanuele di Villa Bianca *et al.*, 2011). As such, NaHS-induced constriction was inhibited by a PLA_2 inhibitor, but remained unaffected by inhibition of COX, LOX or cytochrome p450 (d'Emmanuele di Villa Bianca *et al.*, 2011).

In summary, H_2S induces vasoconstriction in peripheral vessels, which appears to involve decreased NO levels or production, reduced cAMP, or influences on arachidonic acid. The vasoconstrictor effect has not yet been investigated in cerebral vessels. The more thoroughly investigated vasorelaxation effect of H_2S involves contributions from potassium channels, such as K_{ATP}, and from Ca^{2+} channels, bicarbonate exchange, and possibly the endothelium. In cerebral vessels, only three studies have investigated the mechanism of H_2S-induced vasorelaxation, finding roles for K_{ATP} as well as K_{Ca} (Leffler *et al.*, 2010; Liang *et al.*, 2011; Liang *et al.*, 2012). The contribution of other mechanisms to the H_2S-induced vasorelaxation response of cerebral vessels has not yet been investigated.

1.4 Diabetes induced pathophysiology of MCA

H_2S demonstrates antioxidant properties which confer protection of vascular tissues in conditions of oxidative stress, such as hyperglycaemia (see 1.4.4 Diabetic vascular disease and H_2S, p.61). This section provides an overview of diabetic cerebrovascular disease, and the possible involvement of altered H_2S function in this condition.

1.4.1 Diabetes: epidemiology

Diabetes is a highly prevalent health problem, afflicting an estimated 6.4% of adults worldwide (Shaw *et al.*, 2010). It is characterised by elevated blood glucose levels, which can be either diet-induced (Type 2 diabetes) or due to an autoimmune condition involving destruction of pancreatic beta cells (Type 1 diabetes). Type 2 diabetes occurs particularly as a result of western diet and lifestyle, and consequent obesity. Increased incidence is therefore occurring, particularly in developing countries where dietary and life-style habits have changed rapidly (Shaw *et al.*, 2010).

1.4.2 Involvement of cerebrovascular disease in the pathology of diabetes

Insidious development of vascular disease is a feature of both types of diabetes. Vascular disease occurs in both peripheral and cerebral vessels, and entails abnormalities in endothelium and VSM. Cerebrovascular disease is a major contributor to diabetic morbidity and mortality. For example, diabetes confers a 1.5 to 2-fold increased risk of ischaemic stroke (Quinn *et al.*, 2011), a risk which is strongly associated with diabetic cerebrovascular disease (Gunarathne *et al.*, 2009; Nazir *et al.*, 2006; Roquer *et al.*, 2009; Zimmermann *et al.*, 2004). The mortality following stroke is also significantly higher in individuals with diabetes compared to non-diabetic stroke victims (Laing *et al.*, 2003).

1.4.3 Aetiology of diabetic cerebrovascular disease

Diabetes causes atherosclerotic vascular disease, which is associated with endothelial and smooth muscle dysfunction, and a tendency towards thrombosis. A functional endothelium protects against the development of atherosclerosis.

Endothelial dysfunction

Endothelial dysfunction precedes ultrasonic evidence of atherosclerotic plaques, and is considered a fundamental step in atherosclerotic disease (Luscher *et al.*, 1997). NO is a key regulator of endothelial function. In fact, endothelial dysfunction is defined as decreased NO bioavailability, and is determined experimentally by observation of impaired endothelial induced relaxation (Creager *et al.*, 2003). In addition to its vasodilator action (see 1.3.3, Biological effects of H_2S, p.21), NO protects blood vessels from atherosclerosis by prevention of platelet and leukocyte interaction with the vascular wall (Radomski *et al.*, 1987), inhibition of VSM cell proliferation and reduction of pro-inflammatory gene expression (Forstermann, 2010). The reduced NO bioavailability of endothelial dysfunction alters the phenotype of the endothelium, resulting in pro-inflammatory and pro-thrombotic actions (Roquer *et al.*, 2009), as well as promotion of migration of VSM into the intima (Creager *et al.*, 2003). Endothelial dysfunction occurs earlier and is of greater severity in cerebral vessels in several models, including diabetes (Kitayama *et al.*, 2006), aging (Brown *et al.*, 2007) and hypertension (Didion *et al.*, 2002b).

Role of ROS in endothelial dysfunction

Studies in cerebral pial arterioles provided the first evidence that ROS impair endothelial dependent vasorelaxation (Wei *et al.*, 1985). There is now a wealth of evidence implicating increased ROS in the development of endothelial dysfunction. Diabetes causes increased production of ROS in the vascular wall (Hink *et al.*, 2001). A major mechanism of ROS-dependent impairment of endothelial function is the rapid inactivation of NO to $ONOO^-$ by $O_2^{\cdot-}$ (Gryglewski *et al.*, 1986) (figure 1.5). Apart from the influence of ROS on NO bioavailability, ROS may also cause vascular inflammation and remodelling via increased expression of growth factors (Kaneto *et al.*, 2010) and oxidation of proteins such as the redox-activated, pro-inflammatory NF-κB (Anrather *et al.*, 2006) (figure 1.5).

There are several sources of vascular ROS, including NADPH oxidase (Nox), mitochondrial electron transport chain and xanthine oxidase. There is also evidence that persistently elevated ROS, such as in diabetes, uncouples eNOS, resulting in increased $O_2^{\cdot-}$ production in place of NO (Forstermann *et al.*, 2006). Mitochondrial production of $O_2^{\cdot-}$ is enhanced by hyperglycaemia (Naudi *et al.*, 2012), although a causal role between mitochondrial derived $O_2^{\cdot-}$ and endothelial dysfunction has not been established *in vivo*. Nox catalyse the reduction of molecular oxygen to $O_2^{\cdot-}$ and/or H_2O_2 (figure 1.5) and are poised as important mediators of endothelial dysfunction, as their primary function is to produce ROS, they are a major source of ROS in the vasculature (Csanyi *et al.*, 2009), and are activated by stimuli that are known to cause endothelial dysfunction. One homologue of Nox, Nox1, is upregulated in diabetes (San Martin *et al.*, 2007) and by substances which are known to be elevated in diabetes, such as low density lipoproteins and pro-inflammatory cytokines (Lassegue *et al.*, 2010). The effects of ROS are prominent in the cerebral circulation (Faraci, 2011) and the activity and function of Nox is profoundly larger in cerebral compared to peripheral vessels (Miller *et al.*, 2005).

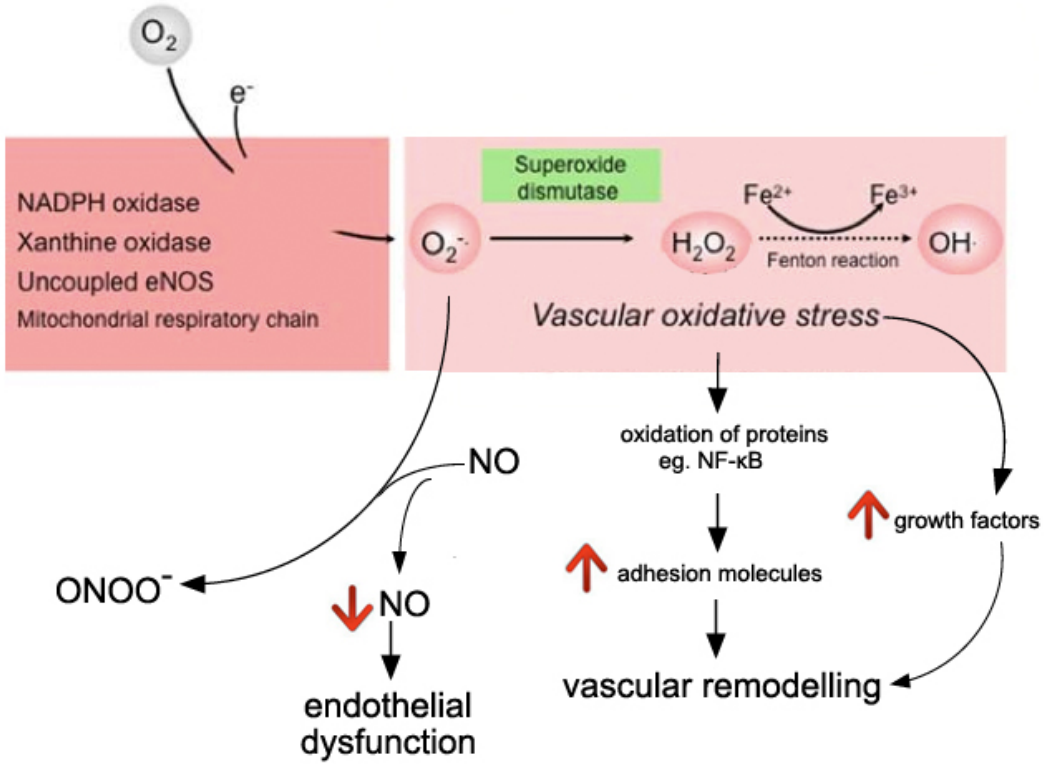

Figure 1.5 Diagram illustrating vascular sources of ROS (top) and consequences of vascular oxidative stress (bottom). Vascular oxidative stress causes endothelial dysfunction by reducing the bioavailability of NO. Oxidative stress also causes vascular remodelling via increased expression of growth factors and adhesion molecules. O_2, oxygen; e^-, electron; $O_2^{\cdot-}$, superoxide; H_2O_2, hydrogen peroxide; $OH^{\cdot}$, hydroxyl; NO, nitric oxide; $ONOO^-$, peroxynitrite; NF-κB, nuclear factor kappa-light-chain-enhancer of activated B cells. Adapted from (Forstermann, 2010).

Vascular smooth muscle dysfunction

The diabetic state is associated with an increase in vascular tone, which is a major contributor to increased vascular risk factors (NHBPEP, 1994). The cellular and molecular mechanisms contributing to this increased tone remain to be fully elucidated. The reduced NO bioavailability in endothelial dysfunction provide part of the puzzle, however, there is also evidence for impaired VSM relaxation. For example, in diabetic humans, impaired endothelium-independent vasorelaxation responses have been demonstrated repeatedly using NO donors (McVeigh *et al.*, 1992; Sivitz *et al.*, 2007). Diabetes can also enhance (Zimmermann *et al.*, 1997) or reduce myogenic tone (Kelly-Cobbs *et al.*, 2011), depending on the age of the animal studied.

Hyperpolarisation-mediated vasorelaxation is also altered by diabetes, due to effects of ROS on VSM K^+ channel function (Liu *et al.*, 2002). Streptozotocin (STZ) treatment, a model of the diabetic state (see 2.4.1 Induction of a diabetic model: streptozotocin treatment, background, p.81) impaired dilator responses to K_{ATP} channel openers in aorta (Kamata *et al.*, 1989) and cerebral arteries (Mayhan *et al.*, 1993), and high glucose impaired K_v channel currents (Liu *et al.*, 2001). This altered function is linked to $O_2^{\cdot-}$ production, since VSM responsiveness to K_{ATP} and K_V channel openers is reduced by $O_2^{\cdot-}$ (Liu *et al.*, 2002). The effect of diabetes on K_{ATP} channel function has also been associated with reduced NO bioavailability and the subsequent membrane depolarisation, since an NO donor restored both membrane potential and sensitivity to a K_{ATP} channel opener (Zimmermann *et al.*, 1997). Moreover, STZ-induced diabetes is associated with impaired activity of vascular K_{Ca} channels (Dong *et al.*, 2008; Leo *et al.*, 2011a; Leo *et al.*, 2011b; McGahon *et al.*, 2007).

Despite the wealth of knowledge regarding diabetic vascular disease, the full picture of this complex and multi-factorial disease state remains to be completed. The possible involvement of H_2S shall now be explored.

1.4.4 Diabetic vascular disease and H_2S

Protective effects of H_2S in the vasculature

H_2S is a chemical reductant (Kim *et al.*, 2007), and has been shown to directly scavenge H_2O_2 and $O_2^{\cdot-}$ in the myocardium in a model of myocardial ischaemia (Geng *et al.*, 2004). Studies have demonstrated protective antioxidant effects of H_2S in VSM and endothelial cells. For example, in A-10 VSM cells, H_2S protected against homocysteine-induced cytotoxicity, and reduced the production of $O_2^{\cdot-}$, H_2O_2 and $ONOO^-$ (Yan *et al.*, 2006). Mechanisms of H_2S-induced protection are not limited to its chemical reductant properties. In human VSM cells, H_2S blocked U46619 (a thromboxane A_2 analogue) induced enhancement of Nox1 expression and inhibited $O_2^{\cdot-}$ formation (Muzaffar *et al.*, 2008). In STZ diabetic rats, four weeks of daily subcutaneous NaHS injections normalised upregulated expression of the Nox subunit, $p22^{phox}$ (Zheng *et al.*, 2010). H_2S has also been shown to protect against high glucose-induced endothelial dysfunction (Suzuki *et al.*, 2011) and apoptosis (Guan *et al.*, 2012). High glucose induced a switch from oxidative phosphorylation to glycolysis and enhanced production of ROS by mitochondria in an endothelial cell culture, both of which were attenuated by H_2S (Suzuki *et al.*, 2011). In human umbilical vein endothelial cells, high glucose increased ROS and reduced SOD activity, both of which were attenuated by H_2S (Guan *et al.*, 2012).

Alteration of vascular response to H_2S and production of H_2S in diabetes

The H_2S producing enzyme, CSE, is expressed in vascular tissue throughout the circulatory system (Fiorucci *et al.*, 2005; Ghasemi *et al.*, 2012; Leffler *et al.*, 2010; Meng *et al.*, 2007; Olson *et al.*, 2010; Yang *et al.*, 2008; Zhao *et al.*, 2001) and endogenous H_2S generation has been demonstrated from aorta homogenates (Brancaleone *et al.*, 2008). These observations,

taken together with the protective effects of H_2S in the vasculature, suggest that an alteration in H_2S signalling may be involved in the development of diabetic vascular disease. Indeed, alterations in H_2S production, and the vasorelaxation induced by H_2S, have been observed in several diabetic studies. Limited evidence suggests that diabetes enhances the response of peripheral vessels to H_2S: vasorelaxation to exogenously applied H_2S was enhanced in the aortas of both non-obese diabetic mice (NOD) (Brancaleone *et al.*, 2008) and STZ-treated rats (Denizalti *et al.*, 2011). However, the effect of diabetes on the vascular production of H_2S remains unclear. In NOD, CSE expression in the aorta was enhanced, although plasma H_2S levels were reduced (Brancaleone *et al.*, 2008). STZ rats had double the expression of CSE in aorta compared to control rats, although this was not significant (Denizalti *et al.*, 2011), and plasma H_2S levels were unaltered by STZ treatment in another study (Yusuf *et al.*, 2005). The effect of diabetes on the cerebrovascular H_2S response has not yet been examined. Understanding the effect of diabetes on the MCA response to and production of H_2S will broaden our understanding of diabetic cerebrovascular disease, perhaps paving the way for the development of novel therapeutics.

1.5 Hypotheses and Aims of Thesis

1.5.1 The role of H_2S in the brain in cardiovascular regulation

The PVN and RVLM are brain regions with profound influences on cardiovascular regulation (Badoer, 2001; Badoer, 2010; Dampney, 1994; Deering *et al.*, 2000). H_2S has both neuromodulatory roles (Abe *et al.*, 1996) and peripheral cardiovascular effects (Zhao *et al.*, 2001), however, its effect on the cardiovascular system via the RVLM or PVN had not been investigated at the time of research.

Hypotheses

- The H_2S producing enzyme, CBS, is present in both the RVLM and PVN
- H_2S is involved in the central regulation of the cardiovascular system
- Abnormal function or production of H_2S is involved in hypertension

Specific Aims

The aims of the study investigating the role of H_2S in the brain in cardiovascular regulation were to:

- investigate the effect of H_2S, or inhibition of endogenous H_2S production in the RVLM and PVN on mean arterial pressure (MAP), heart rate (HR) and LSNA
- determine whether these regions contained either of the H_2S producing enzymes, CBS or CSE
- determine whether a modification of the H_2S response may be responsible for the development of hypertension by investigating the effect of H_2S in the RVLM and PVN on MAP, HR and LSNA in SHR rats

1.5.2 Regulation of middle cerebral artery tone by H_2S

H_2S induces vasorelaxation of peripheral vessels, and systemic administration of a saturated solution of H_2S dose-dependently reduces blood pressure (Zhao *et al.*, 2001). The mechanism of this vasorelaxation in peripheral vessels has been investigated for over a decade, but remains incompletely understood. Only three studies have investigated this mechanism in cerebral vessels, finding roles for K_{ATP} and K_{Ca} channels (Leffler *et al.*, 2010; Liang *et al.*, 2011; Liang *et al.*, 2012). Mechanisms contributing to the H_2S-induced vasodilator response, other than K_{ATP} and K_{Ca} channels, remain to be investigated. Several studies report a biphasic vascular effect of H_2S in peripheral vessels: constriction at low concentrations, and relaxation at higher concentrations (Ali *et al.*, 2006; Geng *et al.*, 2007; Kubo *et al.*, 2007; Lim *et al.*, 2008; Liu *et al.*, 2010). The constrictor effect of H_2S in cerebral vessels has not, to date, been investigated.

Hypotheses

- The H_2S-producing enzyme, CSE is present in MCA endothelium and/or VSM
- Exogenous and endogenous H_2S can dilate MCA
- The mechanism of H_2S-induced vasorelaxation of MCA involves: endothelium, K^+ and Ca^{2+} channels, chloride/bicarbonate exchange or ROS
- The mechanism of H_2S-induced vasoconstriction of MCA involves: endothelium, K^+ and Ca^{2+} channels, chloride/bicarbonate exchange or ROS

Specific Aims

The study investigating regulation of MCA tone by H_2S aimed to

- examine MCA for the presence of the H_2S producing enzyme, CSE
- determine the cell type in which CSE is localised within MCA
- investigate the mechanism of H_2S-induced vasorelaxation and vasoconstriction of MCA

1.5.3 The effect of diabetes on the production and vascular effect of H_2S in MCA

Vascular overproduction of ROS is a major contributor to the pathogenesis of diabetic vascular disease (Creager *et al.*, 2003). H_2S has antioxidant effects in VSM (Muzaffar *et al.*, 2008; Yan *et al.*, 2006) as well as endothelial cells (Suzuki *et al.*, 2011) and has recently been shown to attenuate the decline in endothelial cell viability caused by high glucose (Suzuki *et al.*, 2011). Several studies have shown that H_2S production and vasodilator capacity are altered in peripheral vessels in rat diabetic models (Brancaleone *et al.*, 2008; Denizalti *et al.*, 2011; Yusuf *et al.*, 2005) although the effect of diabetes on the response to and production of H_2S in cerebral vessels has not yet been investigated.

Hypotheses

- The MCA response to H_2S is altered by diabetes
- The mechanism of H_2S-induced relaxation is altered by diabetes
- MCA and tissue production of H_2S is altered by diabetes
- Exogenous H_2S can reduce MCA production of ROS

Specific Aims

The aims of the study investigating the possible involvement of H_2S in diabetic cerebrovascular disease were to:

- determine the effect of STZ treatment on the MCA response to H_2S
- investigate the mechanisms mediating H_2S-induced vasorelaxation in MCA from STZ rats
- examine the effect of STZ treatment on MCA CSE expression, serum sulfide levels, and liver H_2S production
- Examine the effect of exogenous H_2S on ROS production from STZ and control MCA

Chapter 2: General Methods

All procedures were performed to conform to the guidelines set out by the National Health and Medical Research Council of Australia and were approved by the RMIT University Animal Ethics committee.

2.1 Animals

Male WKY and SHR rats weighing 300-350g, aged approximately 8-10 weeks were used in the LSNA recording studies. These animals were housed for a minimum period of one week before undergoing any experimental procedure. Male Sprague Dawley rats weighing 300-350g, aged approximately 8-10 weeks were used in the mechanistic studies on H_2S-induced cerebral vasodilation. For the diabetic studies, Sprague Dawley rats were obtained at either 5 weeks or 15 weeks and kept until 16 weeks of age before study. All animals were obtained from the Animal Resources Centre (ARC, Canning Vale, Western Australia) and then housed in a temperature-controlled room on a 12:12 hour light/dark cycle (lights on at 7:00 AM), in the RMIT Animal Facility (RMIT University, Bundoora West campus, Victoria, Australia).

2.2 Brain injection and LSNA recording studies

2.2.1 Surgical Procedures

Anaesthetics and monitoring

Rats were anaesthetised initially with inhaled isofluorane (1-3% in air), by placing the animal into a sealed container which was subsequently filled with the gas. Once anaesthesia was induced, isofluorane was continually administered via a mask while the femoral vein and artery were cannulated. For cannulation, the right femoral vein and artery were exposed by blunt dissection and blood flow was temporarily obstructed using sutures. A small incision was then made in both the femoral vein and artery for insertion of a separate catheter into both vein and artery. Catheters consisted of polyvinyl chloride tubing (internal diameter 0.28 mm) inserted into a larger bore tubing (internal diameter 0.80 mm), attached using Araldite ® Epoxy Resin (Selleys Pty Ltd; NSW, Australia) glue and filled with heparinised saline (50U/mL). Anaesthesia was maintained using urethane (1-1.5 g/kg IV) with supplemental doses as required (0.1-0.3 g/kg IV), administered through the cannulated vein. The depth of anaesthesia was maintained to ensure the absence of corneal and pedal reflexes, which were tested every 15 minutes. The distal end of the arterial cannula was attached to a blood pressure transducer for direct monitoring of MAP and HR.

Preparation for lumbar sympathetic nerve recording

Following a midline abdominal incision, the left lumbar postganglionic sympathetic nerve trunk was identified and dissected free of surrounding tissue. With the aid of an operating microscope the nerve was placed onto the bared tips of two Teflon – coated silver wire electrodes and the nerve-electrode junction insulated electrically from surrounding tissue with a sealant (Kwik-Cast Sealant, WPI, USA). The nerve activity was amplified using a low-noise differential amplifier (ENG Models 187B and 133, Baker Institute, Victoria, Australia), filtered (bandpass 100-1000Hz), rectified and integrated at 0.5-second intervals. The signal was recorded using a MacLab data acquisition system (ADInstruments, NSW, Australia). The set-up for recording LSNA, HR and MAP is illustrated diagrammatically in figure 2.1, p.70. The signal recorded at the end of the experiment after the injection of phenylephrine (5 µg/kg, IV) was deemed background noise. The LSNA was calculated by subtraction of background noise from the recorded nerve activity. The average integrated LSNA was calculated over a period of 1-2 minutes and expressed as a percentage of the resting period prior to the intracerebral administration of drugs.

Preparation for RVLM and PVN microinjections

For microinjections into the RVLM, each animal was placed prone and the head was mounted in a Stoelting® stereotaxic frame such that both bregma and lambda were positioned on the same horizontal plane. Burr holes were drilled bilaterally into the occipital bone of the skull approximately 2mm lateral of the mid-sagittal suture and 3.8 mm caudal of the lambdoid suture. The pressor region of the RVLM was identified functionally by microinjection of 50 nl of L-glutamate (0.1M) which elicited a pressor response of at least 20mm Hg in arterial pressure (Kantzides *et al.*, 2005). RVLM microinjections were made using the following coordinates; 3.7-4.0 mm caudal to lambdoid suture, 2 mm lateral to the midline, and 8.0 mm ventral to the surface of the dura.

For microinjections into the hypothalamic PVN, a midline reference point was marked 2 mm rostral to bregma. This was necessary because bregma was removed in some instances during the subsequent bone drilling procedure. Holes (approximately 4 mm in diameter) were drilled bilaterally into the skull centred 4.0 mm caudal from the reference point to allow microinjections of drugs into the PVN (stereotaxic coordinates: 3.8-4.1 mm caudal to the reference point, 0.5 mm lateral to midline, and 8.0 mm ventral to the surface of the dura).

All microinjections were made using a fine glass micropipette (Accu-fill 90®, supplied by Clay Adams, Becton, Dickson and Co., NJ, USA) which had been pulled on a P-97 Flaming/Brown micropipette puller (Sutter Instrument Company, CA, USA). The puller was programmed (Program details: Heat 740, Pull 40, Velocity 50, Time duration 110) to produce pipettes with an external tip diameter of 50 – 70 μm.

Microinjections of volume 100 nl were performed bilaterally, and after each microinjection, the micropipette was left in place for approximately 1 min. MAP, HR and LSNA were recorded before, during and after microinjections, as illustrated in figure 2.1. To mark the injection sites, a small amount of rhodamine-tagged fluorescent microspheres was included in the microinjected solution (LumaFluor, NC, USA). The precise location of the microinjections was verified histologically at the end of each experiment.

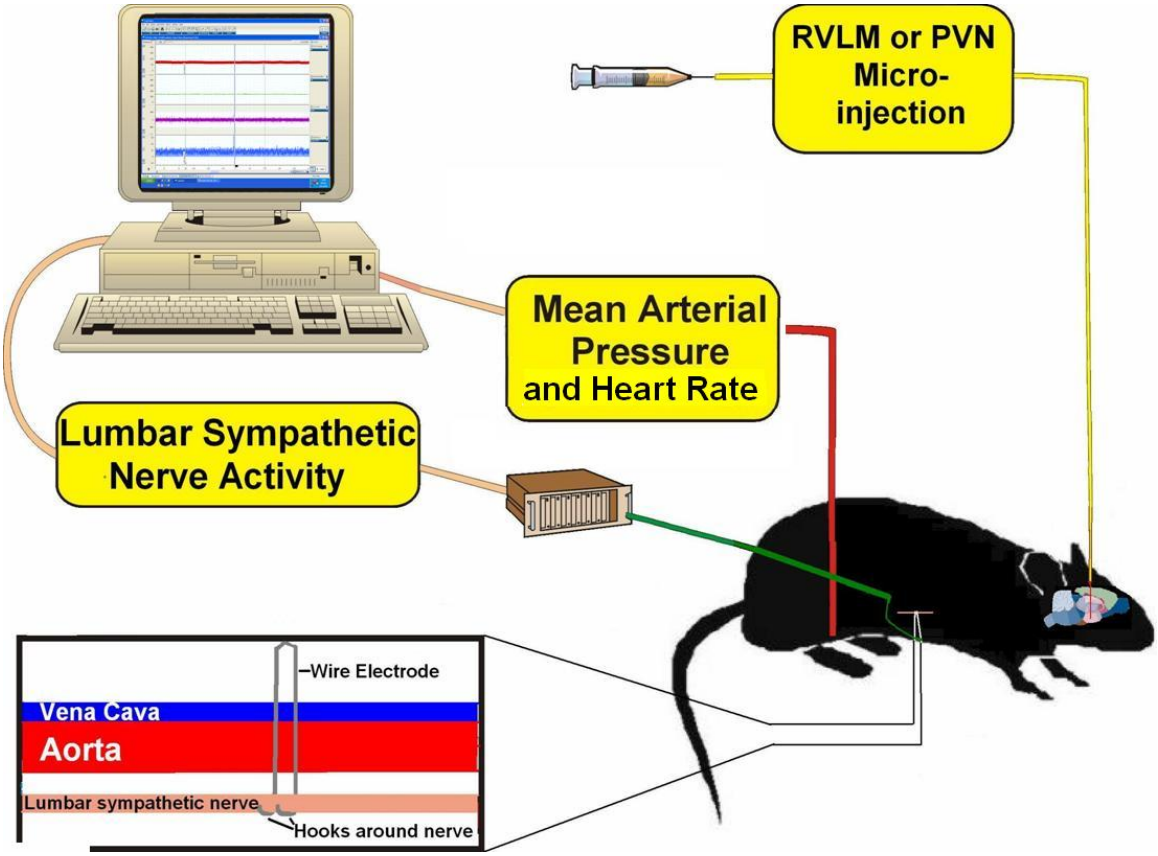

Figure 2.1 Microinjections and recording of MAP, HR and LSNA

MAP, HR and LSNA were recorded before, during and after micro-injection into the RVLM or PVN. MAP and HR were recorded via a blood pressure transducer connected to the cannulated right femoral artery. LSNA was recorded via two wire electrodes hooked under the exposed lumbar sympathetic nerve. MAP, mean arterial pressure; HR, heart rate and LSNA, lumbar sympathetic nerve activity.

2.2.2 Histology

At the end of each experiment, rats were killed using an overdose of pentobarbital sodium (325 mg/kg; Lethabarb, Virbac, NSW, Australia). The brain of each rat was then carefully removed and placed in a solution of 4% paraformaldehyde and 20% sucrose for one week. The medulla (for brains which had been microinjected into the RVLM) or the hypothalamus (for brains which had been microinjected into the PVN) were cut on a cryostat into 40 μm-thick sections and mounted onto gelatin-subbed slides. The sections were then viewed wet under fluorescence microscopy to determine the position of the rhodamine beads which indicated the microinjection site. For the medulla, the caudal end of the facial nucleus, the nucleus ambiguous and the inferior olivary nuclei were identified in the wet sections and the microinjection sites were mapped in relation to those structures. For the hypothalamus, after the centre of the microinjections site was identified, the sections were dried before being stained with cresyl violet and cover-slipped with Depex mounting medium (BDH Lab Supplies, Poole, UK). Light microscopy was then used to re-examine the stained hypothalamic sections to determine the extent of the PVN and adjacent anatomical structures. The microinjection sites were subsequently mapped in relation to the PVN and the anatomical structures.

2.2.3 Data Analysis

The data from the *in vivo* studies were expressed as the change between the level immediately prior to each microinjection and the average of the level observed over a period of 1 min, beginning at 1 and 5 min after drug or vehicle administration. These time points corresponded to those used by others (Dawe *et al.*, 2008), and were therefore considered to be the times at which an effect was most likely to be observed. The average value of the changes was calculated and was subsequently compared between groups using one-way ANOVA, followed by comparisons between the individual doses of drugs and control using Dunnett's post hoc test for multiple comparisons. $P<0.05$ was considered statistically significant.

2.3 Myograph Studies

2.3.1 Cerebral artery collection

Rats were killed humanely by CO_2 inhalation (95% CO_2, 5% O_2), followed by decapitation. The brains were collected into ice-cold Krebs' solution (composition (mM): NaCl, 119; KCl, 4.7; $MgSO_4$ 1.2; $CaCl_2$, 2.5; KH_2PO_4, 1.2; $NaHCO_3$, 25; Glucose 11.1; EDTA 0.26, pH 7.4 and gassed with 95% O_2, 5% CO_2). Proximal lengths of the middle cerebral arteries (approximately 250 μm in diameter) were dissected in ice-cold Krebs' and cleaned of connective tissue.

2.3.2 Isolated cerebral artery preparation

MCA were cut into 2mm segments and each was threaded with two 25 μm diameter gold-plated wires (Goodfellow, Huntington, England) of 2.5 cm in length. The segments were then mounted into a 610M 4-chamber wire myograph (Danish Myotechnology, DMT, Aarhus, Denmark), by attaching one wire to the force transducer, and the other to the micrometer of the myograph chamber (figure 2.2). Each myograph chamber contained 5mL Krebs' solution, maintained at 37 ^{o}C and bubbled with a mixture of 95% O_2 and 5% CO_2. Changes in isometric tension were recorded via Myodaq software (DMT, Aarhus, Denmark). The vessel segments were allowed to rest in the myograph chamber for at least 5 minutes without any tension before a contraction protocol was commenced.

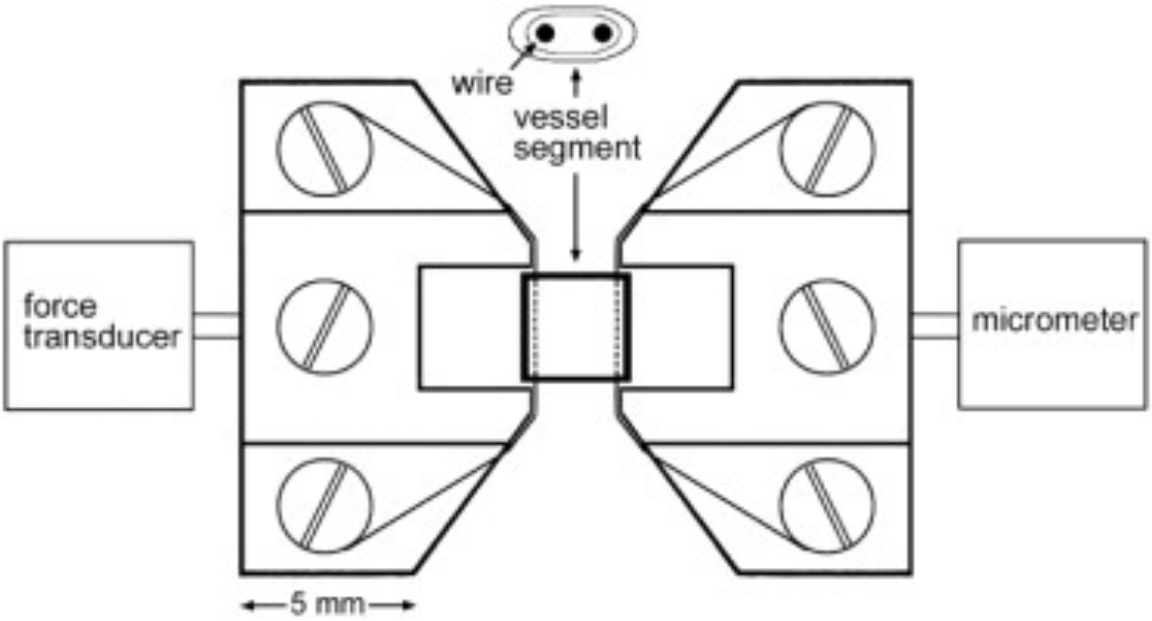

Figure 2.2 Isolated cerebral artery preparation
Segments of middle cerebral artery were mounted into a myograph chamber, in 5mL Krebs solution maintained at 37 ^{o}C and continuously supplied with 95% O_2 and 5% CO_2. The segments were mounted on two wires, one attached to the force transducer, the other to a micrometer for adjustment of tension. Changes in tension were measured throughout the experiment.

Spontaneous developed contraction protocol

Rat middle cerebral arteries possess marked levels of spontaneous myogenic tone. The following protocol was adopted to standardise the level of passive force applied to each vessel (Favaloro *et al.*, 2003). Firstly, a 4 mN force was applied to each segment over a 30 minute period to allow spontaneous tone to develop. During this time, the force was adjusted back to 4 mN, to standardise the amount of tone on the vessels. Subsequently, Krebs' solution was replaced with a calcium free Krebs' solution (composition as above, excluding the $CaCl_2$, and replacing EDTA with EGTA 2mM), causing the vessels to fully relax. The passive force was reset to 4mN, before reintroducing normal Krebs' solution to allow spontaneous redevelopment of tone. The viability of the VSM was confirmed by the redevelopment of spontaneous tone. An increase of at least 2.5 mN in tone was required to deem the VSM viable. Bradykinin (100nM) was then applied to assess the viability of the endothelium. Segments which had a dilation response of >70% of the spontaneous tone development were regarded as having intact endothelium. In some experiments the endothelium was deliberately removed by rubbing the lumen with a wire. Segments which had a dilation response of <20% of the spontaneous tone development were regarded as being denuded of endothelium. The vessels were subsequently washed thoroughly and left until spontaneous tone redeveloped. In experiments where inhibitors or antagonists were used, these agents were added after spontaneous redevelopment of tone to allow observation of any effect of these agents on baseline tone. Concentration-response curves to NaHS were obtained 20 minutes after any inhibitors or antagonists were applied. At the end of each experiment, calcium free Krebs' was administered to define 100% relaxation. Figure 2.3 is a schematic illustrating the spontaneously developed tone protocol.

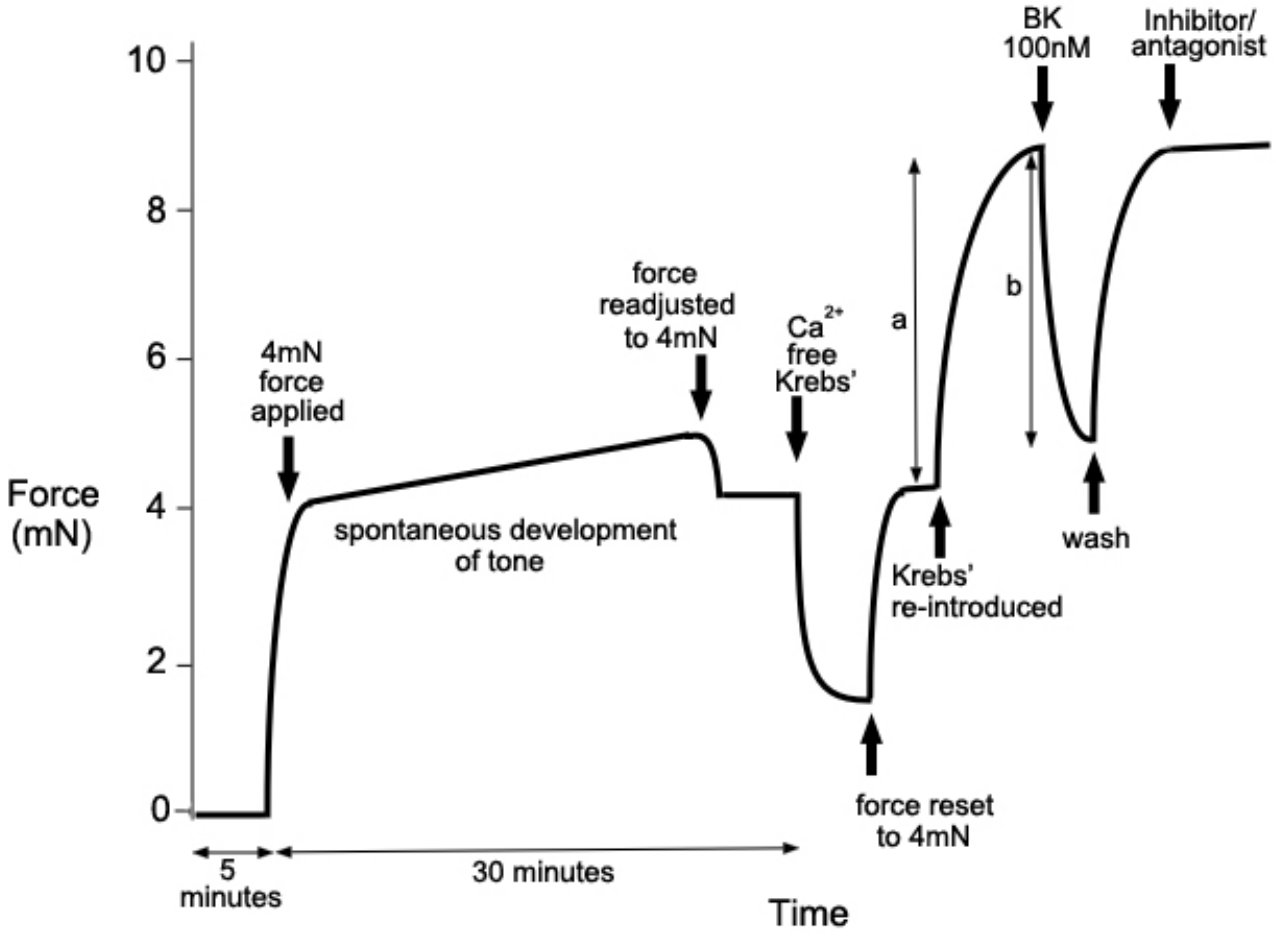

Figure 2.3 Spontaneous tone protocol

Segments of MCA were allowed to equilibrate for 5 min without any tension applied, before adjusting the passive force to 4mN using the micrometer. Spontaneous tone was allowed to develop over 30 min, during which time the force was readjusted to 4 mN. The Krebs' bathing solution was then replaced with calcium free Krebs', allowing the vessels to fully relax. The force was reset to 4mN before re-introducing Krebs' (containing calcium), which resulted in spontaneous development of tone of magnitude 'a'. The viability of VSM was confirmed by a development of tone 'a' > 2.5 mN. The viability of endothelium was then assessed using bradykinin (BK, 100nM). Vessels were deemed as having intact endothelium if the dilation induced by BK, 'b' was greater than 70% of the spontaneous tone 'a'. Vessel segments were then washed, and allowed to redevelop spontaneous tone before application of any inhibitor or agonist.

U46619 induced tone protocol

In some experiments, a different protocol was used for pre-contraction of the vessels. This is because two of the inhibitors used (nifedipine and bicarbonate free Krebs') caused full relaxation of the vessels, so they could not be constricted using the spontaneous tone protocol. For experiments using these inhibitors, a 2 mN force was applied for 30 minutes before the segments were contracted maximally using 125 mM potassium. The vessels were then washed, and titrated concentrations of the thromboxane A_2 mimetic, U46619 (1nM-1μM), were used to constrict the vessels to approximately 50% of the maximal contraction. Endothelial function was assessed using bradykinin (100nM). Vessels were then washed thoroughly, followed by pre-contraction to approximately 50% of the maximal contraction using U46619 (1 nM-1 μM). Incremental doses of U46619 were used to achieve approximately 50% of the maximal contraction, without over or under contracting the vessels. In experiments where inhibitors or antagonists were used, these agents were added prior to the second U46619 contraction, so that this precontraction could be matched between the groups, by adjusting U46619 concentration. Concentration-response curves to NaHS were obtained 20 minutes after any inhibitors or antagonists were applied. At the end of each experiment, calcium free Krebs' was administered to define 100% relaxation. Figure 2.4 is a schematic illustrating the U46619 induced tone protocol.

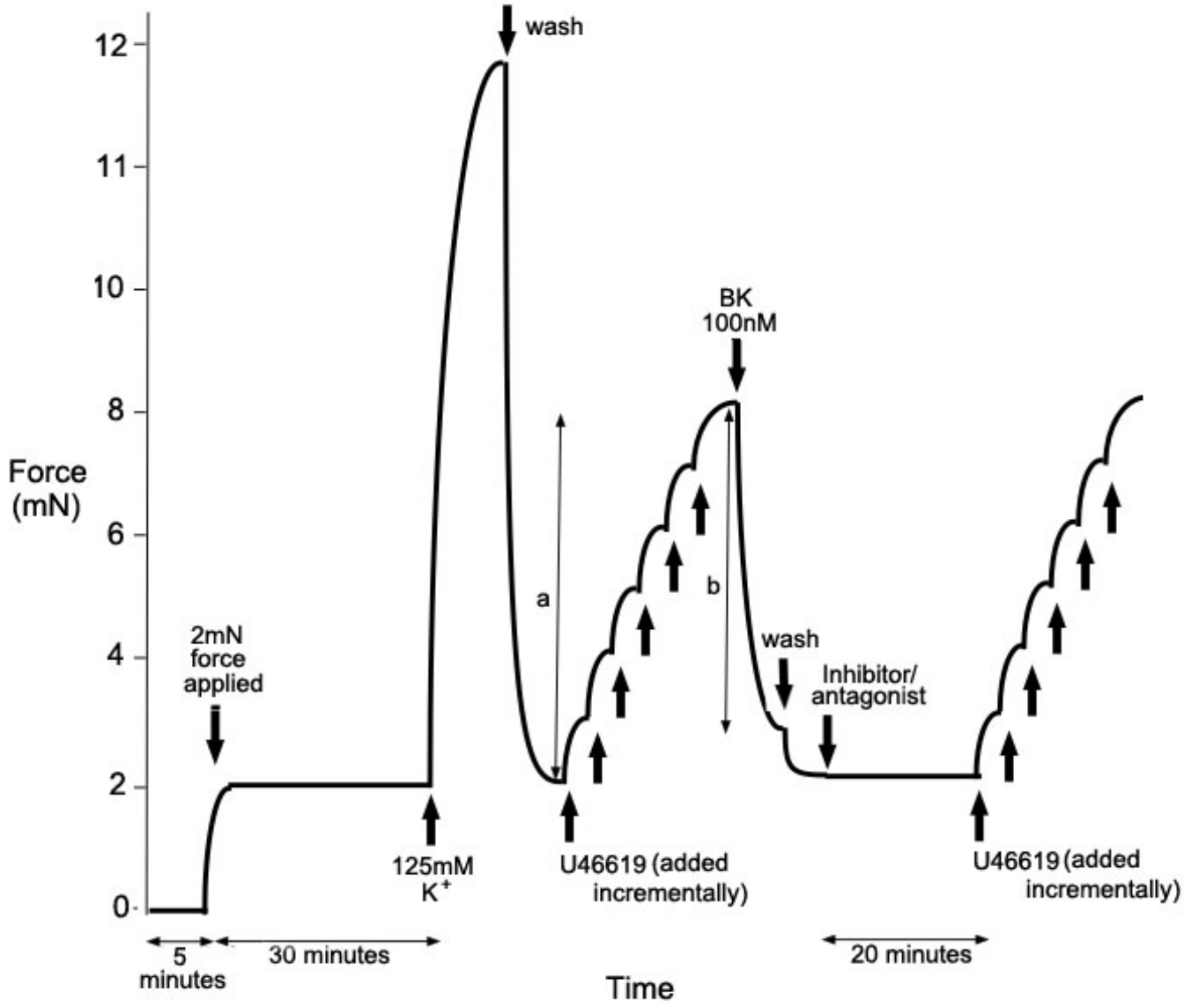

Figure 2.4 U46619 induced tone protocol
Segments were equilibrated at a tension of 2 mN for 30 min before application of 125 mM K^+ to maximally contract the vessels. They were then washed, followed by addition of incremental concentrations of U46619 to contract the vessels to approximately 50% of the maximal contraction. To assess the viability of the endothelium, bradykinin (BK, 100 nM) was applied. Vessels attaining a dilation 'b' of greater than 70% of the U46619 induced contraction (a), were regarded as having intact endothelium. Any inhibitor or antagonist was applied prior to the second U46619 induced contraction.

Constriction to calcium replacement

In a separate set of experiments, the ability of NaHS to influence vascular tone via Ca^{2+} influx through VGCC was assessed. In these experiments a 2mN force was applied to the vessels and the tone was allowed to stabilise for 10 minutes before application of 125mM KCl to assess viability and maximum contractile capacity. The vessels were washed and then incubated in calcium-free Krebs' in the presence of 100 mM KCl (to depolarise the smooth muscle cells, and thus open the VGCCs) for 30 minutes. A concentration response curve to the replacement of $CaCl_2$ in half log unit increments (10 μM-100 mM) was then obtained. The curves were constructed in the presence or absence of nifedipine (3 μM, as a positive control) or NaHS (100 μM-10 mM). Nifedipine was added 20 min prior to construction of the $CaCl_2$ concentration-response curve, whereas NaHS was applied 5 min before the $CaCl_2$ concentration response curve, to minimise the possibility of loss of H_2S as gas from the bath. Each vessel segment was used to obtain only one concentration-response curve. Figure 2.5 is a schematic illustrating the protocol for constriction to calcium replacement.

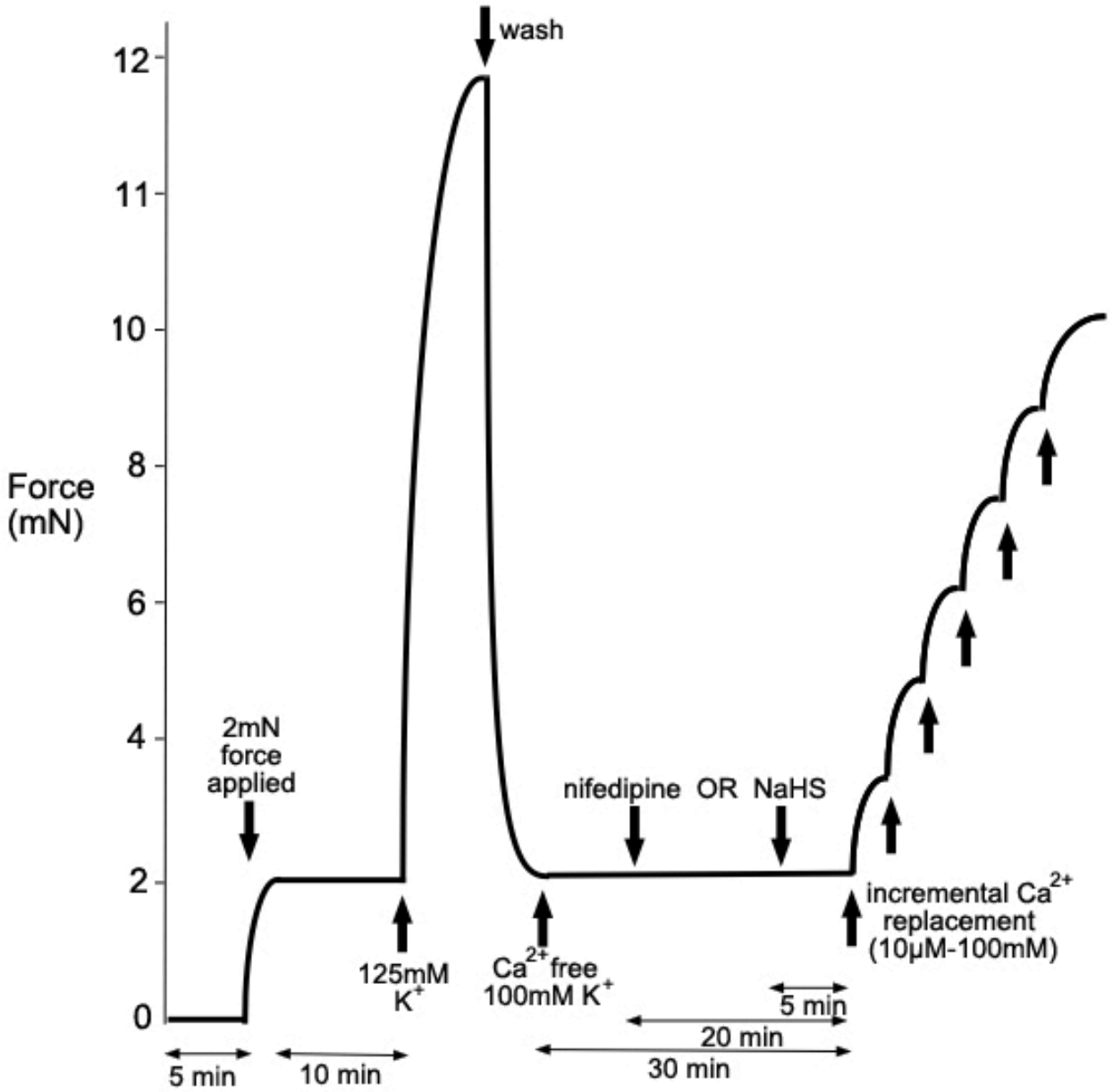

Figure 2.5 Constriction to calcium replacement

After 5 min equilibration, a 2 mN force was applied to the vessels and the tone was allowed to stabilise for 10 minutes. 125 mM KCl was then applied, and vessels were subsequently washed. The vessels were then incubated in calcium-free Krebs' in the presence of 100 mM KCl for 30 minutes. Nifedipine (20 min prior) or NaHS (5 min prior) was applied before a concentration response curve to the replacement of $CaCl_2$ in half log unit increments (10 µM-100 mM) was constructed.

2.3.3 Analysis

Relaxation was expressed as a percentage reversal of the baseline tone prior to NaHS administration, with the final response to calcium free Krebs' defined as 100%. The initial increase in tone caused by each addition of NaHS was also analysed. This increase in tone was expressed as a percentage of the change in tone induced by the relevant preconstriction protocol. For constriction to calcium replacement experiments, the increase in tone was calculated as a percentage of the 125 mM KCl-induced tone.

Average E_{max} (maximum relaxation) and average maximum constriction (caused by calcium replacement, or NaHS addition) were calculated and compared between the groups using the Student's t-test or one-way ANOVA, followed by comparison between individual groups and control using Dunnett's test for multiple comparisons, where appropriate. Individual concentration response curves were each fitted to a sigmoidal curve, and each $logEC_{50}$ (log of concentration of agonist causing 50% relaxation) was calculated. $LogEC_{50}$ values were compared and analysed for differences using the Student's T-test or one-way ANOVA, followed by comparison between individual groups and control using Dunnett's test for multiple comparisons, where appropriate.

All statistical analyses were carried out using Graphpad Prism®, version 5. Results are expressed as mean ± SEM, and statistical significance was accepted at the $P<0.05$ level. *n* values refer to the number of artery segments from separate animals.

2.4 Diabetic Studies

2.4.1 Induction of a diabetic model: streptozotocin treatment

Backgound

Streptozotocin (STZ), derived from the mould, *Streptomyces griseus*, is a glucose analogue, comprised of a glucose moiety attached to a highly reactive nitrosourea group (Bolzan *et al.*, 2002). It selectively accumulates in pancreatic beta cells via the GLUT2 glucose transporter (Tjalve *et al.*, 1976), followed by a splitting of the molecule into its composite moieties. The nitrosourea group then alkylates DNA (Bennett *et al.*, 1981), resulting in cytotoxicity to the pancreatic beta cells. STZ doses of 50-60 mg/kg intravenously lead to hyperglycaemia (20-30mM) (Wei *et al.*, 2003). After 8-10 weeks, the model induces many of the signs and symptoms characteristic of chronic Type 1 diabetes, including micro- (Maric-Bilkan *et al.*, 2012) and macrovascular pathology (Mavrikakis *et al.*, 1998; Searls *et al.*, 2012).

Protocol

Male Sprague Dawley rats were obtained at 5 weeks of age for the diabetic group. A period of 1 week was allowed for animals to acclimatise before any experimental manipulations were undertaken. Animals were then fasted for 12 hours followed by administration of STZ (50 mg/kg) in sodium citrate buffer (10 mM, pH 4.5) via tail vein injection. Development of diabetes was confirmed one week after STZ injection and again on the day of experiment by a non-fasting blood glucose of > 15 mmol/L, read using an Accu-Check Performa® blood glucose meter (Roche diagnostic, Castle Hill, NSW). Diabetic animals were housed until 16 weeks of age before experiment, to allow for development of vascular disease. Animals for the control group were obtained at 15 weeks and housed until 16 weeks before exsanguination.

2.4.2 Lucigenin Assay

Background

The lucigenin assay is an assay for $O_2^{\cdot -}$ production using lucigenin-enhanced chemiluminescence. Lucigenin is a di-acridium compound which emits light upon reaction with superoxide. This reaction involves an initial reduction of lucigenin (Luc^{2+}) to form a radical anion $Luc^{\cdot +}$, followed by a radical-radical coupling of $Luc^{\cdot +}$ to $O_2^{\cdot -}$. This coupling leads to the formation of an unstable dioxetane intermediate, which emits light upon return to the ground state (Okajima *et al.*, 2003). The emitted light is measured using a microplate reader. The lucigenin assay is a reliable method of $O_2^{\cdot -}$ detection, since it is highly selective and sensitive to $O_2^{\cdot -}$ production, and is also able to detect intracellular $O_2^{\cdot -}$, due to the cell permeability of lucigenin (Afanasev, 2009).

Tissue collection

MCA were utilised in the wire myogaphy experiments. In the interest of animal ethics, alternate cerebral arteries were utilised in the lucigenin assay. Cerebral arteries utilised for the lucigenin assay were the basilar artery and the arteries forming the circle of Willis - the posterior communicating arteries, posterior cerebral arteries and anterior cerebral arteries (see figure 1.3, p.30). The basilar artery, circle of Willis and thoracic aorta from diabetic male Sprague Dawley rats and their age-matched controls were dissected and cleaned of connective tissue. Arteries from the circle of Willis and the basilar artery were pooled and divided in half for separate treatments in the lucigenin assay (one rat had only enough cerebral vascular tissue for 2 separate treatments). The thoracic aorta was cut into several 2mm segments for analysis using the lucigenin assay.

Detection of vascular superoxide by lucigenin enhanced chemiluminescence

Reagent preparation: On the day of experiment, HEPES buffered Krebs' solution (composition (mM): HEPES, 20; NaCl, 2.5; KCl, 2.5; $CaCl_2$, 2.7; $MgCl_2$, 1; glucose, 16; pH adjusted to 7.4 using HCl) was prepared for use as a vehicle and incubation solution. Solutions of lucigenin, NADPH and diethyldithio-carbamic acid (DETCA) were prepared on the day and NaHS was prepared immediately before use. All were dissolved in HEPES buffer. Aliquots of diphenyleneiodonium (DPI) dissolved in dimethylsulfoxide (DMSO) were prepared prior to the experimental day and stored at -20˚C.

Stimulation and measurement of superoxide production: The following protocol was used to observe the effects of a prior incubation of H_2S on NADPH oxidase stimulated superoxide production. All segments underwent three treatments in separate 2 mL wells, before reading in a 96-well Optiplate (PerkinElmer, Waltham, USA). The treatments comprised of an initial 30 min incubation, followed by a 45 min incubation and finally a 2 min wash, all at 37 ˚C. The initial 30 min incubation wells contained either: HEPES buffer alone (control), or in the presence of DPI 5 μM, as a positive control to inhibit NADPH oxidase stimulated $O_2^{\cdot-}$ production, or NaHS 100 μM. DPI is a flavoprotein inhibitor (Selemidis *et al.*, 2008), and will therefore inhibit NADPH oxidase. For DPI treated vessels, all subsequent treatments, as well as the Optiplate, contained DPI 5 μM, whereas NaHS treated vessels were treated with NaHS 100 μM only during the initial 30 min incubation. The subsequent 45 min incubation contained NADPH 100 μM to stimulate $O_2^{\cdot-}$ production and DETCA (3 mM) to inhibit breakdown of $O_2^{\cdot-}$ by SOD. Vessels were then transferred to the 2 min wash, containing NADPH 100 μM plus or minus DPI 5 μM, to wash off DETCA. Finally, vessels were transferred to the appropriate well of a 96-well Optiplate containing 300 μL of a solution of NADPH 100 μM plus lucigenin 5 μM and the plate was read in the Polar star microplate reader (POLAR star OPTIMA (BMG LABTECH)) for 12 cycles. A background fluorescence

reading had been previously performed on the vessel-free solution in the Optiplate. At the end of the experiment, tissues were transferred to foil and dried in an oven at 50˚C overnight, before weighing. Figure 2.6 illustrates the protocol for stimulation and measurement of $O_2^{\cdot-}$ production diagrammatically.

Data Analysis

To calculate the amount of superoxide generated by each vessel segment, the background reading was subtracted from the average of the 12-cycle reading performed in the presence of tissue. Superoxide generation was then normalised to tissue weight, by dividing by the weight of the dried sample.

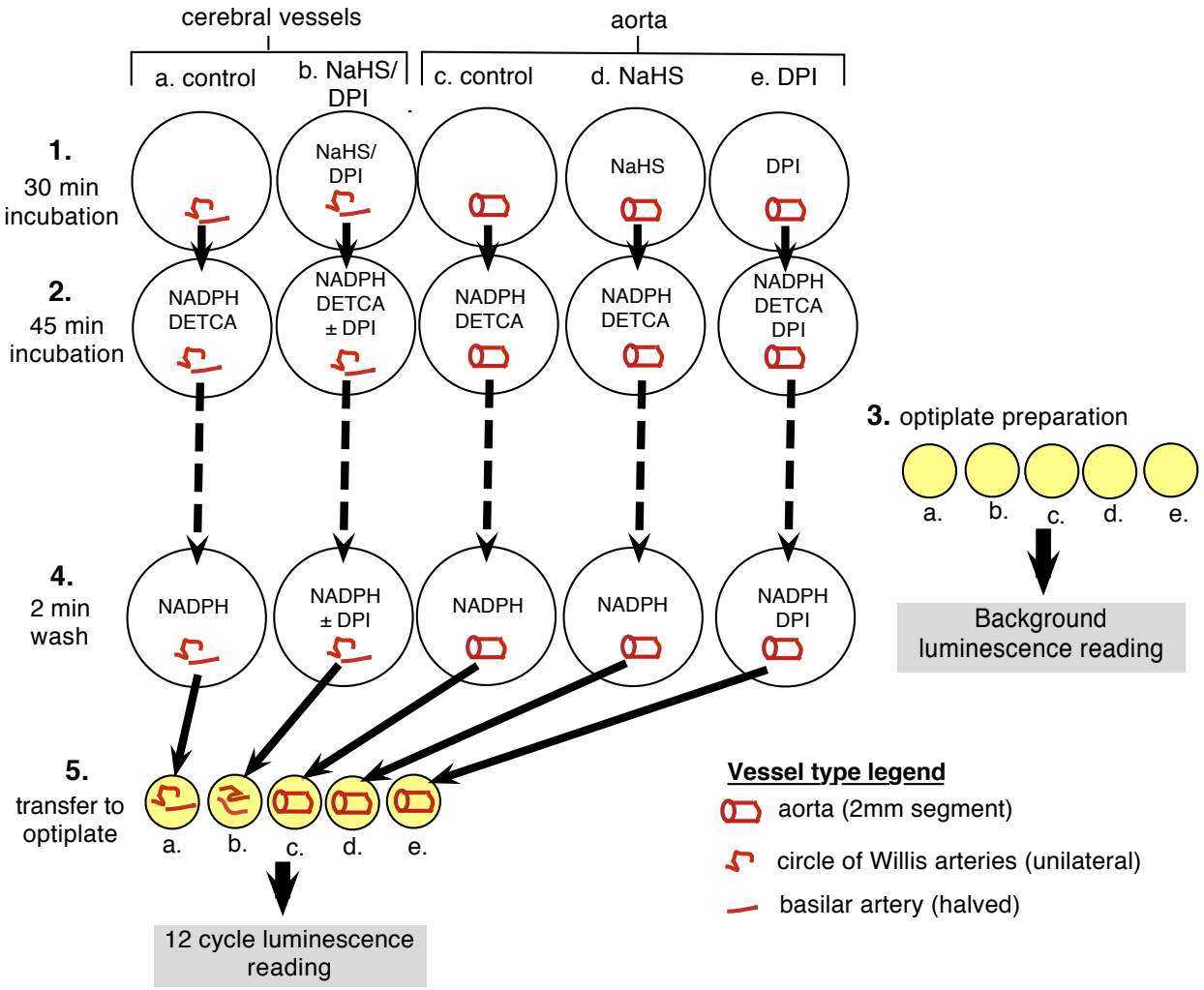

Figure 2.6 Lucigenin assay for superoxide production

Segments of cerebral vessels (a and b) and aorta (c, d and e) each underwent three treatments in 2 mL wells before reading in a 96 well Optiplate. The treatments for cerebral vessels and aorta were identical, except that there was only one treated cerebral vessel (b) for each animal, as compared to two treated aortas (d and e) for each animal. First, segments were incubated in either: HEPES buffer alone (control, a and c); DPI 5µM (b and e); or NaHS 100µM (b and d). For DPI treated vessels (e ± b) all subsequent treatments, as well as the Optiplate, contained DPI 5 µM. Secondly, vessels underwent a 45 minute incubation in NADPH 100µM and DETCA 3 mM. A 96-well Optiplate was prepared by pipetting 300µL of a solution of NADPH 100 µM plus lucigenin 5µM into several wells (one well for each vessel preparation) and a background reading for luminescence was performed. Meanwhile, segments were transferred to their third treatment, a wash containing NADPH. Finally, segments were transferred to the appropriate wells of the Optiplate, and a 12-cycle reading for luminescence was performed. Note: since one rat had only enough cerebral vascular tissue for 2 separate assays (a and b), the NaHS and DPI treatments were performed in separate animals (b= NaHS OR DPI treated).

2.5 Assays for H_2S producing enzymes

2.5.1 Detection of H_2S-producing enzymes via SDS-PAGE and western blotting

WKY rat brains were used for western blot analysis of CSE and CBS. The RVLM (n = 3) or hypothalamic PVN (n = 3) were punched out from frozen sections encompassing the entire rostral – caudal extent of each nucleus, using a blunted 20G needle. For the PVN, the tissues from three animals were combined, as were those from the RVLM. The tissues were homogenised and suspended in sample buffer (sample buffer composition: 5% v/v Glycerine, 2.5% v/v mercaptoethanol, 1.5% w/v SDS, 0.05 M TRIS/HCl pH 8, 0.05mg/ml bromophenol blue). Samples were then heated to 65 °C for 10 minutes. Protein concentration was determined from each sample and the samples were loaded onto 10% gels and separated by SDS-PAGE. After transfer to poly-vilidene difluoride membranes the blots were incubated with primary antibodies suspended in blocking buffer overnight (rabbit anti-CSE antibody, (Proteintech Group Inc, USA) and mouse anti-CBS antibody (Abnova corporation, Taiwan)). The blots were then incubated with the appropriate secondary antibody (goat anti-Rabbit, goat anti-mouse) conjugated to horseradish peroxidase for 1 hr then developed by enhanced chemiluminescence (Millipore Kit). Dual colour marker (Bio-Rad) was used for molecular weight determination. Recombinant protein of CSE and CBS (GST tagged) (Abnova, Taiwan) were loaded on the gel to identify the band of interest.

2.5.2 Detection of H_2S-producing enzymes via immunohistochemistry

Preparation of PVN sections

WKY brains which had been microinjected into the RVLM (in the hind brain) were retained in their entirety, so that the hypothalamus (in the mid brain) could be investigated by immunohistochemical analysis. After fixing in a solution of 4% w/v paraformaldehyde and 20% w/v sucrose for one week, the hypothalamus was cut on a cryostat into 40 μm-thick sections and mounted onto gelatin-subbed slides. The sections were then viewed wet by microscopy, and sections containing the PVN were identified by the proximity of the fornix to the third ventricle. The PVN was then identified as the region around the third ventricle which appeared darker due to the density of neurons in the PVN. The PVN-containing sections were outlined using an ImmEdge® hydrophobic barrier pen (Vector Laboratories, Burlingame, UK) and allowed to dry for 1.5 hours.

Preparation of MCA

MCA from Sprague Dawley rats were dissected and carefully cleaned of connective tissue. They were then placed in 4% w/v paraformaldehyde in phosphate buffered saline (composition (mM): Na_2HPO_4 203; KCl 53.6; KH_2PO_4 35.3; NaCl 2.74) for 10 min.

Antigen retrieval, blocking and permeabilisation

Hypothalamic sections and MCA were transferred to citrate buffer (citric acid 10mM, Triton X 0.05% v/v, adjusted to pH 6 using sodium hydroxide) and microwaved in a 200 W microwave oven for 30 sec for antigen retrieval. For blocking and permeabilisation, the tissue was incubated in 2% v/v rabbit serum and 0.5% v/v Triton X in citrate buffer for 1 hr.

Antibody incubation

Several sections from one brain were then incubated in a mouse monoclonal CBS primary antibody (1:50, M01, ABNOVA), prepared in a solution of phosphate buffer plus 2% v/v rabbit serum, for 18hr at room temperature. Several other sections from the same brain were incubated in the solution alone for 18 hr at room temperature. Similarly for the MCA, several segments were incubated with a mouse monoclonal anti- CSE primary antibody (1:50, ABNOVA) in a solution of citrate buffer plus 2% v/v rabbit serum, whilst other segments were incubated in the solution alone, both for 18 hr at 4˚C. All tissues were then incubated with TRITC-conjugated rabbit anti-mouse secondary antibody (1:50, Dako Cytomation) for 2 hr at room temperature. Finally a Hoechst fluorescent nuclear stain (1:500 (25µg/mL), Thermo Scientific) was applied for 10 min at room temperature. Fluorescent mounting medium (Dako Cytomation) was used to mount the vessels onto slides which were coverslipped then imaged using a C1 confocal mounted on a Nikon Eclipse 90i laser-scanning microscope.

2.5.3 Detection of CSE via RT-PCR

RNA Extraction and Quantification

MCA were collected as described earlier (section 2.3.1) and stored in RNAlater® solution (Invitrogen, Australia) at -20 ˚C. For RNA extraction, MCA were removed from RNAlater® solution and placed in 1 ml of TRIzol® (Invitrogen, Australia) and homogenised with a handheld, motorised Teflon pestle. Samples were allowed to stand for several minutes, after which 200 µl chloroform was added and the sample vigorously shaken. Samples were allowed to stand for 5 min and spun at 12,000 g for 15 min at 4 ˚C after which the upper aqueous phase was transferred to a new tube. The aqueous phase was precipitated by mixing with 500µl ice-cold isopropanol alcohol. Samples were incubated at -20˚C for 1 hr and then centrifuged at 13,200 g for 15 min at room temperature. The supernatant was removed and the resulting pellet was washed with 200 µl of 75% ethanol in RNase-free water. After

centrifugation at 13,200 g for 10 min at room temperature, the ethanol supernatant was removed and the RNA pellets were left to air-dry for 5–10 min before being re-dissolved in 40 µl of RNase-free water by mixing and then incubating at 55˚C for 10 min. The quality and quantity of extracted RNA was determined on a NanoDrop 1000 spectrophotometer (Nanodrop Technologies, Wilmington, USA) by measuring absorbance at 260 nm and 280 nm with a 260/280 ratio of ~ 1.7 recorded for all samples. The RNA samples were diluted as appropriate to equalise concentrations, and stored at -80˚C for subsequent reverse transcription.

Reverse Transcription and Real-Time PCR

First-strand complementary DNA (cDNA) synthesis was performed using commercially available TaqMan Reverse Transcription Reagents (Invitrogen, Melbourne, Australia) in a final reaction volume of 20 µL. A negative sample containing a randomly chosen sample with no Reverse Transcriptase (Superscript®) was prepared to demonstrate an absence of PCR products in amplifications of cDNA during the real-time PCR cycling. A serially diluted pooled RNA sample from the control group was produced and also included to ensure efficiency of reverse transcription and for calculation of a standard curve for real-time quantitative polymerase chain reaction (RT-PCR). All RNA, negative control and standard samples were reverse transcribed to cDNA in a single run from the same reverse transcription master mix. Quantification of mRNA (in duplicate) was performed on a 72-well Rotor-Gene 3000 Centrifugal Real-Time Cycler (Corbett Research, Mortlake, Australia). Taqman-FAM-labelled primer/probe for cystathionine gamma-lyase (Cat No. Rn00567128_m1) was used in a final reaction volume of 20 µL. PCR conditions were 2 min at 50 ºC for UNG activation, 10 min at 95 ºC then 40 cycles of 95 ºC for 15 s and 60 ºC for 60 s. 18S ribosomal RNA (18S rRNA) (Cat No. Hs99999901_s1) was used as a housekeeping gene to normalise threshold cycle (CT) values. The relative amounts of mRNAs were calculated using the relative quantification (ΔΔCT) method (Livak *et al.*, 2001).

2.5.4 Measurement of plasma and liver H_2S

Background

In the present thesis, H_2S generation from liver samples was used to determine CSE activity, via a method developed by Stipanuk and Beck (Stipanuk *et al.*, 1982). The Stipanuk and Beck assay involves the generation of H_2S from tissue by addition of substrate, L-cysteine (for exact details, see below), trapping of H_2S using zinc in solution, and subsequent measurement of the H_2S formed using a colourimetric assay. The colourimetric assay involves the addition of N,N-dimethylphenyldiamine sulphate (NNDP) followed by ferric chloride ($FeCl_3$). Under acidic conditions, NNDP is oxidised by Fe(III), forming an intermediate compound which is then reduced by H_2S to form the phenothiazinium dye, methylene blue (Boltz, 1978). To date, this remains a commonly used method for determination of CSE activity (Brancaleone *et al.*, 2008; Dal-Secco *et al.*, 2008; Li *et al.*, 2011; Yang *et al.*, 2011), since the methylene blue assay allows for specific detection of low micromolar concentrations of H_2S in multiple samples (Siegel, 1965).

In the present thesis, the methylene blue assay was also used to detect H_2S in plasma samples. Application of the methylene blue assay to measurement of free H_2S levels in biological samples has been criticised, since the acidic conditions likely release H_2S from acid labile sulfur stores (Furne *et al.*, 2008). Despite the multiple analytical techniques which have been developed for measurement of H_2S levels, all have limitations to application in biological samples, and most cannot be performed in physiological conditions (for review, see (Olson, 2012)). The present thesis acknowledges the limitation of the methylene blue assay to applications measuring free H_2S in biological samples, and refers to the H_2S measured in plasma as 'sulfide', as it is likely a reflection of both free H_2S and H_2S liberated from acid labile stores. It is noteworthy that acid labile sulfur is unlikely to have contributed to measured H_2S levels in the CSE activity assay, since negative control samples (lacking the substrate, L-cysteine) produced negligible H_2S, which was undetectable using the methylene blue assay (data not shown).

Assay of liver H_2S synthesis: measurement of CSE activity

CSE activity was measured in liver, since it has been demonstrated that CSE expression is relatively high in hepatic tissue (Bao *et al.*, 1998). Liver H_2S synthesising activity was measured using the assay developed by Stipanuk and Beck (Stipanuk *et al.*, 1982), with modifications. Briefly, liver tissue was weighed and homogenised using a Pro Scientific 200 electric homogeniser, then diluted 1 in 10 w/v in ice-cold phosphate buffer (composition (mM): K_2HPO_4, 77.6; KH_2PO_4 22.4). Protein concentration was determined using the Bradford assay (Bio-Rad Laboratories, Milano, Italy). Each liver homogenate was then assayed in triplicate for H_2S synthesising capacity, by adding L-cysteine (1 M, 5 µL), PLP (200 mM, 5 µL) and phosphate buffer 10 µL to 480 µL of homogenate, in 1.5mL eppendorfs. To confirm that H_2S production was due to CSE, a positive control was prepared for each liver homogenate, contents as above, except phosphate buffer was replaced with PPG (0.5 M, 10 µL). Negative controls containing PLP (200 mM, 5 µL) and phosphate buffer 15 µL (without L-cysteine substrate) in 480 µL of homogenate were prepared for n = 3 liver homogenates in each group. Eppendorfs were sealed using parafilm and the reaction was initiated by transferring to a shaking water bath at 37 ºC. After incubation for 30 min, zinc acetate (1% w/v, 250 µL) was injected into each eppendorf to trap the generated H_2S. Subsequently, trichloroacetic acid (10% w/v, 250 µL) was injected into each eppendorf, to precipitate the protein, thus stopping the reaction. 80 µL of each sample was then added to 560 µL of water, followed by addition of NNDP (20 mM, 80 µL) in 7.2 M HCl then $FeCl_3$ (30 mM, 80 µL) in 1.2 M HCl. Standard concentrations of NaHS were prepared (0-5000 µM, *n*=14), and 80 µL of each was again added to 560 µL of water, followed by addition of NNDP (20 mM, 80 µL) in 7.2 M HCl then $FeCl_3$ (30 mM, 80 µL) in 1.2 M HCl. The sample solutions were vortexed at 9,000 g for 1 min, and 250 µL of each sample and standard was pipetted into a 96-well plate (Sarstedt, Newton, NC, USA). 20 min after the addition of $FeCl_3$,

the absorbance was measured at 670 nm in a Multiskan® Spectrum spectrophotometer (Thermo Scientific).

Determination of plasma sulfide content

Determination of sulfide in plasma was performed without addition of L-cysteine or PLP. Plasma samples (80 μL) were added to zinc acetate (1% w/v, 80 μL), followed by addition of trichloroacetic acid (10% w/v, 80 μL). Standard concentrations of NaHS were prepared (0-200 μM, n = 12), and 80 μL of each was also added to zinc acetate (1% w/v, 80 μL), followed by addition of trichloroacetic acid (10% w/v, 80 μL). Subsequently, NNDP (20 mM, 80 μL) in 7.2 M HCl was added to each of the samples and standards, followed by $FeCl_3$ (30mM, 80 μL) in 1.2 M HCl. The sample solutions were vortexed at 9,000 g for 1 min, and 250 μL of each sample and standard was pipetted into a 96-well plate (Sarstedt). 20 min after the addition of $FeCl_3$, the absorbance was measured at 670 nm in a Multiskan® Spectrum spectrophotometer.

Analysis of plasma sulfide content, and liver CSE activity

The final H_2S concentration in treated plasma and liver samples was calculated against the calibration curve of the appropriate NaHS standards. For plasma, the calculated value was referred to as plasma sulfide concentration (as discussed above, under background p.90) and expressed in μM. The difference between diabetic and control plasma sulfide concentration was compared using the Student's t-test. For liver samples (CSE activity), the amount of H_2S was calculated by multiplying by the volume of homogenate (0.048 L). Results were then divided by the number of minutes of reaction (30 min) and normalised to protein content (mg). For CSE activity, results were thus expressed as amount of H_2S produced per mg of protein per minute (nmol per mg per min), and the difference between diabetic and control H_2S production rate was compared using the Student's t-test.

2.6 Materials

2.6.1 Chemicals

9-Amino-5-imino-5H-benzo[a]-phenoxazine salt, (cresyl violet) (Sigma Chemical CO, MO, USA)
4-aminopyridine (Sigma, A0152)
Apamin (Sigma, A9459)
Barium chloride-dihydrate (Merck, A749419 719)
Catalase (Simga, C-10)
Charybdotoxin (Sigma, C7802)
Diethyldithio-carbamic acid (DETCA) sodium salt (Sigma, D-3506)
Dimethylsulfoxide (Sigma-Aldrich, 472301)
D-glucose anhydrous (APS Finechem, 50-99-7)
4,4'-Diisothiocyanatostilbene-2,2'-disulfonic acid disodium salt hydrate (Sigma, D3514)
Diphenylene iodonium (Sigma, D-2926)
DL-Propargylglycine (Sigma, P7888)
Ferric chloride, anhydrous (Merck, S4976445807)Glibenclamide (Sigma, G-0639)
heparin (5000IU/5mL vials, Pharmacia Australia, Rydalmere, NSW, SIN5192P)
Hydroxylamine hydrochloride (Sigma, 159417)
Indomethacin (Sigma I-7378)
L-glutamic acid (glutamate) (Sigma G-1626)
L-N^G-Nitroarginine methyl ester (L-NAME) (Sigma, N5751)
HEPES, Free acid, ULTROL Grade (EMD chemicals, Inc. San Diego, CA, cat#391998)
HEPES sodium salt (Sigma, H3784)
4-hydroxy-TEMPO (tempol) (Aldrich, 17, 614-1)
Hypoxanthine (Sigma, H9377)
β-nicotinamide adenine dinucleotide 2'-phosphate reduced tetrasodium salt hydrate (Sigma, N1630)
Nifedipine (Sigma, N7634)
Niflumic acid (Sigma, N0630)
N,N'-dimethyl-9,9'-biacridium dinitrate, (lucigenin) (Sigma, M8010)
N,N-Dimethyl-p-pheylenediamine sulfate salt (Sigma, D-4790)
O-(Carboxymethyl)hydroxylamine hemihydrochloride (amino-oxyacetate) (Aldrich, C13408)
Paraformaldehyde (Sigma, P6148)
Phenylephrine (Sigma, P6125)
Pyridoxal 5'- phosphate hydrate (Sigma, P9255)
Sodium hydrogen carbonate (APS Finechem, 144-55-8)
Sodium hydrosulfide hydrate (sodium hydrogen sulfide) (Sigma, 161527)
Streptozotocin (Sigma, S01030)
Sucrose (Merck, 10274.7E)
Superoxide Dismutase (Sigma, S7571)
Trichloroacetic acid (BDH chemicals, 10286)
urethane (Sigma, U2500)
Xanthine oxidase, from bovine milk (Sigma, X4376-25UN)
Zinc acetate dihydrate (Sigma, Z0625)

2.6.2 Products

Antifoam (Sigma, A5758)
Depex mounting medium (BDH Lab Supplies, Poole, UK)
Delvet isoflurane inhalation anaesthetic (Delvet Pty Ltd, Seven Hills, NSW, AP/DRUGS/220/96)
ImmEdge® hydrophobic barrier pen (Vector Laboratories, Burlingame, UK)
Kwik-Cast Sealant (WPI, USA)
Lethabarb (pentobarbitone 325mg/mL,Virbac animal health, 1P064 3-2)
Rhodamine (LumaFluor, NC, USA)
RNAlater® Soln (Ambion, AM7024)
Triton X-100 (BDH, 30632)
TRIzol® (Invitrogen, 15596-026)

Chapter 3: The role of hydrogen sulfide in the RVLM and PVN in cardiovascular regulation

3.1 Introduction

H_2S has several neuromodulatory effects, as well as peripheral cardiovascular actions (Gadalla *et al.*, 2010; Kimura, 2002; Mustafa *et al.*, 2009a). The first demonstration that H_2S could act as an endogenous biological mediator was by Kimura et al. in 1996, and showed that H_2S facilitated long-term potentiation in the rat hippocampus (Abe *et al.*, 1996). H_2S has also been shown to induce calcium waves in rat astrocytes (Nagai *et al.*, 2004) and protect against neurodegenerative diseases including Alzheimer's Disease, vascular dementia and Parkinson's Disease, by attenuating oxidative stress and hypoxia induced neuronal cell death in rats (Zhou *et al.*, 2011). In the cardiovascular system, H_2S has been reported to have protective effects against cardiac ischemia-reperfusion injury in mice (Calvert *et al.*, 2009). H_2S donors, such as NaHS, have been shown to relax rat blood vessels *in vitro* (Zhao *et al.*, 2002) (Cheang *et al.*, 2010) and systemic administration of NaHS reduces rat blood pressure in a dose dependent manner (Zhao *et al.*, 2001) indicating H_2S can influence blood pressure *in vivo*.

H_2S is also produced in the central nervous system, suggesting it may have central cardiovascular actions, in addition to its peripheral effects (Gadalla *et al.*, 2010; Kimura, 2002; Mustafa *et al.*, 2009a), as is the case for the gaseous transmitter, nitric oxide. Thus, the question arises as to whether H_2S can regulate the cardiovascular system via actions in the central nervous system as well as systemically. It has been reported that H_2S acts within the posterior hypothalamus of rats to produce a small reduction in blood pressure (Dawe *et al.*, 2008). However, in another study, an infusion of NaHS into the lateral cerebral ventricle increased blood pressure in rats (Ufnal *et al.*, 2008). More recent studies indicate that H_2S can augment pre-synaptic transmission in the NTS (Austgen *et al.*, 2011), and reduces renal sympathetic nerve activity via action in the RVLM of rats (Guo *et al.*, 2011). Thus, it appears unclear as to the central cardiovascular action of H_2S. Furthermore, at the time of research,

brain regions with key regulatory cardiovascular actions, such as the RVLM and PVN, had not been investigated.

Regulating the activity of the sympathetic nervous system is a key mechanism through which the brain can influence the level of blood pressure. There are several areas in the brain that are known to influence sympathetic nerve activity via projections to the intermediolateral cell column of the spinal cord, where sympathetic preganglionic motor neurons are located. These key autonomic regions have important cardiovascular regulatory functions and include the RVLM and the PVN (Guyenet, 2006; Shafton *et al.*, 1998). The RVLM plays a pivotal role in the tonic and reflex control of sympathetic vasomotor activity, such that bilateral inhibition or destruction of neurons in the RVLM results in dramatic decreases in both arterial pressure and sympathetic vasomotor activity (Guyenet, 2006). The PVN is a major integrative nucleus that can markedly influence blood pressure, sympathetic nerve activity and the haemodynamic sequelae (Badoer, 2001; Badoer, 2010). Activation of the PVN can elicit increases or decreases in sympathetic nerve activity and blood flow (Badoer, 2001; Deering *et al.*, 2000), suggesting both sympatho-inhibitory and sympatho-excitatory outflows may emanate from the PVN.

Nitric oxide can influence neuronal function in the RVLM and PVN, and contributes to the regulation of sympathetic nerve activity in normal and pathophysiological conditions (Patel *et al.*, 2001). Whether H_2S microinjected into the RVLM can influence SNA to vascular organs other than the kidney and whether it can act in the PVN to influence SNA is unclear. Additionally, there is no data available on whether H_2S acting in those brain regions has different effects in normotensive and hypertensive conditions. Therefore, the aims of the present study were: to determine whether H_2S could alter LSNA, MAP or HR by acting within the RVLM or PVN in normotensive as well as hypertensive rats; to determine whether CBS inhibitors could alter LSNA, MAP or HR by acting within the RVLM or PVN and to establish whether CBS and CSE were present in the RVLM or PVN of rats.

3.2 Methods

3.2.1 Preparation for recording of MAP, HR and LSNA and intracerebral micro-injections

Animals were anaesthetised initially with inhaled isoflurane, and the right femoral vein was cannulated for maintenance of anaesthesia using intravenous urethane (1-1.5 g/kg IV). The right femoral artery was cannulated for recording of MAP and HR. The left lumbar sympathetic nerve was then exposed and placed onto a probe for recording of nerve activity using a MacLab data acquisition system (ADInstruments, NSW, Australia). Animals were then placed prone and the head was mounted into a Stoelting stereotaxic frame. The skull was exposed, and burr holes were drilled in the appropriate positions for either RVLM or PVN micro-injections. See 2.2.1 for a detailed description of these surgical procedures.

3.2.2 Experimental Protocol

In WKY rats, bilateral microinjections were made into the RVLM (n = 16), PVN (n = 19) and into the area adjacent to the PVN (n = 8). Animals receiving microinjections into the RVLM were given vehicle (artificial cerebrospinal fluid (aCSF) containing NaCl 124mM, KCl 3.0mM, $NaH_2PO_4.2H_2O$ 1.3mM, $MgCl_2.6H_2O$ 2.0mM, $NaHCO_3$ 26mM, glucose 10mM, $CaCl_2$ 2.0mM in Milli-Q water, buffered with carbogen), followed by either (i) five sequential doses of NaHS (0.2, 2, 20, 200 and 2000 pmol/side) or (ii) HA (0.2, and 2 nmol/side, sequentially) and AOA (0.1 and 1 nmol/side, sequentially) the order of HA and AOA was randomised. For microinjections into or out of the PVN the same protocol was followed except only three sequential doses of NaHS were administered (20, 200 and 2000 pmol/side). In SHR rats, NaHS (20-2000 pmol/side) was microinjected into the RVLM (n = 3) and PVN (n = 5). For all experiments, 10 - 15 minutes were allowed between each microinjection of drug. MAP, HR and LSNA were monitored continuously. Resting levels prior to drug administration were recorded at 20 minutes before and immediately prior to the first intracerebral microinjection. At 1, 5 and 10 min after the administration of each dose of drug,

MAP, HR and LSNA were recorded for a duration of 1-2 min. For a description of the data analysis, see 2.2.3 Data Analysis, p.71. Briefly, the average value of changes in MAP, HR and LSNA were calculated. For each parameter, the average value was subsequently compared between groups using one-way ANOVA, followed by comparisons between the individual doses of drugs and control (vehicle administration) using Dunnett's post hoc test for multiple comparisons. $P<0.05$ was considered statistically significant.

3.2.3 Histology

To mark the injection sites, a small amount of rhodamine-tagged fluorescent microspheres was included in the microinjected solution (LumaFluor, NC, USA). Brain slices from experimental animals were subsequently viewed under fluorescence microscopy to determine the exact position of injection sites (see 2.2.2 for a detailed description of histology).

3.2.4 Detection of H_2S-producing enzymes via western blotting and immunohistochemistry

Samples of PVN tissue ($n = 3$) from WKY rats were dissected and pooled, as were those from the RVLM ($n = 3$). The pooled samples were then analysed for CSE and CBS content using western blotting (see 2.5.1). The brains of several WKY rats were fixed using 4% w/v paraformaldehyde and 20% w/v sucrose for one week before sectioning the hypothalamus into 40 μm-thick sections using a cryostat. These sections were then analysed for the presence of CBS using immunohistochemistry (see 2.5.2).

3.3 Results

WKY Rats

3.3.1 Presence of CBS and CSE in RVLM and PVN

Figure 3.1a shows examples of the western blots used to determine the presence of CSE and CBS in the RVLM and PVN. The results show that the PVN and RVLM contain CBS protein. By contrast, in neither region was CSE protein detectable, despite being detected in liver and aorta (figure 3.1b). The control proteins eluted out at the expected size.

Immunohistochemical analysis showed staining for CBS within the PVN (figure 3.2). Combined staining using Hoescht nuclear stain and immunohistochemistry for CBS demonstrated that CBS was localised specifically within cells of the PVN (figure 3.2).

3.3.2 Effect of NaHS microinjected into the rostral ventrolateral medulla

NaHS (0.2 – 2000 pmol / side) microinjected into the RVLM had no significant effect on MAP, HR and LSNA compared to control (figure 3.3). This indicates that exogenous hydrogen sulfide in the RVLM did not have any major effect on MAP, HR or LSNA.

3.3.3 Effect of HA and AOA microinjected into the rostral ventrolateral medulla

The CBS inhibitors, AOA (0.1 – 1.0 nmol / side) and HA (0.2 – 2.0 nmol / side) microinjected into the RVLM did not significantly change any of the cardiovascular variables measured compared to control (figure 3.4). Thus, inhibition of the production of endogenous hydrogen sulfide in the RVLM did not have any major influence on MAP, HR or LSNA.

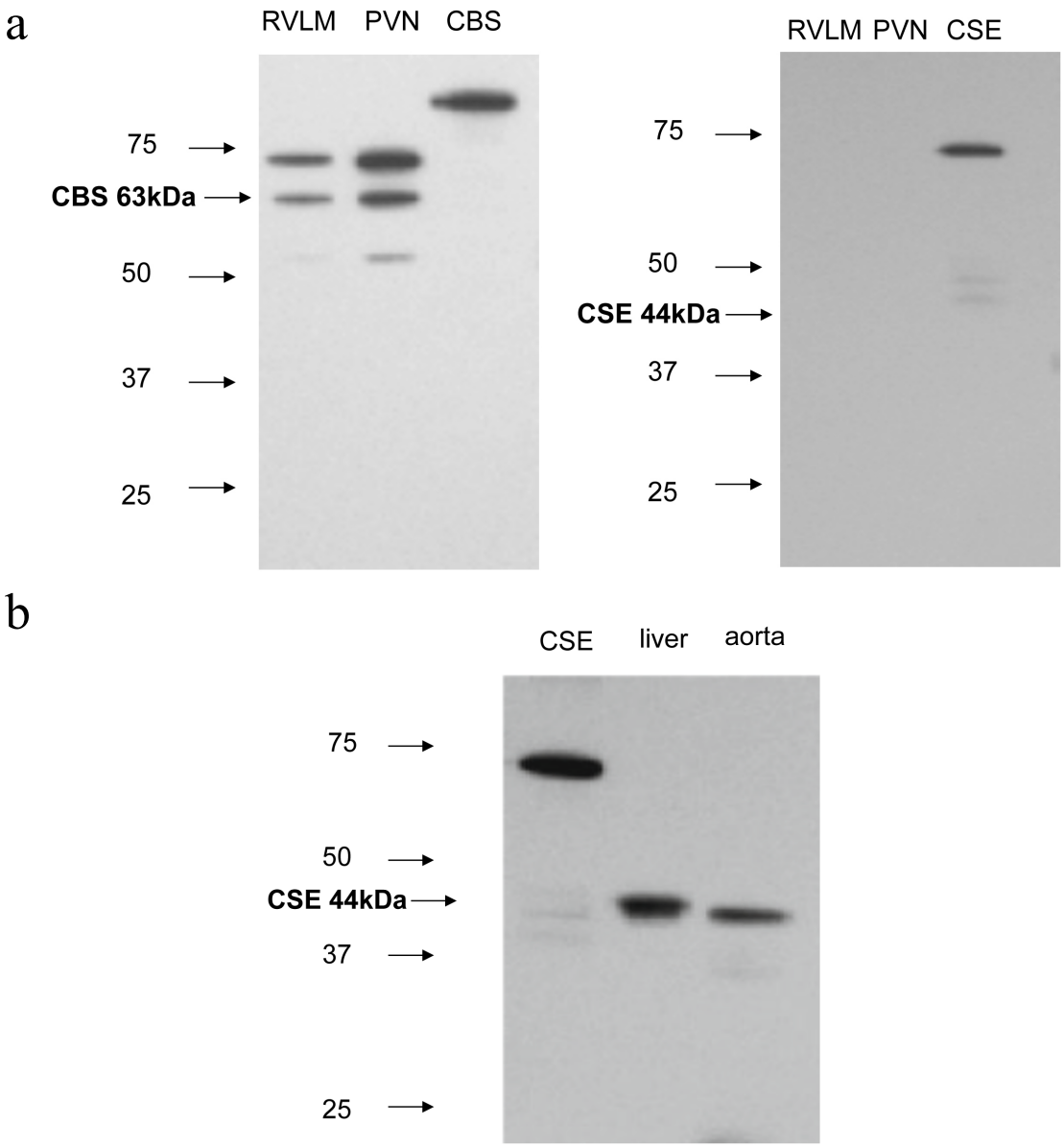

Figure 3.1 Western blots for CBS and CSE in RVLM and PVN

Typical western blots of cystathionine β lyase (CBS) and cystathionine γ lyase (CSE) in punched out homogenates of rostral ventrolateral medulla (RVLM) and hypothalamic paraventricular nucleus (PVN) **(a)**. The native CBS protein (63 kDa) was labelled in both PVN and RVLM samples. No bands for native CSE protein (44kDa) were observed in the PVN or RVLM, despite being observed in liver and aorta homogenates **(b)**. The third lanes in **'a'** and first lane in '**b**' show the GST-tagged human recombinant CBS (86kDa) or CSE (70kDa) protein.

a

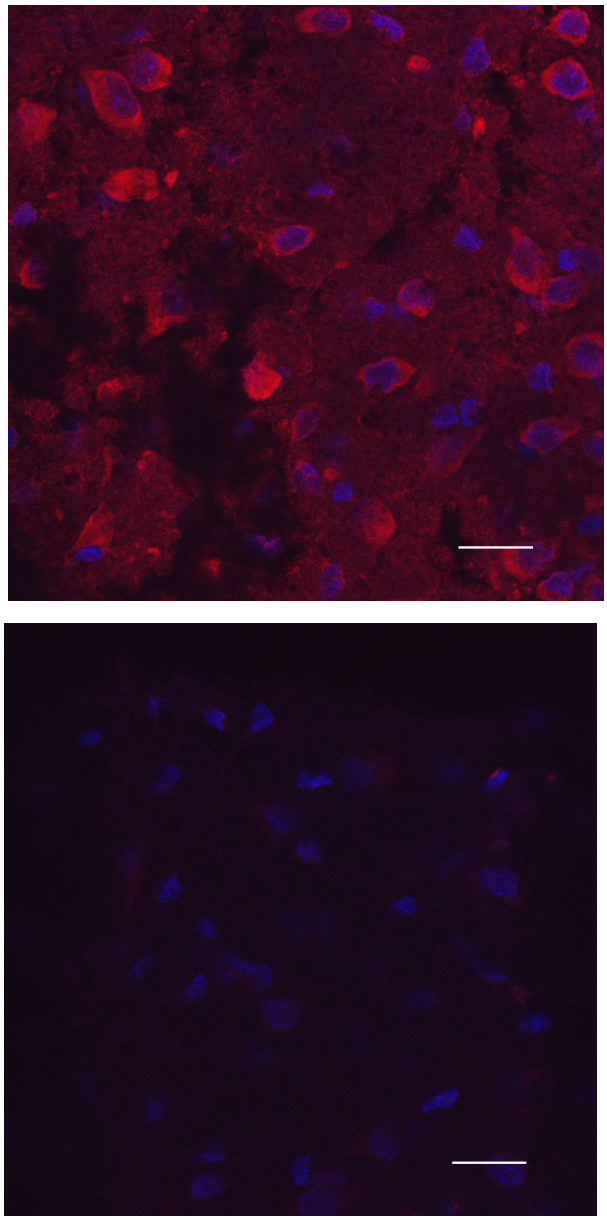

b

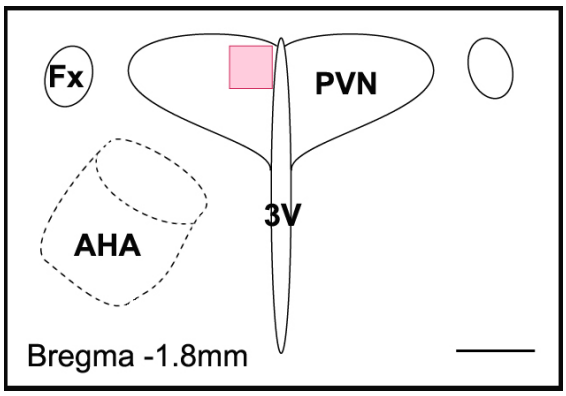

Figure 3.2 CBS staining in the PVN

(a) Immunohistochemistry images demonstrating presence of CBS within the PVN (paraventricular nucleus). Top panel is in the presence of the primary antibody for CBS, bottom panel is a negative control processed in the absence of the primary antibody for CBS. Both images show a merge of CBS (red) and Hoescht nuclei (blue) staining. No specific staining for CBS was observed in the negative control. Calibration scale bar = 20 μm **(b)** Schematic demonstrating the region of the PVN where the images in 'a' were taken (pink square). Calibration scale bar = 500 μm. Fx, fornix; AHA, anterior hypothalamic area, 3V, third ventricle.

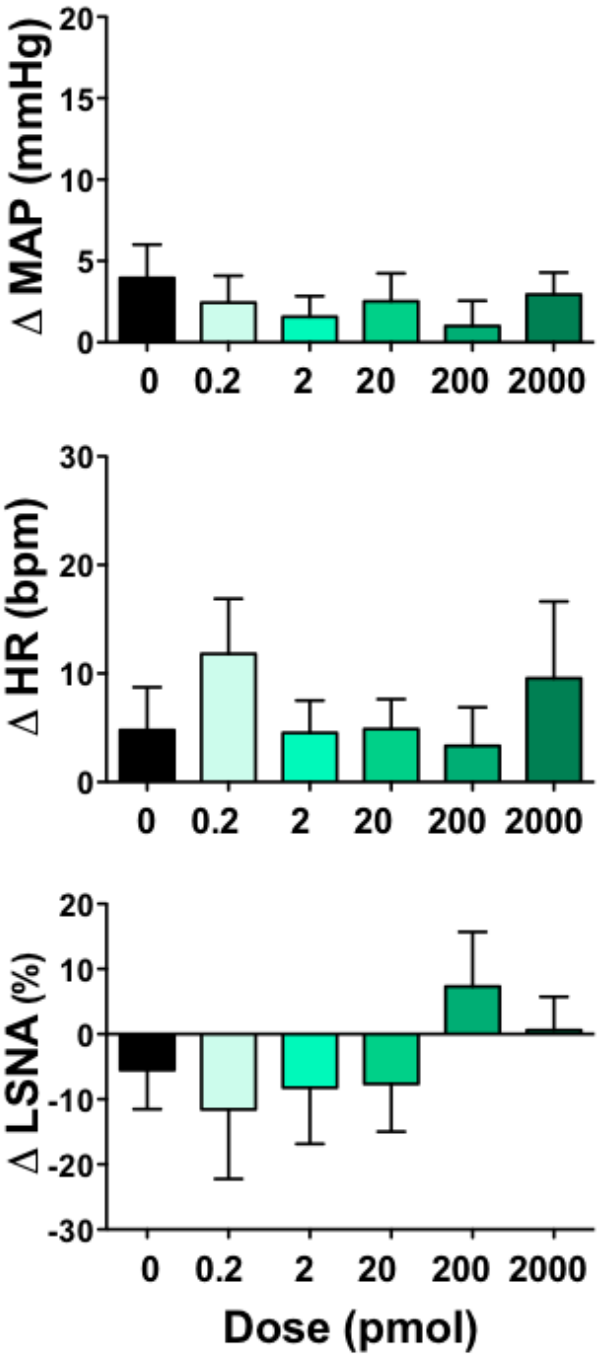

Figure 3.3 Effect of NaHS in the RVLM

Changes in mean arterial pressure (MAP), heart rate (HR) and lumbar sympathetic nerve activity (LSNA) following vehicle (n = 13 for MAP and HR and n = 6 for LSNA) and the H_2S donor, (NaHS, 0.2 – 2000 pmol/side) (n = 8 for MAP and HR and n = 5 for LSNA) microinjected into the rostral ventrolateral medulla (RVLM) of WKY rats.

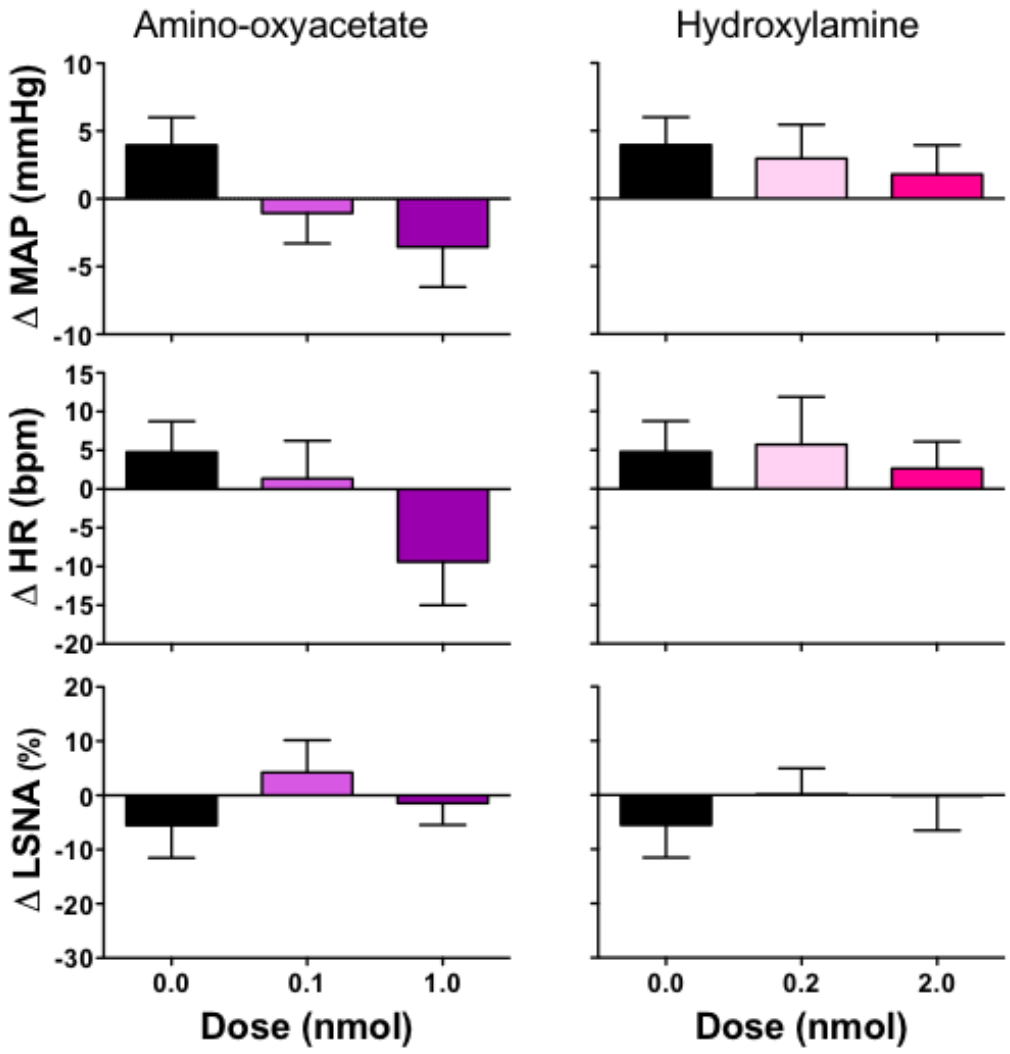

Figure 3.4 Effect of CBS inhibitors in the RVLM

Changes in mean arterial pressure (MAP), heart rate (HR) and lumbar sympathetic nerve activity (LSNA) following vehicle (n = 13 for MAP and HR and n = 6 for LSNA) and amino-oxyacetate (AOA) (0.1 – 1.0 nmol/side) and hydroxylamine (HA) (0.2 – 2.0 nmol/side) (n = 8 for MAP and HR and n = 5 for LSNA) microinjected into the rostral ventrolateral medulla (RVLM) in WKY rats. AOA and HA are inhibitors of the enzyme cystathionine β synthase.

3.3.4 Effect of NaHS microinjected into the paraventricular nucleus

The average changes in MAP, HR and LSNA following NaHS (20 – 2000 pmol) were not significantly different from control (Figure 3.5). These data indicate that exogenous hydrogen sulfide microinjected into the PVN has no significant effect on MAP, HR or LSNA. NaHS microinjected into the area surrounding the PVN also had no significant effect on MAP, HR or LSNA (figure 3.6).

3.3.5 Effect of HA and AOA microinjected into the paraventricular nucleus

Microinjection of AOA (0.1 – 1.0 nmol / side) into the PVN produced no significant change in MAP, HR or LSNA compared to control (figure 3.7). Microinjection of HA (0.2 nmol / side) into the PVN resulted in a small but significant decrease in MAP and HR compared to the control group (figure 3.7). Microinjection of the higher dose of HA (2.0 nmol / side) into the PVN, however, did not elicit any significant effect on MAP and HR compared to control (figure 3.7). Neither dose of HA had any significant effect on LSNA compared to control. Additionally, AOA and HA microinjected into the area surrounding the PVN also had no significant effect on MAP, HR or LSNA (figure 3.8).

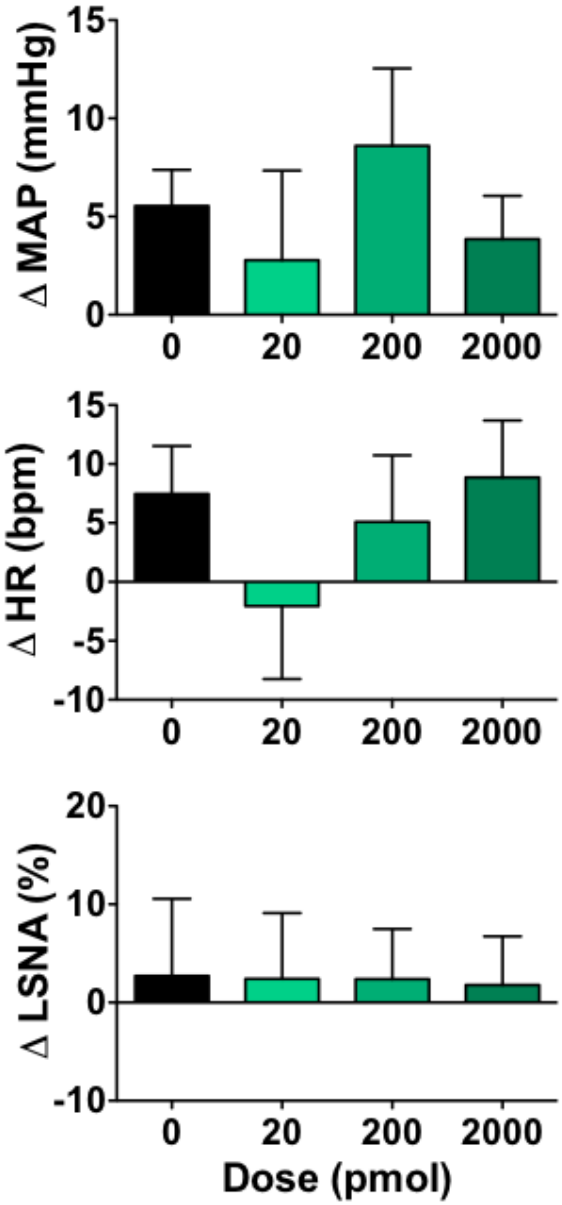

Figure 3.5 Effect of NaHS in the PVN

Changes in mean arterial pressure (MAP), heart rate (HR) and lumbar sympathetic nerve activity (LSNA) following vehicle (n = 14 for MAP and HR and *n* = 7 for LSNA) and the H_2S donor, NaHS, (20 – 2000 pmol/side) (n = 6 for MAP and HR and *n* = 5 for LSNA) microinjected into the hypothalamic paraventricular nucleus (PVN) in WKY rats.

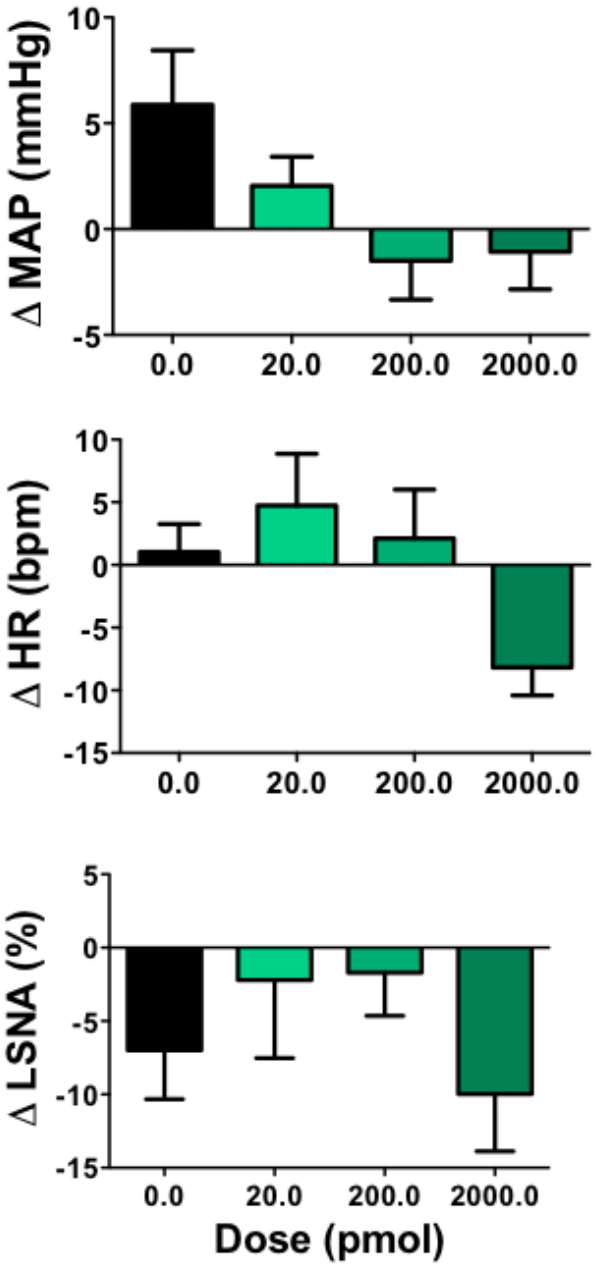

Figure 3.6 Effect of NaHS in the area surrounding the PVN,

Changes in mean arterial pressure (MAP), heart rate (HR) and lumbar sympathetic nerve activity (LSNA) following vehicle (n = 9 for MAP and HR and n = 3 for LSNA) and the H_2S donor, NaHS, (20 – 2000 pmol/side) (n = 5 for MAP, HR and LSNA) microinjected into the area surrounding the hypothalamic paraventricular nucleus (PVN) in WKY rats.

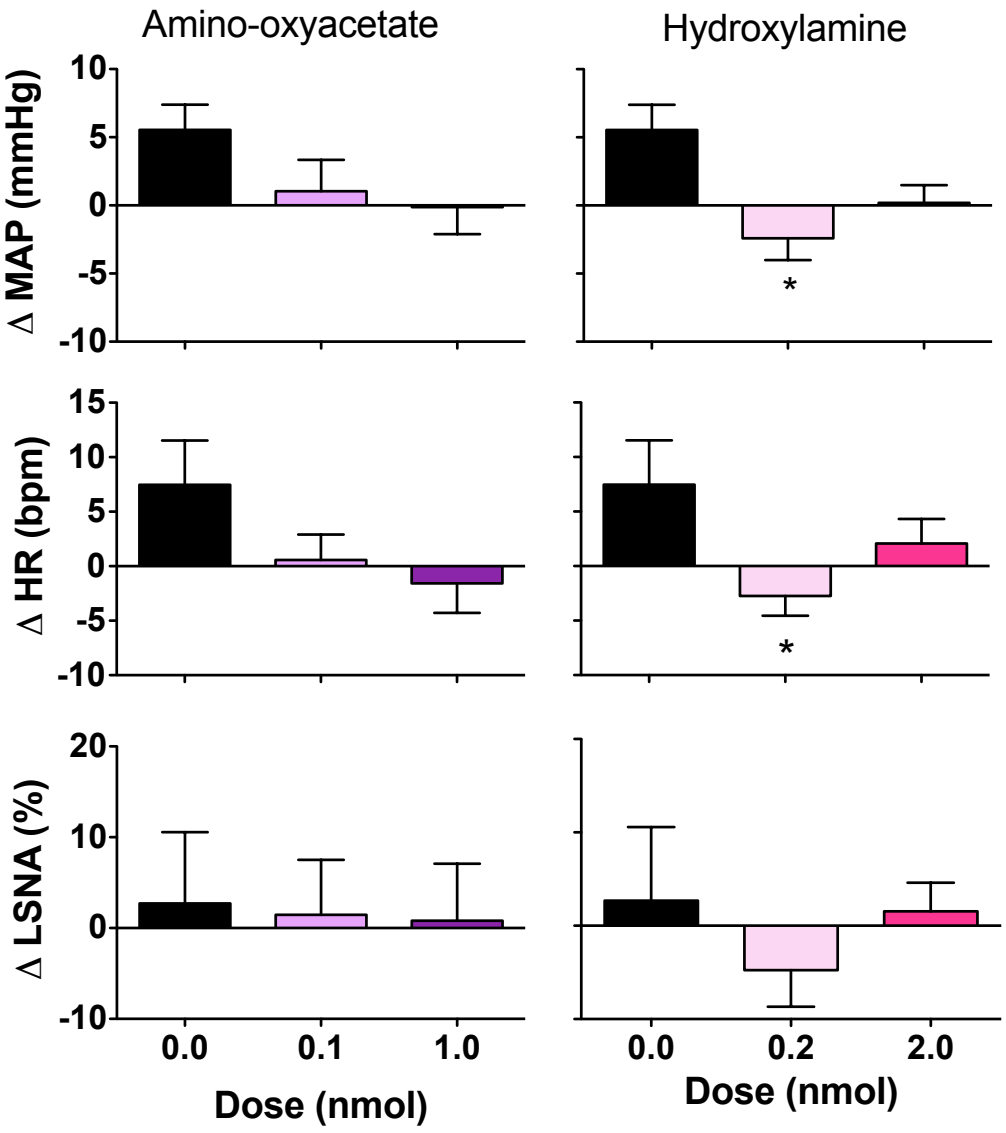

Figure 3.7 Effect of CBS inhibitors in the PVN

Changes in mean arterial pressure (MAP), heart rate (HR) and lumbar sympathetic nerve activity (LSNA) following vehicle (n = 14 for MAP and HR and n = 6 for LSNA) and amino-oxyacetate (AOA) (0.1 – 1.0 nmol/side) and hydroxylamine (HA) (0.2 – 2.0 nmol/side) (n = 13 for MAP and HR and n = 6 for LSNA) microinjected into the paraventricular nucleus (PVN) in WKY rats. AOA and HA are inhibitors of the enzyme cystathionine β synthase. *P<0.05 compared to vehicle.

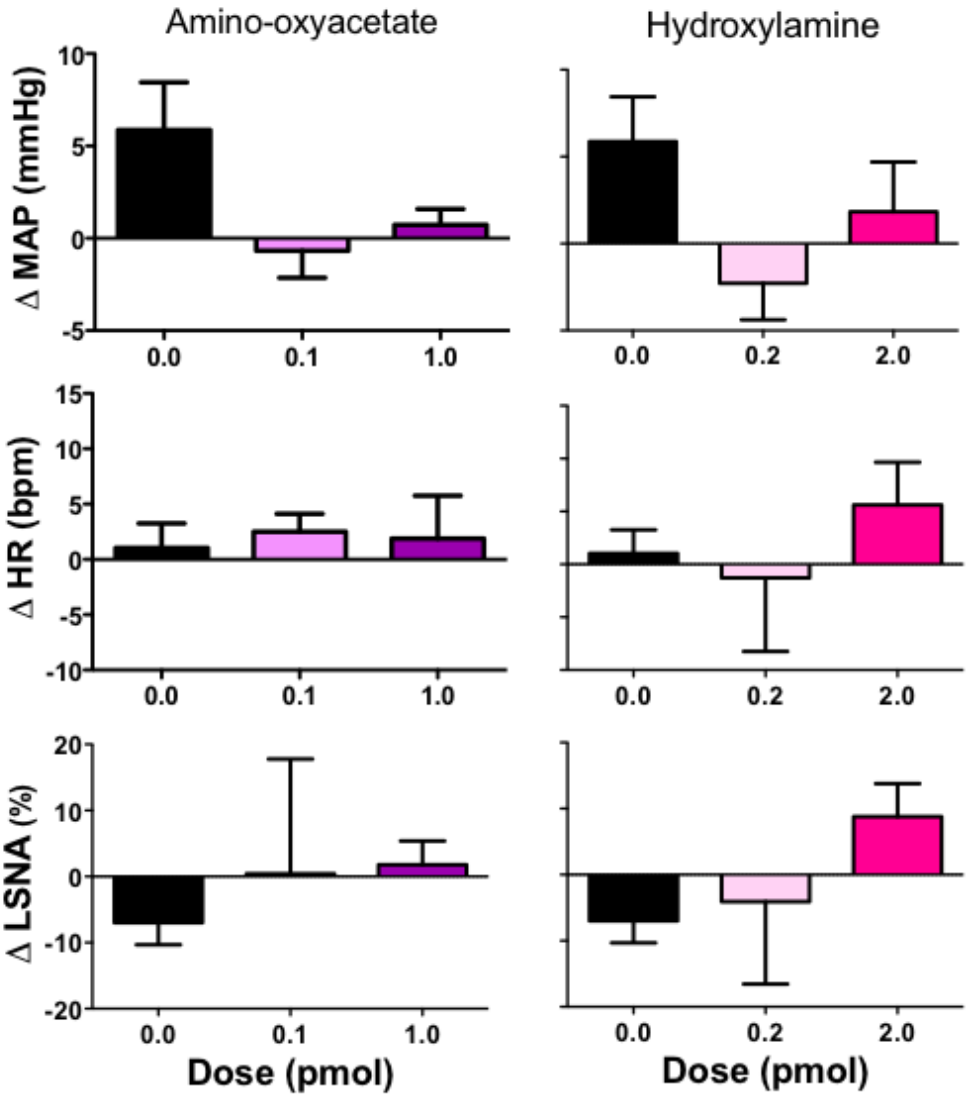

Figure 3.8 Effect of CBS inhibitors in the area surrounding the PVN

Changes in mean arterial pressure (MAP), heart rate (HR) and lumbar sympathetic nerve activity (LSNA) following vehicle (*n* = 9 for MAP and HR and n=3 for LSNA) and amino-oxyacetate (AOA) (0.1 – 1.0 nmol/side) and hydroxylamine (HA) (0.2 – 2.0 nmol/side) (*n* = 7 for MAP and HR and *n* = 3 for LSNA) microinjected into the area surrounding the paraventricular nucleus in WKY rats. AOA and HA are inhibitors of the enzyme cystathionine β synthase.

SHR Rats

3.3.6 Effect of NaHS microinjected into the rostral ventrolateral medulla or paraventricular nucleus in SHR rats

When NaHS (20-2000pmol / side) was microinjected into the RVLM, there was no significant effect on MAP, HR and LSNA compared to vehicle (n = 3) (figure 3.9). Similarly, microinjections of NaHS into the PVN of SHR rats did not significantly affect the cardiovascular variables monitored (n = 5) (figure 3.9).

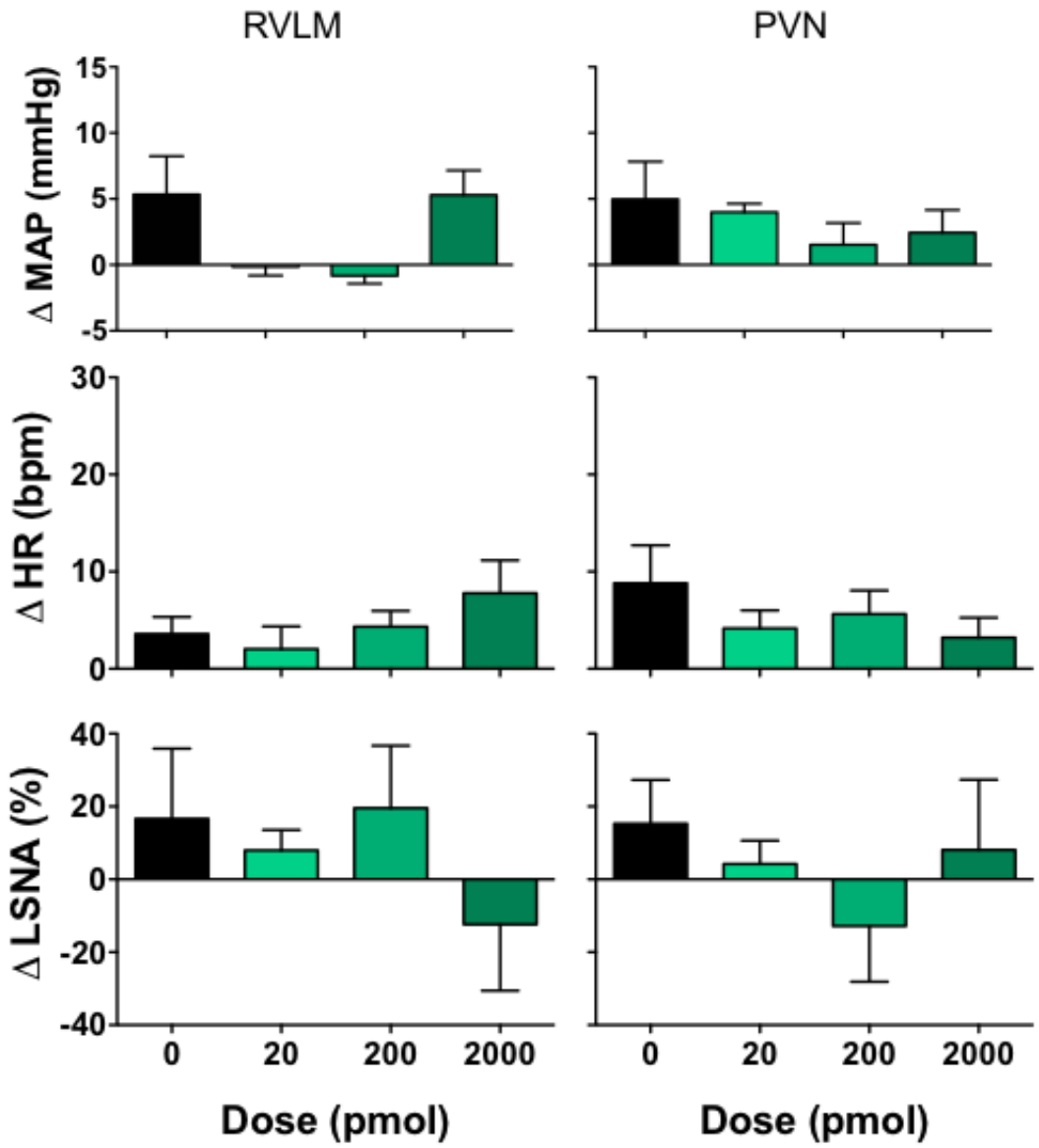

Figure 3.9 Effect of NaHS in the RVLM and PVN of SHR rats

(a) Changes in mean arterial pressure (MAP), heart rate (HR) and lumbar sympathetic nerve activity (LSNA) following vehicle and the H_2S donor, (NaHS, 20– 2000 pmol/side) (n = 3) microinjected into the rostral ventrolateral medulla (RVLM) of SHR rats. **(b)** Changes in mean arterial pressure (MAP), heart rate (HR) and lumbar sympathetic nerve activity (LSNA) following vehicle and the H_2S donor, NaHS, (20 – 2000 pmol/side) (n = 5) microinjected into the hypothalamic paraventricular nucleus (PVN) in SHR rats.

3.3.7 Microinjection sites in the rostral ventrolateral medulla

The sites of microinjection into the RVLM (defined as within 0.0 – 0.6 mm caudal of the facial nucleus) are shown in figure 3.10. The microinjection sites were mainly located towards the rostral end of the RVLM predominantly within 0.0 to 0.2 mm caudal of the caudal pole of the facial nucleus. The distribution of the microinjection sites for NaHS, AOA and HA were similar.

3.3.8 Microinjection sites in the paraventricular nucleus

The sites of microinjection into the PVN are shown in figure 3.11. The centre of the injection sites were found to be within 1.4 to 2.1mm caudal of the bregma and covered the rostral-caudal extent of the PVN. The distribution of the microinjection sites with NaHS and that of the inhibitors of the enzyme that produces H_2S, were similar. Microinjections made adjacent to the PVN were centred dorsal to the PVN, in the ventral portion of the nucleus reunions, at levels 1.3 - 2.3 mm caudal to bregma (figure 3.12).

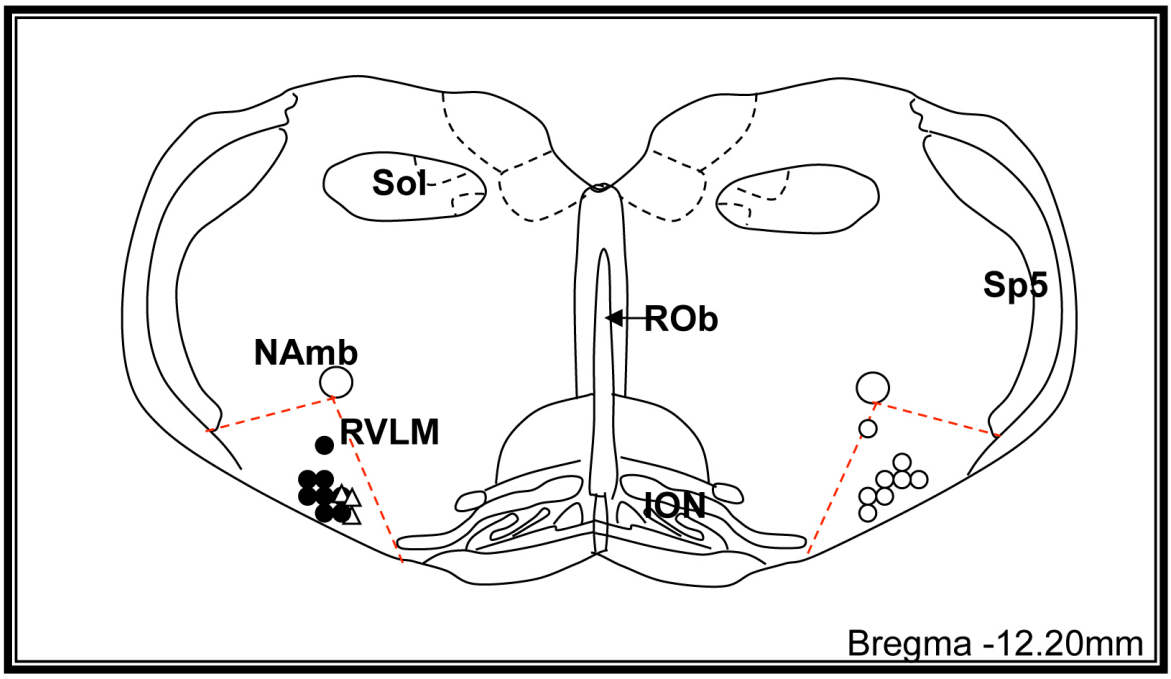

Figure 3.10 Injection sites into RVLM of SHR and WKY rats

Schematic illustration showing the centre of the microinjection sites within the rostral ventrolateral medulla (RVLM). Microinjections were made bilaterally but only unilateral sites are shown. Closed circles represent microinjection sites of NaHS in WKY rats, open triangles represent microinjection sites of NaHS in SHR rats and open circles represent microinjection sites of amino-oxyacetate and hydroxylamine in WKY rats. Sol, nucleus tractus solitarius; NAmb, nucleus ambiguus; Sp5, spinal trigeminal tract; Rob, raphe obscurus; ION inferior olivary nucleus.

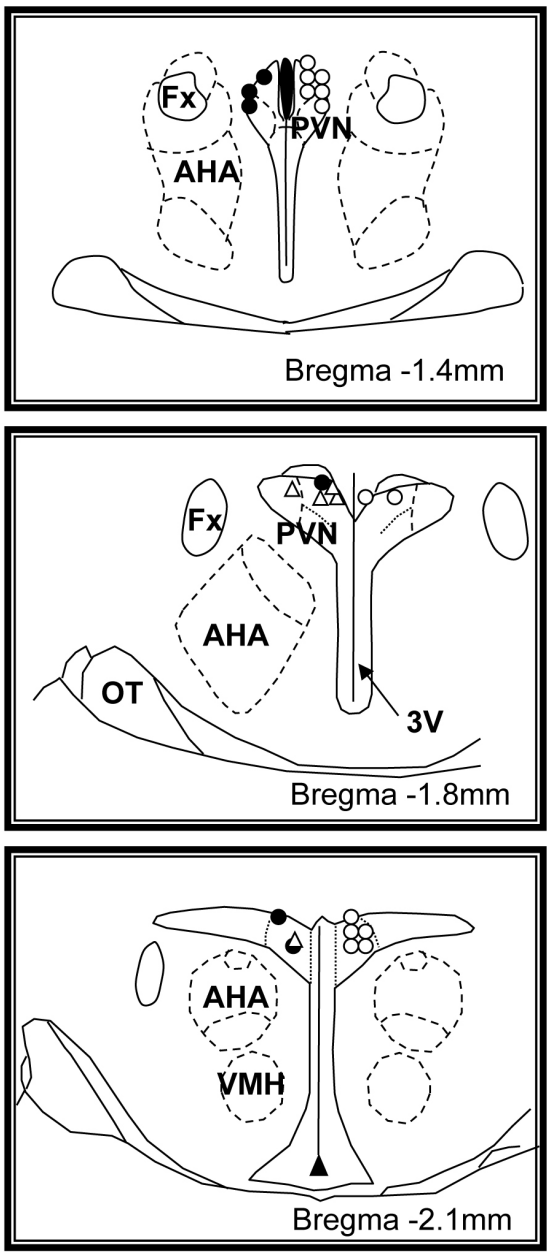

Figure 3.11 Injection sites into the PVN of SHR and WKY rats

Schematic illustration showing the centre of the microinjection sites within the hypothalamic paraventricular nucleus (PVN). Microinjections were made bilaterally but only unilateral sites are shown. Closed circles represent microinjection sites of NaHS into WKY rats, open triangles represent microinjection sites of NaHS into SHR rats and open circles represent microinjection sites of amino-oxyacetate and hydroxylamine into WKY rats. 3V, third ventricle; AHA, anterior hypothalamic area; VMH ventromedial hypothalamus; OT, optic tract; Fx, fornix.

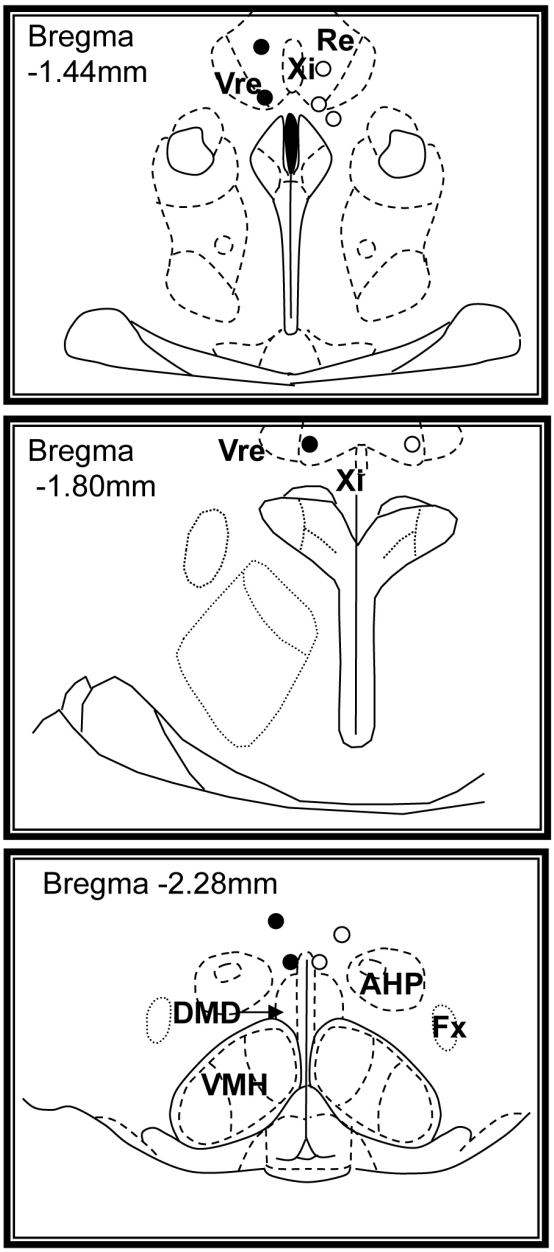

Figure 3.12 Injection sites into the area surrounding the PVN of WKY rats

Schematic illustration showing the centre of the microinjection sites in the region surrounding hypothalamic paraventricular nucleus (PVN). Microinjections were made bilaterally but only unilateral sites are shown. Closed circles represent microinjection sites of NaHS and open circles represent microinjection sites of amino-oxyacetate and hydroxylamine. Re, reunions thalamus nucleus; Vre, ventral reunions nucleus; Xi, xiphoid thalamus nucleus; Fx, fornix; DMD, dorsomedial hypothalamic nucleus; AHP, anterior hypothalamic area; VMH, ventromedial hypothalamus.

3.4 Discussion

In the present study, the enzyme CBS, but not CSE, was demonstrated in the RVLM and PVN, suggesting H_2S may be endogenously produced in these regions. Microinjection of the H_2S donor, NaHS, directly into these brain regions, however, did not significantly alter blood pressure, heart rate or lumbar sympathetic nerve activity in WKY and SHR rats. In WKY rats, inhibition of the production of H_2S, using inhibitors of CBS, in those brain regions also had no marked effects on the cardiovascular variables. The results suggest that hydrogen sulfide in the RVLM and PVN may not have a significant role in cardiovascular regulation.

The present work, using western blot analysis, is the first to report that CBS is present specifically in the RVLM and PVN, two important autonomic brain regions involved in the regulation of sympathetic nerve activity and the cardiovascular system. Previous studies have found that the activity of CBS varies with the brain area examined, and that the hypothalamus of rats had the highest activity (Kohl *et al.*, 1979). Changes in CBS expression have also been observed in mice during development; the levels of CBS increased postnatally, particularly in the hippocampus and cerebellum (Robert *et al.*, 2003). In the present study a second band was observed in the western blots for CBS at approximately 70kDa the reason for this band is not clear, but is possibly due to proteolysis, splice variation or non-specificity of the antibody. There have been several reports demonstrating weak expression of CSE in whole brain tissues of rats and mice (Abe *et al.*, 1996; Ishii *et al.*, 2004), however, the present results indicate that CSE is absent in the specific areas of the RVLM and PVN. Bands for CSE were none-the-less detected in tissues known to express CSE, including aorta and liver.

The RVLM is a key brain region involved in generating tonic sympathetic outflow (Guyenet, 2006). In the RVLM, microinjection of NaHS did not cause significant changes in MAP, HR or LSNA compared to control. This was observed in WKY as well as SHR rats. This contrasts

with the marked influence of another gaseous transmitter, nitric oxide, on blood pressure and sympathetic nerve regulation (Kimura *et al.*, 2009; Patel *et al.*, 2001; Zanzinger, 1999). The present results suggest that H_2S may not be a key player in cardiovascular regulation in the RVLM in normotensive or hypertensive conditions.

In order to observe the effects of endogenous H_2S, two inhibitors of CBS were employed, HA and AOA. Since both inhibitors affect the association of CBS with its co-factor, PLP (Braunstein *et al.*, 1971; McMaster *et al.*, 1991), the effects could be attributable to inhibition of PLP-dependent enzymes other than CBS. However, neither inhibitor microinjected into the RVLM significantly affected MAP, HR or LSNA. These results indicate that, although CBS is present in the RVLM, H_2S in the RVLM does not have a major influence on BP, HR or LSNA. Since the present study found no evidence to suggest a role for endogenous H_2S in WKY rats nor for exogenous H_2S in WKY and SHR rats, the effects of HA or AOA were not further investigated in the SHR rats.

In contrast to the present work, a recent study reported that NaHS microinjected into the RVLM of anaesthetised rats induced dose-dependent, and relatively large, reductions in MAP, HR and renal sympathetic nerve activity (RSNA), and HA elicited opposite cardiovascular effects (Guo *et al.*, 2011). It is noteworthy that the researchers omitted to buffer any of their drugs in solution. In the present experiments, artificial CSF, buffered with carbogen and 25mM $NaHCO_3$, was used as the vehicle for all drugs. The concentrations of NaHS used by Guo *et al*. (2, 4 and 8mM) would be expected to cause a significant increase in the pH when dissolved in unbuffered saline, since it has been observed that NaHS dissolved in a low capacity buffer (containing 2.4mM $NaHCO_3$) increased the pH by approximately 0.6 and 3 pH units at concentrations of 1mM and 10mM, respectively, at 22 ^{o}C (Dombkowski *et al.*,

2005). Given the proximity of the RVLM to regions with chemosensitive neurons that participate in the central sympathetic chemoreflex (Guyenet *et al.*, 2010), a drastic change in pH in this area might have significant influences on blood pressure.

The study by Guo et al. also observed that HA can increase MAP, HR and RSNA via the RVLM (Guo *et al.*, 2011), which contrasts with the lack of effect of HA observed in the present study. HA is a weak base, and therefore may also cause pH-induced haemodynamic effects. Although unbuffered solutions of NaHS and HA are both basic, NaHS and HA induced opposite haemodynamic effects in the study by Guo et al, indicating that HA may have acted by mechanisms other than altered pH. Another possible explanation for the discrepancies between the present study and the study by Guo *et al*. lies in the difference in methodological approach (Guo *et al.*, 2011). In the present study, rats were placed in the prone position for a dorsal approach to the RVLM, the pressor region was functionally identified, and the rats breathed spontaneously, whereas in the work by Guo and colleagues, rats were placed supine for a ventral approach and visual identification of the RVLM, and the rats were ventilated. Stretching the chest wall during ventilation is known to enhance the excitatory drive arising from the RVLM and this can alter the responses to drugs administered into the RVLM (Cox *et al.*, 1988). Functional identification of the pressor region of the RVLM was important in the present study to indicate (i) the correct placement of the microinjection and (ii) the RVLM was functional under the present experimental conditions and cardiovascular responses were clearly obtainable. It has been demonstrated previously that body positional changes influence haemodynamic parameters in rats, and inconsistent body position can lead to conflicting results (Siepe *et al.*, 2005).

The PVN can influence the cardiovascular system via hormonal and neural mechanisms, and

it contains neurons that project to the spinal cord and directly influence sympathetic nerve activity (Badoer, 2001; Shafton *et al.*, 1998). Since the present study found CBS was present in the PVN and its activity was reportedly high in the hypothalamus (Kohl *et al.*, 1979), we investigated whether exogenously administered or endogenously produced H_2S could influence MAP, HR and LSNA. As there was no effect with any of the five doses of NaHS in the RVLM, only the three higher doses of NaHS were used in the PVN. NaHS microinjected into the PVN of WKY rats did not significantly influence MAP, HR or LSNA compared to the microinjection of vehicle. Similarly micro-injection of NaHS into the area surrounding the PVN, mainly in the ventral reunions nucleus, did not significantly influence MAP, HR or LSNA. These findings suggest that exogenous administration of H_2S into the PVN, or closely surrounding region, cannot influence the cardiovascular variables.

After microinjection of HA into the PVN, there was no effect on LSNA and there were minimal effects on MAP and HR which gained statistical significance, compared to control, only with the lowest dose of HA used. Given there was no consistent significant effect of HA on MAP and HR between the two doses of HA, the physiological relevance of the statistical differences observed is questionable. This view is supported by the fact that AOA microinjected into the PVN did not significantly alter MAP, HR or LSNA. Thus, we conclude that endogenous H_2S within the PVN does not appear to play a major role in the regulation of BP, HR or LSNA in the normotensive state. In SHR rats we investigated the effects of NaHS microinjected into the PVN. As in the WKY rats, we could not find any evidence suggesting H_2S in the PVN contributed to the regulation of the MAP, HR and LSNA in the hypertensive state. Given the negative findings in the WKY rats, we did not pursue further investigations with HA and AOA in the PVN of SHR rats.

In a previous study, exogenous as well as endogenous H_2S in the posterior hypothalamus produced a small, but significant, reduction in blood pressure suggesting that H_2S has some depressor activity within the posterior hypothalamus (Dawe *et al.*, 2008). Bolus intracerebroventricular injections of NaHS (3-303 μmol) also resulted in significant reductions of blood pressure (Liu *et al.*, 2011a). In contrast, a 60 min intracerebroventricular infusion of NaHS resulted in a small, significant increase in blood pressure (Ufnal *et al.*, 2008). However, intracerebroventricular AOA did not affect blood pressure in the latter study (Ufnal *et al.*, 2008). The effects on sympathetic nerve activity were not examined in any of these reports. Therefore, H_2S may act in brain regions other than key areas like the RVLM and PVN, to influence cardiovascular regulation.

Opening of K_{ATP} channels is believed to contribute to the effects of H_2S, including vasodilation and cardioprotection (Bian *et al.*, 2006; Zhao *et al.*, 2001). Opening K_{ATP} channels could decrease cell firing as a result of hyperpolarisation. Indeed, a reduced discharge rate in spontaneously firing units in the RVLM after administration of a K_{ATP} channel opener, adenosine, has been reported but there was no effect on blood pressure or heart rate (Chen *et al.*, 1998). A study on hypothalamic slices showed that the spontaneous firing of PVN neurons with projections to the spinal cord was reduced by adenosine; an effect mediated by opening of K_{ATP} channels (Li *et al.*, 2010). The effect on sympathetic outflow, blood pressure or heart rate, however, could not be examined in that *in vitro* study. The present findings suggest that if H_2S opens K_{ATP} channels in the RVLM or PVN, then K_{ATP} channels in those brain regions have little influence in the regulation of MAP, HR or LSNA.

In the brain K_{ATP} channels are distributed widely. In the PVN, relatively high mRNA levels of the Kir6.2 subtype of the K_{ATP} channel have been demonstrated (Dunn-Meynell *et al.*,

1998). These channels are involved in altering firing rates of glucose and may couple metabolic activity with neuronal excitability (Ashford *et al.*, 1990). The expression of these channels in the PVN can be influenced by peripheral glucose administration and may be involved in the predisposition to obesity (Levin *et al.*, 1997). Thus, although our studies suggest H_2S in the PVN has no major role in MAP, HR and LSNA, H_2S in the PVN may perform other functions, which require further investigation.

Methodological Aspects

Exogenously applied free H_2S is sequestered and stored as bound sulfane within minutes, therefore, an effect of exogenously applied H_2S would be expected to be quite short-lived (Ishigami *et al.*, 2009). This is unlikely to explain the lack of any significant effect of NaHS on the cardiovascular variables measured in the present study since previous studies in which 100 nl of NaHS was infused into the posterior hypothalamus over 4 minutes reported significant changes (Dawe *et al.*, 2008) In the present study we used 100 nl injected over a shorter time frame (i.e. less than a minute).

In the course of completing these studies, another enzyme, 3-MST, in addition to CBS, was reported to contribute to the production of endogenous H_2S in the brain (Shibuya *et al.*, 2009a). However, the role of 3-MST in the production of H_2S remains to be fully elucidated, in light of studies using astrocytic, microglial and neuroblastoma SH-SY5Y cell lines in which H_2S production was drastically reduced by inhibition of CBS using hydroxylamine (Lee *et al.*, 2009).

Conclusion

The present study demonstrates for the first time the presence of the enzyme CBS in two important cardiovascular regulatory areas, the RVLM and PVN. By contrast CSE was not observed in those brain regions. This is consistent with the current view that, of those two enzymes, CBS is the main enzyme in the brain involved in the production of H_2S. The present work also showed there was no significant effect on MAP, HR and LSNA upon administration of the H_2S donor, NaHS, into the RVLM and PVN of WKY and SHR rats, or following inhibition of CBS in the RVLM and PVN in WKY. Thus, we suspect that H_2S in those regions is not playing a critical role in the regulation of MAP, HR and LSNA, at least in the short term.

Chapter 4: Regulation of middle cerebral artery tone by hydrogen sulfide

4.1 Introduction

H_2S possesses important cardiovascular effects, including protection against cardiac ischaemia-reperfusion injury, inhibition of VSM hypertrophy and attenuation of ROS or inflammatory mediator-induced endothelial dysfunction (Calvert *et al.*, 2009; Muzaffar *et al.*, 2008; Pan *et al.*, 2011). H_2S is also well established as a vasodilator. The H_2S donor, NaHS, induces concentration-dependent vasorelaxation in conduit arteries (Al-Magableh *et al.*, 2011; Kiss *et al.*, 2008; Kubo *et al.*, 2007; Lee *et al.*, 2007; Schleifenbaum *et al.*, 2010; Zhao *et al.*, 2001), as well as in resistance artery beds, (Cheng *et al.*, 2004; d'Emmanuele di Villa Bianca *et al.*, 2011; Jackson-Weaver *et al.*, 2011). H_2S may be an important physiological vasodilator, given that lowered plasma H_2S levels have been observed in SHR (Ahmad *et al.*, 2012) as well as hypertensive humans (Sun *et al.*, 2007). Furthermore, in one study, mice deficient in CSE had pronounced hypertension (Yang *et al.*, 2008), although CSE deletion did not influence blood pressure in another study (Ishii *et al.*, 2010).

H_2S-induced vasorelaxation in peripheral blood vessels has been attributed to various mechanisms, both endothelium dependent (Cheng *et al.*, 2004; Zhao *et al.*, 2001) and independent (Al-Magableh *et al.*, 2011; Hosoki *et al.*, 1997). In particular, opening of potassium channels, such as K_{ATP} (Al-Magableh *et al.*, 2011; Cheng *et al.*, 2004; Mustafa *et al.*, 2011; Zhao *et al.*, 2001), KCNQ-type voltage-dependent (Schleifenbaum *et al.*, 2010) and K_{Ca} (Jackson-Weaver *et al.*, 2011), has been reported to play a role. There is also evidence for a role of the Cl^-/HCO_3^- exchanger (Kiss *et al.*, 2008; Lee *et al.*, 2007, Al-Magableh, 2011 #73) and Ca^{2+} channels (Al-Magableh *et al.*, 2011; Zhao *et al.*, 2002). Even within the same vessel type, controversy about the responsible mechanism exists; for example, in the rat aorta, the

K_{ATP} channel blocker, glibenclamide, strongly inhibited the H_2S-induced vasorelaxation in one study (Zhao *et al.*, 2001), had no effect in another report (Kiss *et al.*, 2008), and caused partial blockade in another (Al-Magableh *et al.*, 2011). The size and origin of the blood vessel, as well as species, seem to influence the degree to which each mechanism contributes to the vasorelaxation mediated by H_2S. To date, studies on the effects of H_2S on cerebrovascular tone have been few, but have demonstrated a vasorelaxant action (Leffler *et al.*, 2010; Liang *et al.*, 2011; Liang *et al.*, 2012; Liu *et al.*, 2012).

In peripheral vessels, several studies have reported that the vascular action of H_2S is biphasic, depending on its concentration: NaHS causes constriction at low concentrations (10-100 μM) and dilation at higher concentrations (100-1600 μM) (Ali *et al.*, 2006; Kubo *et al.*, 2007; Lim *et al.*, 2008). The vasoconstrictor effects have been attributed to endothelium-dependent mechanisms, including reduction of NO levels by direct reaction with NO (Ali *et al.*, 2006; Whiteman *et al.*, 2006), or inhibition of eNOS (Kubo *et al.*, 2007). There is also evidence for an endothelium independent mechanism – down-regulation of cAMP in smooth muscle cells (Lim *et al.*, 2008). The contractile effect of H_2S in cerebral vessels has not been investigated. H_2S has been reported to have cerebroprotective effects in certain pathophysiological conditions, including attenuating cerebral ischemia-reperfusion injury (Ren *et al.*, 2010) and decreasing the risk of delayed cerebral ischaemia following subarachnoid haemorrhage (Grobelny *et al.*, 2011). Neuroprotection by H_2S has been reported in models of brain diseases that are associated with dysfunctional cerebral blood flow, such as Parkinson's disease and vascular dementia (Hu *et al.*, 2010; Zhang *et al.*, 2009). However, little is known about the mechanism of H_2S-induced cerebral vasodilation or vasoconstriction. Determining these aspects of H_2S biology may provide new insights into the regulation of cerebral blood

flow. Exploiting any cerebroprotective therapeutic potential of H_2S will undoubtedly require further understanding of its mechanism.

The aim of this study was to undertake a detailed analysis of the mechanisms potentially mediating the vasorelaxant and vasoconstrictor effects of H_2S in rat isolated MCA. The localisation of the H_2S producing enzyme, CSE, was also examined in these cerebral vessels using immunohistochemistry.

4.2 Methods

4.2.1 Wire myography

MCA were collected (see 2.3.1) and cut into 2mm segments, which were mounted into a wire myograph (see 2.3.2 and figure 2.2). The vessels were then constricted via one of two pre-constriction protocols, depending which inhibitor was subsequently applied. The 'spontaneous tone protocol' (see 2.3.2 and figure 2.3) was used in all vessel segments, except those using nifedipine or bicarbonate free Krebs', for which the 'U46619 protocol' (see 2.3.2 and figure 2.4) was used. After pre-constriction, the viability of the endothelium was assessed using bradykinin 100 nM, vessel segments were washed and an inhibitor (or vehicle as control) was applied 20 minutes prior to constructing a concentration-response curve.

Mechanism of H_2S-induced vasorelaxation and vasoconstriction

The vascular response to cumulative concentrations of the H_2S donor, NaHS (10 μM-3 mM), was examined in the presence or absence of one (or more) of the following: glibenclamide (10 μM), a K_{ATP} channel blocker; charybdotoxin (100 nM), an inhibitor of large and intermediate conductance K_{Ca} channels together with apamin (1 μM), an inhibitor of small conductance K_{Ca} channels; 4-aminopyridine (4-AP, 1 mM), a K_V channel blocker; barium (Ba^{2+}, 30 μM), a blocker of K_{IR} channels; potassium chloride (KCl, 50 mM), to inhibit K^+ conductance; L-NAME (100 μM), an inhibitor of nitric oxide synthase; indomethacin (10 μM), an inhibitor of cyclo-oxygenase; DIDS (300 μM), an inhibitor of chloride channels and chloride-bicarbonate (Cl^-/HCO_3^-) exchange; bicarbonate free Krebs' (composition same as Krebs' solution, except $NaHCO_3$ was replaced with HEPES free acid 10 mM as a buffer, NaCl concentration was increased to 238mM to maintain the osmolarity, and pH was adjusted to 7.4 using NaOH) to inhibit bicarbonate exchange; niflumic acid (30 μM), a chloride ion channel blocker; nifedipine (3 μM), an L-type voltage-gated calcium channel blocker; catalase (1000 U/mL), an enzyme that selectively decomposes hydrogen peroxide; diphenylene iodonium (DPI, 1

μM), an Nox inhibitor; or tempol (1 mM), a SOD mimetic. Each was added 20 minutes prior to construction of the NaHS concentration-response curve. At the completion of each experiment, maximal relaxation was recorded using calcium free Krebs'. Each vessel segment was used to obtain only one concentration-response curve.

The effect of H_2S on VGCC was also assessed in a separate set of experiments, by examining the constriction to calcium replacement in the presence of NaHS or nifedipine, as described in detail in section 2.3.2 (influence of VGCC) (see also figure 2.5).

Vasorelaxation to endogenous H_2S

For these studies, the spontaneous developed tone protocol was used. Vasorelaxation to cumulative (0.5 log-unit) concentrations of L-cysteine (10 μM-100 mM), a precursor to H_2S, in the presence of the cofactor PLP (1 mM), was examined. Concentration response curves to L-cysteine were obtained in the presence and absence of PPG (20 mM), a CSE inhibitor, applied 20 minutes prior to L-cysteine.

For a detailed description of the data analysis, see 2.3.3 Data Analysis, p.80. Briefly, comparisons were made between average E_{max}, maximum constriction, and $logEC_{50}$ values using T-tests for comparisons between two data sets, and one-way ANOVA with a post-hoc Dunnett's test for comparisons between multiple data sets.

4.2.2 Immunohistochemistry for CSE

Immunohistochemistry was performed on whole MCA using standard protocols (Dan *et al.*, 2003), as detailed in chapter 2, section 2.5.2. Briefly, MCA were incubated in either mouse monoclonal CBS primary antibody (1:50, M01, ABNOVA), or vehicle alone as a negative control. Vessels were then incubated separately in TRITC-conjugated rabbit anti-mouse secondary antibody (1:50, Dako Cytomation), followed by application of a Hoechst fluorescent nuclear stain (1:500).

4.3 Results

4.3.1 Immunofluorescence for CSE in endothelium and smooth muscle

Immunohistochemical analysis of MCA showed staining for CSE in endothelial (figure 4.1a) and smooth muscle cells (figure 4.1b). Immunohistochemical analysis of mesenteric artery and aorta both also show staining for CSE in endothelial (figure 4.2a) and smooth muscle cells (figure 4.2b).

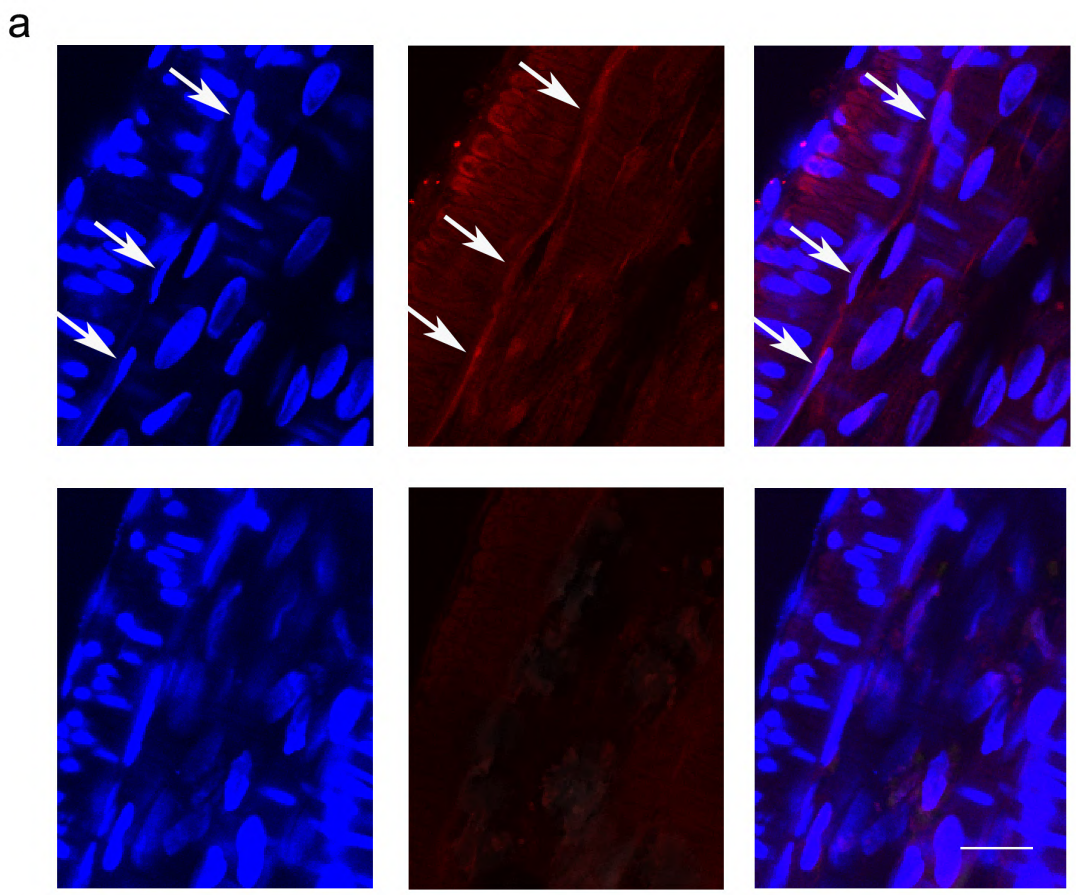

Figure 4.1 a CSE staining in MCA endothelium.

Top panels are in the presence of the primary antibody for CSE, bottom panels are negative controls processed in the absence of the primary antibody for CSE (red). Left panels highlight the presence of nuclei as identified by Hoechst nuclear staining (blue). Middle top panels highlight presence of CSE and right panel shows the merged images. These Images are focused for observation of endothelial cell layer. Arrows demonstrate examples of co-staining, where CSE is clearly staining endothelial cells. No specific staining for CSE was observed in the negative control.

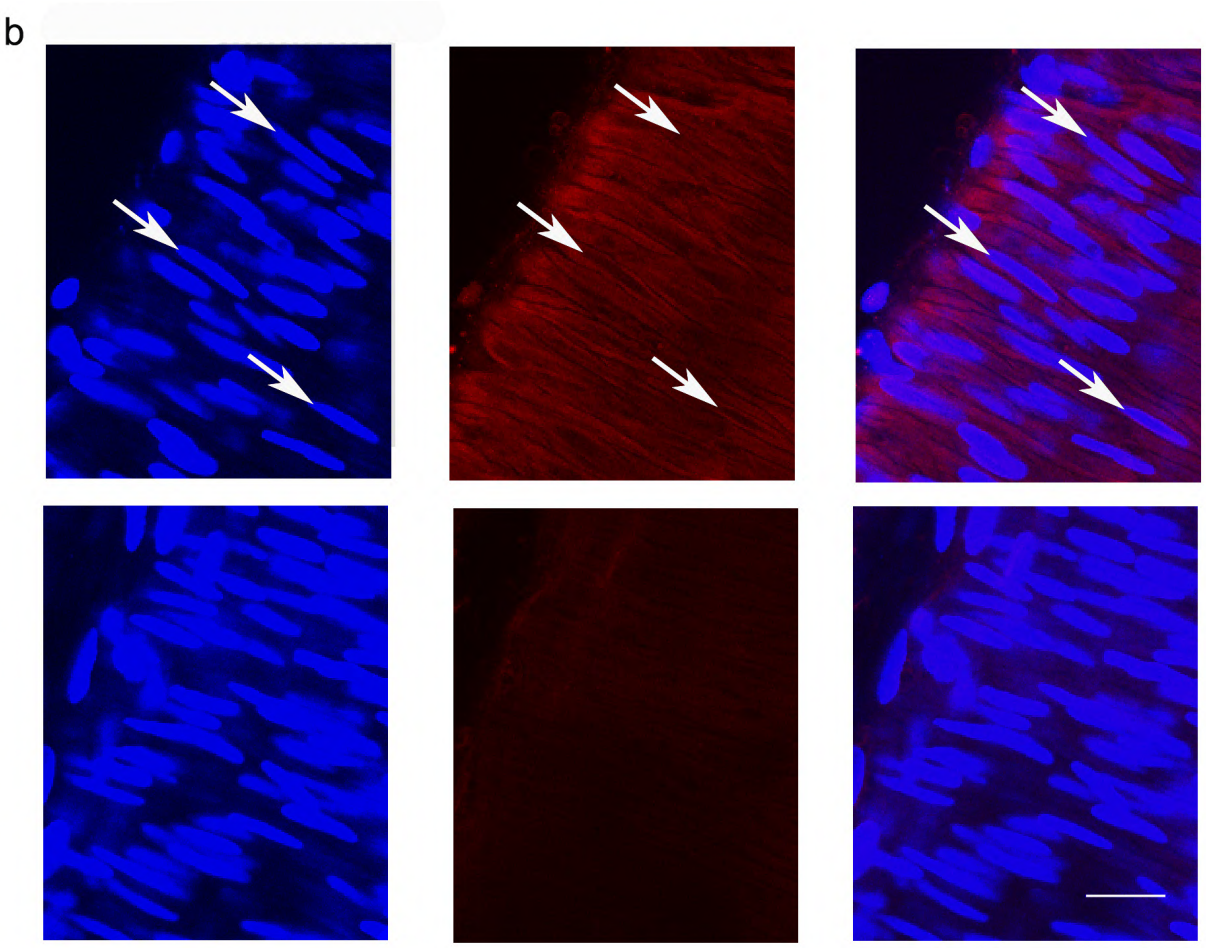

Figure 4.1 b CSE staining in MCA smooth muscle.

Top panels are in the presence of the primary antibody for CSE, bottom panels are negative controls processed in the absence of the primary antibody for CSE (red). Left panels highlight the presence of nuclei as identified by Hoechst nuclear staining (blue). Middle top panels highlight presence of CSE and right panel shows the merged images. These images are focused for observation of smooth muscle cell layer. Arrows demonstrate examples of co-staining, where CSE is clearly staining vascular smooth muscle cells. No specific staining for CSE was observed in the negative control. Calibration scale bar = 20 μm.

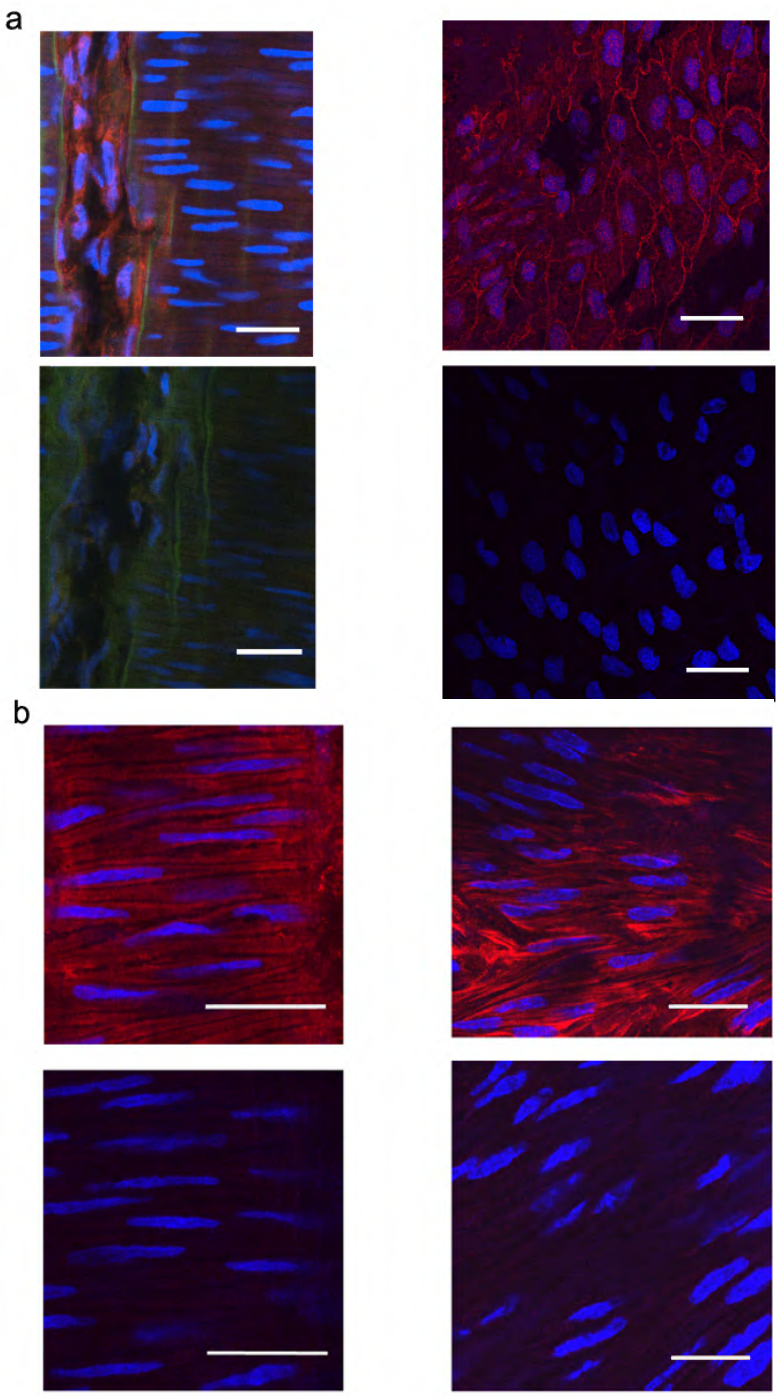

Figure 4.2 CSE staining in mesenteric artery and aorta.

Left panels are images taken of the mesenteric artery and right panels are of aorta. Top panels in '**a**' and '**b**' are in the presence of the primary antibody for CSE, bottom panels in '**a**' and '**b**' are negative controls processed in the absence of the primary antibody for CSE. All images show a merge of CSE (red) and Hoescht nuclei (blue) staining. The green in '**a**' is inherent fluorescence of the internal elastic lamina. Images are focused for observation of the endothelial cell layer **(a)** or smooth muscle cell layer **(b)**. No specific staining for CSE was observed in any negative control. Calibration scale bar = 20μm.

4.3.2 Vasorelaxation response to exogenous H_2S

The hydrogen sulfide donor, NaHS, (10 μM-3 mM) produced a full, concentration-dependent vasorelaxation of MCA that was unaffected by the preconstriction protocol - spontaneous tone or U46619. The threshold for the response was 72±11 μM and the pEC_{50}=4.00±0.02 in vessels preconstricted using the spontaneous tone protocol (figure 4.3a, table 4.1).

4.3.3 Vasorelaxation response to endogenous H_2S

The precursor for endogenous H_2S formation, L-cysteine (10 μM-100 mM), caused concentration dependent vasorelaxation of MCA (E_{max}= 83±3%, pEC_{50}= 2.28±0.04, *n*=6), which was not affected by the removal of endothelium (figure 4.3b). The CSE inhibitor, PPG (20mM) significantly attenuated the maximum vasorelaxation response to L-cysteine (E_{max}= 69±5%, P<0.05, *n*=5) and induced a rightward shift of the L-cysteine concentration-response curve, significantly increasing the EC_{50} (pEC_{50}= 2.02±0.06, P<0.05, *n*=5, figure 4.3b) by approximately two fold. The absence of endothelium did not significantly influence the response to L-cysteine in the presence of PPG (E_{max}= 69±2%, pEC_{50}= 1.91±0.04, *n*=7, figure 4.3b).

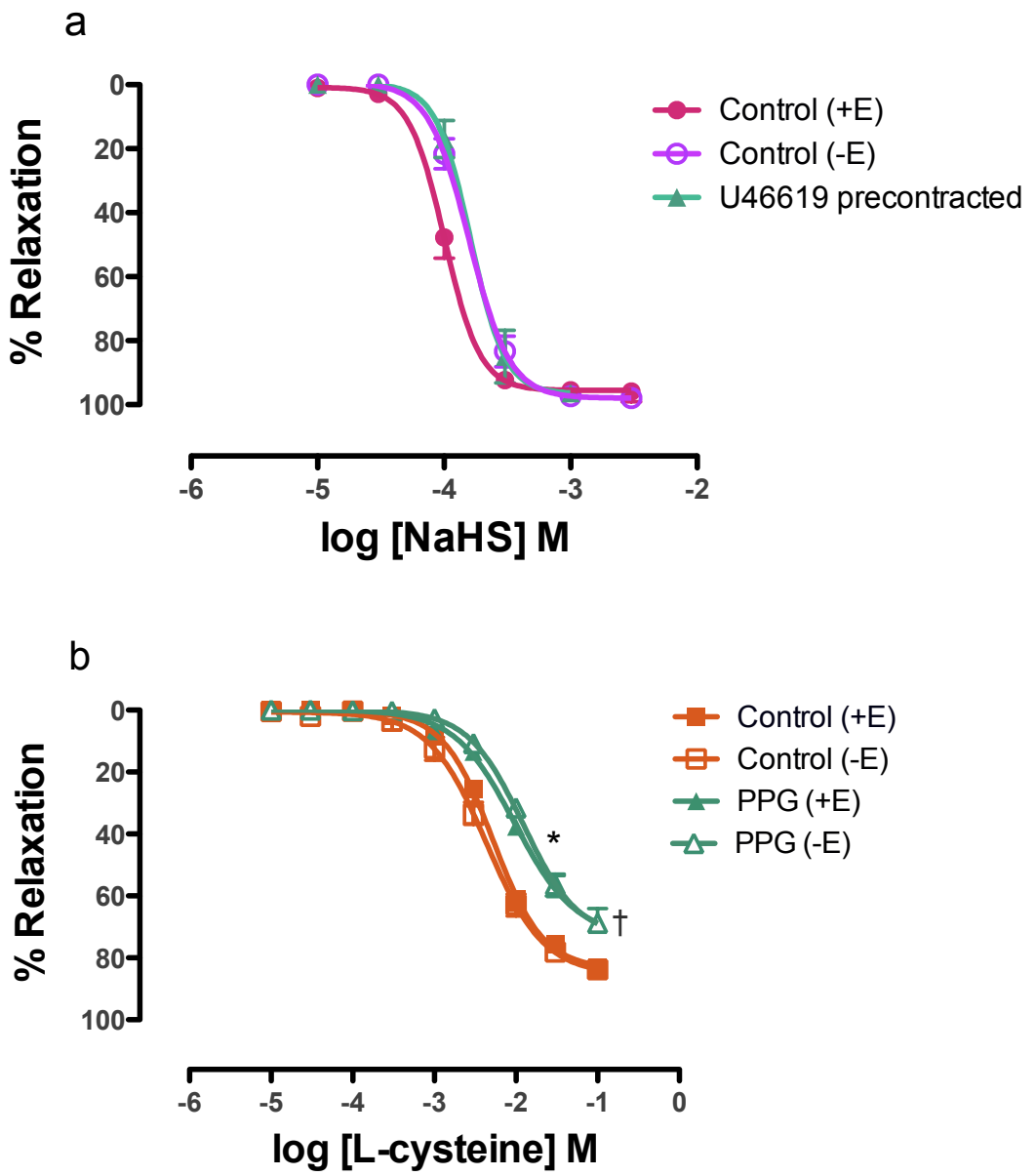

Figure 4.3 MCA vasorelaxation response to exogenous and endogenous H_2S.

(a) Cumulative concentration response curves to (i) NaHS in the presence (+E, closed circles, *n*=13) or absence of endothelium (-E, open circles, *n*=7) and (ii) NaHS in endothelium-intact middle cerebral artery segments preconstricted with U46619 (closed triangles, *n*=4) **(b)** Cumulative concentration response curves to (i) L-cysteine in the presence (closed squares, *n*=6) or absence of endothelium (open squares, *n*=6) and (ii) L-cysteine with propargylglycine (PPG, 20mM) to block cystathionine gamma lyase in the presence (closed triangles, *n*=5) or absence of endothelium (open triangles, *n*=7). *P<0.05 EC_{50} L-cysteine in the presence of PPG versus L-cysteine alone, in both the presence and absence of endothelium, †P<0.05 E_{max} L-cysteine in the presence of PPG versus L-cysteine alone, in both the presence and absence of endothelium. *n* = the number of middle cerebral artery segments from separate rats.

4.3.4 Mechanism of H_2S-induced vasorelaxation

Role of the endothelium: NaHS-induced vasorelaxation was not affected by the removal of endothelium (figure 4.3a, table 4.1). Accordingly, inhibition of the production of nitric oxide using the NOS inhibitor, L-NAME (100μM) or the production of prostanoids with the cyclo-oxygenase inhibitor, indomethacin (10μM) did not significantly alter the NaHS concentration-response curve (figure 4.4, table 4.1). Blockade of COX did not have any significant effect on the level of spontaneously generated tone in these vessels (table 4.2). Blockade of NOS and removal of endothelium both produced a significant increase in the baseline tone (table 4.2).

Role of Potassium channels: Reduction of K^+ conductance using 50mM KCl significantly decreased the pEC_{50} (figure 4.5a, table 4.1) and attenuated the E_{max} of NaHS-induced vasorelaxation, suggesting involvement of K^+ channels. However, selective individual blockade of $K_{ATP,}$ (with glibenclamide), SK_{Ca} and IK_{Ca} (with charybdotoxin/apamin), K_V (with 4-aminopyridine) or K_{IR} (with barium) channels did not significantly alter pEC_{50} or E_{max} (figure 4.5b, table 4.1). Similarly, the combination of glibenclamide, charybdotoxin, apamin and 4-aminopyridine did not affect the response to NaHS (table 4.1). The basal tone was not affected by the presence of glibenclamide or 4-aminopyridine, but the addition of 50mM KCl produced a significant increase in the baseline tone, similar to that produced by L-NAME (table 4.2). Application of charybdotoxin/apamin and barium both also significantly increased baseline tone (table 4.2).

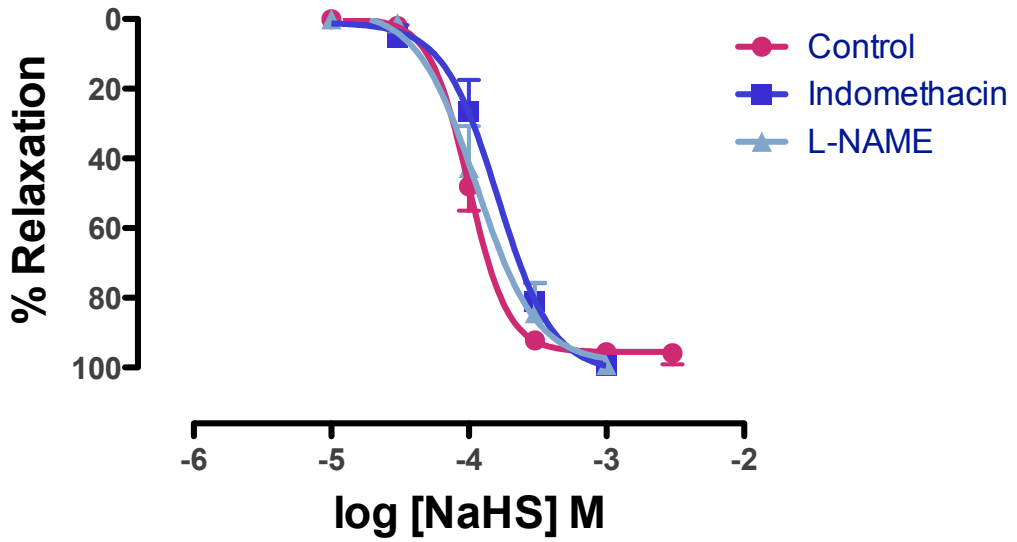

Figure 4.4 Effect of inhibition of the synthesis of endothelial-derived factors on NaHS-induced vasorelaxation.

Cumulative concentration response curves to NaHS in endothelium-intact MCA segments in the absence (control, closed circles, *n*=13), or presence of indomethacin (10 µM, closed squares, *n*=5), or L-NAME (100 µM, closed triangles, n=9). *n* = the number of middle cerebral artery segments from separate rats.

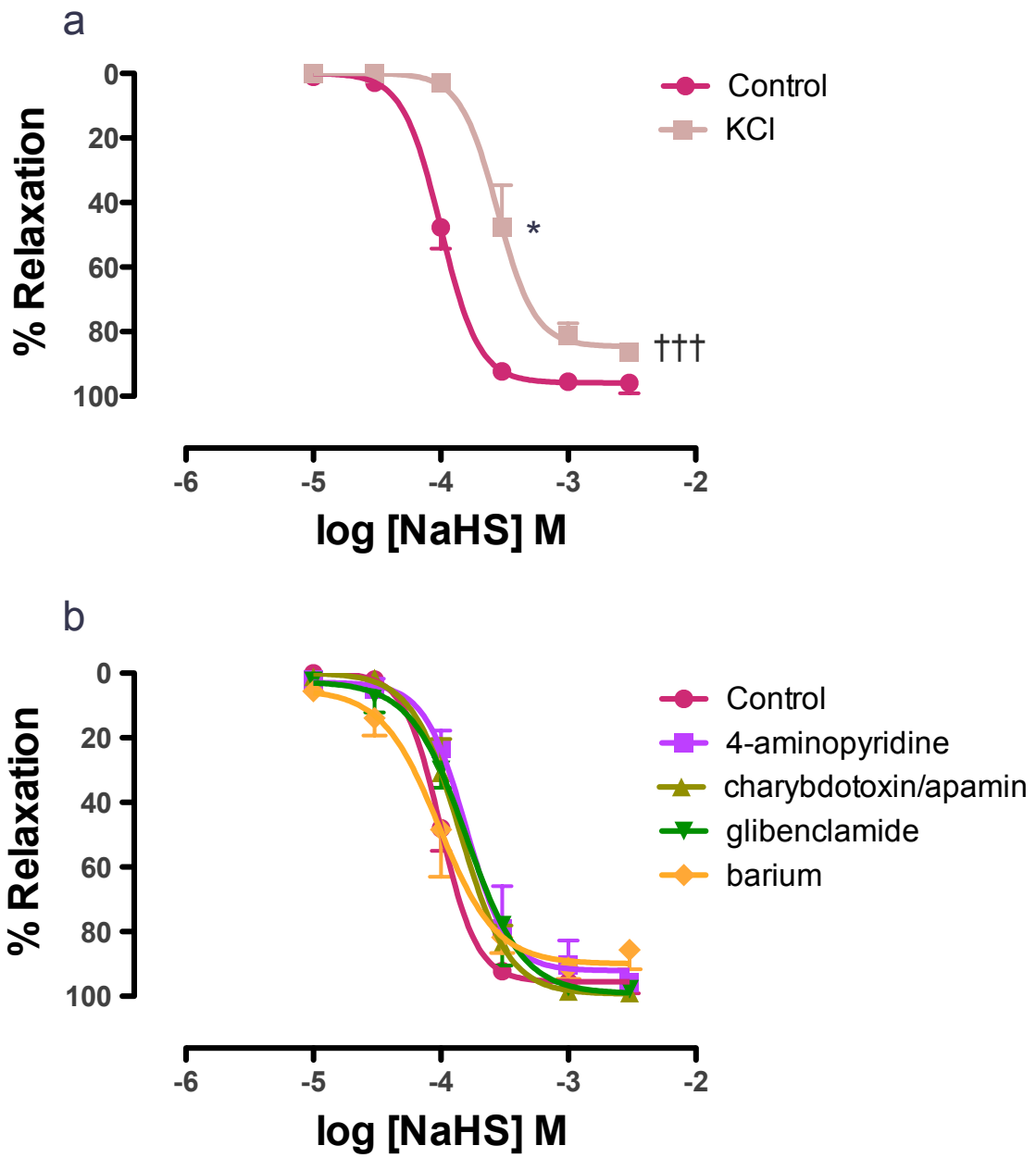

Figure 4.5 Effect of potassium channel inhibition on NaHS-induced vasorelaxation. Cumulative concentration response curves to NaHS in endothelium intact MCA segments in the absence (control, closed circles, n = 13), or presence of **(a)** KCl (50mM, closed squares, n = 7), *P<0.05 $EC_{50,}$ †††P<0.001 E_{max} compared to control, or **(b)** 4-AP (1 mM, closed squares, n = 7); charybdotoxin (100 nM) together with apamin (1 µM, closed triangles, n = 7); glibenclamide (10 µM, closed upside-down triangles n = 7) or Ba^{2+} (30 µM, closed diamonds, n = 5). n = the number of middle cerebral artery segments from separate rats.

Efficacy of glibenclamide: Since K_{ATP} channel opening is reported as a key mechanism for H_2S-mediated vasodilation in the periphery, we investigated the efficacy of our K_{ATP} channel blocker, glibenclamide, in MCA. Levcromakalim (10 nM-100 μM), a K_{ATP} channel opener, induced concentration-dependent vasorelaxation of MCA (figure 4.6). Glibenclamide (10 μM) induced a large rightward shift of the levcromakalim concentration response curve, significantly increasing the EC_{50} by nearly 100 fold (figure 4.6).

Role of reactive oxygen species: Inhibiting the formation of reactive oxygen species (ROS) using the NADPH oxidase inhibitor, DPI (1 μM), did not significantly alter the vasorelaxation to NaHS (figure 4.7, table 4.1). Scavenging ROS using the superoxide dismutase mimetic, tempol (1 mM), also failed to alter NaHS-induced vasorelaxation (figure 4.7, table 4.1). The possibility of involvement of hydrogen peroxide was also investigated using catalase, an enzyme that selectively decomposes hydrogen peroxide. Catalase (1000 U/mL) had no effect on the vasorelaxation induced by NaHS (figure 4.7, table 4.1). None of the agents used to manipulate ROS had any significant influence on basal tone (table 4.2).

Role of chloride channels and bicarbonate exchange: Application of DIDS (300 μM), an inhibitor of both chloride channels and chloride-bicarbonate exchange, produced a significant rightward shift of the NaHS concentration-response curve (figure 4.8, table 4.1). Whether the effect of DIDS was due to chloride channels was investigated using the chloride channel blocker, niflumic acid. Niflumic acid (30 μM) did not produce any significant shift of the NaHS concentration-response curve (figure 4.8, table 4.1). Bicarbonate free Krebs' was used to inhibit the bicarbonate exchanger, however this also failed to alter the NaHS concentration-response curve (figure 4.8, table 4.1). Basal tone was significantly reduced by niflumic acid, but not influenced by DIDS or bicarbonate free Krebs' (table 4.2).

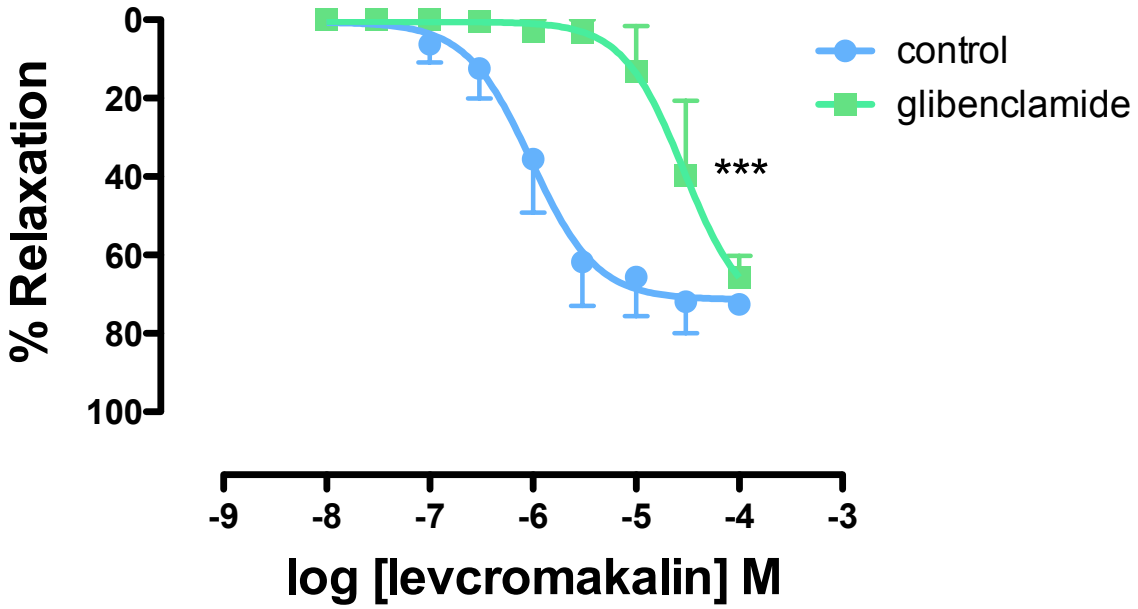

Figure 4.6 Effect of glibenclaminde on levcromakalim induced vasorelaxation.

Cumulative concentration response curves to levcromakalim in endothelium intact MCA segments in the absence (control, closed circles, *n*=4), or presence of glibenclamide (10µM, closed squares, *n* = 4). ***P<0.001 EC_{50} compared to control. *n* = the number of middle cerebral artery segments from separate rats.

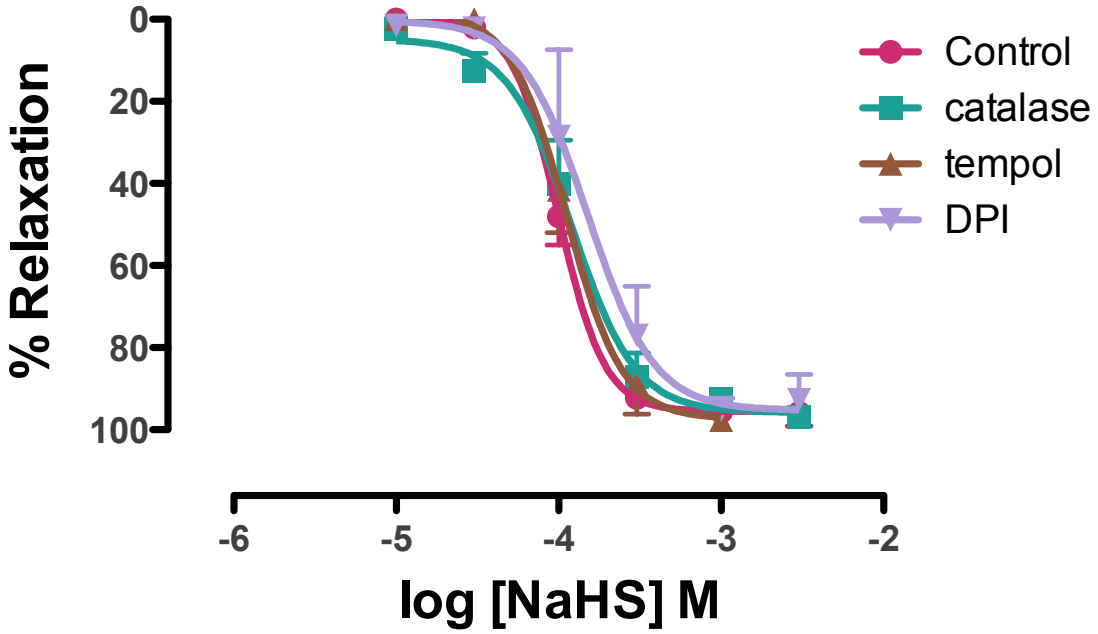

Figure 4.7 Effect of ROS manipulation on NaHS-induced vasorelaxation.

Cumulative concentration response curves to NaHS in endothelium intact MCA segments in the absence (control, closed circles, *n* = 4), or presence of catalase (1000 U/mL, closed squared, *n* = 4), tempol (1 mM, closed triangles, *n* = 3) or DPI (1 μM, closed upside-down triangles, *n* = 4). *n* = the number of middle cerebral artery segments from separate rats.

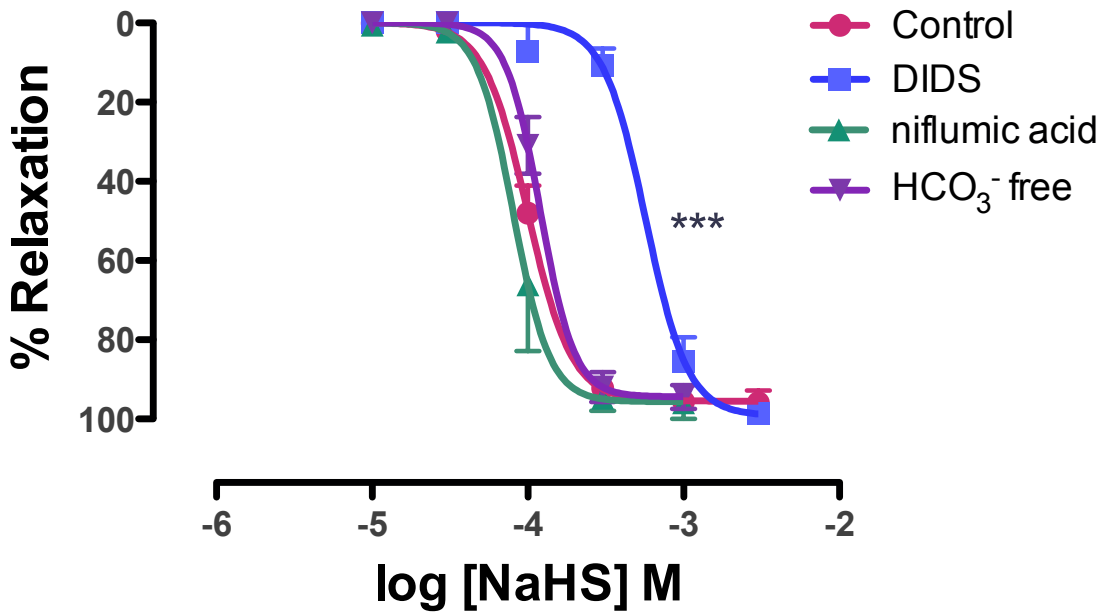

Figure 4.8 Effect of inhibition of chloride channels or chloride-bicarbonate exchange on NaHS-induced vasorelaxation.

Cumulative concentration response curves to NaHS in endothelium intact MCA segments in the absence (control, closed circles, n = 13), or presence of DIDS (300µM, closed squares, n = 5), niflumic acid (30µM, closed triangles, n = 3) or HCO_3^- free Krebs' (closed upside down triangles, n = 4), ***P<0.001 EC_{50} DIDS compared to control. n = the number of middle cerebral artery segments from separate rats.

Role of voltage-gated calcium channels: Nifedipine (3 μM) significantly attenuated the maximum relaxation to NaHS in MCA, although the pEC_{50} was not significantly affected (figure 4.9a). Application of nifedipine produced a significant reduction of basal tone, similar to that induced by niflumic acid (supplementary table 1). The ability of NaHS to inhibit voltage-gated calcium channels was investigated using calcium free Krebs' plus 100 mM KCl to depolarise VSM cells. Concentration response curves to calcium replacement were unaffected by NaHS (100 μM and 1 mM), however, NaHS 10mM significantly attenuated the maximum constriction to calcium by approximately 80% (figure 4.9b), without significantly influencing the pEC_{50}. Nifedipine (3 μM), as a positive control, also significantly reduced the maximum constriction to calcium replacement by approximately 80% (figure 4.9b).

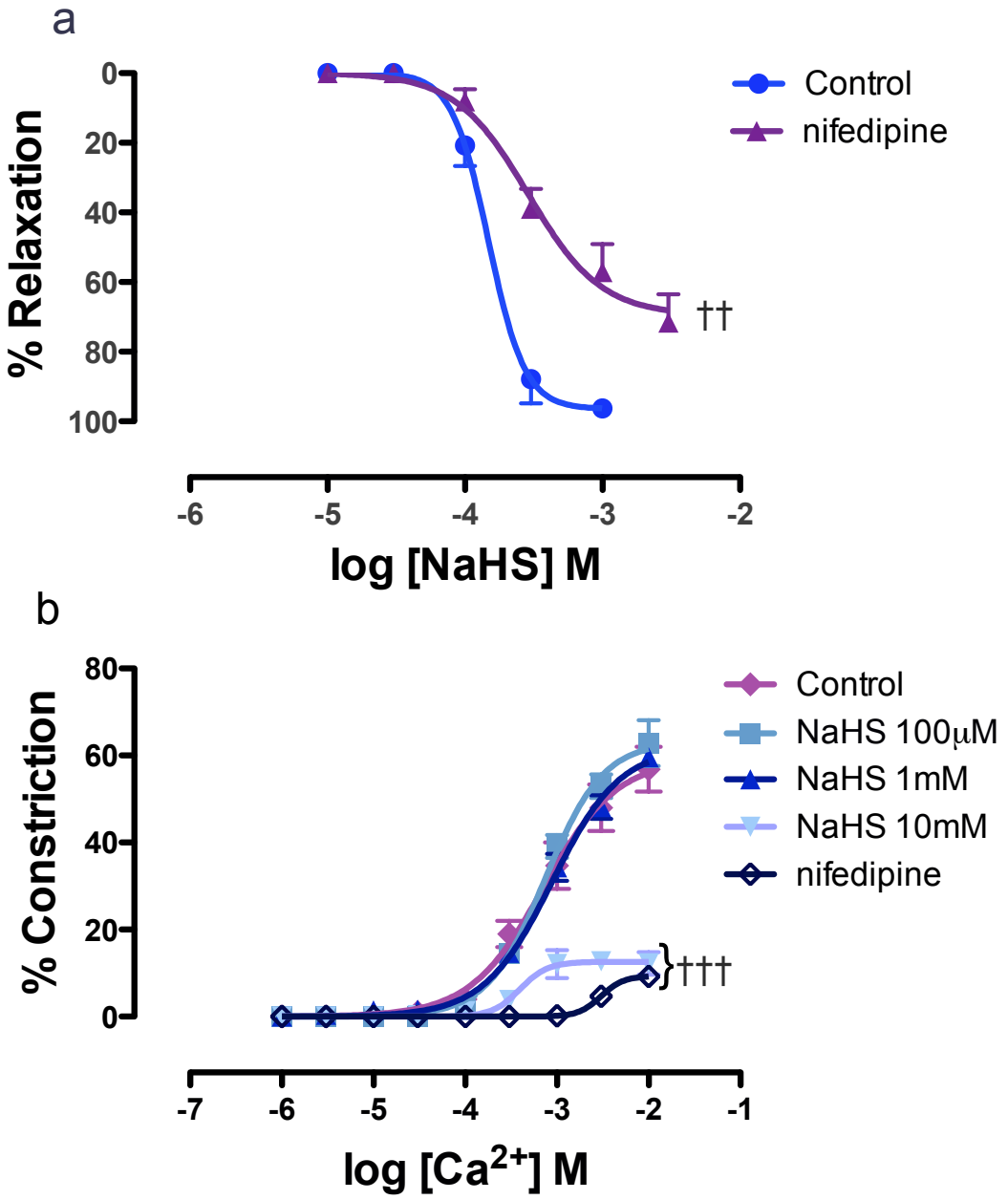

Figure 4.9 Role of voltage-gated calcium channels

Cumulative concentration response curves to NaHS in endothelium intact MCA segments in the absence (control, closed circles, *n* = 5), or presence of nifedipine (3μM, closed triangles, *n* = 6). ††P<0.01 E_{max} compared to control. *n* = the number of middle cerebral artery segments from separate rats. These vessels were preconstricted with U46619 **(b)** Cumulative concentration response curves to $CaCl_2$ in endothelium intact MCA incubated in the Ca^{2+}-free Krebs in the absence (control, closed diamonds, *n* = 5), or presence of NaHS 100μM (closed squares, *n*=3), 1mM (closed triangles, *n* = 4), 10mM (closed upside down triangles, *n* = 5) and nifedipine (3μM, open diamonds, *n* = 5). †††P<0.001 E_{max} compared to control. *n* = the number of middle cerebral artery segments from separate rats.

Table 4.1 pEC_{50} and E_{max} of NaHS-induced vasorelaxation the presence or absence of pharmacological inhibitors.

Drug	*n*	pEC_{50}	E_{max} (%)
Control (spontaneous tone)	13	4.00±0.02	98±0.7
Control (U46619)	4	3.79±0.04	96±1
KCl (50mM)	7	3.56±0.04*	87±1†††
glibenclamide (10μM)	7	3.81±0.08	98±0.5
4-aminopyridine (1mM)	7	3.82±0.07	98±0.7
charybdotoxin/apamin (100nM/1μM)	7	3.85±0.05	99±0.2
barium (30μM)	6	4.05±0.09	92±3
cocktail (glibenclamide+ 4-AP+chtx/apa)	3	3.74±0.09	99±0.6
NaHS (-E)	7	3.80±0.03	98±1
indomethacin (10μM)	5	3.79±0.05	99±0.3
L-NAME (100μM)	9	3.94±0.08	99±0.4
DIDS (300μM)	5	3.24±-0.05***	99± 0.6
HCO_3^- free	4	3.92±0.05	96± 2
niflumic acid (30μM)	3	4.10±0.07	97±2
nifedipine (3μM)	6	3.54±0.09	69±7††
catalase (1000U/mL)	4	3.95±0.05	97±1
tempol (1mM)	3	3.95±0.05	98±2
DPI (1μM)	4	3.82±0.1	96±3

n = the number of middle cerebral artery segments from separate rats. Values are expressed as mean ± standard error of the mean. *P<0.05, ***P<0.001 EC_{50}; ††P<0.01, †††P<0.001 E_{max}.

Table 4.2. Influence of drugs on basal tone.

Drug	Tone (pre inhibitor) (mN)	Baseline tone (pre NaHS) (mN)
Control (spontaneous tone)	6.8±0.3	7.2±0.3
Control (U46619)	N/A	6.6±0.5
KCl (50mM)	5.6±0.6	9.5±0.5***
glibenclamide (10μM)	7.2±0.6	7.6±0.6
4-aminopyridine (1mM)	6.6±0.5	7.1±0.7
charybdotoxin/apamin (100nM/1μM)	6.9±0.5	8.2±0.4**
barium (30μM)	7.4±0.8	7.9±0.9*
NaHS (-E)	N/A	9.1±0.5***
indomethacin (10μM)	7.7±0.6	7.7±0.8
L-NAME (100μM)	6.8±0.6	9.6±0.7***
DIDS (300μM)	7.0	7.7±1
HCO_3^- free	N/A	6.7±0.8
niflumic acid (30μM)	8.0	5.8±0.7*
Nifedipine (3μM)	N/A	5.1±0.7*
catalase (1000U/mL)	6.1±0.5	7.7±1
tempol (1mM)	6.0±0.6	7.3±1
DPI (1μM)	7.3±1	7.0±1

'Tone (pre inhibitor)' is the average tone on vessel segments immediately prior to addition of any pharmacological inhibitor. 'Baseline tone' is the average tone on vessel segments immediately prior to the NaHS dose response curve (approximately 20 minutes after addition of any pharmacological inhibitor). Values are expressed as mean ± standard error of the mean. *P<0.05, **P<0.01, ***P<0.001 'baseline tone' compared to 'tone (pre-inhibitor)'. In vessel segments where an inhibitor was not applied (endothelium denuded), or that were pre-constricted using the U46619 protocol, the tone 'pre-inhibitor' is not applicable. In these groups, 'baseline tone' was compared to the control 'tone (pre-inhibitor)'. mN, milliNewtons

4.3.5 Mechanism of H_2S-induced vasoconstriction

NaHS induced a biphasic effect on MCA tone, consisting of constriction, followed quickly by a robust relaxation (figure 4.10). This biphasic effect was observed after each addition of NaHS at concentrations greater than 30-100 μM (threshold for constriction response = 84 ± 23 μM). The magnitude of constriction caused by NaHS was concentration-dependent. Concentration-response curves to the constriction caused by NaHS in the presence and absence of all inhibitors were also analysed. Reduction of K^+ conductance using 50mM KCl almost abolished constriction to NaHS ($P<0.001$, figure 4.11a, table 4.3). Application of the chloride channel and anion exchange inhibitor, DIDS (300 μM), produced a significant rightward shift of the NaHS concentration-response curve ($P<0.05$, figure 4.11b, table 4.3b). Blockade of L-type Ca^{2+} channels using nifedipine (3μM) significantly decreased maximum constriction ($P<0.05$) and induced a rightward shifted the NaHS concentration-response curve ($P<0.01$, figure 4.11c, table 4.3). Selective decomposition of H_2O_2 using catalase (1000U/mL) significantly decreased the maximum constriction to NaHS ($P<0.05$, figure 4.11d, table 4.3). None of the other inhibitors used significantly influenced the constriction to NaHS (table 4.3).

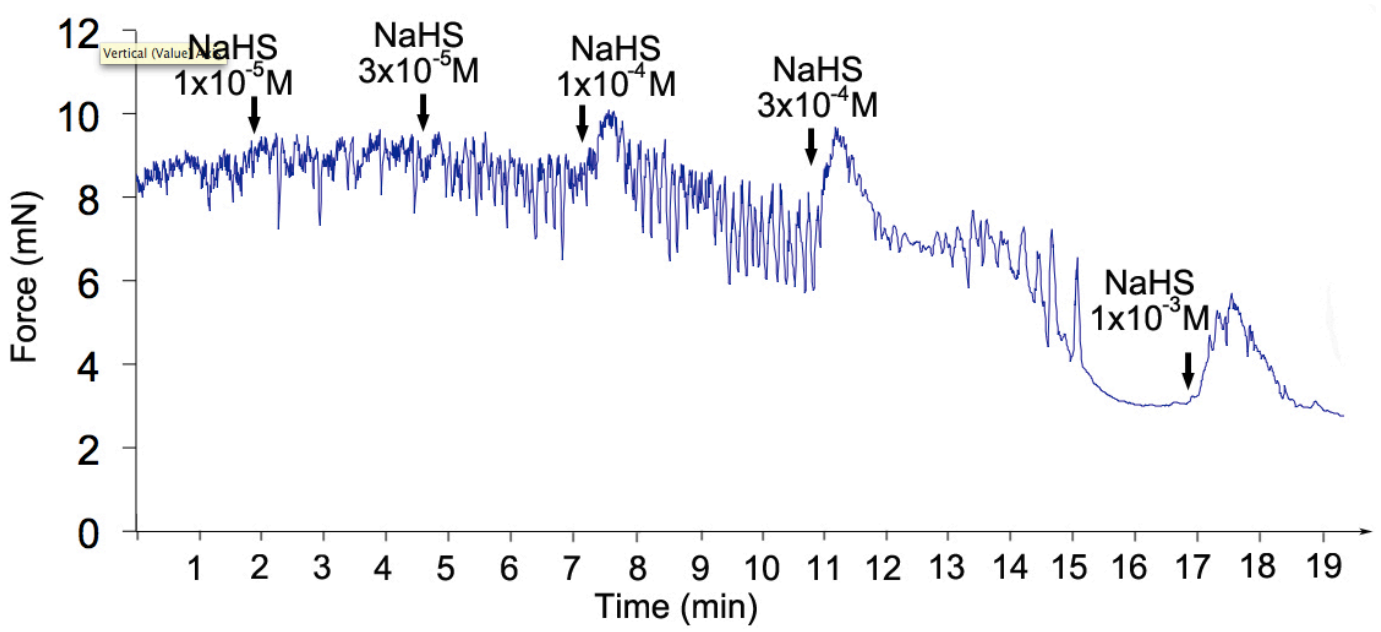

Figure 4.10 Example of original trace showing effects of NaHS on MCA vascular tone

Original trace of tone on an MCA during a concentration-response curve to NaHS, as recorded by Myodaq® software. The MCA had been preconstricted using the spontaneous tone protocol. Arrows indicate the time at which each concentration was administered into the myograph chamber.

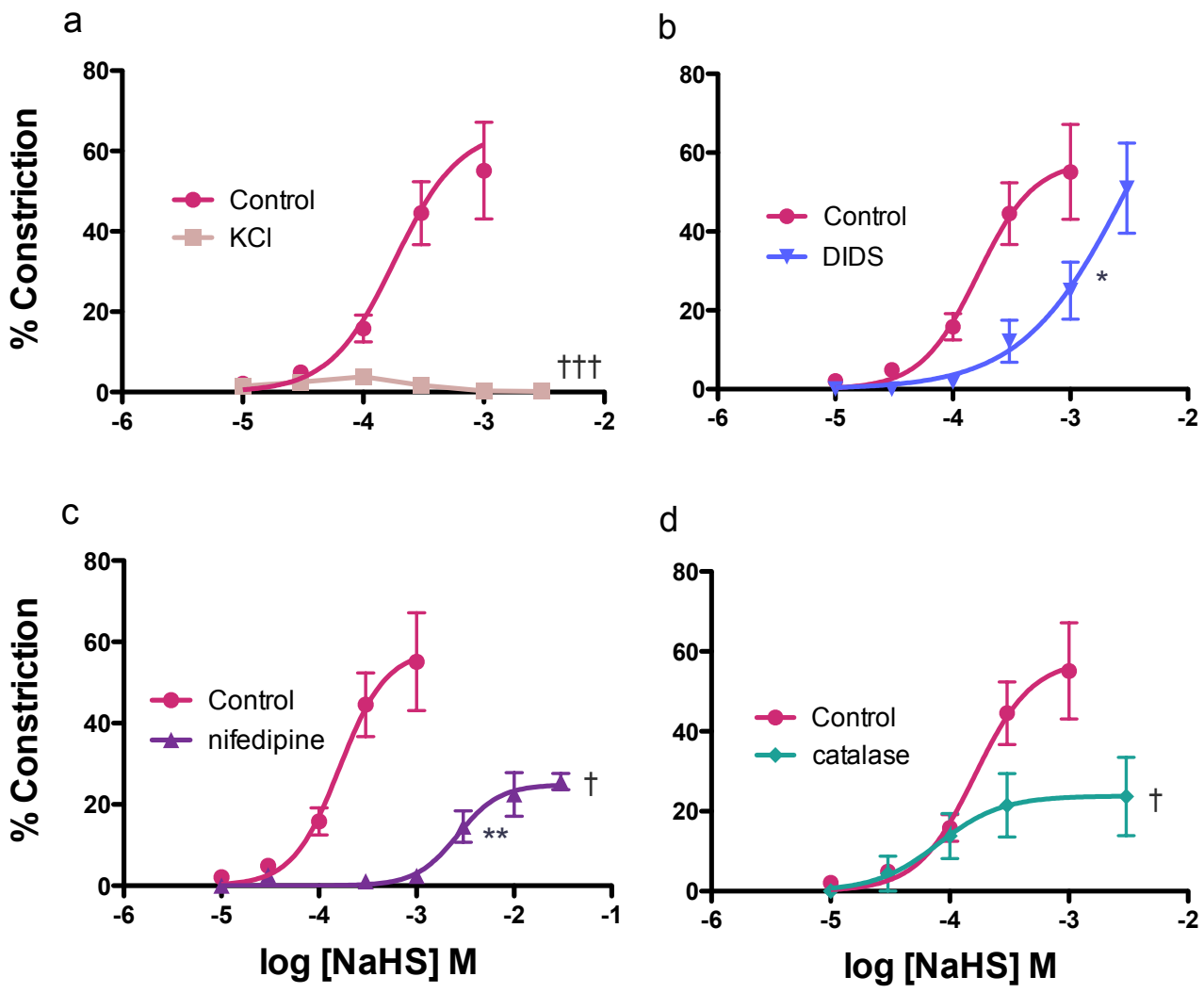

Figure 4.11 Effect of various inhibitors on NaHS-induced vasoconstriction
Cumulative concentration response curves pertaining to NaHS-induced vasoconstriction of endothelium intact MCA segments in the absence (control, closed circles, *n* = 12), or presence of **(a)** KCl (100mM, closed squares, *n* = 7); **(b)** DIDS (300 µM, closed upside-down triangles, *n* = 5); **(c)** nifedipine (3µM, closed triangles, *n* = 6) or **(d)** catalase (1000U/mL, closed diamonds, *n* = 4). *P<0.05 pEC_{50} DIDS compared to control; **P<0.01 pEC_{50} nifedipine compared to control; †††P<0.001 maximum constriction (%) KCl compared to control; †P<0.05 maximum constriction (%) nifedipine and catalase compared to control. *n* = the number of middle cerebral artery segments from separate rats.

Table 4.3 pEC_{50} of NaHS-induced vasoconstriction and maximum constriction to NaHS in the presence or absence of pharmacological inhibitors.

Drug	*n*	pEC_{50}	Max constriction (%)
Control (spontaneous tone)	12	3.79±0.13	56±8
Control (U46619)	4	3.43±0.22	62±12
KCl (50mM)	7	-	5.7±1†††
glibenclamide (10μM)	4	3.60±0.29	47±8
4-aminopyridine (1mM)	6	3.60±0.08	61±15
charybdotoxin/apamin (100nM/1μM)	7	3.60±0.13	62±7
barium (30μM)	3	3.86±0.17	65±20
NaHS (-E)	6	3.82±0.23	55±8
indomethacin (10μM)	5	3.78±0.17	54±9
L-NAME (100μM)	7	3.53±0.13	68±8
DIDS (300μM)	5	2.66±0.08*	59± 12
HCO_3^- free	4	3.98±0.33	50± 9
niflumic acid (30μM)	3	4.10±0.18	79±10
nifedipine (3μM)	6	2.58±0.11**	29±4†
catalase (1000U/mL)	4	4.09±0.28	27±8†
tempol (1mM)	3	3.64±0.43	44±11
DPI (1μM)	3	3.54±1.1	58±24

n = the number of middle cerebral artery segments from separate rats. Values are expressed as mean ± standard error of the mean. *P<0.05, **P<0.01 EC_{50}; †P<0.05, †††P<0.001 E_{max}. Note that the pEC_{50} for NaHS in the presence of KCl (50mM) could not be calculated, due to the almost complete abolishment of the response by KCl (50mM), resulting in a lack of concentration-response curve (see figure 4.11a).

4.4 Discussion

The present study is the first to demonstrate the presence of CSE specifically within endothelial cells and smooth muscle cells of MCA, and to examine in detail the mechanism of NaHS-mediated vasorelaxation in rat middle cerebral arteries. The CSE substrate, L-cysteine caused a PPG-sensitive vasorelaxation, suggesting a role for endogenous H_2S in the regulation of cerebral vascular function. Each addition of the H_2S donor, NaHS, (above a threshold concentration of 84±24μM) caused an initial constriction response, which was followed quickly by a robust relaxation (above a threshold concentration of 72±11 μM). Both constriction and relaxation were concentration dependent. Application of nifedipine produced a significant attenuation of the maximum vasorelaxation elicited by NaHS, suggesting that NaHS may block L-type VGCC. The data also show that relaxation of MCA elicited by NaHS is not endothelium dependent and that NaHS-induced vasorelaxation is only partially due to potassium channel opening, as reducing K^+ conductance produced a modest inhibition of the NaHS-induced relaxation. This role for potassium channels could not be attributed to $K_{ATP,}$ K_{Ca}, K_V or K_{IR} channels as selective blockade of those channels did not have any effect. NaHS relaxation was DIDS sensitive, although the effect could not be explained by inhibition of chloride channels or Cl^-/HCO_3^- exchange, as selective blockade of these mechanisms had no effect. Maximal NaHS-induced constriction was inhibited by KCl, nifedipine and catalase. DIDS induced a rightward shift of the concentration-response curve for NaHS-induced constriction.

This study demonstrates, for the first time, the presence of CSE within endothelial cells and VSM in MCA, confirming a previous report of the presence of CSE in cerebral arterioles (Leffler *et al.*, 2010). The immunohistochemistry data also demonstrates the presence of CSE in endothelial cells and VSM of both mesenteric artery and aorta. The presence of CSE

in endothelium of peripheral vessels remains controversial (Jackson-Weaver *et al.*, 2011; Mustafa *et al.*, 2011; Shibuya *et al.*, 2009a; Yang *et al.*, 2008; Zhao *et al.*, 2001). However, the present findings are in agreement with a study demonstrating the presence of CSE in mouse mesenteric artery endothelium and human umbilical vein endothelial cells by immunohistochemistry and western blotting, respectively (Yang *et al.*, 2008). Furthermore, cultured bovine aortic endothelial cells could generate H_2S, and CSE gene silencing inhibited this H_2S production (Yang *et al.*, 2008). In support of the present findings in VSM, CSE has been demonstrated in rat and mouse aorta smooth muscle cells, by immunohistochemistry or real-time PCR (Al-Magableh *et al.*, 2011; Hosoki *et al.*, 1997; Zhao *et al.*, 2001).

Given that CSE was shown to be present in MCA, the ability of the vessels to relax to endogenously generated H_2S was examined. L-cysteine elicited concentration-dependent relaxation, which was attenuated by the CSE inhibitor, PPG, indicating that the relaxation involved endogenous production of H_2S. The effect of PPG was relatively small suggesting that either (i) only a small proportion of the vasorelaxation induced by L-cysteine was due to H_2S production, (ii) L-cysteine was being converted to H_2S via an alternate enzyme, for example 3-MST (the presence of which has been demonstrated in vascular tissues (Shibuya *et al.*, 2009a) or (iii) there was incomplete inhibition of CSE by PPG. The latter could be due to the relatively poor cell permeability of PPG (Marcotte *et al.*, 1976). It should also be noted that PPG acts by covalently binding to the pyridoxal 5'-phosphate (PLP) (co-factor) binding site of the CSE enzyme, thus may also influence other PLP-dependent enzymes (Johnston *et al.*, 1979). Despite these limitations, PPG is a widely used inhibitor of endogenous H_2S production and is the best available pharmacological tool at this time. L-cysteine-induced relaxation in MCA was independent of endothelium, suggesting that conversion of L-cysteine to H_2S occurs mainly in the sub-endothelial tissue, for example, in smooth muscle cells.

Thus, although our immunohistochemistry data demonstrate the presence of CSE in the endothelium, the vasorelaxation studies indicate that the production of H_2S from the endothelial layer does not make a major contribution to the vasorelaxation mediated by endogenous H_2S in MCA.

In rat mesenteric arteries L-cysteine-induced relaxation was attenuated by endothelium removal (Jackson-Weaver *et al.*, 2011), suggesting that the contribution of endothelial derived H_2S to vasorelaxation is tissue-type specific. Furthermore, there is evidence to suggest that H_2S may be a candidate for endothelium-derived hyperpolarizing factor (EDHF), such that $CSE^{-/-}$ mice have attenuated cholinergic vasorelaxation (Yang *et al.*, 2008) and hyperpolarisation (Mustafa *et al.*, 2011) in mesenteric artery and aorta. The present findings are not supportive of a role for H_2S as an EDHF in MCA. The discrepancy may be due to an anomaly introduced by the $CSE^{-/-}$ model: this model has been shown to induce hyperhomocysteinaemia (HHcy), thus, the findings of the aforementioned studies may have been confounded by endothelial dysfunction induced by HHcy generated ROS (Edwards *et al.*, 2012). However, it is possible that H_2S acts as an EDHF in mesenteric, but not cerebral vessels, given evidence that the candidate for EDHF is different in cerebral and mesenteric arteries (Dong *et al.*, 2000).

In the present study, the maximum relaxation induced by NaHS was significantly reduced by nifedipine, a highly selective L-type calcium channel blocker (Furukawa *et al.*, 1999), suggesting a role for voltage-gated calcium channels. To investigate this further, the effect of NaHS on calcium-mediated vasoconstriction was determined. NaHS significantly inhibited the ability of calcium to constrict rat middle cerebral arteries, supporting the view that vasorelaxation induced by NaHS involved inhibition of voltage-gated calcium channels.

NaHS inhibition of L-type calcium channel conductance has also been demonstrated in rat cardiac myocytes (Sun *et al.*, 2008). In the present study, the concentration of NaHS required to significantly block the calcium-induced constriction was at least 10 fold higher than that which produced maximum vasorelaxation. This difference has been observed previously (Al-Magableh *et al.*, 2011) and is probably due to the different methodological conditions used to examine the vasorelaxation compared to the vasoconstriction responses. In these latter experiments it is necessary to depolarise the VSM cells, so that the VGCC are open. The level of depolarisation achieved with 100mM K^+ would be expected to be greater than either that of a spontaneously contracted artery, or an artery sub-maximally contracted with U46619. Therefore a higher concentration of NaHS may be required to counteract this depolarisation.

The present work indicates an endothelium independent mechanism for H_2S-induced vasorelaxation, since removal of endothelium had no effect on the NaHS-induced relaxation of MCA. This is in agreement with our data showing that inhibition of the synthesis of the endothelium derived vasodilators, nitric oxide and prostacyclin, had no effect. In a recent report, removal of the endothelium attenuated the effect of NaHS (Liu *et al.*, 2012), however, that report examined the effect of NaHS on myogenic tone development, as opposed to the present study investigating the vasorelaxant mechanisms. The discrepancy is likely due to a difference in mechanism of H_2S between the two models: inhibition of myogenic tone development compared to vasorelaxation. The role of the endothelium in the vasorelaxation mediated by H_2S in peripheral vessels also remains controversial. Several studies using mouse and rat aorta report that removal of endothelium had no effect on H_2S-mediated vasorelaxation (Al-Magableh *et al.*, 2011; Hosoki *et al.*, 1997; Kubo *et al.*, 2007). In contrast, other studies, using rat aorta and mesenteric vessels, have reported an attenuation of H_2S-

mediated relaxation when the endothelium was removed (Cheng *et al.*, 2004; Zhao *et al.*, 2001).

The present data suggests only a partial role for potassium channels in mediating vasorelaxation to NaHS, as 50mM KCl significantly reduced the maximum relaxation by approximately 10% and sensitivity by 4 fold. The contribution of specific potassium channels to the H_2S-mediated vasorelaxation was also investigated. Using glibenclamide to block K_{ATP} channels had no effect on the vasorelaxation to NaHS, but effectively blocked the vasorelaxation elicited by the specific K_{ATP} channel opener, levcromakalim. Similarly, blockade of K_V, K_{Ca} and K_{IR} channels had no effect. The role of two-pore domain K^+ channels was not investigated and it is conceivable that the observed minor role for K^+ channels in the H_2S-induced vasorelaxation may be attributable to this potassium channel subtype. An alternative explanation for the ability of 50mM K^+ to attenuate the H_2S-mediated vasorelaxation is that the strong depolarisation induced by the high concentration of K^+ may influence voltage operated mechanisms, for example, opening voltage-gated calcium channels (see later in discussion). This view would not support a role for K^+ channels in the H_2S-mediated vasorelaxation in MCA.

A very recent study demonstrates that H_2S increases the frequency of Ca^{2+} sparks in piglet cerebral arteriole smooth muscle cells, causing an increase in the frequency of transient K_{Ca} current, and thus vasorelaxation (Liang *et al.*, 2012). In the present study, combined BK_{Ca} and SK_{Ca} blockade did not influence H_2S-mediated vasorelaxation, indicating that this mechanism does not contribute to H_2S-mediated vasorelaxation of rat MCA. This may be due to a difference in the contribution of K_{Ca} to resting tone. Inhibition of BK_{Ca} and SK_{Ca} resulted in a significant increase in resting tone on adult rat MCA in the present study

(supplemental table 1) in agreement with previous work (Gollasch *et al.*, 1998), but in newborn rats or newborn pigs the increased tone is not observed (Gollasch *et al.*, 1998; Liang *et al.*, 2012). These observations suggest the influence of H_2S on K_{Ca} may be age dependent. In peripheral vessels, age also influences the effect of H_2S on K_{Ca} (d'Emmanuele di Villa Bianca *et al.*, 2011; van der Sterren *et al.*, 2011).

The present study finds no role for K_{ATP} channels in H_2S-mediated relaxation of MCA. Three other studies have investigated the role of K_{ATP} channels in cerebral vessels. In an *in vivo* study, using piglet pial arterioles (50 μm), the vasorelaxation response to H_2S solution was found to be entirely mediated by K_{ATP} channels (Leffler *et al.*, 2010). In a separate study, using piglet cerebral arterioles (200μm) *in vitro*, only 55% of the vasorelaxation could be attributed to K_{ATP} channels (Liang *et al.*, 2011). Additionally, the latter study showed that the Na_2S (a H_2S donor) -mediated vasorelaxation of cerebral vessels of SUR2 (a K_{ATP} subunit) knockout mice was only 50% of the wild type mice (Liang *et al.*, 2011). In a more recent study, glibenclamide reportedly reduced the NaHS-induced reduction in myogenic tone at intraluminal pressures between 20-60mmHg, but not between 80-120mmHg (Liu *et al.*, 2012). While these studies show that K_{ATP} channels play a role, the data strongly suggests that other mechanisms are also involved. The disparity between the present study and these previous reports on the role of K_{ATP} channels, may be due to different vessel types, species, and age of the animals. Indeed it is known that the sensitivity of lemakalim-induced cerebral vasorelaxation is different in newborn compared to adult cerebral arteries *in vitro* (Pearce *et al.*, 1994). Additionally, in the present study, the vessels were investigated under isometric compared to isobaric conditions (Liang *et al.*, 2011), or pressure-induced myogenic tone (Liu *et al.*, 2012). Although these different conditions can influence the reactivity of vessels, the influence is not dramatic (McPherson, 1992), and it is unlikely to account for the marked

differences between the studies in the contribution of K_{ATP} channels in the vasorelaxation mediated by H_2S. The role of K_{ATP} channels in the H_2S-mediated vasorelaxation in peripheral vessels is also controversial. In some studies, using rat and mouse aorta, only partial inhibition of the relaxation induced by NaHS was demonstrated by blockade of K_{ATP} channels (Al-Magableh *et al.*, 2011; Cheng *et al.*, 2004; Zhao *et al.*, 2001). By contrast, other studies using rat mesenteric arteries, and rat and mouse aorta, failed to demonstrate any role of K_{ATP} channels in the vasorelaxation mediated by H_2S (Jackson-Weaver *et al.*, 2011; Kiss *et al.*, 2008; Kubo *et al.*, 2007).

Since the present findings suggested only a partial role for K^+ channels in the H_2S-mediated vasorelaxation, other potential mechanisms that could contribute were investigated. DIDS was used to explore the role of Cl^- channels and Cl^-/HCO_3^- exchange and was found to significantly attenuate the vasorelaxation induced by NaHS. However, the more selective Cl^- channel blocker, niflumic acid, did not affect the response to NaHS, suggesting Cl^- channels were not involved. To investigate the role of Cl^-/HCO_3^- exchange, HCO_3^- free solution was used but also had no effect on the NaHS vasorelaxation response. Thus, Cl^-/HCO_3^- exchange does not appear to play a role in the vasorelaxation mediated by H_2S. Since DIDS is known to be non-specific in its actions, the ability of DIDS to attenuate the NaHS response may involve some other action(s) of this drug, for example, inhibition of Na^+ current or influences on the ryanodine receptor (Hill *et al.*, 2002; Liu *et al.*, 1998; Lu *et al.*, 2007). This requires further investigation.

ROS are generated at low levels in cerebral vessels and are essential for normal vascular cell physiology, having multiple functions, including regulation of tone (Miller *et al.*, 2005). Under basal conditions, ROS are maintained at low levels by production of NO, which

rapidly reacts with superoxide (Rubanyi *et al.*, 1986). H_2S has also been shown to directly scavenge ROS (Whiteman *et al.*, 2005) and to influence ROS production (Samhan-Arias *et al.*, 2009). It was therefore examined whether the vascular effects of H_2S were due to an influence on ROS. Since tempol, DPI and catalase had no effect on the vasorelaxation induced by NaHS, the present findings do not support a role for ROS in the vasorelaxation mediated by H_2S. This is in contrast with a finding that Tiron, a superoxide dismutase mimetic, enhanced the vasorelaxant action of H_2S in aortic rings (Liu *et al.*, 2010). The difference is probably due to a marked difference between the reaction of cerebral and peripheral vessels to ROS (Faraci, 2006). There is evidence that K^+ channels, such as K_{ATP} and K_{Ca}, mediate vasodilator effects of ROS in cerebral vessels (Faraci, 2006). Our findings that selective K_{ATP} and K_{Ca} blockade had no effect on the vasorelaxation induced by NaHS therefore also support the view that ROS are not involved in H_2S-induced vasorelaxation of MCA.

In peripheral vessels, several studies demonstrate that H_2S has a biphasic effect on vascular tone, consisting of constriction at low concentrations, followed by dilation at high concentrations (Ali *et al.*, 2006; Kubo *et al.*, 2007; Lim *et al.*, 2008; Liu *et al.*, 2010). The present study is the first to investigate the constrictor action of H_2S in cerebral vessels and demonstrates a 'dual vascular response' of cerebral vessels to H_2S, consisting of a transient vasoconstriction, followed by a robust vasorelaxation. The response is referred to as 'dual' as opposed to 'biphasic', since both constriction and relaxation were observed after administration of a single concentration of NaHS (compared to the biphasic response to NaHS which consists of constriction at low concentrations, and dilation at high concentrations, with only one of these responses occurring after a single addition of NaHS). A similar dual vascular response to H_2S has also been observed in mesenteric arteries

(d'Emmanuele di Villa Bianca *et al.*, 2011). In the present study, the magnitude of NaHS-induced constriction was concentration-dependent. While the subsequent robust vasorelaxation has been the main subject of this study, as an aside, it was also possible to observe the effect of each of the treatments on the constriction response.

The maximum constriction to NaHS was nearly completely abolished by 50 mM K^+, indicating a possible involvement of K^+ channels, although this could not be attributed specifically to any of K_{ATP}, K_V, K_{Ca} or K_{IR}, since selective blockade of each of these pathways had no effect. Similarly in rat aorta, although K_{ATP} channels do not appear to be involved in the H_2S-induced constrictor response (Kubo *et al.*, 2007; Lim *et al.*, 2008), the response was inhibited by 50mM KCl (Kubo *et al.*, 2007). The lack of efficacy of the selective K^+ channel blockers indicates that 50mM K^+ may block the constrictor action of H_2S via inhibition of K^+ channels other than those targeted in the present study, for example, two-pore-domain K^+ channels, or a subtype of K_V, K_{V7}, which are insensitive to the K_V blocker 4-aminopyridine (Mackie *et al.*, 2008). Alternatively, the constrictor action of H_2S may be due to opening of VGCC, and thus the depolarising effect of 50mM K^+, and ensuing increased open probability of VGCC, would reduce the population of VGCC upon which H_2S could act. In support of this view, blockade of L-type calcium channels using nifedipine significantly inhibited NaHS-induced constriction in the present study, and also in a study using rainbow trout branchial arteries (Dombkowski *et al.*, 2004).

DIDS caused a significant rightward shift of the constriction concentration-response curve, although this could not be specifically attributed to either bicarbonate exchange or inhibition of chloride channels, as selective blockade of each of these pathways had no effect. DIDS has also been shown to attenuate H_2S-induced constriction of rat aortic rings (Liu *et al.*,

2010), however, this effect was attributed to DIDS' inhibition of bicarbonate exchange, since a bicarbonate-free medium also blocked the constriction. The authors concluded that H_2S stimulates the anion exchanger to transport bicarbonate for intracellular O_2^-, which inactivates NO to induce vasoconstriction. Thus the difference observed in terms of efficacy of the bicarbonate-free medium may be attributed to a difference in reactivity of the two vessel types to O_2^-. Selective decomposition of H_2O_2 using catalase also significantly inhibited H_2S- induced vasoconstriction in the present study. Since H_2O_2 generally acts to dilate VSM (Wolin, 2009) including MCA (Faraci, 2006), the efficacy of catalase is suggestive that H_2S induces constriction via reducing H_2O_2 levels, although this hypothesis requires further investigation.

A striking similarity is observed when comparing the agents that inhibited vasodilation to those that inhibited constriction. Of the 14 agents investigated in this study, only three – 50mM KCl, nifedipine and DIDS - significantly inhibited vasorelaxant effects of H_2S, and all three also inhibited vasoconstriction. Only one agent, catalase, was effective at blocking vasoconstriction but not vasorelaxation. Although speculative, the similarity in mechanism between constriction and relaxation could be taken to indicate that both constriction and relaxation are a consequence of one initiating effect of H_2S. For example, H_2S may induce a hypoxia-like state, by its inhibition of cytochrome c oxidase (Groeger *et al.*, 2012), leading to influences on vascular tone. Observations of various other studies support the hypothesis that the vascular actions of H_2S are due to inhibition of cytochrome c oxidase. Firstly, cyanide, a cytochrome c oxidase inhibitor, also induces constriction followed by relaxation (Mathew *et al.*, 1991). Secondly, vascular responses to H_2S and hypoxia have been compared, and found temporally and quantitatively identical in a range of vessel types (Olson *et al.*, 2006; Olson *et al.*, 2008; Olson *et al.*, 2001). Finally, similar mechanisms contribute to H_2S-induced and

hypoxia-induced vasodilation, including K_{ATP} (Adebiyi *et al.*, 2011), BK_{Ca} (Armstead, 1998) and generation of NO (Pearce, 1995). Interestingly, the precise mechanism of hypoxic vasodilation remains unresolved, and similar controversies exist regarding the contribution of various mechanisms, for example K_{ATP} channels (Adebiyi *et al.*, 2011). However, whether the dual vascular effect of H_2S in MCA observed in the present study was due to metabolic inhibition requires further investigation.

Methodological Aspects

In the present study the EC_{50} of NaHS (100±5 μM) to induce vasorelaxation was similar to that observed in other studies using mouse and rat aorta (Al-Magableh *et al.*, 2011; Kiss *et al.*, 2008; Lee *et al.*, 2007; Zhao *et al.*, 2001). However, a study in cerebral vessels observed a higher potency of Na_2S at relaxing piglet pial arterioles (EC_{50} (Na_2S)= 30±5 μM) (Liang *et al.*, 2011). The discrepancy between this and the present study may be due to any number of differences, including; i) vessel type and species – H_2S is more potent at relaxing mesenteric vessels than aorta (EC_{50}= 25±4 μM; 125±14 μM in mesenteric and aorta, respectively, (Cheng *et al.*, 2004; Zhao *et al.*, 2001)) so a similar variation between cerebral vessel types is possible; ii) H_2S donor used – the NaHS used in the present study may have different H_2S releasing properties to the Na_2S used by Liang *et al*. This could account for the observation that double the concentration of NaHS was required to produce a similar response to Na_2S (Liang *et al.*, 2011); iii) method used to observe vasorelaxant response – although vessels treated with isometric compared to isobaric conditions may show different reactivity, the difference is not great (McPherson, 1992). Even within vessels under isometric conditions, the present study indicates that the preconstriction protocol does not influence the reactivity of the vessels to H_2S - NaHS produced a similar concentration-response curve in MCA preconstricted with either U46619 or the spontaneous tone protocol. We therefore used the spontaneous tone method to preconstrict MCA whilst avoiding confounding influences of preconstriction drugs.

Plasma concentrations of H_2S have been reported to be between 40-300 μM, which places the vasorelaxant responses observed in our study within the physiological range (Kimura, 2002). However, more recent studies suggest that these are overestimations, and the actual concentration may, in fact, be in the nanomolar range (Furne *et al.*, 2008; Whitfield *et al.*, 2008). It should be noted that the amount of H_2S actually reaching the target vascular tissue is probably much lower than the concentration of NaHS applied to the bath for several reasons. Firstly, a previous report indicates that the final concentration of H_2S in solution is less than 10% of the concentration of NaHS used, (Al-Magableh *et al.*, 2011), probably due to volatility and equilibrium with HS^- (see 1.1.2, Pharmacological tools, H_2S donors, p.17). Secondly, free H_2S applied to various tissue types is promptly sequestered and stored as bound sulfur (Ishigami *et al.*, 2009). Furthermore, as a small molecule of gas, H_2S diffuses rapidly, making it difficult, if not impossible, to measure local concentrations of H_2S at the site of action and production: the smooth muscle cell. It is, therefore, entirely plausible that H_2S acts as a physiological vasorelaxant in MCA, despite the relatively low potency of NaHS observed in this study.

It is also important to note that some of the treatments used in the present study altered basal tone, however, such changes cannot account for the effects of the treatments which influenced the H_2S-mediated relaxation, because similar changes to basal tone were observed with other treatments that had no effect on the H_2S-mediated relaxation. In the case of 50 mM K^+, the increase in basal tone was similar to those observed with L-NAME, which had no effect on the H_2S-mediated vasorelaxation. In the case of nifedipine, the reduction in basal tone observed was similar in amplitude to that observed with niflumic acid, which had no influence on H_2S-mediated vasorelaxation. Taken together, these observations suggest that effects of 50 mM K^+ and nifedipine on H_2S-mediated relaxation were independent of their effects on basal tone.

Conclusion

The presence of the H_2S producing enzyme, CSE, was demonstrated in endothelium and smooth muscle cells of MCA, thus, endogenously generated H_2S may play a role in regulating cerebrovascular tone. Vasorelaxation mediated by H_2S in rat middle cerebral arteries was found to be endothelium independent and involved a contribution from voltage-gated calcium channels as well as from K^+ channels. There was no contribution from reactive oxygen species. The response was sensitive to DIDS, but inhibition of chloride channels or the anion exchanger had no effect. H_2S-induced vasoconstriction also involved contributions from voltage gated calcium channels, potassium channels and was DIDS-sensitive. The vasoconstriction was inhibited by catalase, indicating this effect is partly due to an influence of H_2S on H_2O_2.

Chapter 5: Effect of STZ-induced diabetes on the vascular response to H_2S in rat middle cerebral arteries

5.1 Introduction

H_2S is well established as a vasodilator in the periphery (d'Emmanuele di Villa Bianca *et al.*, 2011; Hart, 2011; Hosoki *et al.*, 1997; Jackson-Weaver *et al.*, 2011; Liu *et al.*, 2011b; Schleifenbaum *et al.*, 2010; Zhao *et al.*, 2001) and there are now several lines of evidence that it also dilates cerebral vessels (Leffler *et al.*, 2010; Liang *et al.*, 2011; Liang *et al.*, 2012; Streeter *et al.*, 2012). Genetic deletion of CSE results in pronounced hypertension, as well as reduced endothelium dependent vasorelaxation (Yang *et al.*, 2008). There is a growing body of evidence that H_2S also protects against endothelial dysfunction via anti-inflammatory (Pan *et al.*, 2011) and antioxidant effects (Guan *et al.*, 2012; Suzuki *et al.*, 2011) (see 1.4.4, Diabetic vascular disease and H_2S, p.61). H_2S protects against atherosclerosis in animal models, for example, NaHS significantly inhibited neointima formation after balloon injury in rats (Meng *et al.*, 2007) and reduced the size of atherosclerotic plaques in apolipoprotein E knockout mice (Wang *et al.*, 2009).

Diabetes causes peripheral and cerebrovascular disease, the hallmarks of which are endothelial dysfunction and atherosclerosis. Diabetes increases the risk of ischaemic stroke by one and a half to two-fold (Quinn *et al.*, 2011), and this increased risk has been associated with diabetic cerebrovascular disease (Gunarathne *et al.*, 2009; Nazir *et al.*, 2006). Furthermore, diabetes is associated with cognitive decline and impairment, Alzheimer's disease and vascular dementia, and there is mounting evidence linking all of these conditions with cerebrovascular disease (Humpel, 2011; Steffens *et al.*, 2007; Wakefield *et al.*, 2010).

Despite the severe risks associated with diabetic vascular disease, it remains incompletely understood. There is a general consensus in the literature that excessive vascular production of ROS and resulting decreased availability of nitric oxide are major contributors to diabetic endothelial dysfunction (Creager *et al.*, 2003) (see 1.4.3 Aetiology of diabetic cerebrovascular disease, Role of ROS in endothelial dysfunction, p.58). Interestingly, H_2S has been shown to decrease mitochondrial membrane potential and decrease overproduction of ROS in PC12 cells (Tang *et al.*, 2008). In a recent study, elevated glucose was found to reduce H_2S levels in the supernatant of endothelial cells *in vitro*, an effect which was attributed to consumption of H_2S by mitochondrial ROS (Suzuki *et al.*, 2011). Furthermore, administration of H_2S attenuated the decline in endothelial cell viability and reduced ROS production *in vitro*, as well as protecting against endothelial dysfunction in STZ-induced diabetic rats *ex vivo* (Suzuki *et al.*, 2011).

There is evidence that H_2S production and vasodilation capacity are altered in diabetic peripheral vessels, further suggesting that H_2S may be involved in diabetic vascular disease. In aorta, mesenteric and pulmonary arteries, STZ-induced diabetes has been shown to enhance the vasodilator action of H_2S (Denizalti *et al.*, 2011). Aorta from non-obese diabetic mice have enhanced vasodilation by H_2S, as well as increased CSE mRNA expression (Brancaleone *et al.*, 2008). In cerebral vessels, the effect of diabetes on the vasodilator response or production of H_2S has not, to date, been studied. To further our understanding of the cerebrovascular pathological changes induced by diabetes, we have investigated whether diabetes alters the middle cerebral artery's vascular response to H_2S or tissue production of H_2S.

5.2 Methods

5.2.1 Streptozocin treatment

Induction of the diabetic model is described in detail in section 2.4.1. Animals were fasted for 12 hours followed by administration of STZ (50 mg/kg) in sodium citrate buffer (10 mM, pH 4.5) via tail vein injection. Development of diabetes was confirmed one week after STZ injection and again on the day of experiment by a non-fasting blood glucose of >15 mmol/L.

5.2.2 Wire myography

Middle cerebral arteries were collected (see 2.3.1) and cut into 2mm segments, which were mounted into a wire myograph (see 2.3.2 and figure 2.2). The vessels were then constricted using the 'spontaneous tone protocol' (see 2.3.2 and figure 2.3), except vessels to be treated with nifedipine, for which the 'U46619 protocol' (see 2.3.2 and figure 2.4) was used.

Assessment of endothelial function

A single dose of bradykinin (BK, 100nM) was applied to control and diabetic vessel segments to assess the function of endothelium.

Mechanism of H_2S-induced vasorelaxation and vasoconstriction

The vascular response to cumulative concentrations of the H_2S donor, NaHS (10 μM-3 mM), was examined in the presence or absence of one (or more) of the following: KCl (50 mM), to inhibit K^+ conductance; DIDS (300 μM), an inhibitor of chloride channels and Cl^-/HCO_3^- exchange; nifedipine (3 μM), an L-type voltage-gated calcium channel blocker. Each was added 20 minutes prior to construction of the NaHS concentration-response curve. At the completion of each experiment, maximal relaxation was recorded using calcium free Krebs'. Each vessel segment was used to obtain only one concentration-response curve.

Vasorelaxation to endogenous H_2S

For these studies, the spontaneous developed tone protocol was used. The relaxation response of vessel segments from diabetic and control rats to cumulative (0.5 log unit) concentrations of L-cysteine (10μM-100mM) was assessed in the presence and absence of PPG (20mM).

For a detailed description of the data analysis, see 2.3.3 Data Analysis, p.80. Briefly, comparisons were made between average E_{max} and $logEC_{50}$ values using T-tests for comparisons between two data sets, and one-way ANOVA with a post-hoc Dunnett's test for comparisons between multiple data sets.

5.2.3 Lucigenin Assay

The methods for the lucigenin assay are described in detail in section 2.4.2 and figure 2.6. Briefly, the circle of Willis, basilar artery and thoracic aorta from control and diabetic rats were dissected and cleaned of connective tissue. The aorta was cut into several 2mm segments and the cerebral arteries were pooled, before being divided in half for separate treatments. Once prepared, the arteries were immediately transferred to a 24-well plate for a series of two incubations followed by a wash. Artery segments were then transferred into separate wells of an Optiplate containing a solution with lucigenin (5 μM). $O_2^{\cdot -}$ production was subsequently measured by reading for luminescence using a Polar star microplate reader.

5.2.4 Detection of CSE via RT-PCR

Since MCA from the present study were utilised in the myograph experiments, MCA for the PCR experiments were obtained from additional diabetic and control groups. MCA were dissected and placed into RNAlater® and stored at -20 ˚C until assay for CSE expression (see 2.5.3).

5.2.5 Measurement of plasma sulfide and liver CSE activity

The liver of diabetic and control animals was snap frozen using liquid nitrogen and stored at -80 ˚C, for later analysis of CSE activity using the assay developed by Stipanuk and Beck (Stipanuk *et al.*, 1982) (see 2.5.4). Whole blood was collected and spun at 1,300 g for 10 minutes for separation of plasma, which was drawn off and stored at -20 ˚C until assay for sulfide content (see 2.5.4).

5.3 Results

5.3.1 STZ rats had high blood glucose and endothelial dysfunction in MCA

STZ rats had significantly higher blood glucose than controls, as measured on the day of experiment, confirming induction of the diabetic model (table 5.1). The level of tone developed in MCA segments using the spontaneous tone protocol was not significantly different between vessels from control and STZ treated animals (table 5.2). The maximal contractile capacity (to 125mM KCl) was not significantly different in MCA from STZ treated, compared to control animals (table 5.2). However, relaxation of MCAs to BK 100nM was significantly reduced in STZ treated animals, indicating endothelial dysfunction (figure 5.1).

5.3.2 Vasorelaxation response to exogenous H_2S

The hydrogen sulfide donor, NaHS, (10 μM-3 mM) produced a full, concentration-dependent vasorelaxation of MCA which was not altered by the STZ diabetic model (figure 5.2). The pEC_{50} for NaHS-induced relaxation of MCA was 3.94±0.06 in control compared to 4.03±0.07 in diabetic MCA.

5.3.3 Mechanisms of H_2S-induced vasorelaxation of diabetic MCA

The contribution of K^+ conductance, chloride-bicarbonate exchange and L-type Ca^{2+} channels to H_2S-induced vasorelaxation in diabetic MCA were investigated. Application of DIDS (300 μM), an inhibitor of both chloride channels and chloride-bicarbonate exchange, produced a significant rightward shift of the NaHS concentration-response curve (figure 5.3a). Reduction of K^+ conductance using 50mM KCl significantly decreased the pEC_{50} and attenuated the E_{max} of NaHS-induced vasorelaxation (figure 5.3b). Nifedipine (3 μM) significantly attenuated the maximum relaxation to NaHS in MCA, although the pEC_{50} was not significantly affected (figure 5.3c).

Table 5.1 Blood glucose levels

	Control	Diabetic
Blood glucose (mmol)	8.7±0.5	30.9±0.8

Blood glucose levels as measured on the day of experiment using an Accu-Check Performa® blood glucose monitor of control (n = 17) and diabetic (n = 13) rats. Values are expressed as average ± standard error.

Table 5.2 Vascular parameters

	Control	Diabetic
Tone induced by preconstriction (mN)	7.7±0.5	8.0±0.3
Tone induced by 125 mM KCl (mN)	8.7±0.4	8.9±0.6

Tone induced by the spontaneous-preconstriction protocol (middle column) and maximal contractile capacity, as measured by application of 125 mM KCl, in control (n = 9) and diabetic (n = 9) middle cerebral artery (MCA) segments. Values are expressed as average ± standard error. n = the number of MCA segments from separate rats.

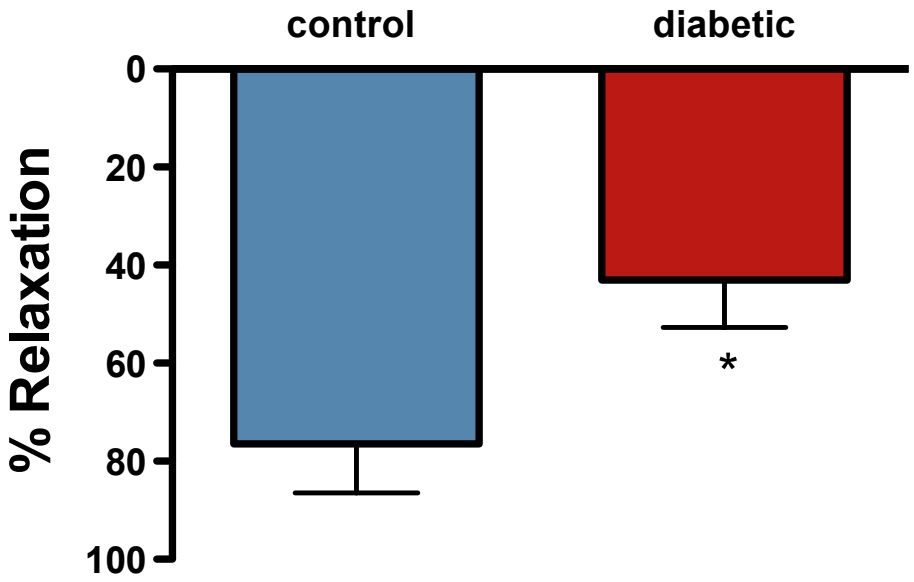

Figure 5.1 Relaxation of MCA to bradykinin

Relaxation induced by the endothelium-dependent vasorelaxant, bradykinin (100nM), in control (blue, n = 5) and diabetic (red, n = 6) MCA. * $P<0.05$, n = the number of middle cerebral artery segments from separate rats.

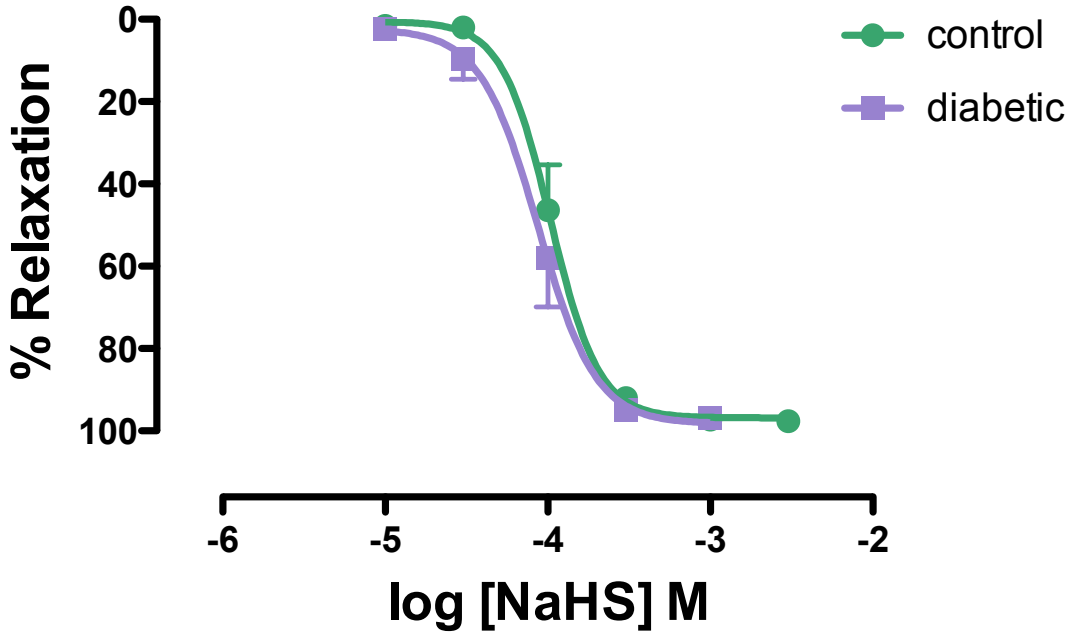

Figure 5.2 Vasorelaxation of diabetic and control MCA to exogenous H_2S

Cumulative concentration-response curves to NaHS in control (closed circles, *n*=7) or diabetic (closed squares, *n* = 9) MCA. *n* = the number of middle cerebral artery segments from separate rats.

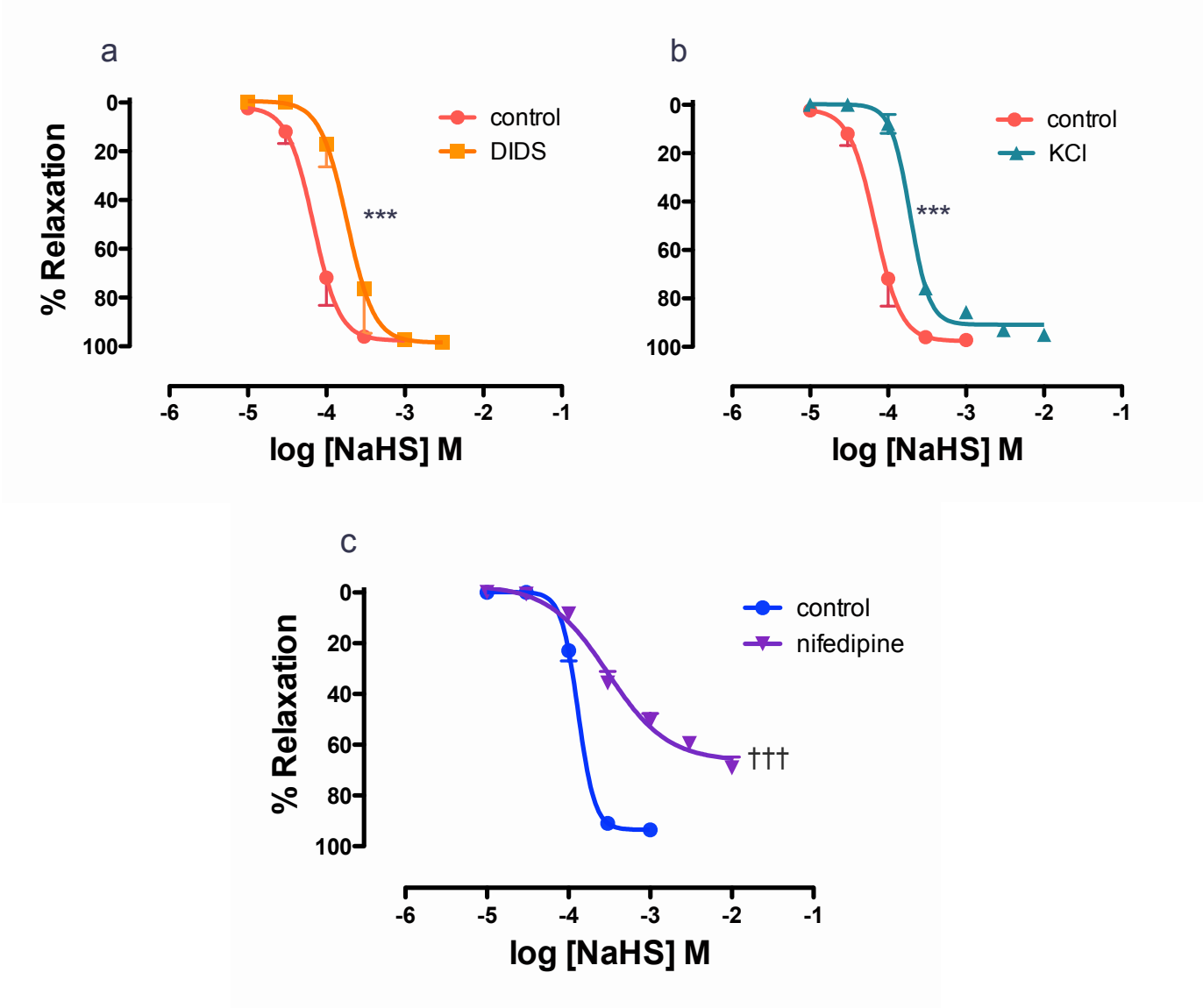

Figure 5.3 Mechanisms contributing to H_2S-induced vasorelaxation of diabetic MCA

Cumulative concentration response curves to NaHS in diabetic MCA segments in the absence (control, closed circles, n=9), or presence of **(a)** DIDS (300µM, closed squares, *n* = 5); **(b)** KCl (50mM, closed triangles, n=5); or **(c)** nifedipine (3 µM, closed upside-down triangles n=9). Note: the vessels in '**c**' were preconstricted with U46619. ***P<0.001 EC_{50} DIDS and KCl compared to control; †††P<0.001 E_{max} nifedipine compared to control. *n* = the number of middle cerebral artery segments from separate rats. DIDS, 4,4-diisothiocyanatostilbene-2,2-disulfonic acid

5.3.4 Effect of diabetes on the vasorelaxation response to endogenous H_2S

The precursor for endogenous H_2S formation, L-cysteine (10 μM-100 mM), caused concentration-dependent vasorelaxation of control MCA (E_{max}= 82±3%, pEC_{50}= 2.30±0.06, *n*=8, figure 5.4) which was significantly enhanced by the diabetic model (E_{max}= 92±1%, pEC_{50}= 2.63±0.08, P<0.05 pEC_{50}, p<0.01 E_{max}, *n*=6, figure 5.4). The CSE inhibitor, PPG (20mM) attenuated vasorelaxation to L-cysteine in control (E_{max}= 78±5%; pEC_{50}= 1.95±0.07, P<0.05 pEC_{50}, *n*=6) and diabetic (E_{max}= 75±5%, P<0.05 E_{max}; pEC_{50}= 2.10±0.08, P<0.01 pEC_{50}, *n*=8) MCA to a similar level, indicating that the enhanced L-cysteine-induced vasorelaxation observed in diabetic MCA was due to enhanced conversion of L-cysteine to H_2S via CSE (figure 5.4).

5.3.5 Effect of diabetes on the ability of tissues to produce hydrogen sulfide

Liver CSE activity was significantly greater in diabetics compared to control animals (P<0.001, figure 5.5). The mRNA expression of the H_2S producing enzyme, CSE, as detected by real-time PCR, was increased in diabetic compared to control MCA, although the increase did not attain statistical significance (figure 5.6). Serum sulfide levels were not significantly altered by the diabetic model (figure 5.7). Although the assay determines the final concentration of H_2S in each sample, it is referred to here as 'sulfide' levels, since the assay process is likely to release H_2S from acid labile sulfide stores.

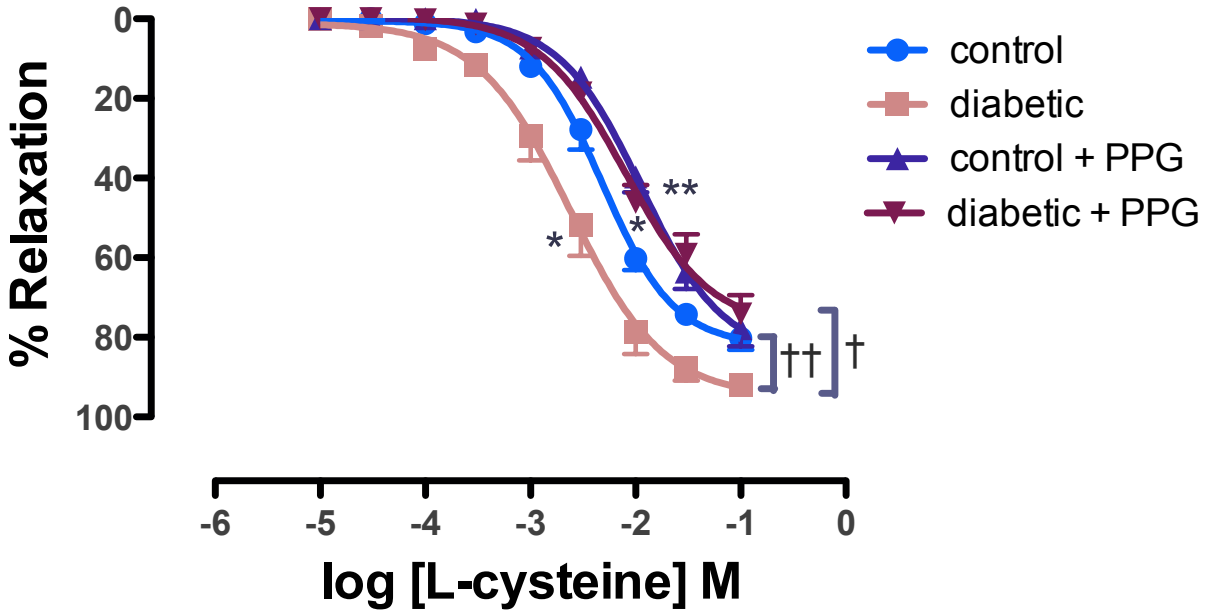

Figure 5.4 Vasorelaxation response of diabetic and control MCA to endogenous H_2S

Cumulative concentration-response curves to i) L-cysteine in control (closed circles, *n*=8) or diabetic MCA (closed squares, *n*=6) and ii) L-cysteine with propargylglycine (PPG, 20mM) in control (closed triangles, *n*=7) or diabetic MCA (closed upside-down triangles, *n*=8). *P<0.05 pEC_{50} L-cysteine in diabetic compared to control MCA; *P<0.05 pEC_{50} L-cysteine compared to L-cysteine with PPG in control MCA; **P<0.01 pEC_{50} L-cysteine compared to L-cysteine with PPG in diabetic MCA; ††P<0.01 E_{max} L-cysteine in diabetic compared to control MCA; †P<0.05 L-cysteine compared to L-cysteine with PPG in diabetic MCA. *n* = the number of middle cerebral artery segments from separate rats.

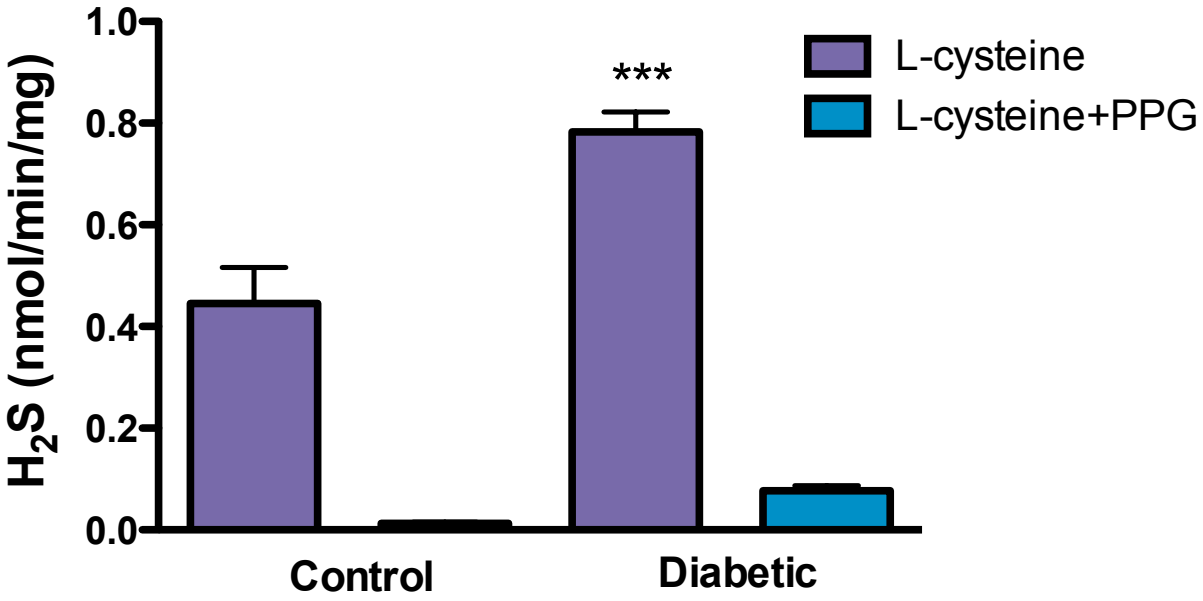

Figure 5.5 CSE activity in control and diabetic liver

L-cysteine-induced H_2S production in control (n=6) and diabetic (n=8) liver homogenates in the absence (purple) and presence (blue) of the CSE inhibitor, PPG (10mM). ***P<0.001 L-cysteine-induced H_2S production in control compared to diabetic rats, in the absence of PPG. PPG, propargylglycine.

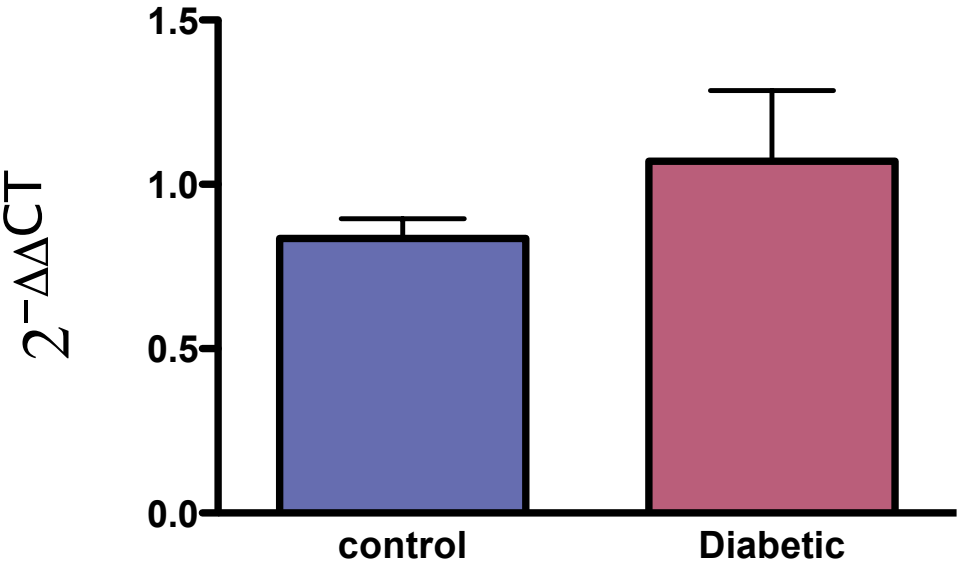

Figure 5.6 CSE mRNA expression in control and diabetic MCA

Level of mRNA expression of the H_2S producing enzyme, cystathionine gamma lyase (CSE) in control (*n*=7) and diabetic (*n*=4) MCA, normalised to 18S ribosomal RNA.

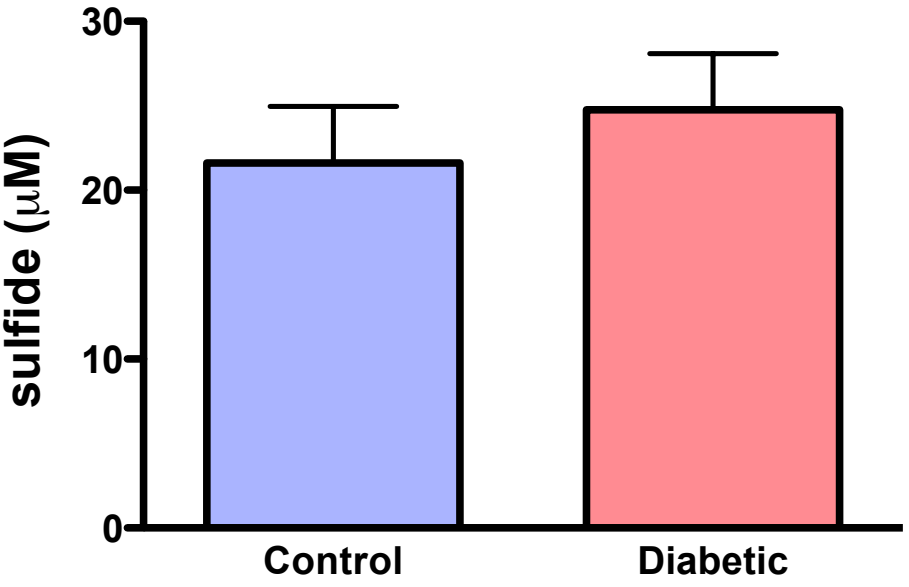

Figure 5.7 Sulfide levels in control and diabetic serum

Sulfide levels in control (n = 7) and diabetic (n = 9) serum.

5.3.6 Effect of exogenous hydrogen sulfide on vascular superoxide production

For $O_2^{\cdot-}$ detection in cerebral arteries, the basilar artery was pooled with circle of Willis arteries. NADPH-stimulated $O_2^{\cdot-}$ production was 22 fold higher in cerebral arteries than aorta. The diabetic model significantly enhanced NADPH-stimulated $O_2^{\cdot-}$ production in both cerebral arteries and aorta ($P<0.05$ diabetic compared to control in both cerebral vessels and aorta, figure 5.8a and b). DPI (5 μM), a flavoprotein inhibitor, which inhibits NADPH oxidase (Selemidis *et al.*, 2008), almost abolished $O_2^{\cdot-}$ production in cerebral arteries and aorta from both diabetic and control animals (figure 5.8a and b). A prior incubation of arteries in hydrogen sulfide using the donor, NaHS (100 μM), significantly reduced $O_2^{\cdot-}$ production in diabetic cerebral arteries (figure 5.8a), but had no influence on control cerebral arteries (figure5.8b). This prior incubation in NaHS had no influence on aortic superoxide production in aorta from either control or diabetic animals (figure 5.8a and b).

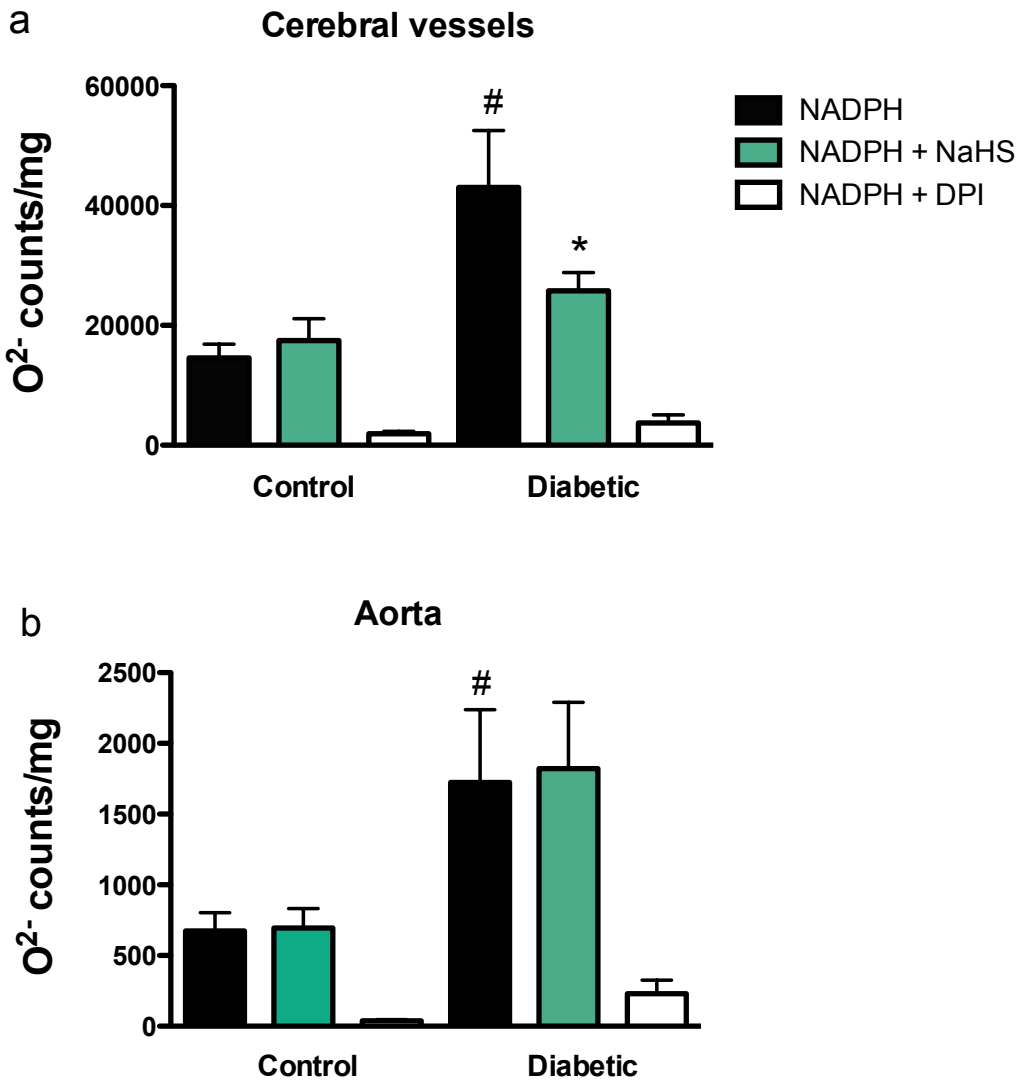

Figure 5.8 NADPH stimulated $O_2^{\cdot-}$ production in cerebral vessels and aorta

NADPH stimulated $O_2^{\cdot-}$ production as detected by lucigenin-enhanced chemiluminescence in **(a)** cerebral vessels (basilar artery pooled with circle of Willis arteries) of control (n = 9) and diabetic (n = 9) animals and **(b)** aorta of control (n = 3) and diabetic (n = 4) animals. In both **(a)** and **(b)** NADPH was applied either: alone (black); after an incubation in NaHS (100 μM) (green); or in the presence of DPI (5 μM) (white). #P<0.05, control compared to diabetic NADPH stimulated $O_2^{\cdot-}$ production in both cerebral vessels and aorta; *P<0.05 diabetic NADPH stimulated $O_2^{\cdot-}$ production compared to that with prior incubation in NaHS in cerebral vessels.

5.4 Discussion

The present study is the first to investigate the influence of diabetes on the cerebrovascular response to H_2S. The findings demonstrate that diabetic MCA display endothelial dysfunction, as the response to bradykinin (which relaxes via EDHF, not NO (Smeda *et al.*, 2010)) were significantly attenuated, however smooth muscle cell function was retained. The vasorelaxation response of MCA to exogenous H_2S was unaffected by diabetes. However, CSE-dependent vasorelaxation elicited by L-cysteine was significantly enhanced by diabetes. This suggests that diabetes upregulates the endogenous production of H_2S in MCA. Indeed, there was a trend toward increased CSE expression in diabetic compared to control MCA, which was supported by the finding that liver tissue of diabetic animals had significantly enhanced CSE activity. The effect of exogenous H_2S on vascular $O_2^{\cdot-}$ production was also examined. In control animals, NADPH-stimulated $O_2^{\cdot-}$ production was 40 times higher in MCA compared to aorta. In addition, diabetes caused a doubling of MCA $O_2^{\cdot-}$ production. This increase was significantly reduced by acute exogenous H_2S treatment, but only in diabetic, not control MCA. The reduction is likely due to H_2S inhibition of Nox, since NADPH-stimulated $O_2^{\cdot-}$ production would be expected to be catalysed mainly by Nox.

In the present study, NaHS caused full relaxation of control MCA. In several studies using rat and mouse aorta, the maximal relaxation to NaHS in control aorta was approximately 70% (Brancaleone *et al.*, 2008; Denizalti *et al.*, 2011). This difference in reactivity is unlikely to be explained by the different protocols used for precontraction of the vessels in the separate studies, since similar concentration-response curves, obtaining full relaxation to NaHS, were observed in U46619-precontracted MCA (figure 5.3c). Thus, the present findings highlight a stark difference in the reactivity of peripheral and cerebral vessels to H_2S.

The present study demonstrates that STZ-induced diabetes does not alter the sensitivity or maximum vasorelaxation of MCA to exogenous H_2S. Interestingly, peripheral vessels demonstrate an enhanced maximal relaxation to exogenously applied H_2S in aorta of STZ-treated rats (Denizalti *et al.*, 2011) and NOD mice, but only those with severe disease (Brancaleone *et al.*, 2008). The discrepancy is likely due to the already high sensitivity of healthy MCA to the vasodilator effects of H_2S, which relax fully to H_2S, meaning that the maximum response cannot be enhanced by the diabetic state. In line with the observation that the vasorelaxant efficacy of H_2S was not altered, the mechanisms contributing to the H_2S-induced vasorelaxation in diabetic MCA were similar to those observed in chapter 4. As such, NaHS-induced vasorelaxation was again sensitive to inhibition by nifedipine and 50mM KCl, indicating involvement of L-type calcium channels and potassium channels. NaHS-induced vasorelaxation was also sensitive to DIDS in the diabetic animals, although, based on the previous chapter, it is not entirely clear as to the mechanism behind the DIDS-sensitivity, which probably involves pathways other than Cl^- channels or Cl^-/HCO_3^- exchange.

The ability of MCA to relax to endogenously generated H_2S was assessed using the H_2S precursor, L-cysteine. L-cysteine induced a relaxation of MCA that was attenuated by the CSE inhibitor, PPG, indicating that the relaxation involved endogenous production of H_2S. Possible reasons for the incomplete blocking of L-cysteine-induced vasorelaxation by PPG are discussed in detail in section 4.4, p.149. Diabetic MCA were more sensitive to the vasorelaxant effects of L-cysteine, and PPG attenuated the vasorelaxation to levels similar to those seen in control (i.e. non-diabetic) MCA. These results indicate an enhanced conversion of L-cysteine to H_2S via CSE in diabetic MCA. In contrast, the biosynthesis of H_2S was impaired in the aorta of NOD mice, as evidenced by attenuated relaxation to L-cysteine, and reduced CSE activity (Brancaleone *et al.*, 2008). The discrepancy may be due to the different

models of diabetes, or may highlight a difference between the response of peripheral and cerebral vessels to the diabetic state.

The enhanced vasorelaxant efficacy of L-cysteine in diabetic MCA suggests enhanced generation of H_2S via either enhanced activity or expression of CSE. Although there was a trend towards increased CSE mRNA expression in diabetic compared to control MCA, the difference did not attain statistical significance (n = 4 in the diabetic group). Previous observations suggest that diabetes may indeed upregulate vascular CSE expression - in the aorta of NOD mice, CSE mRNA and protein expression were enhanced in a manner that correlated with disease severity (Brancaleone *et al.*, 2008). However, in another study, CSE mRNA and protein expression in aorta of STZ treated diabetic rats were not significantly different from control, as determined by RT-PCR and western blotting (Denizalti *et al.*, 2011). It is possible that enhanced MCA synthesis of H_2S in diabetes occurs via enhanced CSE activity, rather than expression.

Although little is known about the regulation of CSE activity, a very recent study demonstrated that platelet derived growth factor upregulates CSE mRNA, protein levels and activity, with concurrent increased formation of ROS (Hassan *et al.*, 2012). Antioxidants, including DPI, a flavoprotein inhibitor, which inhibits NADPH oxidase (Selemidis *et al.*, 2008), attenuated the enhanced CSE expression, suggesting that CSE gene expression, and possibly activity, is redox-regulated (Hassan *et al.*, 2012). It should be noted, however, that DPI also inhibits flavin-containing enzymes (Selemidis *et al.*, 2008), NOS (Stuehr *et al.*, 1991), reversibly blocks K^+ and Ca^{2+} currents in type I carotid body cells (Selemidis *et al.*, 2008) and has inhibitory effects on mitochondrial respiration, albeit at higher concentrations than those required to inhibit NADPH oxidase (Hancock *et al.*, 1987). Whether diabetes

induced vascular ROS generation may similarly result in upregulation of CSE activity remains to be investigated.

CSE expression is relatively high in hepatic tissue (Bao *et al.*, 1998), thus the CSE activity of hepatic tissue was determined. The liver of diabetic animals had an increased propensity to generate H_2S from L-cysteine, which was nearly abolished by PPG, demonstrating enhanced CSE activity. Enhanced tissue H_2S synthesis (Yusuf *et al.*, 2005), as well as increased CSE expression have previously been demonstrated in liver (Jacobs *et al.*, 1998) and pancreas of STZ diabetic rats (Yusuf *et al.*, 2005). Altered transsulfuration rates in diabetic humans are indicative that a similar upregulation may occur in the livers of human diabetic patients (Abu-Lebdeh *et al.*, 2006). In the present study, upregulated tissue H_2S production was not correlated with plasma sulfide levels, which were unaltered by STZ-induced diabetes. This is in agreement with a study in STZ rats showing no change in plasma H_2S concentration, despite upregulation of tissue CSE (Yusuf *et al.*, 2005). In contrast, decreased plasma H_2S levels have been observed in NOD mice (Brancaleone *et al.*, 2008) and diabetic humans (Jain *et al.*, 2010). One reason for the observed discrepancy between tissue CSE activity and plasma H_2S levels is that CSE may only influence local H_2S levels. An alternate hypothesis is that the reductant H_2S may react with excess ROS generated from diabetic vascular tissue. This is supported by an observation that exposure of endothelial cells to elevated glucose decreased H_2S concentration, an effect which was rescued by incubation with the ROS scavenger, Tempol (Suzuki *et al.*, 2011).

H_2S is not only a direct ROS scavenger (Geng *et al.*, 2004), it can also perturb upregulated Nox expression in diabetes (Zheng *et al.*, 2010). It has been suggested that upregulated H_2S production in diabetes may thus form part of a self-protecting mechanism against excessive

ROS generation (Hassan *et al.*, 2012; Kaneko *et al.*, 2009; Yusuf *et al.*, 2005). The effects of exogenous H_2S on vascular NADPH-stimulated $O_2^{\cdot-}$ generation were therefore assessed in diabetic compared to control MCA and aorta. Diabetes enhanced NADPH-stimulated $O_2^{\cdot-}$ generation in both aorta and MCA, indicating that Nox expression or activity is upregulated by diabetes in the vasculature, in line with the literature (Shen, 2010). A prior incubation of vessels in H_2S (using the donor, NaHS) attenuated $O_2^{\cdot-}$ production in diabetic MCA back to control levels, but did not influence $O_2^{\cdot-}$ production in control MCA, indicating that H_2S can selectively normalise $O_2^{\cdot-}$ production in MCA from diabetic animals. The design of the experiment was such that the effects of H_2S could not be due to its direct scavenging effect, since it was washed off before NADPH-stimulated $O_2^{\cdot-}$ production, suggesting that H_2S acted by inhibition of $O_2^{\cdot-}$ generating enzymes, such as Nox.

In peripheral vessels there is, indeed, evidence that H_2S can normalise enhanced Nox expression caused by either U46619 in VSM *in vitro* (Muzaffar *et al.*, 2008) or STZ treatment in aorta *in vivo* (Zheng *et al.*, 2010). However, H_2S was not effective at inhibiting $O_2^{\cdot-}$ production from either control or diseased aorta in the present study. The discrepancy may be due to differences in experimental approach: in the present study NaHS was applied for only 30 minutes *in vitro*, compared to 6 weeks' worth of daily subcutaneous NaHS injections in the study by Zheng *et al*. (Zheng *et al.*, 2010). The findings of the present study that a short-term *in vitro* application of H_2S can normalise $O_2^{\cdot-}$ production in diabetic MCA, but not aorta, suggest that diabetic MCA are more sensitive to the effects of H_2S on ROS production than diabetic aorta.

The findings of this and other studies (Kaneko *et al.*, 2009; Yusuf *et al.*, 2005) are suggestive that H_2S may form part of an important adaptive response to oxidative stress in diabetes.

Given the vasodilator action of H_2S, such an adaptive response could also counteract the enhanced level of tone in diabetic cerebral vessels associated with reduced NO bioavailability and enhanced myogenic reactivity (see 1.4.3 Aetiology of diabetic cerebrovascular disease, p.57). Despite the wealth of knowledge regarding the damaging effects of oxidative stress in diabetic vascular disease, antioxidants have so far failed as therapeutics in the clinical setting (Bjelakovic *et al.*, 2012). A frequently sited possible reason for this failure is the requirement of low levels of ROS for normal physiological function in the vasculature (Droge, 2002), which would be upset by powerful antioxidants. The suggestion that H_2S may play part in the endogenous homeostatic control of redox signalling is therefore promising in terms of its potential efficacy as a therapeutic tool. However, more research will be required to confirm whether the CSE-H_2S pathway forms part of a regulatory response to diabetic oxidative stress, and whether manipulation of this system can be applied to therapeutics.

Conclusion

The key findings of the present study were that STZ-induced diabetes increased the vasorelaxant efficacy of endogenous H_2S in MCA and enhanced tissue biosynthesis of H_2S. Vasorelaxation responses mediated by exogenous H_2S were retained under diabetic conditions. A selective attenuation of pathologically increased $O_2^{\cdot-}$ by exogenous H_2S was also observed in diabetic MCA. The study implicates the CSE-H_2S pathway as a possible new avenue for research into the therapy of diabetic cerebrovascular disease.

Chapter 6: General discussion

The present thesis initially examined the central cardiovascular role of H_2S in the important cardiovascular regulatory brain regions, the RVLM and PVN. It was found that H_2S in the RVLM or PVN was not crucial in central cardiovascular regulation, thus changing the direction of the original study. Since H_2S is a known peripheral vasodilator, and there have been no detailed analyses of the mechanism of H_2S-induced relaxation of cerebral vessels, studies moved to investigation of the mechanism of H_2S in vasorelaxation of MCA. H_2S caused vasorelaxation of MCA that was DIDS-sensitive and involved closure of VGCC, plus a small contribution from K^+ channel opening. Additional evidence was obtained to support the role of endogenous H_2S in the regulation of the cerebral blood vessels. The final study investigated the possible involvement of H_2S in diabetic cerebrovascular disease by examining the effect of diabetes on the cerebrovascular response to H_2S. Although the vasorelaxant efficacy of exogenous H_2S was not altered by diabetes, diabetic MCA had an enhanced response to a precursor for endogenous generation of H_2S, indicating an enhanced ability to generate H_2S in diabetic cerebral vessels. It was also demonstrated that H_2S effectively inhibited excessive $O_2^{\cdot -}$ production from diabetic cerebral vessels, which suggests a role for H_2S in vasoprotection.

The possibility that H_2S may be involved in central cardiovascular regulation via the RVLM and PVN was investigated by first examining the potential of these regions to produce H_2S. The presence of the H_2S producing enzyme, CBS, was demonstrated in both the RVLM and PVN. The effect of H_2S on MAP, HR and LSNA via each of these regions was therefore examined by microinjection of the H_2S donor, NaHS, or inhibitors of CBS specifically into either the RVLM or PVN of rats. In the RVLM, neither exogenous H_2S, nor inhibition of endogenous H_2S formation had any influence on MAP, HR or LSNA. This is in direct contrast to a study in rats showing that exogenous H_2S significantly decreased MAP, HR and

RSNA, while the CBS inhibitor, HA, elicited the opposite cardiovascular effects (Guo *et al.*, 2011). The discrepancy between the studies could be due to the omission of Guo *et al.* to buffer their NaHS, despite their use of concentrations known to increase pH (Dombkowski *et al.*, 2004). Chemosensitive neurons, which can influence sympathetic nerve activity upon sensing alterations in pH, exist in close proximity to the RVLM (Guyenet *et al.*, 2010). Thus it is possible that the effects observed by Guo *et al.* are pH induced. Alternatively, the discrepancy may be due to differences in methodological approach between the studies, for example, rats were ventilated in the study by Guo *et al.* but breathed spontaneously in the present study. Ventilation is known to influence cardiovascular responses (Cox *et al.*, 1988).

The present work is the first to investigate the haemodynamic effect of H_2S via the PVN. Micro-injection of NaHS, or the CBS inhibitor, AOA, into the PVN did not significantly influence MAP, HR or LSNA, indicating that H_2S does not regulate the cardiovascular system via the PVN. Although there are currently no other studies investigating the effect of H_2S in the PVN, several studies indicate that H_2S may be involved in central cardiovascular regulation via alternate brain regions. In the posterior hypothalamus, NaHS caused a small, but apparently significant reduction in MAP and HR, whereas both AOA and HA increased MAP (Dawe *et al.*, 2008). In the NTS, H_2S augmented synaptic transmission and caused increased presynaptic Ca^{2+} concentration, whereas AOA decreased synaptic transmission. Thus, endogenous H_2S may be involved in central cardiovascular regulation via specific regions in the brain, such as the NTS and posterior hypothalamus, but not the PVN. Two studies have observed a central cardiovascular response following intracerebroventricular administration of a H_2S donor. A rapid bolus injection of high doses of NaHS (3-303 μmol over 30 seconds) significantly reduced MAP and HR, (Liu *et al.*, 2011a), whereas a slow infusion of a lower NaHS dose (0.4 μmol over 60 min) significantly increased MAP and HR (Ufnal *et al.*, 2008). It appears that the effect of exogenous H_2S administered

intracerebroventricularly is dependent on dose and/or infusion rate. These studies did not determine which brain region(s) were involved in these responses to H_2S. The infusion of inhibitors of CBS was not supportive of a role for endogenous H_2S in central cardiovascular regulation in either study (Liu *et al.*, 2011a; Ufnal *et al.*, 2008), in line with the present findings that endogenous H_2S does not influence cardiovascular parameters via the PVN or RVLM.

The present thesis found no role for H_2S in the short-term central control of the cardiovascular system via the RVLM or PVN. However, this does not rule out the hypothesis that long-term manipulation of H_2S or its production could protect against cardiovascular disease, such as hypertension. In support of this hypothesis, upregulated Nox in both the RVLM and PVN is involved in the pathogenesis of hypertension (Peterson *et al.*, 2006; Xue *et al.*, 2012), and although short-term application of NaHS (30 minute *in vitro*) had no influence on Nox stimulated O_2^- production in aorta (present thesis, chapter 5), repeated long term administration of NaHS (6 weeks, daily IP injections) attenuated enhanced Nox subunit expression in diabetic aorta (Zheng *et al.*, 2010). It is apparent that this hypothesis warrants further investigation.

Numerous studies have shown that H_2S causes relaxation of peripheral vessels. In light of this, the present studies shifted focus to the cerebrovascular action of H_2S, specifically in MCA. NaHS-induced relaxation of MCA with an EC_{50} of 100±5μM, which is similar to that observed in the aorta reported in several studies (Al-Magableh *et al.*, 2011; Kiss *et al.*, 2008; Lee *et al.*, 2007; Zhao *et al.*, 2001). This is well outside the physiological range of H_2S concentrations in plasma and tissues, according to recent reports (Furne *et al.*, 2008; Whitfield *et al.*, 2008). However, despite the development of various methods to measure H_2S levels, all have limitations, and none are able to measure intracellular production of H_2S in real-time and under physiological conditions (for review, see (Olson, 2012)). Furthermore,

the amount of H_2S reaching a putative intracellular target in SMC is likely considerably lower than the amount of NaHS applied, due to the equilibrium between H_2S and HS^- favouring HS^- production (see 1.1.2 Pharmacological tools, H_2S donors, p.17-18), as well as the rapid loss of H_2S which has been observed in biological experiments including myography (DeLeon *et al.*, 2012). Thus it is feasible that physiologically produced H_2S could relax MCA. This is supported by the observation from the present study that a precursor to H_2S production, L-cysteine induced relaxation of MCA that was sensitive to the CSE inhibitor, PPG. The presence of the H_2S producing enzyme, CSE, was also demonstrated in endothelial and smooth muscle cells of MCA.

Endogenously produced H_2S (from addition of L-cysteine) caused vasorelaxation of MCA that was insensitive to the removal of endothelium. Thus, although the presence of CSE was demonstrated in endothelium of MCA, it appears that endothelial derived H_2S is not important in endogenous H_2S-induced vasorelaxation of MCA. Taken together with the observation that H_2S-induced relaxation was insensitive to blockade of IK_{Ca} and SK_{Ca} channels, this suggests that H_2S does not act as an EDHF in MCA. Two studies have provided evidence that H_2S acts as an EDHF in mouse mesenteric artery and aorta (Mustafa *et al.*, 2011; Yang *et al.*, 2008). Numerous studies show that H_2S-induced relaxation is sensitive to blockade of IK_{Ca} and SK_{Ca} in rat aorta (Zhao *et al.*, 2002; Zhao *et al.*, 2001), rat mesenteric artery (Cheng *et al.*, 2004; d'Emmanuele di Villa Bianca *et al.*, 2009) and mouse mesenteric artery (Al-Magableh *et al.*, 2011; Mustafa *et al.*, 2011), however this is not without contention, as one study shows blockade of these channels had no influence on H_2S-induced relaxation of rat aorta (Li *et al.*, 2008). Indeed, whether H_2S is an EDHF in peripheral vessels remains a topic of debate. A recent study demonstrated that cholinergic VSM hyperpolarisation is virtually abolished in mesenteric arteries of $CSE^{-/-}$ mice, and the K_{ATP} channel blocker, glibenclamide, attenuated cholinergic VSM hyperpolarisation in wild-

type mice in the presence of NOS and COX inhibitors (Mustafa *et al.*, 2011). The study was criticised because over 20 years of accumulated evidence from various groups suggests strongly that, after NOX and COX blockade, the remaining EDHF-dependent relaxation is independent of K_{ATP} channels (Edwards *et al.*, 2012). One possible reason for the discrepancy is that, although glibenclamide is routinely used as a K_{ATP} blocker, it does have alternate effects, such as blockade of a non-selective stretch-activated cation channel (Simard *et al.*, 2006). Regardless, the observations of Mustaffa et al. do not conflict with the present studies, given the lack of consistent dilator effect of ACh in rat MCA (Gorlach *et al.*, 1998).

H_2S-induced vasorelaxation was sensitive to DIDS, 50mM KCl and nifedipine in MCA. However, the mechanism was insensitive to blockade of selective potassium channels, including K_{ATP}, K_V, K_{Ca} and K_{IR}. The lack of involvement of K_{ATP} and K_{Ca} channels in the present study contrasts with several studies in peripheral vessels (see table 1.1, p.52-53), as well as three recent studies in cerebral vessels (Leffler *et al.*, 2010; Liang *et al.*, 2011; Liang *et al.*, 2012). The discrepancy between the present study and other cerebrovascular studies may be due to differences in species, age, or the specific vessels studied (pial compared to MCA) (Leffler *et al.*, 2010; Liang *et al.*, 2011; Streeter *et al.*, 2012). It should be noted that in peripheral vessels, controversy exists regarding the contribution of K_{ATP} and K_{Ca} channels even within the same species and vessel type (see table 1.1, p.52-53). Interestingly, Dombkowski *et al.* observed that K_{ATP} channel blockade attenuated H_2S-induced vasodilation, despite repeated observations that K_{ATP} channel opening was ineffective at relaxing the same vessel type (Dombkowski *et al.*, 2004). This suggests that the K_{ATP} sensitivity does not necessarily implicate K_{ATP} channel opening in H_2S-induced vasodilation, and instead the K_{ATP} channel blocker may be acting as a functional antagonist to the H_2S-induced response. Such functional antagonism could be caused by downstream effects of K_{ATP} channel blockade (or indeed other K^+ channel blockade), for example, membrane depolarisation.

These downstream effects might vary with minor differences in methodology between laboratories, providing a possible explanation for the observed controversy regarding the contribution of K_{ATP} and K_{Ca} channels within a single species and vessel type. Such downstream effects might also explain the contentious observations of Mustafa *et al.*, 2011, regarding inhibition of cholinergic VSM hyperpolarisation with glibenclamide in the presence of NOS and COX inhibitors (Mustafa *et al.*, 2011)(see above).

The present study is the first to investigate the role of K_V channels or the endothelium in cerebral H_2S-induced vasodilation, demonstrating no role for either pathway in MCA. Controversy also exists regarding the contribution of K_V channels or endothelium to H_2S-induced vasorelaxation of peripheral vessels (see table 1.1 p.52-53).

In the present study, a dual vascular response to H_2S was observed in MCA. A similar vascular response to H_2S has been reported in mesenteric arteries (d'Emmanuele di Villa Bianca *et al.*, 2011), although this is the first report of such a response in cerebral vessels. Interestingly, of the 14 agents used to examine the mechanism of H_2S-induced vascular effects, the same three agents - DIDS, 50mM KCl and nifedipine – inhibited both the initial constriction, and the ensuing relaxation induced by H_2S. Constriction was additionally sensitive to catalase, which had no influence on relaxation. As speculated in the chapter 4 discussion, this similarity in mechanism for constriction and relaxation could be taken to indicate that one effect of H_2S results in both vascular actions. Observations of various studies are supportive of a hypothesis that the H_2S-induced vascular effects are due to its inhibition of cytochrome c oxidase (see 4.4 p.157). Exactly how inhibition of cytochrome c oxidase might result in constriction followed by relaxation was not determined by the present studies. One hypothesis is that the constriction involves increased intracellular Ca^{2+} ($[Ca^{2+}]_i$) due to decreased extrusion via ATP-dependent pumps, with an additional contribution from

lowered mitochondrial generation of $O_2^{\cdot-}$, thus lowered levels of the vasodilator, H_2O_2. The ensuing relaxation may be due to decreased pH_i as a result of accumulated lactic acid from the reliance of the cell on anaerobic glycolysis for energy production. However, this hypothesis remains entirely speculative, and investigation would require substantial amounts of further experimentation, which was beyond the scope of the present thesis.

The final study of this thesis investigated whether diabetes alters the function or production of H_2S in the cerebral vasculature. It was shown that the vasorelaxation to exogenous H_2S was not altered in diabetic MCA, but the precursor to endogenous H_2S production, L-cysteine, induced greater relaxation in diabetic MCA. This suggests that diabetic MCA have an enhanced ability to generate H_2S via CSE, however, there was no significant difference in CSE mRNA expression between control and diabetic MCA. The discrepancy may be due to the low numbers available for PCR in the diabetic group (n=4), meaning that the difference in mRNA expression did not obtain significance. Alternatively, it is possible that CSE activity is enhanced, without enhancement of mRNA expression (see 5.4 p.179). In the present study it was indeed observed that CSE activity was enhanced in the liver of diabetic rats. This is supported by observations of enhanced CSE expression in liver of STZ-diabetic rats (Jacobs *et al.*, 1998) and aorta of NOD mice (Brancaleone *et al.*, 2008) and higher transsulfuration rates, reflecting enhanced activity of the transsulfuration enzymes, CSE and CBS, in diabetic humans without renal complications (Abu-Lebdeh *et al.*, 2006). However, the aorta of the NOD mice had lowered relaxation to L-cysteine, and had lower CSE activity (Brancaleone *et al.*, 2008). This deviates from the present results, which suggest enhanced tissue CSE activity, a discrepancy which may be due to the different model of diabetes.

The transsulfuration pathway has been of some interest in diabetic research, due to its involvement in the breakdown of homocysteine. Hypohomocysteineamia is observed in diabetes without renal complications and is partly due to enhanced CBS and CSE activity

(Abu-Lebdeh *et al.*, 2006; Jacobs *et al.*, 1998), while hyperhomocysteinaemia (HHcy) occurs in the advanced stages of diabetic disease where renal dysfunction is present, and is an independent risk-factor for both cardiovascular disease (Refsum *et al.*, 1998) and cerebrovascular disease (Hogervorst *et al.*, 2002). This suggests that the flux of homocysteine through the transsulfuration pathway, and thus subsequent H_2S generation, alters according to the stage and severity of the diabetic state, which may explain the differences in CSE activity and L-cysteine response between the present study and that of Brancaleone *et al*. (Brancaleone *et al.*, 2008). Despite the known association between HHcy and cardiovascular disease, large-scale trials using folic acid and vitamin B6 and B12 have achieved lowered homocysteine levels, without any concomitant change in cardiovascular outcomes (Albert *et al.*, 2008; Bonaa *et al.*, 2006). One possible explanation is that the cardiovascular disease observed in HHcy is due to reduced generation of one or more of the bi-products of homocysteine catabolism, for example, H_2S.

It is possible that upregulated CSE activity, and accompanying hypohomocysteinaemia and enhanced H_2S generation, which occurs in early diabetic disease forms part of a regulatory mechanism to protect the vasculature against oxidative stress. In chapter 4 of the present thesis, immunohistochemistry demonstrated staining for the H_2S producing enzyme, CSE. However, the endothelium was not required for endogenously produced H_2S to induce vasorelaxation, suggesting that endothelium-derived H_2S may have regulatory functions independent of vasorelaxation. There are various lines of evidence that H_2S can protect both VSM and endothelium against oxidative insults, including that induced by high glucose (see 1.4.4 Diabetic vascular disease and H_2S, p.61). In the final study of this thesis, it was demonstrated that exogenous H_2S could normalise excessive ROS production in diabetic MCA, but did not influence ROS production in control MCA. Thus, the hypothesis that

upregulated CSE activity in early diabetes forms part of a self-protecting mechanism warrants further investigation.

The limitations of pharmacological and analytical tools have often hindered attainment of quality evidence regarding the effect of exogenous and endogenous H_2S in this field. At the outset, the sulfide salt donors were exclusively used to deliver H_2S (apart from H_2S gas solutions). These salts release a bolus dose of H_2S, which has been shown to be rapidly lost from solutions in *in vitro* biological experiments (DeLeon *et al.*, 2012). However, the recent development of sustained release donors which are now becoming readily available will undoubtedly help progress in the field immensely. There are still no specific inhibitors of CSE, CBS or 3-MST available for use. Methods for reliable measurement of tissue levels of H_2S are still in development. Improvements in tools will assist in clarifying many of the lingering questions regarding H_2S production and function in physiology and pathophysiology.

Finally, there is now a vast array of physiological and pathophysiological effects attributed to H_2S. The present thesis shows that H_2S has no role in acute central regulation of blood pressure, but that H_2S does contribute to endogenous cerebral vasoregulation. Importantly, exogenous H_2S normalised the enhanced ROS production in diabetic cerebral blood vessels. Furthermore, cerebrovascular H_2S production is enhanced in diabetes, which suggests that this molecule may have a role as a vasoprotective factor.

References

Aalkjaer C, Peng HL (1997). pH and smooth muscle. *Acta Physiologica Scandinavica* **161**(4)**:** 557-566.

Abe K, Kimura H (1996). The possible role of hydrogen sulfide as an endogenous neuromodulator. *The Journal of Neuroscience* **16**(3)**:** 1066-1071.

Abu-Lebdeh HS, Barazzoni R, Meek SE, Bigelow ML, Persson XM, Nair KS (2006). Effects of insulin deprivation and treatment on homocysteine metabolism in people with type 1 diabetes. *The Journal of Clinical Endocrinology and Metabolism* **91**(9)**:** 3344-3348.

Adebiyi A, McNally EM, Jaggar JH (2011). Vasodilation induced by oxygen/glucose deprivation is attenuated in cerebral arteries of SUR2 null mice. *American Journal of Physiology. Heart and Circulatory Physiology* **301**(4)**:** H1360-1368.

Afanasev I (2009). Detection of superoxide in cells, tissues and whole organisms.*Frontiers in Bioscience (Elite Edition)* **1:** 153-160.

Ahmad FU, Sattar MA, Rathore HA, Abdullah MH, Tan S, Abdullah NA*, et al.* (2012). Exogenous hydrogen sulfide (H2S) reduces blood pressure and prevents the progression of diabetic nephropathy in spontaneously hypertensive rats. *Renal Failure* **34**(2)**:** 203-210.

Aickin CC (1988). Movement of acid equivalents across the mammalian smooth muscle cell membrane. *Ciba Foundation Symposium* **139:** 3-22.

Al-Magableh MR, Hart JL (2011). Mechanism of vasorelaxation and role of endogenous hydrogen sulfide production in mouse aorta. *Naunyn-Schmiedeberg's Archives of Pharmacology* **383**(4)**:** 403-413.

Albert CM, Cook NR, Gaziano JM, Zaharris E, MacFadyen J, Danielson E*, et al.* (2008). Effect of folic acid and B vitamins on risk of cardiovascular events and total mortality among women at high risk for cardiovascular disease: a randomized trial. *JAMA : The Journal of the American Medical Association* **299**(17)**:** 2027-2036.

Ali MY, Ping CY, Mok YY, Ling L, Whiteman M, Bhatia M*, et al.* (2006). Regulation of vascular nitric oxide in vitro and in vivo; a new role for endogenous hydrogen sulphide? *British Jounal of Pharmacology* **149**(6)**:** 625-634.

Allen AM (2002). Inhibition of the hypothalamic paraventricular nucleus in spontaneously hypertensive rats dramatically reduces sympathetic vasomotor tone. *Hypertension* **39**(2)**:** 275-280.

Amadasi A, Bertoldi M, Contestabile R, Bettati S, Cellini B, di Salvo ML*, et al.* (2007). Pyridoxal 5'-phosphate enzymes as targets for therapeutic agents. *Current Medicinal Chemistry* **14**(12)**:** 1291-1324.

Andrews KL, Irvine JC, Tare M, Apostolopoulos J, Favaloro JL, Triggle CR*, et al.* (2009). A role for nitroxyl (HNO) as an endothelium-derived relaxing and hyperpolarizing factor in resistance arteries. *British Jounal of Pharmacology* **157**(4)**:** 540-550.

Anrather J, Racchumi G, Iadecola C (2006). NF-kappaB regulates phagocytic NADPH oxidase by inducing the expression of gp91phox. The *Journal of Biological Chemistry* **281**(9)**:** 5657-5667.

Armstead WM (1998). Contribution of kca channel activation to hypoxic cerebrovasodilation does not involve NO. *Brain Research* **799**(1)**:** 44-48.

Ashford ML, Boden PR, Treherne JM (1990). Glucose-induced excitation of hypothalamic neurones is mediated by ATP-sensitive K+ channels. *Pflugers Archiv* **415**(4)**:** 479-483.

Austgen JR, Hermann GE, Dantzler HA, Rogers RC, Kline DD (2011). Hydrogen sulfide augments synaptic neurotransmission in the nucleus of the solitary tract. *Journal of Neurophysiology* **106**(4)**:** 1822-1832.

Badoer E (2001). Hypothalamic paraventricular nucleus and cardiovascular regulation. *Clinical and Experimental Pharmacology and Physiology* **28**(1-2)**:** 95-99.

Badoer E (2010). Role of the hypothalamic PVN in the regulation of renal sympathetic nerve activity and blood flow during hyperthermia and in heart failure. *American Journal of Physiology. Renal Physiology* **298**(4)**:** F839-846.

Bago M, Dean C (2001). Sympathoinhibition from ventrolateral periaqueductal gray mediated by 5-HT(1A) receptors in the RVLM. *American Journal of Physiology. Regulatory Integrative and Comparative Physiology* **280**(4)**:** R976-984.

Bao L, Vlcek C, Paces V, Kraus JP (1998). Identification and tissue distribution of human cystathionine beta-synthase mRNA isoforms. *Archives of Biochemistry and Biophysics* **350**(1)**:** 95-103.

Bennett RA, Pegg AE (1981). Alkylation of DNA in rat tissues following administration of streptozotocin. *Cancer Research* **41**(7)**:** 2786-2790.

Bian JS, Yong QC, Pan TT, Feng ZN, Ali MY, Zhou S*, et al.* (2006). Role of hydrogen sulfide in the cardioprotection caused by ischemic preconditioning in the rat heart and cardiac myocytes. *The Journal of Pharmacology and Experimental Therapeutics* **316**(2)**:** 670-678.

Bjelakovic G, Nikolova D, Gluud LL, Simonetti RG, Gluud C (2012). Antioxidant supplements for prevention of mortality in healthy participants and patients with various diseases. *Cochrane Database of Systematic Reviews (Online)* **3:** CD007176.

Boedtkjer E, Praetorius J, Matchkov VV, Stankevicius E, Mogensen S, Fuchtbauer AC*, et al.* (2011). Disruption of Na+,HCO(3)(-) cotransporter NBCn1 (slc4a7) inhibits NO-mediated vasorelaxation, smooth muscle Ca(2)(+) sensitivity, and hypertension development in mice. *Circulation* **124**(17)**:** 1819-1829.

Bogatcheva NV, Sergeeva MG, Dudek SM, Verin AD (2005). Arachidonic acid cascade in endothelial pathobiology. *Microvascular Research* **69**(3)**:** 107-127.

Boltz H (1978). Colorimetric determination of nonmetals. *Wiley, New York***:** 474-477.

Bolzan AD, Bianchi MS (2002). Genotoxicity of streptozotocin. *Mutation Research* **512**(2-3)**:** 121-134.

Bonaa KH, Njolstad I, Ueland PM, Schirmer H, Tverdal A, Steigen T*, et al.* (2006). Homocysteine lowering and cardiovascular events after acute myocardial infarction. *The New England Journal of Medicine* **354**(15)**:** 1578-1588.

Brancaleone V, Roviezzo F, Vellecco V, De Gruttola L, Bucci M, Cirino G (2008). Biosynthesis of H2S is impaired in non-obese diabetic (NOD) mice. *British Journal Pharmacology* **155**(5)**:** 673-680.

Braunstein AE, Goryachenkova EV, Tolosa EA, Willhardt IH, Yefremova LL (1971). Specificity and some other properties of liver serine sulphhydrase: evidence for its identity with cystathionine - synthase. *Biochimica et Biophysica Acta* **242**(1)**:** 247-260.

Brayden JE (2002). Functional roles of KATP channels in vascular smooth muscle. *Clinical and Experimental Pharmacology Physiology* **29**(4)**:** 312-316.

Brian JE, Jr., Faraci FM, Heistad DD (1996). Recent insights into the regulation of cerebral circulation. *Clinical and Experimental Pharmacology Physiology* **23**(6-7)**:** 449-457.

Briones AM, Alonso MJ, Hernanz R, Miguel M, Salaices M (2002). Alterations of the nitric oxide pathway in cerebral arteries from spontaneously hypertensive rats. *Journal of Cardiovascular Pharmacology* **39**(3)**:** 378-388.

Brown KA, Didion SP, Andresen JJ, Faraci FM (2007). Effect of aging, MnSOD deficiency, and genetic background on endothelial function: evidence for MnSOD haploinsufficiency. *Arteriosclerosis, Thrombosis, and Vascular Biology* **27**(9)**:** 1941-1946.

Calvert JW, Jha S, Gundewar S, Elrod JW, Ramachandran A, Pattillo CB*, et al.* (2009). Hydrogen sulfide mediates cardioprotection through Nrf2 signaling. *Circulatory Research* **105**(4)**:** 365-374.

Campbell WB, Falck JR (2007). Arachidonic acid metabolites as endothelium-derived hyperpolarizing factors. *Hypertension* **49**(3)**:** 590-596.

Campos RR, Oliveira-Sales EB, Nishi EE, Boim MA, Dolnikoff MS, Bergamaschi CT (2011). The role of oxidative stress in renovascular hypertension. *Clinical and Experimental Pharmacology Physiology* **38**(2)**:** 144-152.

Carr P, McKinnon W, Poston L (1995). Mechanisms of pHi control and relationships between tension and pHi in human subcutaneous small arteries. *American Journal of Physiology* **268**(3 Pt 1)**:** C580-589.

Catterall WA, Perez-Reyes E, Snutch TP, Striessnig J (2005). International Union of Pharmacology. XLVIII. Nomenclature and structure-function relationships of voltage-gated calcium channels. *Pharmacological Reviews* **57**(4)**:** 411-425.

Chai W, Wang Y, Lin JY, Sun XD, Yao LN, Yang YH*, et al.* (2012). Exogenous hydrogen sulfide protects against traumatic hemorrhagic shock via attenuation of oxidative stress. *The Journal of Surgical Research* **176**(1)**:** 210-219.

Cheang WS, Wong WT, Shen B, Lau CW, Tian XY, Tsang SY*, et al.* (2010). 4-Aminopyridine-sensitive K(+) channels contributes to NaHS-induced membrane hyperpolarization and relaxation in the rat coronary artery. *Vascular Pharmacology* **53**(3-4)**:** 94-98.

Chen F, Liu F, Badoer E (2011). AT1 receptors in the paraventricular nucleus mediate the hyperthermia-induced reflex reduction of renal blood flow in rats. *American Journal of Physiology. Regulatory Integrative and Comparative Physiology* **300**(2)**:** R479-485.

Chen S, He RR (1998). Effect of intracarotid injection of adenosine on the activity of RVLM neurons in barodenervated rats. *Sheng Li Xue Bao* **50**(6)**:** 629-635.

Cheng Y, Ndisang J, Tang G, Cao K, Wang R (2004). Hydrogen sulfide-induced relaxation of resistance mesenteric artery beds of rats. *American Journal of Physiology - Heart and Circulatory Physiology* **287:** 2316-2323.

Cheng Z, Jiang X, Kruger WD, Pratico D, Gupta S, Mallilankaraman K*, et al.* (2011). Hyperhomocysteinemia impairs endothelium-derived hyperpolarizing factor-mediated vasorelaxation in transgenic cystathionine beta synthase-deficient mice. *Blood* **118**(7)**:** 1998-2006.

Cho AH, Kang DW, Kwon SU, Kim JS (2007). Is 15 mm size criterion for lacunar infarction still valid? A study on strictly subcortical middle cerebral artery territory infarction using diffusion-weighted MRI. *Cerebrovascular diseases (Basel, Switzerland)* **23**(1)**:** 14-19.

Cipolla MJ, McCall AL, Lessov N, Porter JM (1997). Reperfusion decreases myogenic reactivity and alters middle cerebral artery function after focal cerebral ischemia in rats. *Stroke* **28**(1)**:** 176-180.

Coetzee WA, Amarillo Y, Chiu J, Chow A, Lau D, McCormack T*, et al.* (1999). Molecular diversity of K+ channels. *Annals of the New York Academy of Sciences* **868:** 233-285.

Coote JH, Yang Z, Pyner S, Deering J (1998). Control of sympathetic outflows by the hypothalamic paraventricular nucleus. *Clinical and Experimental Pharmacology and Physiology* **25**(6)**:** 461-463.

Cox BF, Brody MJ (1988). Tidal volume affects the response to inactivation of the rostral ventrolateral medulla. *Hypertension* **11**(2 Pt 2)**:** I186-189.

Creager MA, Luscher TF, Cosentino F, Beckman JA (2003). Diabetes and vascular disease: pathophysiology, clinical consequences, and medical therapy: Part I. *Circulation* **108**(12)**:** 1527-1532.

Cribbs LL (2001). Vascular smooth muscle calcium channels: could "T" be a target? *Circulation Research* **89**(7)**:** 560-562.

Csanyi G, Taylor WR, Pagano PJ (2009). NOX and inflammation in the vascular adventitia. *Free Radical Biology & Medicine* **47**(9)**:** 1254-1266.

d'Emmanuele di Villa Bianca R, Sorrentino R, Coletta C, Mitidieri E, Rossi A, Vellecco V*, et al.* (2011). Hydrogen sulfide-induced dual vascular effect involves arachidonic acid cascade in rat mesenteric arterial bed. *The Journal of Pharmacology and Experimental Therapeutics* **337**(1)**:** 59-64.

d'Emmanuele di Villa Bianca R, Sorrentino R, Maffia P, Mirone V, Imbimbo C, Fusco F*, et al.* (2009). Hydrogen sulfide as a mediator of human corpus cavernosum smooth-muscle relaxation. *Proceedings of the National Academy of Sciences of the United States of America* **106**(11)**:** 4513-4518.

Dal-Secco D, Cunha TM, Freitas A, Alves-Filho JC, Souto FO, Fukada SY*, et al.* (2008). Hydrogen sulfide augments neutrophil migration through enhancement of adhesion molecule expression and prevention of CXCR2 internalization: role of ATP-sensitive potassium channels. *Journal of Immunology (Baltimore, Md. : 1950)* **181**(6)**:** 4287-4298.

Dampney RA (1994). Functional organization of central pathways regulating the cardiovascular system. *Physiological Reviews* **74**(2)**:** 323-364.

Dan P, Cheung JC, Scriven DR, Moore ED (2003). Epitope-dependent localization of estrogen receptor-alpha, but not -beta, in en face arterial endothelium. *American Journal of Physiology. Heart and Circulatory Physiology* **284**(4)**:** H1295-1306.

Dawe GS, Han SP, Bian JS, Moore PK (2008). Hydrogen sulphide in the hypothalamus causes an ATP-sensitive K+ channel-dependent decrease in blood pressure in freely moving rats. *Neuroscience* **152**(1)**:** 169-177.

Deering J, Coote JH (2000). Paraventricular neurones elicit a volume expansion-like change of activity in sympathetic nerves to the heart and kidney in the rabbit. *Experimental Physiology* **85**(2)**:** 177-186.

DeLeon ER, Stoy GF, Olson KR (2012). Passive loss of hydrogen sulfide in biological experiments. *Analytical Biochemistry* **421**(1)**:** 203-207.

Dello Russo C, Tringali G, Ragazzoni E, Maggiano N, Menini E, Vairano M*, et al.* (2000). Evidence that hydrogen sulphide can modulate hypothalamo-pituitary-adrenal axis function: in vitro and in vivo studies in the rat. *Journal of Neuroendocrinology* **12**(3)**:** 225-233.

Demchenko IT, Oury TD, Crapo JD, Piantadosi CA (2002). Regulation of the brain's vascular responses to oxygen. *Circulatory Research* **91**(11)**:** 1031-1037.

Denizalti M, Bozkurt TE, Akpulat U, Sahin-Erdemli I, Abacioglu N (2011). The vasorelaxant effect of hydrogen sulfide is enhanced in streptozotocin-induced diabetic rats. *Naunyn-Schmiedeberg's Archives of Pharmacology* **383**(5)**:** 509-517.

di Villa Bianca R, Coletta C, Mitidieri E, De Dominicis G, Rossi A, Sautebin L*, et al.* (2010). Hydrogen sulphide induces mouse paw oedema through activation of phospholipase A2. *British Journal of Pharmacology* **161**(8)**:** 1835-1842.

Didion SP, Faraci FM (2002a). Effects of NADH and NADPH on superoxide levels and cerebral vascular tone. *American Journal of Physiology. Heart and Circulatory Physiology* **282**(2)**:** H688-695.

Didion SP, Ryan MJ, Baumbach GL, Sigmund CD, Faraci FM (2002b). Superoxide contributes to vascular dysfunction in mice that express human renin and angiotensinogen. *American Journal of Physiology. Heart and Circulatory Physiology* **283**(4)**:** H1569-1576.

Diedler J, Sykora M, Rupp A, Poli S, Karpel-Massler G, Sakowitz O*, et al.* (2009). Impaired cerebral vasomotor activity in spontaneous intracerebral hemorrhage. *Stroke* **40**(3)**:** 815-819.

Dombkowski RA, Russell MJ, Olson KR (2004). Hydrogen sulfide as an endogenous regulator of vascular smooth muscle tone in trout. *American Journal of Physiology. Regulatory Integrative and Comparative Physiology* **286**(4)**:** R678-685.

Dombkowski RA, Russell MJ, Schulman AA, Doellman MM, Olson KR (2005). Vertebrate phylogeny of hydrogen sulfide vasoactivity. *American Journal of Physiology. Regulatory Integrative and Comparative Physiology* **288**(1)**:** R243-252.

Dong H, Jiang Y, Cole WC, Triggle CR (2000). Comparison of the pharmacological properties of EDHF-mediated vasorelaxation in guinea-pig cerebral and mesenteric resistance vessels. *British Journal of Pharmacology* **130**(8)**:** 1983-1991.

Dong L, Zheng YM, Van Riper D, Rathore R, Liu QH, Singer HA*, et al.* (2008). Functional and molecular evidence for impairment of calcium-activated potassium channels in type-1 diabetic cerebral artery smooth muscle cells. *Journal of Cerebral Blood Flow and Metabolism* **28**(2)**:** 377-386.

Droge W (2002). Free radicals in the physiological control of cell function. *Physiological Reviews* **82**(1)**:** 47-95.

Dunn-Meynell AA, Rawson NE, Levin BE (1998). Distribution and phenotype of neurons containing the ATP-sensitive K+ channel in rat brain. *Brain Research* **814**(1-2)**:** 41-54.

Edvinsson LI, Povlsen GK (2011). Vascular plasticity in cerebrovascular disorders. *Journal of Cerebral Blood Flow and Metabolism* **31**(7)**:** 1554-1571.

Edwards G, Feletou M, Weston AH (2010). Endothelium-derived hyperpolarising factors and associated pathways: a synopsis. *Pflugers Archiv* **459**(6)**:** 863-879.

Edwards G, Feletou M, Weston AH (2012). Hydrogen sulfide as an endothelium-derived hyperpolarizing factor in rodent mesenteric arteries. *Circulation Research* **110**(1)**:** e13-14.

Elsey DJ, Fowkes RC, Baxter GF (2010). L-cysteine stimulates hydrogen sulfide synthesis in myocardium associated with attenuation of ischemia-reperfusion injury. *Journal of Cardiovascular Pharmacology and Therapeutics* **15**(1)**:** 53-59.

Escobar C, Bravo L, Hernandez J, Herrera L (2007). Hydrogen sulfide production from elemental sulfur by Desulfovibrio desulfuricans in an anaerobic bioreactor. *Biotechnology and Bioengineering* **98**(3)**:** 569-577.

Esler M (2010). The 2009 Carl Ludwig Lecture: Pathophysiology of the human sympathetic nervous system in cardiovascular diseases: the transition from mechanisms to medical management. *Journal of Applied Physiology (Bethesda, Md. : 1985)* **108**(2)**:** 227-237.

Eto K, Kimura H (2002). A novel enhancing mechanism for hydrogen sulfide-producing activity of cystathionine beta-synthase. *Journal of Biological Chemistry* **277**(45)**:** 42680-42685.

Fagan SC, Hess DC, Hohnadel EJ, Pollock DM, Ergul A (2004). Targets for vascular protection after acute ischemic stroke. *Stroke* **35**(9)**:** 2220-2225.

Fang L, Zhao J, Chen Y, Ma T, Xu G, Tang C*, et al.* (2009). Hydrogen sulfide derived from periadventitial adipose tissue is a vasodilator. *Journal of Hypertension* **27**(11)**:** 2174-2185.

Faraci FM (1993). Endothelium-derived vasoactive factors and regulation of the cerebral circulation. *Neurosurgery* **33**(4)**:** 648-658; discussion 658-649.

Faraci FM (2011). Protecting against vascular disease in brain. *American Journal of Physiology. Heart and Circulatory Physiology* **300**(5)**:** H1566-1582.

Faraci FM (2006). Reactive oxygen species: influence on cerebral vascular tone. *Journal of Applied Physiology* **100**(2)**:** 739-743.

Faraci FM, Heistad DD (1990). Regulation of large cerebral arteries and cerebral microvascular pressure. *Circulation Research* **66**(1)**:** 8-17.

Faraci FM, Heistad DD (1998). Regulation of the cerebral circulation: role of endothelium and potassium channels. *Physiological Reviews* **78**(1)**:** 53-97.

Favaloro JL, Andrews KL, McPherson GA (2003). Novel imidazoline compounds that inhibit Kir-mediated vasorelaxation in rat middle cerebral artery. *Naunyn-Schmiedeberg's Archives of Pharmacology* **367**(4)**:** 397-405.

Feletou M, Vanhoutte PM (1988). Endothelium-dependent hyperpolarization of canine coronary smooth muscle. *British Journal of Pharmacology* **93**(3)**:** 515-524.

Filosa JA, Bonev AD, Straub SV, Meredith AL, Wilkerson MK, Aldrich RW*, et al.* (2006). Local potassium signaling couples neuronal activity to vasodilation in the brain. *Nature Neuroscience* **9**(11)**:** 1397-1403.

Finkelstein JD, Kyle WE, Martin JL, Pick AM (1975). Activation of cystathionine synthase by adenosylmethionine and adenosylethionine. *Biochemical and Biophysical Research Communications* **66**(1)**:** 81-87.

Fiorucci S, Antonelli E, Mencarelli A, Orlandi S, Renga B, Rizzo G*, et al.* (2005). The third gas: H2S regulates perfusion pressure in both the isolated and perfused normal rat liver and in cirrhosis. *Hepatology* **42**(3)**:** 539-548.

Forstermann U (2010). Nitric oxide and oxidative stress in vascular disease. *Pflugers Archiv* **459**(6)**:** 923-939.

Forstermann U, Munzel T (2006). Endothelial nitric oxide synthase in vascular disease: from marvel to menace. *Circulation* **113**(13)**:** 1708-1714.

Fraile ML, Conde MV, Sanz L, Moreno MJ, Marco EJ, Lopez de Pablo AL (1994). Different influence of superoxide anions and hydrogen peroxide on endothelial function of isolated cat cerebral and pulmonary arteries. *General Pharmacology* **25**(6)**:** 1197-1205.

Franklin KA (2002). Cerebral haemodynamics in obstructive sleep apnoea and Cheyne-Stokes respiration. *Sleep Medicine Reviews* **6**(6)**:** 429-441.

Fukao M, Hattori Y, Kanno M, Sakuma I, Kitabatake A (1995). Thapsigargin- and cyclopiazonic acid-induced endothelium-dependent hyperpolarization in rat mesenteric artery. *British Journal Pharmacology* **115**(6)**:** 987-992.

Furne J, Saeed A, Levitt MD (2008). Whole tissue hydrogen sulfide concentrations are orders of magnitude lower than presently accepted values. *American Journal of Physiology. Regulatory Integrative and Comparative Physiology* **295**(5)**:** R1479-1485.

Furukawa T, Yamakawa T, Midera T, Sagawa T, Mori Y, Nukada T (1999). Selectivities of dihydropyridine derivatives in blocking Ca(2+) channel subtypes expressed in Xenopus oocytes. *The Journal of Pharmacology and Experimental Therapeutics* **291**(2)**:** 464-473.

Gadalla MM, Snyder SH (2010). Hydrogen sulfide as a gasotransmitter. *Journal of Neurochemistry* **113**(1)**:** 14-26.

Gardner JP, Diecke FP (1988). Influence of pH on isometric force development and relaxation in skinned vascular smooth muscle. *Pflugers Archiv* **412**(3)**:** 231-239.

Geng B, Chang L, Pan C, Qi Y, Zhao J, Pang Y*, et al.* (2004). Endogenous hydrogen sulfide regulation of myocardial injury induced by isoproterenol. *Biochemical and Biophysical Research Communications* **318**(3)**:** 756-763.

Geng B, Cui Y, Zhao J, Yu F, Zhu Y, Xu G*, et al.* (2007). Hydrogen sulfide downregulates the aortic L-arginine/nitric oxide pathway in rats. *American Journal of Physiology. Regulatory Integrative and Comparative Physiology* **293**(4)**:** R1608-1618.

Ghasemi M, Dehpour AR, Moore KP, Mani AR (2012). Role of endogenous hydrogen sulfide in neurogenic relaxation of rat corpus cavernosum. *Biochemical Pharmacology* **83**(9)**:** 1261-1268.

Gollasch M, Wellman GC, Knot HJ, Jaggar JH, Damon DH, Bonev AD*, et al.* (1998). Ontogeny of local sarcoplasmic reticulum Ca2+ signals in cerebral arteries: Ca2+ sparks as elementary physiological events. *Circulation Research* **83**(11)**:** 1104-1114.

Goodwin LR, Francom D, Dieken FP, Taylor JD, Warenycia MW, Reiffenstein RJ*, et al.* (1989). Determination of sulfide in brain tissue by gas dialysis/ion chromatography: postmortem studies and two case reports. *Journal of Analytical Toxicology* **13**(2)**:** 105-109.

Gorlach C, Benyo Z, Wahl M (1998). Dilator effect of bradykinin and acetylcholine in cerebral vessels after brain lesion. *Kidney International. Supplement* **67:** S226-227.

Grobelny BT, Ducruet AF, Derosa PA, Kotchetkov IS, Zacharia BE, Hickman ZL*, et al.* (2011). Gain-of-function polymorphisms of cystathionine beta-synthase and delayed cerebral ischemia following aneurysmal subarachnoid hemorrhage. *Journal of Neurosurgery* **115**(1)**:** 101-107.

Groeger M, Matallo J, McCook O, Wagner F, Wachter U, Bastian O*, et al.* (2012). Temperature and Cell-type Dependency of Sulfide-Effects on Mitochondrial Respiration. *Shock (Augusta, Ga.)*.

Gryglewski RJ, Palmer RM, Moncada S (1986). Superoxide anion is involved in the breakdown of endothelium-derived vascular relaxing factor. *Nature* **320**(6061)**:** 454-456.

Guan Q, Zhang Y, Yu C, Liu Y, Gao L, Zhao J (2012). Hydrogen sulfide protects against high-glucose-induced apoptosis in endothelial cells. *Journal of Cardiovascular Pharmacology* **59**(2)**:** 188-193.

Gunarathne A, Patel JV, Kausar S, Gammon B, Hughes EA, Lip GY (2009). Glycemic status underlies increased arterial stiffness and impaired endothelial function in migrant South Asian stroke survivors compared to European Caucasians: pathophysiological insights from the West Birmingham Stroke Project. *Stroke* **40**(7)**:** 2298-2306.

Guo Q, Jin S, Wang XL, Wang R, Xiao L, He RR*, et al.* (2011). Hydrogen sulfide in the rostral ventrolateral medulla inhibits sympathetic vasomotor tone through ATP-sensitive K+ channels. *The Journal of Pharmacology and Experimental Therapeutics* **338**(2)**:** 458-465.

Guyenet PG (2006). The sympathetic control of blood pressure. *Nature Reviews Neuroscience* **7**(5)**:** 335-346.

Guyenet PG, Stornetta RL, Abbott SB, Depuy SD, Fortuna MG, Kanbar R (2010). Central CO2 chemoreception and integrated neural mechanisms of cardiovascular and respiratory control. *Journal of Applied Physiology (Bethesda, Md. : 1985)* **108**(4)**:** 995-1002.

Han Y, Shi Z, Zhang F, Yu Y, Zhong MK, Gao XY*, et al.* (2007). Reactive oxygen species in the paraventricular nucleus mediate the cardiac sympathetic afferent reflex in chronic heart failure rats. *European Journal of Heart Failure* **9**(10)**:** 967-973.

Hancock JT, Jones OT (1987). The inhibition by diphenyleneiodonium and its analogues of superoxide generation by macrophages. *The Biochemical Journal* **242**(1)**:** 103-107.

Hart JL (2011). Role of sulfur-containing gaseous substances in the cardiovascular system. *Frontiers in Bioscience (Elite Edition)* **3:** 736-749.

Hassan MI, Boosen M, Schaefer L, Kozlowska J, Eisel F, von Knethen A*, et al.* (2012). Platelet-derived growth factor-BB induces cystathionine gamma-lyase expression in rat mesangial cells via a redox-dependent mechanism. *British Journal of Pharmacology* 166(8):2231-42.

Henrion D, Laher I, Klaasen A, Bevan JA (1994). Myogenic tone of rabbit facial vein and posterior cerebral artery is influenced by changes in extracellular sodium. *American Journal of Physiology* **266**(2 Pt 2)**:** H377-383.

Hill AP, Sitsapesan R (2002). DIDS modifies the conductance, gating, and inactivation mechanisms of the cardiac ryanodine receptor. *Biophysical Journal* **82**(6)**:** 3037-3047.

Hink U, Li H, Mollnau H, Oelze M, Matheis E, Hartmann M*, et al.* (2001). Mechanisms underlying endothelial dysfunction in diabetes mellitus. *Circulation Research* **88**(2)**:** E14-22.

Hogervorst E, Ribeiro HM, Molyneux A, Budge M, Smith AD (2002). Plasma homocysteine levels, cerebrovascular risk factors, and cerebral white matter changes (leukoaraiosis) in patients with Alzheimer disease. *Archives of Neurology* **59**(5)**:** 787-793.

Hosoki R, Matsuki N, Kimura H (1997). The possible role of hydrogen sulfide as an endogenous smooth muscle relaxant in synergy with nitric oxide. *Biochemical and Biophysical Research Communications* **237**(3)**:** 527-531.

Hsu P, Haffner J, Albuquerque ML, Leffler CW (1996). pHi in piglet cerebral microvascular endothelial cells: recovery from an acid load. *Proceedings of the Society for Experimental Biology and Medicine* **212**(3)**:** 256-262.

Hu LF, Lu M, Tiong CX, Dawe GS, Hu G, Bian JS (2010). Neuroprotective effects of hydrogen sulfide on Parkinson's disease rat models. *Aging Cell* **9**(2)**:** 135-146.

Hughes JM, Riddle MA, Paffett ML, Gonzalez Bosc LV, Walker BR (2010). Novel role of endothelial BKCa channels in altered vasoreactivity following hypoxia. *American Journal of Physiology. Heart and Circulatory Physiology* **299**(5)**:** H1439-1450.

Humpel C (2011). Chronic mild cerebrovascular dysfunction as a cause for Alzheimer's disease? *Experimental Gerontology* **46**(4)**:** 225-232.

Iadecola C (2004). Neurovascular regulation in the normal brain and in Alzheimer's disease. *Nature Reviews Neuroscience* **5**(5)**:** 347-360.

Iadecola C, Davisson RL (2008). Hypertension and cerebrovascular dysfunction. *Cell Metabolism* **7**(6)**:** 476-484.

Iadecola C, Zhang F, Niwa K, Eckman C, Turner SK, Fischer E*, et al.* (1999). SOD1 rescues cerebral endothelial dysfunction in mice overexpressing amyloid precursor protein. *Nature Neuroscience* **2**(2)**:** 157-161.

Ishigami M, Hiraki K, Umemura K, Ogasawara Y, Ishii K, Kimura H (2009). A source of hydrogen sulfide and a mechanism of its release in the brain. *Antioxidants and Redox Signalling* **11**(2)**:** 205-214.

Ishii I, Akahoshi N, Yamada H, Nakano S, Izumi T, Suematsu M (2010). Cystathionine gamma-Lyase-deficient mice require dietary cysteine to protect against acute lethal myopathy and oxidative injury. The *Journal of Biological Chemistry* **285**(34)**:** 26358-26368.

Ishii I, Akahoshi N, Yu XN, Kobayashi Y, Namekata K, Komaki G*, et al.* (2004). Murine cystathionine gamma-lyase: complete cDNA and genomic sequences, promoter activity, tissue distribution and developmental expression. *The Biochemical Journal* **381**(Pt 1)**:** 113-123.

Jackson WF (2000). Ion channels and vascular tone. *Hypertension* **35**(1 Pt 2)**:** 173-178.

Jackson-Weaver O, Paredes DA, Bosc LV, Walker BR, Kanagy NL (2011). Intermittent hypoxia in rats increases myogenic tone through loss of hydrogen sulfide activation of large-conductance Ca2+-activated potassium channels. *Circulation Research* **108**(12)**:** 1439-1447.

Jacobs RL, House JD, Brosnan ME, Brosnan JT (1998). Effects of streptozotocin-induced diabetes and of insulin treatment on homocysteine metabolism in the rat. *Diabetes* **47**(12)**:** 1967-1970.

Jaggar JH, Porter VA, Lederer WJ, Nelson MT (2000). Calcium sparks in smooth muscle. *American Journal of Physiology. Cell Physiology* **278**(2)**:** C235-256.

Jain SK, Bull R, Rains JL, Bass PF, Levine SN, Reddy S*, et al.* (2010). Low levels of hydrogen sulfide in the blood of diabetes patients and streptozotocin-treated rats causes vascular inflammation? *Antioxidants and Redox Signalling* **12**(11)**:** 1333-1337.

Johnson TD, Marrelli SP, Steenberg ML, Childres WF, Bryan RM, Jr. (1998). Inward rectifier potassium channels in the rat middle cerebral artery. *American Journal of Physiology* **274**(2 Pt 2)**:** R541-547.

Johnston M, Jankowski D, Marcotte P, Tanaka H, Esaki N, Soda K*, et al.* (1979). Suicide inactivation of bacterial cystathionine gamma-synthase and methionine gamma-lyase during processing of L-propargylglycine. *Biochemistry* **18**(21)**:** 4690-4701.

Kamata K, Miyata N, Kasuya Y (1989). Functional changes in potassium channels in aortas from rats with streptozotocin-induced diabetes. *European journal of Pharmacology* **166**(2)**:** 319-323.

Kaneko Y, Kimura T, Taniguchi S, Souma M, Kojima Y, Kimura Y*, et al.* (2009). Glucose-induced production of hydrogen sulfide may protect the pancreatic beta-cells from apoptotic cell death by high glucose. *FEBS letters* **583**(2)**:** 377-382.

Kaneto H, Katakami N, Matsuhisa M, Matsuoka TA (2010). Role of reactive oxygen species in the progression of type 2 diabetes and atherosclerosis. *Mediators of Inflammation* **2010:** 453892.

Kang YM, He RL, Yang LM, Qin DN, Guggilam A, Elks C*, et al.* (2009). Brain tumour necrosis factor-alpha modulates neurotransmitters in hypothalamic paraventricular nucleus in heart failure. *Cardiovascular Research* **83**(4)**:** 737-746.

Kannan H, Hayashida Y, Yamashita H (1989). Increase in sympathetic outflow by paraventricular nucleus stimulation in awake rats. *American Journal of Physiology* **256**(6 Pt 2)**:** R1325-1330.

Kannan H, Niijima A, Yamashita H (1987). Inhibition of renal sympathetic nerve activity by electrical stimulation of the hypothalamic paraventricular nucleus in anesthetized rats. *Journal of the Autonomic Nervous System* **21**(1)**:** 83-86.

Kantzides A, Badoer E (2005). nNOS-containing neurons in the hypothalamus and medulla project to the RVLM. *Brain Research* **1037**(1-2)**:** 25-34.

Kasprowicz M, Czosnyka M, Soehle M, Smielewski P, Kirkpatrick PJ, Pickard JD*, et al.* (2012). Vasospasm shortens cerebral arterial time constant. *Neurocritical Care* **16**(2)**:** 213-218.

Kelley BJ, Petersen RC (2007). Alzheimer's disease and mild cognitive impairment. *Neurologic Clinics* **25**(3)**:** 577-609, v.

Kelly-Cobbs A, Elgebaly MM, Li W, Ergul A (2011). Pressure-independent cerebrovascular remodelling and changes in myogenic reactivity in diabetic Goto-Kakizaki rat in response to glycaemic control. *Acta physiologica (Oxford, England)* **203**(1)**:** 245-251.

Khan AA, Schuler MM, Prior MG, Yong S, Coppock RW, Florence LZ*, et al.* (1990). Effects of hydrogen sulfide exposure on lung mitochondrial respiratory chain enzymes in rats. *Toxicology and Applied Pharmacology* **103**(3)**:** 482-490.

Kiely JM, Gordon FJ (1994). Role of rostral ventrolateral medulla in centrally mediated pressor responses. *American Journal of Physiology* **267**(4 Pt 2)**:** H1549-1556.

Kim C, Lan Y, Deng B (2007). Kinetic study of hexavalent Cr(VI) reduction by hydrogen sulfide through goethite surface catalytic reaction. *Geochemical Journal* **41:** 397-405.

Kimura H (2002). Hydrogen sulfide as a neuromodulator. *Molecular Neurobiology* **26**(1)**:** 13-19.

Kimura H (2011). Hydrogen sulfide: its production, release and functions. *Amino Acids* **41**(1)**:** 113-121.

Kimura Y, Dargusch R, Schubert D, Kimura H (2006). Hydrogen sulfide protects HT22 neuronal cells from oxidative stress. *Antioxidants and Redox Signalling* **8**(3-4)**:** 661-670.

Kimura Y, Goto Y, Kimura H (2010). Hydrogen sulfide increases glutathione production and suppresses oxidative stress in mitochondria. *Antioxidants and Redox Signalling* **12**(1)**:** 1-13.

Kimura Y, Hirooka Y, Kishi T, Ito K, Sagara Y, Sunagawa K (2009). Role of inducible nitric oxide synthase in rostral ventrolateral medulla in blood pressure regulation in spontaneously hypertensive rats. *Clinical and Experimental Hypertension (New York, N.Y. : 1993)* **31**(3)**:** 281-286.

Kishi T, Hirooka Y, Kimura Y, Ito K, Shimokawa H, Takeshita A (2004). Increased reactive oxygen species in rostral ventrolateral medulla contribute to neural mechanisms of hypertension in stroke-prone spontaneously hypertensive rats. *Circulation* **109**(19)**:** 2357-2362.

Kiss L, Deitch EA, Szabo C (2008). Hydrogen sulfide decreases adenosine triphosphate levels in aortic rings and leads to vasorelaxation via metabolic inhibition. *Life Sciences* **83**(17-18)**:** 589-594.

Kitayama J, Faraci FM, Gunnett CA, Heistad DD (2006). Impairment of dilator responses of cerebral arterioles during diabetes mellitus: role of inducible NO synthase. *Stroke; a Journal of Cerebral Circulation* **37**(8)**:** 2129-2133.

Klockner U, Isenberg G (1994). Intracellular pH modulates the availability of vascular L-type Ca2+ channels. *The Journal of General Physiology* **103**(4)**:** 647-663.

Knot HJ, Nelson MT (1995). Regulation of membrane potential and diameter by voltage-dependent K+ channels in rabbit myogenic cerebral arteries. *American Journal of Physiology* **269**(1 Pt 2)**:** H348-355.

Koenitzer JR, Isbell TS, Patel HD, Benavides GA, Dickinson DA, Patel RP*, et al.* (2007). Hydrogen sulfide mediates vasoactivity in an O2-dependent manner. *American Journal of Physiology. Heart and Circulatory Physiology* **292**(4)**:** H1953-1960.

Kohl RL, Quay WB (1979). Cystathionine synthase in rat brain: regional and time-of-day differences and their metabolic implications. *Journal of Neuroscience Research* **4**(3)**:** 189-196.

Koide M, Nystoriak MA, Brayden JE, Wellman GC (2011). Impact of subarachnoid hemorrhage on local and global calcium signaling in cerebral artery myocytes. *Acta Neurochirurgica. Supplement* **110**(Pt 1)**:** 145-150.

Komori K, Lorenz RR, Vanhoutte PM (1988). Nitric oxide, ACh, and electrical and mechanical properties of canine arterial smooth muscle. *American Journal of Physiology.* **255**(1 Pt 2)**:** H207-212.

Kontos HA (2001). Oxygen radicals in cerebral ischemia: the 2001 Willis lecture. *Stroke* **32**(11)**:** 2712-2716.

Koshiya N, Guyenet PG (1996). Tonic sympathetic chemoreflex after blockade of respiratory rhythmogenesis in the rat. *Journal of Physiology* **491 (Pt 3):** 859-869.

Kubo S, Doe I, Kurokawa Y, Nishikawa H, Kawabata A (2007). Direct inhibition of endothelial nitric oxide synthase by hydrogen sulfide: contribution to dual modulation of vascular tension. *Toxicology* **232**(1-2)**:** 138-146.

Kumagai H, Oshima N, Matsuura T, Iigaya K, Imai M, Onimaru H*, et al.* (2012). Importance of rostral ventrolateral medulla neurons in determining efferent sympathetic nerve activity and blood pressure. *Hypertension Research* **35**(2)**:** 132-141.

Kuo IY, Wolfle SE, Hill CE (2011). T-type calcium channels and vascular function: the new kid on the block? *Journal of Physiology* **589**(Pt 4)**:** 783-795.

Laing SP, Swerdlow AJ, Carpenter LM, Slater SD, Burden AC, Botha JL*, et al.* (2003). Mortality from cerebrovascular disease in a cohort of 23 000 patients with insulin-treated diabetes. *Stroke* **34**(2)**:** 418-421.

Lam E, Skarsgard P, Laher I (1998). Inhibition of myogenic tone by mibefradil in rat cerebral arteries. *European Journal of Pharmacology* **358**(2)**:** 165-168.

Lassegue B, Griendling KK (2010). NADPH oxidases: functions and pathologies in the vasculature. *Arteriosclerosis, Rhrombosis, and Vascular Biology* **30**(4)**:** 653-661.

Lee M, Schwab C, Yu S, McGeer E, McGeer PL (2009). Astrocytes produce the antiinflammatory and neuroprotective agent hydrogen sulfide. *Neurobiology and Aging* **30**(10)**:** 1523-1534.

Lee SW, Cheng Y, Moore PK, Bian JS (2007). Hydrogen sulphide regulates intracellular pH in vascular smooth muscle cells. *Biochemical and Biophysical Research Communications* **358**(4)**:** 1142-1147.

Leffler CW, Parfenova H, Basuroy S, Jaggar JH, Umstot ES, Fedinec AL (2010). Hydrogen sulfide and cerebral microvascular tone in newborn pigs. *American Journal of Physiology. Heart and Circulatory Physiology* **300**(2)**:** H440-447.

Leo CH, Hart JL, Woodman OL (2011a). 3',4'-Dihydroxyflavonol reduces superoxide and improves nitric oxide function in diabetic rat mesenteric arteries. *PloS one* **6**(6)**:** e20813.

Leo CH, Hart JL, Woodman OL (2011b). Impairment of both nitric oxide-mediated and EDHF-type relaxation in small mesenteric arteries from rats with streptozotocin-induced diabetes. *British Journal Pharmacology* **162**(2)**:** 365-377.

Levin BE, Dunn-Meynell AA (1997). In vivo and in vitro regulation of [3H]glyburide binding to brain sulfonylurea receptors in obesity-prone and resistant rats by glucose. *Brain Research* **776**(1-2)**:** 146-153.

Li DP, Chen SR, Pan HL (2010). Adenosine inhibits paraventricular pre-sympathetic neurons through ATP-dependent potassium channels. *Journal of Neurochemistry* **113**(2)**:** 530-542.

Li L, Whiteman M, Guan YY, Neo KL, Cheng Y, Lee SW, *et al.* (2008). Characterization of a novel, water-soluble hydrogen sulfide-releasing molecule (GYY4137): new insights into the biology of hydrogen sulfide. *Circulation* **117**(18)**:** 2351-2360.

Li W, Tang C, Jin H, Du J (2011). Regulatory effects of sulfur dioxide on the development of atherosclerotic lesions and vascular hydrogen sulfide in atherosclerotic rats. *Atherosclerosis* **215**(2)**:** 323-330.

Li YF, Patel KP (2003). Paraventricular nucleus of the hypothalamus and elevated sympathetic activity in heart failure: the altered inhibitory mechanisms. *Acta Physiologica Scandinavica* **177**(1)**:** 17-26.

Liang GH, Adebiyi A, Leo MD, McNally EM, Leffler CW, Jaggar JH (2011). Hydrogen sulfide dilates cerebral arterioles by activating smooth muscle cell plasma membrane KATP channels. *American Journal of Physiology. Heart and Circulatory Physiology* **300**(6)**:** H2088-2095.

Liang GH, Xi Q, Leffler CW, Jaggar JH (2012). Hydrogen sulfide activates Ca2+ sparks to induce cerebral arteriole dilation. *Journal Physiology* **590:** 2709-2720.

Liew HC, Khoo HE, Moore PK, Bhatia M, Lu J, Moochhala SM (2007). Synergism between hydrogen sulfide (H(2)S) and nitric oxide (NO) in vasorelaxation induced by stonustoxin (SNTX), a lethal and hypotensive protein factor isolated from stonefish Synanceja horrida venom. *Life Sciences* **80**(18)**:** 1664-1668.

Lim JJ, Liu YH, Khin ES, Bian JS (2008). Vasoconstrictive effect of hydrogen sulfide involves downregulation of cAMP in vascular smooth muscle cells. *American Journal of Physiology. Cell Physiology* **295**(5)**:** C1261-1270.

Lin Y, Matsumura K, Kagiyama S, Fukuhara M, Fujii K, Iida M (2005). Chronic administration of olmesartan attenuates the exaggerated pressor response to glutamate in the rostral ventrolateral medulla of SHR. *Brain Research* **1058**(1-2)**:** 161-166.

Liu J, Lai ZF, Wang XD, Tokutomi N, Nishi K (1998). Inhibition of sodium current by chloride channel blocker 4,4'-diisothiocyanatostilbene-2,2'-disulfonic acid (DIDS) in guinea pig cardiac ventricular cells. *Journal of Cardiovascular Pharmacology* **31**(4)**:** 558-567.

Liu L, Liu H, Sun D, Qiao W, Qi Y, Sun H, *et al.* (2012). Effects of h(2)s on myogenic responses in rat cerebral arterioles. *Circulatory Journal* **76**(4)**:** 1012-1019.

Liu WQ, Chai C, Li XY, Yuan WJ, Wang WZ, Lu Y (2011a). The cardiovascular effects of central hydrogen sulfide are related to K(ATP) channels activation. *Physiological Research / Academia Scientiarum Bohemoslovaca* **60**(5)**:** 729-738.

Liu Y, Gutterman DD (2002). The coronary circulation in diabetes: influence of reactive oxygen species on K+ channel-mediated vasodilation. *Vascular Pharmacology* **38**(1)**:** 43-49.

Liu Y, Terata K, Rusch NJ, Gutterman DD (2001). High glucose impairs voltage-gated K(+) channel current in rat small coronary arteries. *Circulation Research* **89**(2)**:** 146-152.

Liu YH, Bian JS (2010). Bicarbonate-dependent effect of hydrogen sulfide on vascular contractility in rat aortic rings. *American journal of physiology. Cell Physiology* **299**(4)**:** C866-872.

Liu YH, Yan CD, Bian JS (2011b). Hydrogen sulfide: a novel signaling molecule in the vascular system. *Journal of Cardiovascular Pharmacology* **58**(6)**:** 560-569.

Livak KJ, Schmittgen TD (2001). Analysis of relative gene expression data using real-time quantitative PCR and the 2(-Delta Delta C(T)) Method. *Methods (San Diego, Calif.)* **25**(4)**:** 402-408.

Lohn M, Dubrovska G, Lauterbach B, Luft FC, Gollasch M, Sharma AM (2002). Periadventitial fat releases a vascular relaxing factor. *FASEB Journal* **16**(9)**:** 1057-1063.

Long W, Zhang L, Longo LD (2000). Cerebral artery sarcoplasmic reticulum Ca(2+) stores and contractility: changes with development. *American Journal of Physiology. Regulatory Integrative and Comparative Physiology* **279**(3)**:** R860-873.

Lovick TA (1993). The periaqueductal gray-rostral medulla connection in the defence reaction: efferent pathways and descending control mechanisms. *Behavioural Brain Research* **58**(1-2)**:** 19-25.

Lovick TA, Malpas S, Mahony MT (1993). Renal vasodilatation in response to acute volume load is attenuated following lesions of parvocellular neurones in the paraventricular nucleus in rats. *Journal of the Autonomic Nervous System* **43**(3)**:** 247-255.

Lu J, Boron WF (2007). Reversible and irreversible interactions of DIDS with the human electrogenic Na/HCO3 cotransporter NBCe1-A: role of lysines in the KKMIK motif of TM5. *American journal of physiology. Cell Physiology* **292**(5)**:** C1787-1798.

Luksha L, Agewall S, Kublickiene K (2009). Endothelium-derived hyperpolarizing factor in vascular physiology and cardiovascular disease. *Atherosclerosis* **202**(2)**:** 330-344.

Luscher TF, Barton M (1997). Biology of the endothelium. *Clinical Cardiology* **20**(11 Suppl 2)**:** II-3-10.

Mackie AR, Byron KL (2008). Cardiovascular KCNQ (Kv7) potassium channels: physiological regulators and new targets for therapeutic intervention. *Molecular Pharmacology* **74**(5)**:** 1171-1179.

Maclean KN, Sikora J, Kozich V, Jiang H, Greiner LS, Kraus E*, et al.* (2010). Cystathionine beta-synthase null homocystinuric mice fail to exhibit altered hemostasis or lowering of plasma homocysteine in response to betaine treatment. *Molecular Genetics and Metabolism* **101**(2-3)**:** 163-171.

Madden JA, Ray DE, Keller PA, Kleinman JG (2001). Ion exchange activity in pulmonary artery smooth muscle cells: the response to hypoxia. *American Journal of Physiology. Lung Cellular and Molecular Physiology* **280**(2)**:** L264-271.

Malliani A, Montano N (2002). Emerging excitatory role of cardiovascular sympathetic afferents in pathophysiological conditions. *Hypertension* **39**(1)**:** 63-68.

Marcotte P, Walsh C (1976). Vinylglycine and proparglyglycine: complementary suicide substrates for L-amino acid oxidase and D-amino acid oxidase. *Biochemistry* **15**(14)**:** 3070-3076.

Maric-Bilkan C, Flynn ER, Chade AR (2012). Microvascular disease precedes the decline in renal function in the streptozotocin-induced diabetic rat. *American Journal of Physiology.l Renal Physiology* **302**(3)**:** F308-315.

Mathew R, Burke-Wolin T, Gewitz MH, Wolin MS (1991). O2 and rat pulmonary artery tone: effects of endothelium, Ca2+, cyanide, and monocrotaline. *Journal of Applied Physiology (Bethesda, Md. : 1985)* **71**(1)**:** 30-36.

Mavrikakis ME, Sfikakis PP, Kontoyannis D, Horti M, Kittas C, Koutras DA*, et al.* (1998). Macrovascular disease of coronaries and cerebral arteries in streptozotocin-induced diabetic rats. A

controlled, comparative study. *Experimental and Clinical Endocrinology & Diabetes : Official Journal* **106**(1)**:** 35-40.

Mayhan WG, Faraci FM (1993). Responses of cerebral arterioles in diabetic rats to activation of ATP-sensitive potassium channels. *American Journal of Physiology* **265**(1 Pt 2)**:** H152-157.

McGahon MK, Dash DP, Arora A, Wall N, Dawicki J, Simpson DA*, et al.* (2007). Diabetes downregulates large-conductance Ca2+-activated potassium beta 1 channel subunit in retinal arteriolar smooth muscle. *Circulation Research* **100**(5)**:** 703-711.

McMaster OG, Du F, French ED, Schwarcz R (1991). Focal injection of aminooxyacetic acid produces seizures and lesions in rat hippocampus: evidence for mediation by NMDA receptors. *Experimental Neurology* **113**(3)**:** 378-385.

McPherson GA (1992). Assessing vascular reactivity of arteries in the small vessel myograph. *Clinical and Experimental Pharmacology & Physiology* **19**(12)**:** 815-825.

McVeigh GE, Brennan GM, Johnston GD, McDermott BJ, McGrath LT, Henry WR*, et al.* (1992). Impaired endothelium-dependent and independent vasodilation in patients with type 2 (non-insulin-dependent) diabetes mellitus. *Diabetologia* **35**(8)**:** 771-776.

Meng QH, Yang G, Yang W, Jiang B, Wu L, Wang R (2007). Protective effect of hydrogen sulfide on balloon injury-induced neointima hyperplasia in rat carotid arteries. *The American Journal of Pathology* **170**(4)**:** 1406-1414.

Miller AA, Drummond GR, Schmidt HH, Sobey CG (2005). NADPH oxidase activity and function are profoundly greater in cerebral versus systemic arteries. *Circulation Research* **97**(10)**:** 1055-1062.

Miller AA, Drummond GR, Sobey CG (2006). Novel isoforms of NADPH-oxidase in cerebral vascular control. *Pharmacology & Therapeutics* **111**(3)**:** 928-948.

Mitchell JA, Ali F, Bailey L, Moreno L, Harrington LS (2008). Role of nitric oxide and prostacyclin as vasoactive hormones released by the endothelium. *Experimental Physiology* **93**(1)**:** 141-147.

Moncada S, Gryglewski R, Bunting S, Vane JR (1976). An enzyme isolated from arteries transforms prostaglandin endoperoxides to an unstable substance that inhibits platelet aggregation. *Nature* **263**(5579)**:** 663-665.

Moosmang S, Schulla V, Welling A, Feil R, Feil S, Wegener JW*, et al.* (2003). Dominant role of smooth muscle L-type calcium channel Cav1.2 for blood pressure regulation. *EMBO Journal* **22**(22)**:** 6027-6034.

Moskowitz MA, Lo EH, Iadecola C (2010). The science of stroke: mechanisms in search of treatments. *Neuron* **67**(2)**:** 181-198.

Mustafa AK, Gadalla MM, Sen N, Kim S, Mu W, Gazi SK*, et al.* (2009a). H2S signals through protein S-sulfhydration. *Science Signaling* **2**(96)**:** ra72.

Mustafa AK, Gadalla MM, Snyder SH (2009b). Signaling by gasotransmitters. *Science Signaling* **2**(68)**:** re2.

Mustafa AK, Sikka G, Gazi SK, Steppan J, Jung SM, Bhunia AK*, et al.* (2011). Hydrogen sulfide as endothelium-derived hyperpolarizing factor sulfhydrates potassium channels. *Circulation Research* **109**(11)**:** 1259-1268.

Muzaffar S, Shukla N, Bond M, Newby AC, Angelini GD, Sparatore A*, et al.* (2008). Exogenous hydrogen sulfide inhibits superoxide formation, NOX-1 expression and Rac1 activity in human vascular smooth muscle cells. *Journal of Vascular Research* **45**(6)**:** 521-528.

Myren M, Olesen J, Gupta S (2011). Pharmacological and expression profile of the prostaglandin I(2) receptor in the rat craniovascular system. *Vascular Pharmacoogyl* **55**(1-3)**:** 50-58.

Nagai Y, Tsugane M, Oka J, Kimura H (2004). Hydrogen sulfide induces calcium waves in astrocytes. *FASEB Journal* **18**(3)**:** 557-559.

Nakashima M, Vanhoutte PM (1995). Isoproterenol causes hyperpolarization through opening of ATP-sensitive potassium channels in vascular smooth muscle of the canine saphenous vein. *The Journal of Pharmacology and Experimental Therapeutics* **272**(1)**:** 379-384.

Naudi A, Jove M, Ayala V, Cassanye A, Serrano J, Gonzalo H*, et al.* (2012). Cellular dysfunction in diabetes as maladaptive response to mitochondrial oxidative stress. *Experimental Diabetes Research* **2012:** 696215.

Navarro-Gonzalez MF, Grayson TH, Meaney KR, Cribbs LL, Hill CE (2009). Non-L-type voltage-dependent calcium channels control vascular tone of the rat basilar artery. *Clinical and Experimental Pharmacology and Physiology* **36**(1)**:** 55-66.

Nazir FS, Alem M, Small M, Connell JM, Lees KR, Walters MR*, et al.* (2006). Blunted response to systemic nitric oxide synthase inhibition in the cerebral circulation of patients with Type 2 diabetes. *Diabetic Medicine* **23**(4)**:** 398-402.

Nelson MT, Cheng H, Rubart M, Santana LF, Bonev AD, Knot HJ*, et al.* (1995a). Relaxation of arterial smooth muscle by calcium sparks. *Science* **270**(5236)**:** 633-637.

Nelson MT, Patlak JB, Worley JF, Standen NB (1990). Calcium channels, potassium channels, and voltage dependence of arterial smooth muscle tone. *American Journal of Physiology* **259**(1 Pt 1)**:** C3-18.

Nelson MT, Quayle JM (1995b). Physiological roles and properties of potassium channels in arterial smooth muscle. *American Journal of Physiology* **268**(4 Pt 1)**:** C799-822.

Netzer N, Werner P, Jochums I, Lehmann M, Strohl KP (1998). Blood flow of the middle cerebral artery with sleep-disordered breathing: correlation with obstructive hypopneas. *Stroke* **29**(1)**:** 87-93.

Ng CW, De Matteo R, Badoer E (2004). Effect of muscimol and L-NAME in the PVN on the RSNA response to volume expansion in conscious rabbits. *American Journal of Physiology. Renal Physiology* **287**(4)**:** F739-746.

NHBPEP wg (1994). National High Blood Pressure Education Program Working Group report on hypertension in diabetes. *Hypertension* **23**(2)**:** 145-158; discussion 159-160.

Nishihara M, Hirooka Y, Matsukawa R, Kishi T, Sunagawa K (2012). Oxidative stress in the rostral ventrolateral medulla modulates excitatory and inhibitory inputs in spontaneously hypertensive rats. *Journal of Hypertension* **30**(1)**:** 97-106.

Niwa K, Kazama K, Younkin L, Younkin SG, Carlson GA, Iadecola C (2002). Cerebrovascular autoregulation is profoundly impaired in mice overexpressing amyloid precursor protein. *American Journal of Physiology. Heart and Circulatory Physiology* **283**(1)**:** H315-323.

O'Collins VE, Macleod MR, Donnan GA, Horky LL, van der Worp BH, Howells DW (2006). 1,026 experimental treatments in acute stroke. *Annals of Neurology* **59**(3)**:** 467-477.

O'Neill MJ, Clemens JA (2001). Rodent models of focal cerebral ischemia. *Current Protocols in Neuroscience* **Chapter 9:** Unit9 6.

Okajima T, Ohsaka T (2003). Chemiluminescence of lucigenin by electrogenerated superoxide ions in aqueous solutions. *Luminescence* **18**(1)**:** 49-57.

Oliveira-Sales EB, Colombari DS, Davisson RL, Kasparov S, Hirata AE, Campos RR*, et al.* (2010). Kidney-induced hypertension depends on superoxide signaling in the rostral ventrolateral medulla. *Hypertension* **56**(2)**:** 290-296.

Oliveira-Sales EB, Nishi EE, Carillo BA, Boim MA, Dolnikoff MS, Bergamaschi CT*, et al.* (2009). Oxidative stress in the sympathetic premotor neurons contributes to sympathetic activation in renovascular hypertension. *American Journal of Hypertension* **22**(5)**:** 484-492.

Olson KR (2012). A practical look at the chemistry and biology of hydrogen sulfide. *Antioxidants and Redox Signalling* **17**(1)**:** 32-44.

Olson KR, Dombkowski RA, Russell MJ, Doellman MM, Head SK, Whitfield NL*, et al.* (2006). Hydrogen sulfide as an oxygen sensor/transducer in vertebrate hypoxic vasoconstriction and hypoxic vasodilation. *The Journal of Experimental Biology* **209**(Pt 20)**:** 4011-4023.

Olson KR, Forgan LG, Dombkowski RA, Forster ME (2008). Oxygen dependency of hydrogen sulfide-mediated vasoconstriction in cyclostome aortas. *The Journal of Experimental Biology* **211**(Pt 14)**:** 2205-2213.

Olson KR, Russell MJ, Forster ME (2001). Hypoxic vasoconstriction of cyclostome systemic vessels: the antecedent of hypoxic pulmonary vasoconstriction? *American Journal of Physiology. Regulatory Integrative and Comparative Physiology* **280**(1)**:** R198-206.

Olson KR, Whitfield NL, Bearden SE, St Leger J, Nilson E, Gao Y*, et al.* (2010). Hypoxic pulmonary vasodilation: a paradigm shift with a hydrogen sulfide mechanism. *American Journal of Physiology. Regulatory Integrative and Comparative Physiology* **298**(1)**:** R51-60.

Ospina JA, Krause DN, Duckles SP (2002). 17beta-estradiol increases rat cerebrovascular prostacyclin synthesis by elevating cyclooxygenase-1 and prostacyclin synthase. *Stroke* **33**(2)**:** 600-605.

Ottschytsch N, Raes A, Van Hoorick D, Snyders DJ (2002). Obligatory heterotetramerization of three previously uncharacterized Kv channel alpha-subunits identified in the human genome. *Proceedings of the National Academy of Sciences of the United States of America* **99**(12)**:** 7986-7991.

Pagnussat AS, Faccioni-Heuser MC, Netto CA, Achaval M (2007). An ultrastructural study of cell death in the CA1 pyramidal field of the hippocapmus in rats submitted to transient global ischemia followed by reperfusion. *Journal of Anatomy* **211**(5)**:** 589-599.

Palmer RM, Ferrige AG, Moncada S (1987). Nitric oxide release accounts for the biological activity of endothelium-derived relaxing factor. *Nature* **327**(6122)**:** 524-526.

Pan LL, Liu XH, Gong QH, Wu D, Zhu YZ (2011). Hydrogen sulfide attenuated tumor necrosis factor-alpha-induced inflammatory signaling and dysfunction in vascular endothelial cells. *PloS one* **6**(5)**:** e19766.

Park L, Anrather J, Zhou P, Frys K, Wang G, Iadecola C (2004). Exogenous NADPH increases cerebral blood flow through NADPH oxidase-dependent and -independent mechanisms. *Arteriosclerosis, Thrombosis, and Vascular Biology* **24**(10)**:** 1860-1865.

Parks SK, Tresguerres M, Goss GG (2009). Cellular mechanisms of chloride transport in trout gill mitochondrion-rich cells. *American Journal of Physiology. Regulatory Integrative and Comparative Physiology* **296**(4)**:** R1161-1169.

Patel KP (2000). Role of paraventricular nucleus in mediating sympathetic outflow in heart failure. *Heart Failure Reviews* **5**(1)**:** 73-86.

Patel KP, Li YF, Hirooka Y (2001). Role of nitric oxide in central sympathetic outflow. *Experimental Biology and Medicine (Maywood, N.J.)* **226**(9)**:** 814-824.

Patel KP, Schmid PG (1988). Role of paraventricular nucleus (PVH) in baroreflex-mediated changes in lumbar sympathetic nerve activity and heart rate. *Journal of the Autonomic Nervous System* **22**(3)**:** 211-219.

Patel KP, Zheng H (2012). Central neural control of sympathetic nerve activity in heart failure following exercise training. *American Journal of Physiology. Heart and Circulatory Physiology* **302**(3)**:** H527-537.

Pearce WJ (1995). Mechanisms of hypoxic cerebral vasodilatation. *Pharmacology & Therapeutics* **65**(1)**:** 75-91.

Pearce WJ, Elliott SR (1994). Maturation enhances the sensitivity of ovine cerebral arteries to the ATP-sensitive potassium channel activator lemakalim. *Pediatric Research* **35**(6)**:** 729-732.

Peng HL, Jensen PE, Nilsson H, Aalkjaer C (1998). Effect of acidosis on tension and [Ca2+]i in rat cerebral arteries: is there a role for membrane potential? *American Journal of Physiology* **274**(2 Pt 2)**:** H655-662.

Pesic A, Madden JA, Pesic M, Rusch NJ (2004). High blood pressure upregulates arterial L-type Ca2+ channels: is membrane depolarization the signal? *Circulation Research* **94**(10)**:** e97-104.

Peterson JR, Sharma RV, Davisson RL (2006). Reactive oxygen species in the neuropathogenesis of hypertension. *Current Hypertension Reports* **8**(3)**:** 232-241.

Petersson M (2002). Cardiovascular effects of oxytocin. *Progress in Brain Research* **139:** 281-288.

Pilowsky PM, Goodchild AK (2002). Baroreceptor reflex pathways and neurotransmitters: 10 years on. *Journal of Hypertension* **20**(9)**:** 1675-1688.

Ploug KB, Edvinsson L, Olesen J, Jansen-Olesen I (2006). Pharmacological and molecular comparison of K(ATP) channels in rat basilar and middle cerebral arteries. *European Journal of Pharmacology* **553**(1-3)**:** 254-262.

Poulain DA, Wakerley JB (1982). Electrophysiology of hypothalamic magnocellular neurones secreting oxytocin and vasopressin. *Neuroscience* **7**(4)**:** 773-808.

Predmore BL, Julian D, Cardounel AJ (2011). Hydrogen sulfide increases nitric oxide production from endothelial cells by an akt-dependent mechanism. *Frontiers in Physiology* **2:** 104.

Pyner S (2009). Neurochemistry of the paraventricular nucleus of the hypothalamus: implications for cardiovascular regulation. *Journal of Chemical Neuroanatomy* **38**(3)**:** 197-208.

Qi M, Hang C, Zhu L, Shi J (2011). Involvement of endothelial-derived relaxing factors in the regulation of cerebral blood flow. *Neurological Sciences* **32**(4)**:** 551-557.

Quayle JM, McCarron JG, Brayden JE, Nelson MT (1993). Inward rectifier K+ currents in smooth muscle cells from rat resistance-sized cerebral arteries. *American Journal of Physiology* **265**(5 Pt 1)**:** C1363-1370.

Quayle JM, Nelson MT, Standen NB (1997). ATP-sensitive and inwardly rectifying potassium channels in smooth muscle. *Physiological Reviews* **77**(4)**:** 1165-1232.

Quinn TJ, Dawson J, Walters MR (2011). Sugar and stroke: cerebrovascular disease and blood glucose control. *Cardiovascular Therapeutics* **29**(6)**:** e31-42.

Radomski MW, Palmer RM, Moncada S (1987). The role of nitric oxide and cGMP in platelet adhesion to vascular endothelium. *Biochemical and Biophysical Research Communications* **148**(3)**:** 1482-1489.

Refsum H, Ueland PM, Nygard O, Vollset SE (1998). Homocysteine and cardiovascular disease. *Annual Review of Medicine* **49:** 31-62.

Reid JM, Paterson DJ, Ashcroft FM, Bergel DH (1993). The effect of tolbutamide on cerebral blood flow during hypoxia and hypercapnia in the anaesthetized rat. *Pflugers Archiv* **425**(3-4)**:** 362-364.

Ren C, Du A, Li D, Sui J, Mayhan WG, Zhao H (2010). Dynamic change of hydrogen sulfide during global cerebral ischemia-reperfusion and its effect in rats. *Brain Research* **1345:** 197-205.

Robert K, Vialard F, Thiery E, Toyama K, Sinet PM, Janel N*, et al.* (2003). Expression of the cystathionine beta synthase (CBS) gene during mouse development and immunolocalization in adult brain. *Journal of Histochemistry and Cytochemistry* **51**(3)**:** 363-371.

Roher AE, Esh C, Kokjohn TA, Kalback W, Luehrs DC, Seward JD*, et al.* (2003). Circle of willis atherosclerosis is a risk factor for sporadic Alzheimer's disease. *Arteriosclerosis, Thrombosis, and Vascular Biology* **23**(11)**:** 2055-2062.

Roquer J, Segura T, Serena J, Castillo J (2009). Endothelial dysfunction, vascular disease and stroke: the ARTICO study. *Cerebrovascular Diseases (Basel, Switzerland)* **27 Suppl 1:** 25-37.

Rubanyi GM, Vanhoutte PM (1986). Superoxide anions and hyperoxia inactivate endothelium-derived relaxing factor. *American Journal of Physiology* **250**(5 Pt 2)**:** H822-827.

Salom JB, Barbera MD, Centeno JM, Orti M, Torregrosa G, Alborch E (1999). Relaxant effects of sodium nitroprusside and NONOates in goat middle cerebral artery: delayed impairment by global ischemia-reperfusion. *Nitric Oxide : Biology and Chemistry* **3**(1)**:** 85-93.

Salom JB, Barbera MD, Centeno JM, Orti M, Torregrosa G, Alborch E (1998). Relaxant effects of sodium nitroprusside and NONOates in rabbit basilar artery. *Pharmacology* **57**(2)**:** 79-87.

Samhan-Arias AK, Garcia-Bereguiain MA, Gutierrez-Merino C (2009). Hydrogen sulfide is a reversible inhibitor of the NADH oxidase activity of synaptic plasma membranes. *Biochemical and Biophysical Research Communications* **388**(4)**:** 718-722.

San Martin A, Du P, Dikalova A, Lassegue B, Aleman M, Gongora MC*, et al.* (2007). Reactive oxygen species-selective regulation of aortic inflammatory gene expression in Type 2 diabetes. *American Journal of Physiology. Heart and Circulatory Physiology* **292**(5)**:** H2073-2082.

Savage JC, Gould DH (1990). Determination of sulfide in brain tissue and rumen fluid by ion-interaction reversed-phase high-performance liquid chromatography. *Journal of Chromatography* **526**(2)**:** 540-545.

Schleifenbaum J, Kohn C, Voblova N, Dubrovska G, Zavarirskaya O, Gloe T*, et al.* (2010). Systemic peripheral artery relaxation by KCNQ channel openers and hydrogen sulfide. *Journal of Hypertension* **28**(9)**:** 1875-1882.

Schmidt HH, Walter U (1994). NO at work. *Cell* **78**(6)**:** 919-925.

Schubert R, Krien U, Gagov H (2001). Protons inhibit the BK(Ca) channel of rat small artery smooth muscle cells. *Journal of Vascular Research* **38**(1)**:** 30-38.

Schulz E, Munzel T (2011). Intracellular pH: a fundamental modulator of vascular function. *Circulation* **124**(17)**:** 1806-1807.

Searls Y, Smirnova IV, Vanhoose L, Fegley B, Loganathan R, Stehno-Bittel L (2012). Time-dependent alterations in rat macrovessels with type 1 diabetes. *Experimental Diabetes Research* **2012:** 278620.

Selemidis S, Sobey CG, Wingler K, Schmidt HH, Drummond GR (2008). NADPH oxidases in the vasculature: molecular features, roles in disease and pharmacological inhibition. *Pharmacology & Therapeutics* **120**(3)**:** 254-291.

Shafton AD, Ryan A, Badoer E (1998). Neurons in the hypothalamic paraventricular nucleus send collaterals to the spinal cord and to the rostral ventrolateral medulla in the rat. *Brain Research* **801**(1-2)**:** 239-243.

Shaw JE, Sicree RA, Zimmet PZ (2010). Global estimates of the prevalence of diabetes for 2010 and 2030. *Diabetes Research and Clinical Practice* **87**(1)**:** 4-14.

Shen GX (2010). Oxidative stress and diabetic cardiovascular disorders: roles of mitochondria and NADPH oxidase. *Canadian Journal of Physiology and Pharmacology* **88**(3)**:** 241-248.

Shibuya N, Mikami Y, Kimura Y, Nagahara N, Kimura H (2009a). Vascular endothelium expresses 3-mercaptopyruvate sulfurtransferase and produces hydrogen sulfide. *Journal of Biochemistry* **146**(5)**:** 623-626.

Shibuya N, Tanaka M, Yoshida M, Ogasawara Y, Togawa T, Ishii K*, et al.* (2009b). 3-Mercaptopyruvate sulfurtransferase produces hydrogen sulfide and bound sulfane sulfur in the brain. *Antioxidants and Redox Signalling* **11**(4)**:** 703-714.

Siegel LM (1965). A direct microdetermination for sulfide. *Analytical Biochemistry* **11:** 126-132.

Siepe M, Ruegg DM, Giraud MN, Python J, Carrel T, Tevaearai HT (2005). Effect of acute body positional changes on the haemodynamics of rats with and without myocardial infarction. *Experimental Physiology* **90**(4)**:** 627-634.

Simard JM, Chen M, Tarasov KV, Bhatta S, Ivanova S, Melnitchenko L*, et al.* (2006). Newly expressed SUR1-regulated NC(Ca-ATP) channel mediates cerebral edema after ischemic stroke. *Nature Medicine* **12**(4)**:** 433-440.

Sivitz WI, Wayson SM, Bayless ML, Sinkey CA, Haynes WG (2007). Obesity impairs vascular relaxation in human subjects: hyperglycemia exaggerates adrenergic vasoconstriction arterial dysfunction in obesity and diabetes. *Journal of Diabetes and its Complications* **21**(3)**:** 149-157.

Skarby T, Hogestatt ED, Andersson KE (1985). Influence of extracellular calcium and nifedipine on alpha 1- and alpha 2-adrenoceptor-mediated contractile responses in isolated rat and cat cerebral and mesenteric arteries. *Acta Physiologica Scandinavica* **123**(4)**:** 445-456.

Skoog I, Gustafson D (2006). Update on hypertension and Alzheimer's disease. *Neurological Research* **28**(6)**:** 605-611.

Smeda JS, McGuire JJ, Daneshtalab N (2010). Protease-activated receptor 2 and bradykinin-mediated vasodilation in the cerebral arteries of stroke-prone rats. *Peptides* **31**(2)**:** 227-237.

Sobey CG, Heistad DD, Faraci FM (1997). Mechanisms of bradykinin-induced cerebral vasodilatation in rats. Evidence that reactive oxygen species activate K+ channels. *Stroke* **28**(11)**:** 2290-2294; discussion 2295.

Soltis EE, Cassis LA (1991). Influence of perivascular adipose tissue on rat aortic smooth muscle responsiveness. *Clinical and Experimental Hypertension. Part A, Theory and Practice* **13**(2)**:** 277-296.

Steffens DC, Potter GG, McQuoid DR, MacFall JR, Payne ME, Burke JR*, et al.* (2007). Longitudinal magnetic resonance imaging vascular changes, apolipoprotein E genotype, and development of dementia in the neurocognitive outcomes of depression in the elderly study. *The American Journal of Geriatric Psychiatry* **15**(10)**:** 839-849.

Stipanuk MH, Beck PW (1982). Characterization of the enzymic capacity for cysteine desulphhydration in liver and kidney of the rat. *The Biochemical Journal* **206**(2)**:** 267-277.

Stitham J, Arehart EJ, Gleim SR, Douville KL, Hwa J (2007). Human prostacyclin receptor structure and function from naturally-occurring and synthetic mutations. *Prostaglandins & other Lipid Mediators* **82**(1-4)**:** 95-108.

Streeter E, Hart J, Badoer E (2012). An investigation of the mechanisms of hydrogen sulfide-induced vasorelaxation in rat middle cerebral arteries. *Naunyn-Schmiedeberg's Archives of Pharmacology*.

Stuehr DJ, Fasehun OA, Kwon NS, Gross SS, Gonzalez JA, Levi R*, et al.* (1991). Inhibition of macrophage and endothelial cell nitric oxide synthase by diphenyleneiodonium and its analogs. *FASEB Journal* **5**(1)**:** 98-103.

Sun NL, Xi Y, Yang SN, Ma Z, Tang CS (2007). [Plasma hydrogen sulfide and homocysteine levels in hypertensive patients with different blood pressure levels and complications]. *Zhonghua xin xue guan bing za zhi* **35**(12)**:** 1145-1148.

Sun YG, Cao YX, Wang WW, Ma SF, Yao T, Zhu YC (2008). Hydrogen sulphide is an inhibitor of L-type calcium channels and mechanical contraction in rat cardiomyocytes. *Cardiovascular Research* **79**(4)**:** 632-641.

Surks HK (2007). cGMP-dependent protein kinase I and smooth muscle relaxation: a tale of two isoforms. *Circulation Research* **101**(11)**:** 1078-1080.

Suzuki K, Olah G, Modis K, Coletta C, Kulp G, Gero D*, et al.* (2011). Hydrogen sulfide replacement therapy protects the vascular endothelium in hyperglycemia by preserving mitochondrial function.

Proceedings of the National Academy of Sciences of the United States of America **108**(33)**:** 13829-13834.

Swanson LW, Sawchenko PE (1983). Hypothalamic integration: organization of the paraventricular and supraoptic nuclei. *Annual Review of Neuroscience* **6:** 269-324.

Tai MH, Wang LL, Wu KL, Chan JY (2005). Increased superoxide anion in rostral ventrolateral medulla contributes to hypertension in spontaneously hypertensive rats via interactions with nitric oxide. *Free Radical Biology & Medicine* **38**(4)**:** 450-462.

Taira J, Misik V, Riesz P (1997). Nitric oxide formation from hydroxylamine by myoglobin and hydrogen peroxide. *Biochimica et Biophysica Acta* **1336**(3)**:** 502-508.

Takeda K, Nakata T, Takesako T, Itoh H, Hirata M, Kawasaki S*, et al.* (1991). Sympathetic inhibition and attenuation of spontaneous hypertension by PVN lesions in rats. *Brain Research* **543**(2)**:** 296-300.

Tang XQ, Yang CT, Chen J, Yin WL, Tian SW, Hu B*, et al.* (2008). Effect of hydrogen sulphide on beta-amyloid-induced damage in PC12 cells. *Clinical and Experimental Pharmacology and Physiology* **35**(2)**:** 180-186.

Tjalve H, Wilander E, Johansson EB (1976). Distribution of labelled streptozotocin in mice: uptake and retention in pancreatic islets. *The Journal of Endocrinology* **69**(3)**:** 455-456.

Toda N, Ayajiki K, Okamura T (2009). Cerebral blood flow regulation by nitric oxide: recent advances. *Pharmacological Reviews* **61**(1)**:** 62-97.

Tomioka H, Hattori Y, Fukao M, Sato A, Liu M, Sakuma I*, et al.* (1999). Relaxation in different-sized rat blood vessels mediated by endothelium-derived hyperpolarizing factor: importance of processes mediating precontractions. *Journal of Vascular Research* **36**(4)**:** 311-320.

Tsioufis C, Kordalis A, Flessas D, Anastasopoulos I, Tsiachris D, Papademetriou V*, et al.* (2011). Pathophysiology of resistant hypertension: the role of sympathetic nervous system. *International Journal of Hypertension* **2011:** 642416.

Tsuchihashi T, Kagiyama S, Ohya Y, Abe I, Fujishima M (1998). Antihypertensive treatment and the responsiveness to glutamate in ventrolateral medulla. *Hypertension* **31**(1)**:** 73-76.

Ufnal M, Sikora M, Dudek M (2008). Exogenous hydrogen sulfide produces hemodynamic effects by triggering central neuroregulatory mechanisms. *Acta Neurobiologiae Experimentalis* **68**(3)**:** 382-388.

Ujiie H, Chaytor AT, Bakker LM, Griffith TM (2003). Essential role of Gap junctions in NO- and prostanoid-independent relaxations evoked by acetylcholine in rabbit intracerebral arteries. *Stroke* **34**(2)**:** 544-550.

van Breemen C, Saida K (1989). Cellular mechanisms regulating [Ca2+]i smooth muscle. *Annual Review of Physiology* **51:** 315-329.

van der Sterren S, Kleikers P, Zimmermann LJ, Villamor E (2011). Vasoactivity of the gasotransmitters hydrogen sulfide and carbon monoxide in the chicken ductus arteriosus. *American Journal of Physiology. Regulatory Integrative and Comparative Physiology* **301**(4)**:** R1186-1198.

Verlohren S, Dubrovska G, Tsang SY, Essin K, Luft FC, Huang Y*, et al.* (2004). Visceral periadventitial adipose tissue regulates arterial tone of mesenteric arteries. *Hypertension* **44**(3)**:** 271-276.

Wakefield DB, Moscufo N, Guttmann CR, Kuchel GA, Kaplan RF, Pearlson G*, et al.* (2010). White matter hyperintensities predict functional decline in voiding, mobility, and cognition in older adults. *Journal of the American Geriatrics Society* **58**(2)**:** 275-281.

Wallace JL, Caliendo G, Santagada V, Cirino G, Fiorucci S (2007). Gastrointestinal safety and anti-inflammatory effects of a hydrogen sulfide-releasing diclofenac derivative in the rat. *Gastroenterology* **132**(1)**:** 261-271.

Wang Y, Zhao X, Jin H, Wei H, Li W, Bu D*, et al.* (2009). Role of hydrogen sulfide in the development of atherosclerotic lesions in apolipoprotein E knockout mice. *Arteriosclerosis, Thrombosis, and Vascular Biology* **29**(2)**:** 173-179.

Wei EP, Kontos HA, Beckman JS (1996). Mechanisms of cerebral vasodilation by superoxide, hydrogen peroxide, and peroxynitrite. *American Journal of Physiology* **271**(3 Pt 2)**:** H1262-1266.

Wei EP, Kontos HA, Christman CW, DeWitt DS, Povlishock JT (1985). Superoxide generation and reversal of acetylcholine-induced cerebral arteriolar dilation after acute hypertension. *Circulation Research* **57**(5)**:** 781-787.

Wei M, Ong L, Smith MT, Ross FB, Schmid K, Hoey AJ*, et al.* (2003). The streptozotocin-diabetic rat as a model of the chronic complications of human diabetes. *Heart, Lung & Circulation* **12**(1)**:** 44-50.

Weiss N, Heydrick S, Zhang YY, Bierl C, Cap A, Loscalzo J (2002). Cellular redox state and endothelial dysfunction in mildly hyperhomocysteinemic cystathionine beta-synthase-deficient mice. *Arteriosclerosis, Thrombosis, and Vascular Biology* **22**(1)**:** 34-41.

Whiteman M, Cheung NS, Zhu YZ, Chu SH, Siau JL, Wong BS*, et al.* (2005). Hydrogen sulphide: a novel inhibitor of hypochlorous acid-mediated oxidative damage in the brain? *Biochemical and Biophysical Research Communications* **326**(4)**:** 794-798.

Whiteman M, Li L, Kostetski I, Chu SH, Siau JL, Bhatia M*, et al.* (2006). Evidence for the formation of a novel nitrosothiol from the gaseous mediators nitric oxide and hydrogen sulphide. *Biochemical and Biophysical Research Communications* **343**(1)**:** 303-310.

Whiteman M, Winyard PG (2011). Hydrogen sulfide and inflammation: the good, the bad, the ugly and the promising. *Expert Review of Clinical Pharmacology* **4**(1)**:** 13-32.

Whitfield NL, Kreimier EL, Verdial FC, Skovgaard N, Olson KR (2008). Reappraisal of H2S/sulfide concentration in vertebrate blood and its potential significance in ischemic preconditioning and vascular signaling. *American Journal of Physiology. Regulatory Integrative and Comparative Physiology* **294**(6)**:** R1930-1937.

Wolin MS (2009). Reactive oxygen species and the control of vascular function. *American Journal of Physiology. Heart and Circulatory Physiology* **296**(3)**:** H539-549.

Wray S, Smith RD (2004). Mechanisms of action of pH-induced effects on vascular smooth muscle. *Molecular and Cellular Biochemistry* **263**(1-2)**:** 163-172.

Xu B, Zheng H, Patel KP (2012). Enhanced activation of RVLM-projecting PVN neurons in rats with chronic heart failure. *American Journal of Physiology. Heart and Circulatory Physiology* **302**(8)**:** H1700-1711.

Xu HL, Santizo RA, Baughman VL, Pelligrino DA (2002). ADP-induced pial arteriolar dilation in ovariectomized rats involves gap junctional communication. *American Journal of Physiology. Heart and Circulatory Physiology* **283**(3)**:** H1082-1091.

Xue B, Beltz TG, Johnson RF, Guo F, Hay M, Johnson AK (2012). PVN adenovirus-siRNA injections silencing either NOX2 or NOX4 attenuate aldosterone/NaCl-induced hypertension in mice. *American Journal of Physiology. Heart and Circulatory Physiology* **302**(3)**:** H733-741.

Yan SK, Chang T, Wang H, Wu L, Wang R, Meng QH (2006). Effects of hydrogen sulfide on homocysteine-induced oxidative stress in vascular smooth muscle cells. *Biochemical and Biophysical Research Communications* **351**(2)**:** 485-491.

Yang G, Pei Y, Teng H, Cao Q, Wang R (2011). Specificity protein-1 as a critical regulator of human cystathionine gamma-lyase in smooth muscle cells. *Journal of Biological Chemistry* **286**(30)**:** 26450-26460.

Yang G, Wu L, Jiang B, Yang W, Qi J, Cao K*, et al.* (2008). H2S as a physiologic vasorelaxant: hypertension in mice with deletion of cystathionine gamma-lyase. *Science* **322**(5901)**:** 587-590.

Yang ZW, Zhang A, Altura BT, Altura BM (1998). Endothelium-dependent relaxation to hydrogen peroxide in canine basilar artery: a potential new cerebral dilator mechanism. *Brain Research Bulletin* **47**(3)**:** 257-263.

Yoo KM, Shin HK, Chang HM, Caplan LR (1998). Middle cerebral artery occlusive disease: the New England Medical Center Stroke Registry. *Journal of Stroke and Cerebrovascular Diseases* **7**(5)**:** 344-351.

You J, Johnson TD, Marrelli SP, Bryan RM, Jr. (1999). Functional heterogeneity of endothelial P2 purinoceptors in the cerebrovascular tree of the rat. *American Journal of Physiology* **277**(3 Pt 2)**:** H893-900.

Yusuf M, Kwong Huat BT, Hsu A, Whiteman M, Bhatia M, Moore PK (2005). Streptozotocin-induced diabetes in the rat is associated with enhanced tissue hydrogen sulfide biosynthesis. *Biochemical and Biophysical Research Communications* **333**(4)**:** 1146-1152.

Zanzinger J (1999). Role of nitric oxide in the neural control of cardiovascular function. *Cardiovascular Res*earch **43**(3)**:** 639-649.

Zhang H, Flagg TP, Nichols CG (2010). Cardiac sarcolemmal K(ATP) channels: Latest twists in a questing tale! *Journal of Molecular and Cellular Cardiology* **48**(1)**:** 71-75.

Zhang LM, Jiang CX, Liu DW (2009). Hydrogen sulfide attenuates neuronal injury induced by vascular dementia via inhibiting apoptosis in rats. *Neurochemical Research* **34**(11)**:** 1984-1992.

Zhao W, Wang R (2002). H(2)S-induced vasorelaxation and underlying cellular and molecular mechanisms. *American Journal of Physiology. Heart and Circulatory Physiology* **283**(2)**:** H474-480.

Zhao W, Zhang J, Lu Y, Wang R (2001). The vasorelaxant effect of H(2)S as a novel endogenous gaseous K(ATP) channel opener. *EMBO Journal* **20**(21)**:** 6008-6016.

Zhao ZZ, Wang Z, Li GH, Wang R, Tan JM, Cao X*, et al.* (2011). Hydrogen sulfide inhibits macrophage-derived foam cell formation. *Experimental Biology and Medicine (Maywood, N.J.)* **236**(2)**:** 169-176.

Zheng H, Liu X, Li Y, Sharma NM, Patel KP (2011). Gene transfer of neuronal nitric oxide synthase to the paraventricular nucleus reduces the enhanced glutamatergic tone in rats with chronic heart failure. *Hypertension* **58**(5)**:** 966-973.

Zheng YF, Dai DZ, Dai Y (2010). NaHS ameliorates diabetic vascular injury by correcting depressed connexin 43 and 40 in the vasculature in streptozotocin-injected rats. *The Journal of Pharmacy and Pharmacology* **62**(5)**:** 615-621.

Zhong MK, Gao J, Zhang F, Xu B, Fan ZD, Wang W*, et al.* (2009). Reactive oxygen species in rostral ventrolateral medulla modulate cardiac sympathetic afferent reflex in rats. *Acta Physiologica (Oxford, England)* **197**(4)**:** 297-304.

Zhong XZ, Harhun MI, Olesen SP, Ohya S, Moffatt JD, Cole WC*, et al.* (2010). Participation of KCNQ (Kv7) potassium channels in myogenic control of cerebral arterial diameter. *Journal of Physiology* **588**(Pt 17)**:** 3277-3293.

Zhou CF, Tang XQ (2011). Hydrogen sulfide and nervous system regulation. *Chinese Medical Journal* **124**(21)**:** 3576-3582.

Zimmermann C, Wimmer M, Haberl RL (2004). L-arginine-mediated vasoreactivity in patients with a risk of stroke. *Cerebrovascular Diseases (Basel, Switzerland)* **17**(2-3)**:** 128-133.

Zimmermann PA, Knot HJ, Stevenson AS, Nelson MT (1997). Increased myogenic tone and diminished responsiveness to ATP-sensitive K+ channel openers in cerebral arteries from diabetic rats. *Circulation Research* **81**(6)**:** 996-1004.

Zucker IH, Schultz HD, Li YF, Wang Y, Wang W, Patel KP (2004). The origin of sympathetic outflow in heart failure: the roles of angiotensin II and nitric oxide. *Progress in Biophysics and Molecular Biology* **84**(2-3)**:** 217-232.

Zuckerman SL, Armstead WM, Hsu P, Shibata M, Leffler CW (1996). Age dependence of cerebrovascular response mechanisms in domestic pigs. *American Journal of Physiology* **271**(2 Pt 2)**:** H535-540.

Zygmunt PM, Hogestatt ED (1996). Role of potassium channels in endothelium-dependent relaxation resistant to nitroarginine in the rat hepatic artery. *British Journal of Pharmacology* **117**(7)**:** 1600-1606.